1-1-2011

Correlation Analysis of Treatment Sensitivity and Protein Expresson of pro- and anti-apoptotic Proteins & the Role of the BH3-only Protein Bim during Apoptosis of malignant Gliomas

Birgit Claudia Weyhenmeyer
Royal College of Surgeons in Ireland

RCSI

Correlation Analysis of Treatment Sensitivity and Protein Expression of pro- and anti-apoptotic Proteins

&

the Role of the BH3-only Protein Bim during Apoptosis of malignant Gliomas

Birgit Claudia Weyhenmeyer

Dissertation submitted to the National University of Ireland
Royal College of Surgeons In Ireland for the
acquisition of the academic degree

Doctor of Philosophy

March 2011

Department of Physiology and Medical Physics
Supervisor: Dr. Brona Murphy

Candidate Thesis Declaration

I declare that this thesis, which I submit to RCSI for examination in consideration of the award of a higher degree, Doctor of Philosophy, is my own personal effort. Where any of the content presented is the result of input or data from a related collaborative research program this is duly acknowledged in the text such that it is possible to ascertain how much of the work is my own. I have not already obtained a degree in RCSI or elsewhere on the basis of this work. Furthermore, I took reasonable care to ensure that the work is original, and, to the best of my knowledge, does not breach copyright law, and has not been taken from other sources except where such work has been cited and acknowledged within the text.

Signed  (Birgit Weyhenmeyer)

Student Number: 08500207

Date 12/7/2012

For my parents,
who are always there for me,
and without whose continuous support
I could have never gotten this far!
THANK YOU!

Table of Contents

Summary

GBM (Glioblastoma multiforme) is the most aggressive form of primary brain tumour, with dismal patient outcome. Treatment failure is often associated with intrinsic or acquired apoptosis resistance and aberrant signalling of survival pathways.

In this work, we analysed apoptosis resistance in gliomas in order to improve treatment predictions and the accuracy of prognosis for patients suffering from GBM. We successfully correlated protein expression profiles of 21 pro- and anti-apoptotic proteins in glioma cell lines with chemotherapeutic sensitivity to mono-therapy with TMZ or TRAIL and to combined therapy with TMZ and TRAIL in these cell lines, using single protein analysis, the multivariate principal component analysis and the computational model APOPTO CELL. We found that sensitivity to TMZ was sufficiently predicted by analysing the components involved in the late steps of apoptosis after the release of cytochrome *c*. Sensitivity to TRAIL or a combination of TMZ and TRAIL was best explained by the analysis of all 21 apoptotic proteins, which are involved in an interactive network in extrinsic and intrinsic apoptotic pathways. Our results also revealed a high predictive value of the anti-apoptotic proteins XIAP and Bcl-x_L and the pro-apoptotic protein procaspase-3 in the determination of apoptosis resistance in glioblastomas.

The BH3-only protein Bim was extensively downregulated in most glioma cell lines and all GBM patient samples. Additionally, a glioma cell line with high intrinsic expression of Bim showed further upregulation of Bim levels during treatment, which was also associated with an enhanced cell death following combination therapy with TMZ and TRAIL. Our results suggest that Bim is transcriptionally regulated during TMZ- and TRAIL-induced apoptosis by the transcription factor FoxO3a, which itself is post-transcriptionally controlled by phosphorylation mediated through the Ras/ RAF/ ERK1/2 survival signalling pathway. Thus, we hypothesise that the repression of Bim activity is a pivotal step during tumourigenesis, which is conferred by both the dysregulation of the apoptotic pathway and aberrant survival signalling.

Acknowledgement

I would like to thank many people who have helped me through the completion of this thesis. First and foremost, I would like to thank my supervisor, Dr. Brona Murphy, for the opportunity to work on this project, for her extensive supervision, valuable guidance, her continous encouragement and moral support throughout these three years.
I would also like to thank my collegue Dr. Áine Murphy for her technical advice and her support in this time.

I am grateful to Dr. Leonie Young and Prof. Dr. Peter Daniel for kindly reviewing my PhD thesis as examiners.
Thank you to Prof. Dr. Jochen Prehn and all my colleagues from the physiology department for their support.

Special thanks go to Jasmin Schmid for her statistical expertise and her friendship, to Dr. Caoimhin Concannon for sharing his endless technical knowledge, as well as to Dr. Markus Rehm and Dr. Heiko Düssmann for many inspiring scientific conversations; to Dr. Hans-Georg König, Dr. Eva Jimenez, Dr. Tobias Engel, Dr. Matthew King, Prof. Dr. Nikolaus Plesnila, Dr. Susanne Hector and Tytus Bernas.

I would also like to thank my parents, Dr. Roland Weyhenmeyer and Anne Weyhenmeyer, Amos Matsiko and Jasmin Schmid for critical proofreading of this thesis.

Finally I'd like to thank my friends, collegues and former collegues, who helped me with day-to-day tasks: Thank you, Simone Pöschel, Dr. David Davila, Dr. Robert Schwamborn, Eugenia Delgado, Dr. Beau Fenner, Maximilian Würstle, Claire Ewarts, Dr. Susanne Schwarzmaier, Andreas Lindner, Dr. Lorna Flanagan, Dr. Christian Hellwig, Dr. Takanori Sano, Dr. Mary Cannon, Dr. Maike Laussmann, Dr. Jordi Sebastia, Ina Woods, Sudipto Das, Dr. Amaya Sany Rodriguez, Dr. Sergio Perez, Aurélien Caballero, Franziska Walter, Dr. Gerhardt Boukes, Ross Gallagher Dr. Suzanne Miller-Delaney, Dr. Sean Kilbride Dr. Jackeline White and Dr. Angela Cesari,

Abbreviations

x g	gravity, centrifugal force
Ac-DEVD-AMC	Acetyl-Asp-Glu-Val-Asp-7-amino-4-methylcoumarin
(d) ATP	(Deoxy) adenosine triphosphate
a.U.	Arbitrary units
Akt	AKR mouse T-cell lymphoma kinase
Apaf-1	Apoptotic protease-activating factor-1
AP-1	Activator protein-1
APS	Ammonium persulphate
Bad	Bcl-2 antagonist of cell death
Bak	Bcl-2 antagonist/killer
Bax	Bcl-2-associated protein X
BCA	Bicinochinic acid
Bcl-2	B cell lymphoma 2
Bcl-2A1	Bcl-2 related protein, also known as A1
Bcl-w	Bcl-2-like protein 2
Bcl-X_L	Bcl-2-related protein X (large)
BH1-4	Bcl-2 homology domain 1 – 4
BH3-only	Bcl-2 homology domain 3-only proteins
Bid	Bcl-2 interacting domain death agonist BH Bcl-2 homology domain
Bim	Bcl-2 interacting mediator of cell death
Bmf	Bcl-2 modifying factor
Bok	Bcl-2 related ovarian killer
bp	Base pairs
BSA	Bovine serum albumin
BSP	Bisulfite genomic sequencing Primers
CARD	Caspase activation recruitment domain
Caspase	Cysteine dependent aspartate specific protease
CD95L	CD95 ligand

cFLIP	Cellular FLICE-like inhibitory protein, CFAR
cIAP	Cellular inhibitor of apoptosis protein
c-Jun	Member of Jun family; component of transcription factor AP-1 (activator protein-1) together with c-Fos
c-Fos	member of Fos family; component of transcription factor AP-1 (activator protein-1) together with c-Jun
Ctrl	Control
Cyt *c*	Cytochrome *c*
DD	Death domain
DDB	DNA Binding Domain
DED	Death effector domain
DEVD	Amino acid sequence Asp-Glu-Val-Asp
DISC	Death-inducing signalling complex
DMEM	Dulbecco's modified Eagle Medium
DMSO	Dimethylsulfoxide
DNA	Deoxyribonucleic acid
DR4, DR5	Death receptor 4 (= TRAIL-R1), death receptor 5 (= TRAIL-R2)
DSB	Double strand break
DTT	Dithiothreitol
ECL	Enhanced chemiluminescence
E. coli	*Escherichia coli* DH5α
EGFR	Epidermal growth factor receptor
EDTA	Ethylene diamine tetraacetic acid
EGTA	Ethylene glycol tetraacetic acid
ER	Endoplasmic reticulum
ERK1/2	Extracellular signal-regulated kinases ERK 1 and ERK 2; p44 and p42 MAP Kinases
FADD	Fas-associated death domain
Fas	FS7-associated cell surface antigen
FasL	Fas ligand (CD95 ligand)

FBS	Fetal bovine serum
FLICE	FADD-like interleukin-1 β-converting enzyme
forw	Forward
FoxO3a	Forkhead box O3, transcription factor
h	Hour, hours
HEPES	N-2-hydroxyethylpiperazine-N-2-ethane-sulphonic acid
Hrk	Harakiri
HRP	Horseradish peroxydase
HtrA2/ Omi	High temperature requirement protein A2/ Omi
IAP	Inhibitor of apoptosis proteins
JNK	c-Jun N-terminal protein kinase
kDa	Kilo Dalton
LB	Luria Bertani
LC3	Microtubule-associated protein light chain 3
MAPK	Mitogen-activated protein (MAP) kinase
Mcl-1	Myeloid cell leukaemia-1
MGMT	O^6-methylguanine-DNA methyltransferase
min	Minute, minutes
MMR	Mismatch repair
MOMP	Mitochondrial outer membrane permeabilisation
mRNA	Messenger RNA
MTT	Thiazolyl Blue Tetrazolium Bromide
MZ	Mainz
NOXA	Damage protein, a pro-apoptotic BH3-containing protein
PARP	Poly (ADP-ribose) polymerase
O^6MeG	O^6-methylguanine, adduct formed after TMZ treatment
OS	Overall survival
p53	Protein 53; tumour suppressor
p-Akt	Phospho-Akt, phosphorylated AKT
PBS	Phosphate-buffered saline

p-c-Jun	Phospho-c-Jun, phosphorylated c-Jun
PCR	Polymerase chain reaction
PDGFR	Platelet-derived growth factor receptor
p-ERK1/2	Phospho-ERK1/2, phosphorylated ERK1/2
p-FoxO3a	Phospho-FoxO3a, phosphorylated FoxO3a
PFS	Progression-free survival
rev	Reverse
PI	Propidium iodide
PI3K	Phospatidyl inositol- 3- kinase
RIP	Receptor interacting protein (RIP)
PS	Phosphatidylserine
RTK	Receptor tyrosine kinases
PUMA /BBC3	p53-upregulated modulator of apoptosis
rpm	Rounds per minute
RPMI	Roswell Park Memorial Institute
RT	Room temperature
RT-PCR	Real Time polymerase chain reaction
SDS	Sodium dodecyl sulfate
SDS-PAGE	Sodium dodecyl sulfate polyacrylamide gel electrophoresis
S.E.M	Standard error of the mean
Smac/ DIABLO	Second mitochondrial- derived activator of caspases/ direct inhibitor of apoptosis protein (IAP)-binding protein with low PI
SSB	Single strand break
STS	Staurosporine
tBid	truncated Bid
TBS	Tris buffered saline
TBST	Tris buffered saline with Tween- 20
TEMED	N,N,N',N'-tetramethyl- ethane-1,2-diamine
TM	Transmembrane (domain)
TMZ	Temozolomide

TNF	Tumour necrosis factor
TRAIL	Tumour necrosis factor-related apoptosis-inducing ligand
TRAIL-R1 – R4	TRAIL receptor 1 – 4; R1 = DR4, R2 = DR5
TS	Tissue sample
TT	TMZ and TRAIL in combination
V	Volt
v/v	Volume per volume
w/v	Weight per volume
WHO	World Health Organization
XIAP	X- chromosome linked inhibitor of apoptosis
zVAD	Benzyloxycarbonyl-Val-Ala-Asp(*O*-methyl) fluoromethylketone

List of Figures

List of Tables

1 Introduction

1.1 Glioblastoma multiforme

Cancer is a leading cause of death and accounts for approximately 7 million deaths (13%) worldwide every year (Lenhard 1996; Louis et al. 2007; World Health Organisation (WHO)). It is assumed that on average, one out of every four people will have cancer at one point in their life (Laurier 2003). Primary brain tumours represent about 2% of all cancers. Glioblastoma multiforme (GBM) is probably the most aggressive type of glial tumour and represents with about 60% of the most common form of all diagnosed primary brain tumours (Das et al. 2011; Ghavami et al. 2009; Cao et al. 2009).

Tumours of the central nervous system are graded according to the WHO based on their state of malignancy (Louis et al. 2007). Grade I apply to tumours with low proliferative potential and can be cured by complete surgical resection alone. The highest grade, grade IV, describes the most aggressive and cytological malignant state. These tumours are highly mitotically active and typically display the following properties: areas of necrosis, uncontrolled cellular proliferation, diffuse infiltration, increased angiogenesis and a high rate of recurrence (Louis 2006). GBM is characterized as a grade IV astrocytoma. Patients with GBM that contains a necrotic core tend to possess a substantially shorter overall survival rate than patients with tumours that do not show any signs of necrosis (Miller et al. 2006). The histological classification of tumours is a major influence on the choice of therapy (Louis et al. 2007).

The majority of glioblastomas are primary GBM that occur *de novo* without evidence of a previously existing malignancy (Kesari 2011). About 5 – 10% glioblastomas are secondary GBM, which result from the progression of a lower grade astrocytoma into a higher grade tumour (Louis et al. 2007). Most tumours emerge without a genetic predisposition and with unknown specific risk factors (Furnari et al. 2007).

Two subtypes of glioblastomas are described: small cell glioblastoma form monomorphic cell populations, consisting of small, densely packed cells with round to slightly elongated shapes that occasionally resemble anaplastic oligodendroglioma (Perry et

al. 2004). The nuclei are typically hyperchromatic and cells show high nuclei/ cytoplasmic ratios. The second subtype consists of glioblastoma in variable size and frequency, including giant cell glioblastoma, and are characterized by oligodendroglioma components (Kesari 2011). Common mutations include epidermal growth factor receptor (EGFR) and variant EGFR-vIII amplification, cyclin-dependent kinase inhibitor 2A (p16INK4a) homozygous deletion, loss of heterozygosity on chromosome 10q (LOH 10q) and phosphatase and tensin homolog (PTEN) mutations (Burger et al. 2001; Perry et al. 2004; Homma et al. 2006).

1.1.1 Treatment of glioblastoma multiforme

Current treatment regimes for patients with glioblastoma involve complete surgical resection, followed by extensive radiotherapy with concomitant and adjuvant chemotherapy (Roos et al. 2007). Chemotherapy aims to inhibit cell cycle progression and angiogenesis, the formation of new blood vessels that support the growing tumour (Yanamandra et al. 2004). Chemotherapeutics can also directly or indirectly induce apoptosis, a cellular suicide program, often by causing DNA damage (Kondo et al. 2010).

Temozolomide (TMZ), a DNA-alkylating agent, has greatly improved the prolonged overall survival of patients (Guckenberger et al. 2011). The drug was first introduced in the 90's and is now the current standard-of-care in chemotherapy of GBM (O'Reilly et al. 1993; Mirimanoff et al. 2006). However, despite recent advances in the therapy, the prognosis for most patients suffering from glioblastoma remains poor (Louis et al. 2007). The median survival rate is still only 14.6 months, with little progress been made in the last 25 years (Stupp et al. 2005; Johnson & O'Neill 2011). Therefore, most treatments strategies are primarily palliative and merely aim to extend the patients life (Friedman 2007).

TMZ, also called Temodar™ or Temodal™ in clinical therapy, shows favourable pharmacokinetic properties and a unique chemical structure (Stevens et al. 1987; Friedman et al. 2000). Its small molecular weight enables the therapeutic to efficiently cross the blood-brain barrier, which makes this drug especially suitable for the treatment of brain tumours (Patel et al. 2003; Ray et al. 2002). TMZ is a imidazotetrazine prodrug and can be

taken orally, as it does not require hepatic metabolism for activation (Clark et al. 1995). Instead, TMZ is directly hydrolyzed under physiological conditions to the reactive alkylating agent MTIC (Stevens et al. 1987) (Figure 1-1). MTIC then transfers a methyl group to the O^6 position of guanine on the DNA and gets degraded into AIC, which is excreted via the kidneys (Clark et al. 1995). The resulting O^6-methylguanine (O^6MeG) adduct is the most potent cytotoxic lesion, which, when unrepaired, leads to apoptosis (Roos et al. 2007).

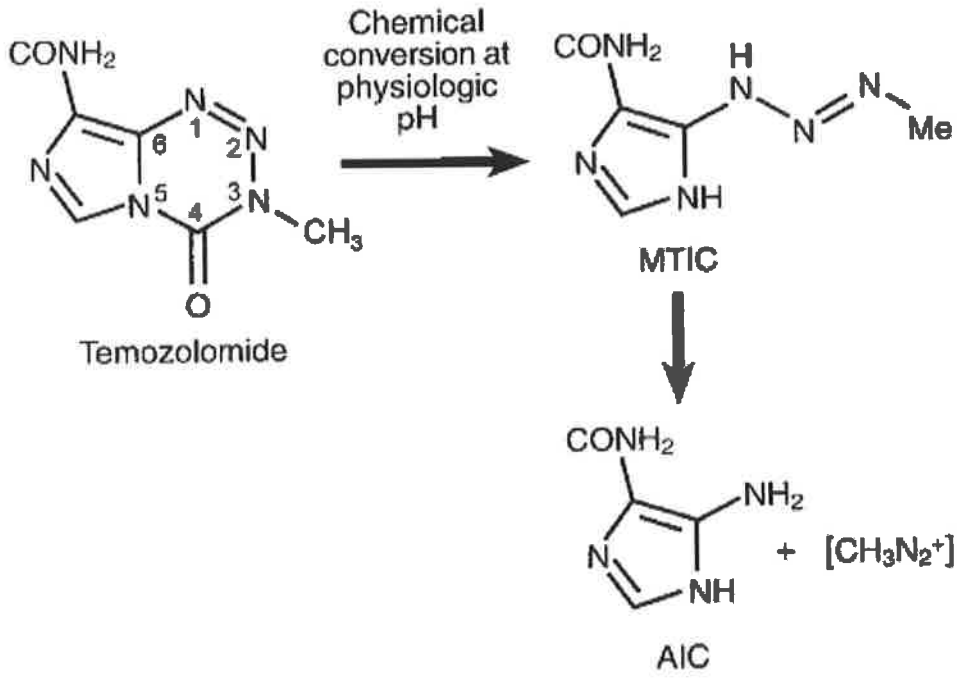

Figure 1-1 Chemical structure of TMZ and MTIC

Chemical structure of the DNA-alkylating drug temozolomide (TMZ). TMZ is converted into MTIC at a physiological pH, which is then degraded to AIC and a methyl group. Adapted from Friedman & Kerby 2000, *Clinical Cancer Research*.

The DNA repair enzyme O^6-methylguanine-DNA methyltransferase (MGMT) can counteract DNA damages caused by alkylating agents such as TMZ by transferring the methyl group irreversibly to a cysteine residue in the catalytic pocket of the MGMT protein (Lindahl et al. 1982; Brennand & Margison 1986; Kaina et al. 2007). MGMT is subsequently degraded.

In some tumours, MGMT function can be suppressed by p53 dysfunction or epigenetic *gene* silencing by MGMT promoter hypermethylation (Blough et al. 2007; Watts et al. 1997). Methylation of the MGMT promoter leads to lower protein expression levels and a reduced activity of the DNA repair enzyme MGMT (Quian & Brent 1997). The assessment of O^6-methylguanine DNA-transferase (MGMT) promoter methylation is so far the most promising predictive marker for sensitivity to temozolomide chemotherapy in patients with glioblastoma (Hegi et al. 2005; Kitange et al. 2009; Sarkaria et al. 2008; Shah et al. 2011). However, this assessment is subject to a controversial debate that has precluded its clinical use (Costa et al. 2010; Tang et al. 2011; Preusser et al. 2008) (see discussion).

In the case of MGMT deactivation, the O^6MeG adducts form O^6MeG:T or O^6MeG:C mismatch pairs during replication (Roos et al. 2007). These mismatches are recognised by the Mismatch repair apparatus (MMR) of the cell, which creates single strand breaks (SSB), causing replication arrest and finally leading to double strand breaks (DSB) (Fulda & Debatin 2006; Roos et al. 2007). DSB are recognised by the tumour suppressor p53, which triggers apoptosis. In the case of p53-mutant cells, cell death can occur via a special case of apoptosis, the mitotic catastrophe, or via the mitochondrial apoptotic pathway (Castedo et al. 2004; Roos et al. 2007)

MGMT can be targeted with the inhibitor O^6benzylG, an O^6MeG analogue (Kokkinakis et al. 1996). MGMT methylation status has been described as a predictive factor for chemotherapeutic sensitivity to TMZ (Hegi et al. 2005).

1.2 Apoptosis and other mechanisms of cell death

Apoptosis or programmed cell death refers to an evolutionary preserved mechanism of controlled cell deletion with characteristic morphological features (Kerr et al. 1972; Jesenberger & Jentsch 2002). The purpose of apoptosis lies in the removal of superfluous or damaged cells from the body of multicellular organisms without the risk of inflammation (Meier et al. 2000; Yuan & Yankner 2000). Cell death via apoptosis is essential during embryogenesis and in maintaining cellular homeostasis (Yuan & Horvitz 2004). It is also fundamental in the defence of infectious microorganism and the removal of cancerous cells. The principles of apoptosis were already proposed in 1842 by Carl Vogt (Vogt 1842). The term apoptosis originates from the greek expression "the falling of leaves from a tree" and was first introduced into scientific literature in 1972, when John Kerr et al. published a detailed description of the distinct morphological features of dying cells (Kerr et al. 1972; Bodey et al. 2004).

The process of apoptosis can be divided into two main phases: In the initial phase, cells undergo a range of morphological and biochemical changes, including cell shrinkage, chromatin condensation, DNA fragmentation and membrane blebbing, which results in the disintegration of the cell into small membrane enclosed vesicles, the so-called apoptotic bodies (Kerr et al. 1972; Llambi & Green 2011; Hector & Prehn 2009) (Figure 1-2). Apoptotic bodies contain pyknotic remnants of nuclei and intact organelles. In the terminal phase, cells present phagocytosis signals, such as phosphatidylserine on the cell surface, which are recognised by macrophages and neighbouring cells who engulf and degrade the remains of the apoptotic cell (Savill et al. 1993; Savill 1997).

Apoptosis differs from necrosis or autophagy, two other types of cell death that occur in cells. Necrosis, greek for "dying", is characterised by uncontrolled swelling of the cell, followed by chromatin digestion and disruption of organelle and plasma membranes (Miller et al. 2006) (Figure 1-2). These events are followed by organelle breakdown, extensive DNA hydrolysis, vacuolation of the endoplasmatic reticulum and plasma membrane rupture. The intracellular content is subsequently released without control, serving as danger signals (DS), which are recognised by specific receptors on the surface of macrophages and drendritic cells. The ligation of DSRs leads to the stimulation of the

inflammatory response. In case of an infection, pathogens can be released from the necrotic cell, which directly interact with Toll-like receptors (TLTs) of the innate immune response (Byrne & Ojcius 2004; Demaria et al. 2010).

Recently, a mode of necrosis called necroptosis or programmed necrosis has been described as an alternative form of a partially controlled cell death that can be induced by regulated signalling pathways (Murakami et al. 2011). Necroptosis is activated by the receptor interacting protein (RIP) when caspase pathways are blocked (Galluzzi et al. 2009).

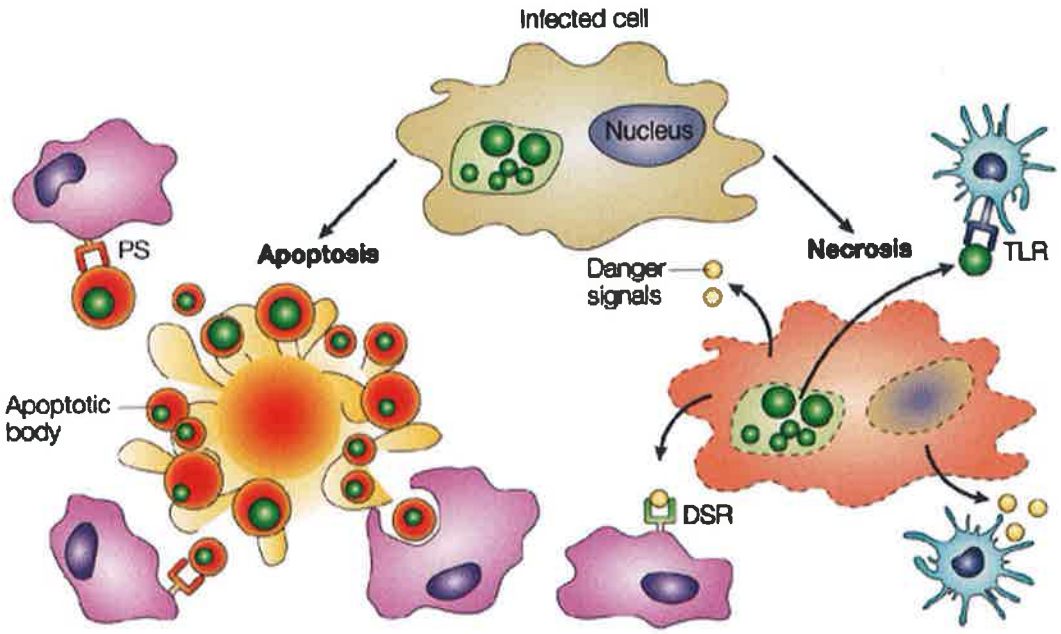

Figure 1-2 Apoptosis and Necrosis

Apoptotic cells shrink, display condensed and fragmented chromatin and disintregrate into small membrane enclosed vesicles without releasing cellular content. As a result of the interaction between these apoptotic bodies and receptors on phagocytic cells, for example via exposed phosphatidylserines (PS) on the surface for example, the inflammatory response is reduced. In contrast, necrotic cells swell, burst open and release intracellular content as danger signals (DS), which is then recognised by danger signal receptors (DSR) on the surface of macrophages. Adapted from Byrne & Ojcius 2004, *Nature review.*

Autophagy, the greek word for "self consumption" is a recycling process that is triggered by food deprivation and cellular stress (Glick et al. 2010). A characteristic of autophagy is the formation of autophagosomes, double-membrane vesicles that contain cellular compounds. Autophagosomes undergo fusion with lysosomes, double-membrane vesicles carrying acid hydrolase enzymes to break down cellular components. Autophagy mainly promotes cell survival, but may result in cell death upon prolonged activation (Maiuri et al. 2007).

1.2.1 Mitochondrial regulators of apoptosis: the Bcl-2 family of proteins

Apoptosis is tightly controlled by a molecular network of protein interactions (Kyprianou et al. 1990; Lopez et al. 2010). The proteins of the apoptotic machinery are constitutively expressed and remain inactive in place until activated by an apoptotic stimulus (Weil et al. 1996). Members of the B cell lymphoma-2 (Bcl-2) family of proteins are pivotal regulators of the mitochondrial apoptotic pathway (Tsujimoto 1998; Nemec & Khaled 2008). The name originates from their first identified member, Bcl-2, an oncoprotein that was activated via chromosome translocation in human follicular lymphoma (Adams & Cory 1998). The discovery that Bcl-2 did not drive cell proliferation, as previously characterised oncogenes, but rather promoted cell survival, led to the view that the inhibition of apoptotic pathways is a critical step in tumourigenesis (Adams & Cory 1998; Adams & Cory 2007; Strasser et al. 1990; Letai 2005). Bcl-2 proteins can form homo- or heterodimers through interaction with Bcl-2 homology (BH) domains (Cosulich et al. 1997; Wong & Puthalakath 2008) (Figure 1-3). All proteins share at least one of four conserved BH regions: BH1, BH2, BH3 and BH4 (Adams & Cory 2007). Some Bcl-2 members also have a C-terminal hydrophobic sequence that enables them to bind to the outer mitochondrial membrane (TM domain).

The Bcl-2 family consists of about 17 proteins, all implicated in apoptosis with sometimes overlapping function (Wong & Puthalakath 2008). Family members can be subdivided into three groups: The first group, the anti-apoptotic Bcl-2-like proteins,

comprises Bcl-2, Bcl-2-related protein X large (Bcl-x_L), Bcl-w, Bfl-1, myeloid cell leukemia-1 (Mcl-1) and A1 (Jette et al. 2008). Anti-apoptotic Bcl-2-like proteins possess all four BH domains proteins and have similar 3D structures (Strasser et al. 2005). The three domains, BH1, BH2 and BH3, form a hydrophobic groove on the surface of Bcl-2-like proteins that enables interaction with the BH3-domain of BH3-only proteins. Members of the Bcl-2-like proteins can bind to and inhibit all pro-apoptotic Bcl-2 family members. Overexpression of the Bcl-2 like proteins prevents apoptosis induced by various stimuli (Giam et al. 2008). The second group, the pro-apoptotic multidomain proteins, comprises Bcl-associated-x (Bax), BH3-homologuous agonist killer (Bak) and Bcl-2 related ovarian killer (Bok), among others (Mckenzie et al. 2010). Characteristic for Bax/ Bak-like proteins are two to three BH domains (BH1, BH2 and BH3). Multidomain proteins also show a high resemblance to pro-apoptotic Bcl-x_L in their three-dimensional structure (Du et al. 2011; Strasser et al. 2005). Bax/ Bak-like proteins are the main effectors of the Bcl-2 regulated pathway. They function downstream of BH3-only proteins and participate in mitochondrial outer membrane permeabilization (MOMP) by pore formation into the mitochondrial outer membrane (Narita et al. 1998). The third group, the pro-apoptotic BH3-only proteins share only the BH3 domain with each other and the rest of the Bcl-2 family members (Strasser et al. 2006). The BH3-only domain is an amphipathic α helix that can be inserted into a hydrophobic groove on the surface of anti-apoptotic proteins. The domain also contains the highly conserved motif LXXXGD (the X stands for any aminoacid). BH3-only group members include the proteins Bcl-2 interacting mediator (Bim), p53-upregulated modulator of apoptosis (PUMA), BH3-interacting domain death agonist (Bid), Noxa (latin for damage), Bcl-2 interacting killer (Bik), Bcl-2 modifying factor (Bmf), Bcl-2 associated death promoter (Bad) and Harakiri (Hrk) (Labi et al. 2006). The activity of BH3-only proteins is essential for the initiation of the mitochondrial apoptotic pathway, but requires the presence of either Bax or Bak (Mérino et al. 2009).

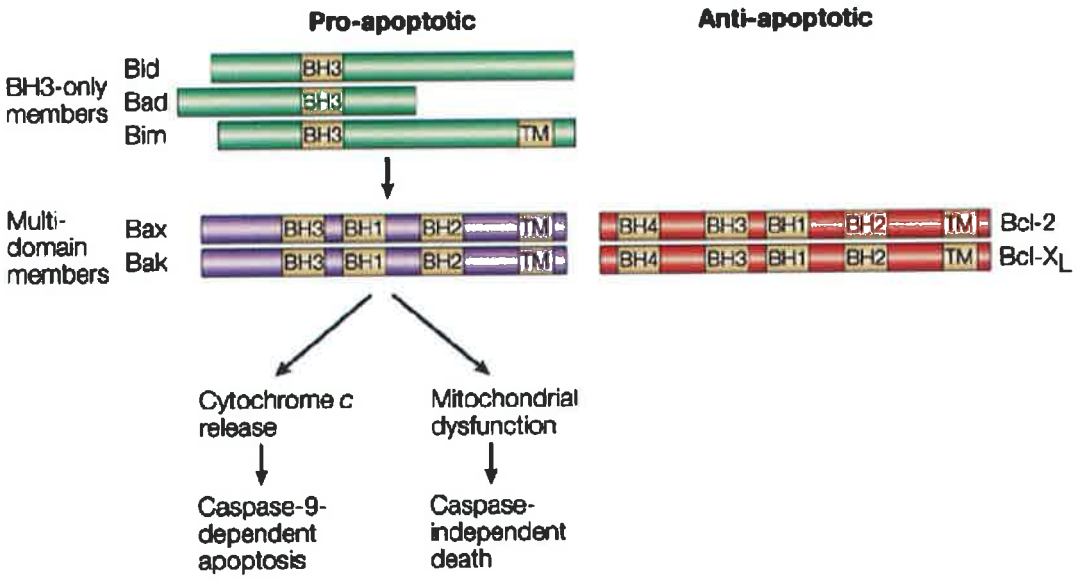

Figure 1-3 Mitochondrial regulator of apoptosis: the Bcl-2 family of proteins

Molecular structure of Bcl-2 family members. Anti-apoptotic Bcl-2 like family members contain all BH domains, BH1-BH4, and the TM domain, pro-apoptotic multidomain-members carry three domains, BH1-BH3 and the TM domain, and pro-apoptotic BH3-only members have just one BH domain; Bim also contains a TM domain. Anti-apoptotic Bcl-2 members primarily function by suppressing the pro-apoptotic family members. BH3-only proteins can activate multidomain members Bak and Bax to trigger mitochondrial apoptosis. Adapted from Jesenberger & Jentsch 2002, *Nature Review*.

BH3-only proteins are activated in response to apoptotic stimuli such as DNA damage, ER stress or exposure to cytotoxic drugs (Willis & Adams 2010). How Bcl-2 proteins interact with each other has been controversially discussed (Giam et al. 2008; Labi et al. 2006; Strasser et al. 2006). One model proposes that certain members of the BH3-only family (Bim, PUMA and Bid) can bind to all anti-apoptotic proteins, while other proteins, such as Bad and Noxa, only interact with a limited number of Bcl-2-like proteins (Chen et al. 2007) (Figure 1-4 A). The interaction of pro-apoptotic BH3-only proteins and anti-apoptotic Bcl-2-like proteins can lead to the release of Bak and Bax (Narita et al. 1998). The second model suggests that BH3-only proteins Bim, Bid and maybe PUMA act as "direct activators" and the rest of the BH3- only proteins act as "de-repressors" (Kuwana et al. 2003) (Figure 1-4 B). Members of both classes are sequestered by anti-apoptotic Bcl-2 family members. High amounts of "de-repressors" would cause the release of "direct activators" from binding to the anti-apoptotic Bcl-2-like proteins. "Direct activators" would then directly interact with Bak and Bax, leading to Bak/ Bax homo-dimerisation (Chipuk et al. 2010). Increased levels of "de-repressors" may result from transcriptional upregulation in response to DNA damage, as demonstrated for PUMA and Noxa (Labi et al. 2006). The ability to directly activate Bax was believed to be specific for Bim, PUMA and Bid (Ren et al. 2011). However, it was recently demonstrated that BH3-only domains other than Bim, PUMA and Bid can also induce Bak and Bax (Du et al. 2011).

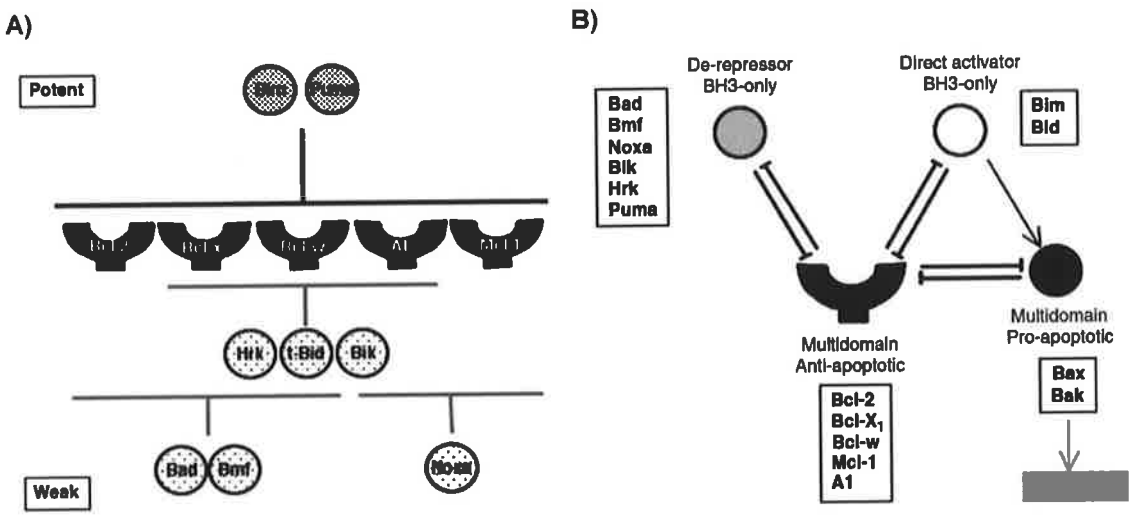

Figure 1-4 Different models describing the mode of BH3-only protein action

A) The action of BH3-only proteins is influenced by their selective affinities for individual Bcl-2-like proteins. Bim and PUMA can bind to Bcl-2, Bcl-x_L, Bcl-w, A1 and Mcl-1 with high affinity, while other BH3-only proteins such as Bmf and Bad bind a subset of anti-apoptotic Bcl-2 like proteins. **B)** BH3-only function can also be explained by the ability of Bim or tBid to bind and activate Bax and Bak directly. Overexpression of "de-repressors" would release "direct activators", which would then induce Bak/ Bax homo-dimerisation. Adapted from Labi et al. 2006, *Nature Reviews*.

Inactive Bax localises in the cytosol or is loosely associated with the mitochondrial outer membrane, whereas Bak is constitutively bound to the mitochondrial membrane (Chen et al. 2007; Reed 2008). On activation, Bax and Bak undergo allosteric changes, leading to the exposure of the BH3 domains and the C-terminal membrane-anchoring domain of Bax. Bax translocates to the mitochondria and inserts into the membrane (Chen et al. 2007). Bax and Bak homo-oligomerise and form pores in the outer mitochondrial membrane (Dewson et al. 2008). Pore formation leads to the release of apoptotic factors such as cytochrome *c* from the mitochondrial inter-membrane space into the cytosol, which triggers apoptosome formation and activation of effector caspases (Garrido et al. 2006; Munoz-Pinedo et al. 2006).

1.2.1.1 Regulation of the BH3-only protein Bim

BH3-only proteins underlie transcriptional, translational and post-translational control through various mechanisms (Sunters et al. 2003; San José-Enerez et al. 2009; Labi et al. 2006; Youle & Strasser 2008). The regulation often varies in a cell type- and stimulus-specific manner (Putcha et al. 2003). The pro-apoptotic Bcl-2 family member Bim, a BH3-only protein, was first identified in a screen for interactors with the anti-apoptotic protein Bcl-2 (O'Connor et al. 1998). Bim plays a pivotal role in the regulation of the mitochondrial pathway after stress-induced apoptosis (O'Connor et al. 1998; Nordigården et al. 2009; Essafi et al. 2005). Cytokine withdrawal, chemotherapeutic agents and anoikis (cell detachment) all trigger apoptosis through upregulation of Bim (Shinjyo et al. 2001; Akiyama et al. 2009; Woods et al. 2007; Reginato et al. 2003).

The *Bim* promoter sequence reveals specific binding sites for several transcription factors that regulate Bim activity at the transcriptional level (Gilley et al. 2003b; Essafi et al. 2005; Biswas et al. 2007; Puthalakath & Strasser 2002). Two conserved forkhead box O3 (FoxO3a /FKHR) binding sites were identified, indicating the regulation of Bim expression through binding of the transcription factor FoxO3a (Gilley et al. 2003a; Essafi et al. 2005). FoxO3a itself is under negative control by the Ras/ RAF/ ERK1/2 – and the PI3K/ Akt survival signalling pathways (Roy et al. 2010; Wang et al. 2011). ERK1/2- and

Akt-mediated phosphorylation leads to the retention of FoxO3a in the cytosol, which is thus unable to promote gene expression in the nucleus (Sunters et al. 2006). Extracellular signal-regulated kinases (ERK1/2) are part of a chain of mitogen-activated protein kinases (MAPK) that are activated in response to extracellular ligand binding to receptor tyrosine kinases (RTK) such as the epidermal growth factor receptor (EGFR) or the Platelet-derived growth factor receptor (PDGFR) (Reginato et al. 2003). The MAPK cascade regulates cell proliferation, differentiation and cell death. Phospatidylinositol 3-kinase (P13K)/ Akt signalling can also be activated via EGFR signalling. The *Bim* promoter also contains binding sites for the transcription factors c-Jun and Myb (Biswas et al. 2007). c-Jun in combination with c-fos forms the activator protein-1 (AP-1) (Hess et al. 2004). AP-1 is an early response transcription factor involved in several processes such as cell proliferation, differentiation and apoptosis. c-Jun is positively regulated by phosphorylation by another class of MAP kinases, the N-terminal c-Jun activating kinase (JNK) (Biswas et al. 2007). The transcription factor Myb is cell cycle controlled through Cdk4/ E2F signalling (Biswas et al. 2007).

Post-transcriptional regulation of Bim activity is partly enabled by differential RNA splicing: The analysis of *Bim* cDNAs revealed that Bim proteins exist as multiple isoforms, which are the result of alternative splicing of the *Bim* mRNA (O'Connor et al. 1998; Bouillet et al. 2001). The splice variants show different potencies to induce apoptosis (O'Connor et al. 1998; Puthalakath et al. 1999). Three major isoforms have been identified: Bim_S (108 base pairs (bp)), Bim_L (138 bp) and Bim_{EL} (198 bp) (Figure 1-6). The shortest form, Bim_S, lacks exons 3 and 4, giving rise to a polypeptide of approximately 13 kilo Daltons (kDa) that only contains the BH3-only domain and a hydrophobic C-terminal region to mediate membrane interactions (TM domain). Bim_L (15 kDa) and Bim_{EL} (23 kDa) both contain exon 4, which encodes for a domain that interacts with the 8 kDa light chain (LC8), a component of the microtubule-associated dynein motor complex (Puthalakath et al. 1999). Bim_L and Bim_{EL} are post-translationally regulated by binding to the dynein motor complex, which sequesters and inactivates both isoforms in healthy cells. Certain apoptotic stimuli induce the dissociation and translocation of Bim_L and Bim_{EL} from the dynein motor complex to the mitochondria. This event was shown to occur upstream of caspase

activation during apoptotic signalling (Puthalakath et al. 1999). Exon 4 also contains phosphorylation sites for JNK (Marani et al. 2004). Direct phosphorylation of Bim by JNK potentiates the proapoptotic activity of Bim (Putcha et al. 2003). Thus, JNK positively controls Bim activity both transcriptionally and post-translationally. Additional regulation of the Bim_{EL} variant occurs via regulatory unites encoded in exon 3: Bim_{EL} contains several ERK phosphorylation sites and at least one Akt phosphorylation site, Ser87 (Luciano et al. 2003; Ewings et al. 2007; Qi et al. 2006). Akt and ERK1/2 mediated phosphorylation targets Bim for ubiquitination and proteasomal degradation. Supposedly due to its lack of the LC8 binding domain, Bim_S is the most potent killer of the three isoforms, while Bim_{EL} is the most abundant form (Puthalakath et al. 1999; O'Connor et al. 1998; Bouillet et al. 2001).

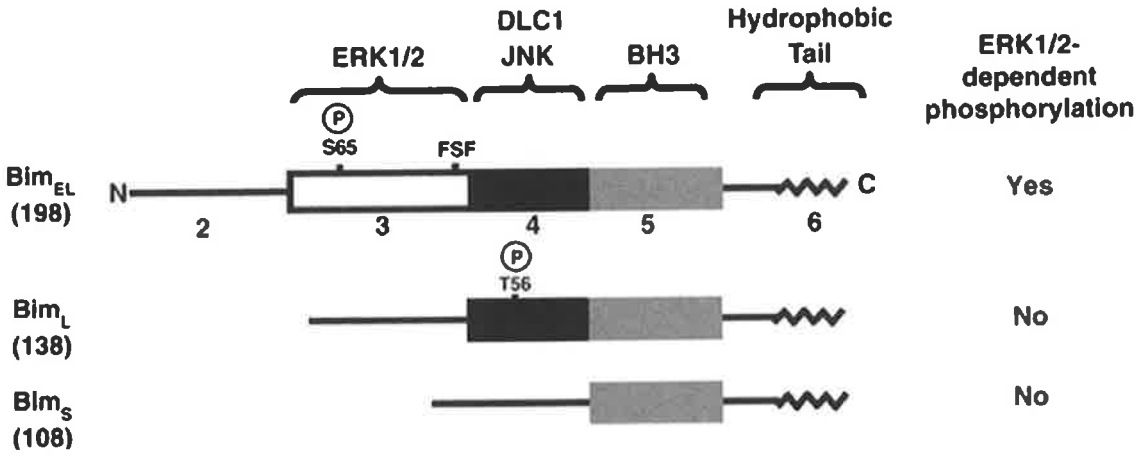

Figure 1-5 Alternative *Bim* mRNA splice variants and Bim domain structure

Alternative splicing of *Bim* mRNA results in at least three major forms: the extra long form Bim_{EL} (198 bp), the long form Bim_L (138 bp) and the short variant Bim_S (108 bp). All Bim splice variants carry exon 2, 5 and 6, which encode for the BH3-only domain (exon 5) and a hydrophobic membrane anker (exon 6). Bim_S lacks both exon 3 and exon 4 and is not susceptible to post-translational regulation by ERK1/2-, Akt- or JNK. Bim_L and Bim_{EL} are both positively regulated by JNK phosphorylation due to the presence of exon 4. Only the isoform Bim_{EL} includes exon 3, which encodes for several ERK1/2 and Akt (not shown) phosphorylation sites. Adapted and modified from Ley et al. 2005, *Cell Death and Differentiation.*

1.2.2 Caspases

Cellular proteases called caspases play a central role in the regulation and execution of apoptotic cell death, but also during necrosis and inflammation (Nicholson et al. 1995; Bodey et al. 2004). Caspases are a family of cysteinyl aspartate-specific proteinases (Stennicke et al. 1999; Li et al. 1997; Garcia-Calvo et al. 1999). The caspase family comprises 11 members in humans (Lavrik et al. 2005). Caspases exist as zymogens called procaspases, inactive enzyme precursors that undergo biochemical modification and conformational changes to become active (Stennicke & Salvesen 2000; Degterev et al. 2003). Most caspases contain an N-terminal prodomain of variable length followed by a large subunit of about 20 kDa (p20) and a small subunit of about 10 kDa (p10), which in some cases are separated by a small linker sequence (Lavrik et al. 2005) (Figure 1-6 A). Three groups can be distinguished: Executioner or effector caspases, including caspase 3, 6 and 7, are the final inducers and executers of the morphological and biochemical changes that are the hallmarks of apoptosis. Initiator or activator caspases, caspase 2, 8, 9 and 10 activate the effector caspases. The third group consists of caspase 1, 4, 5 and 14 and are part of the inflammatory response, but play no prominent role in apoptosis (Stennicke & Salvesen 2000). Activator and inflammatory caspases contain caspase-recruitment domains (CARD) or death-effector domains (DED) to interact with apoptosis signalling molecules (Kischkel et al. 1995; Bertin et al. 1997). Initiator caspase 9 interacts with effector caspases such as caspase-3 and caspase-7 through its CARD domain in a multiprotein complex called apoptosome, which is involved in the intrinsic apoptotic pathway. The DED domain of initiator caspase-8 mediates effector caspase activation in the death-inducing signalling complex (DISC) as part of extrinsic apoptotic signalling. Caspases are activated by proteolytic cleavage and fold into heterotetramers of two cleaved caspase dimers containing two active sites (Garcia-Calvo et al. 2000; Chai et al. 2001) (Figure 1-6 B).

A)

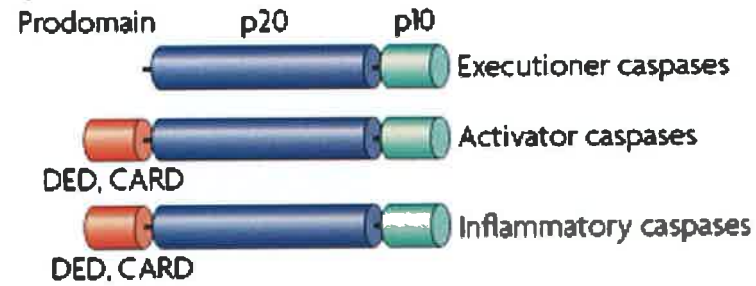

B)

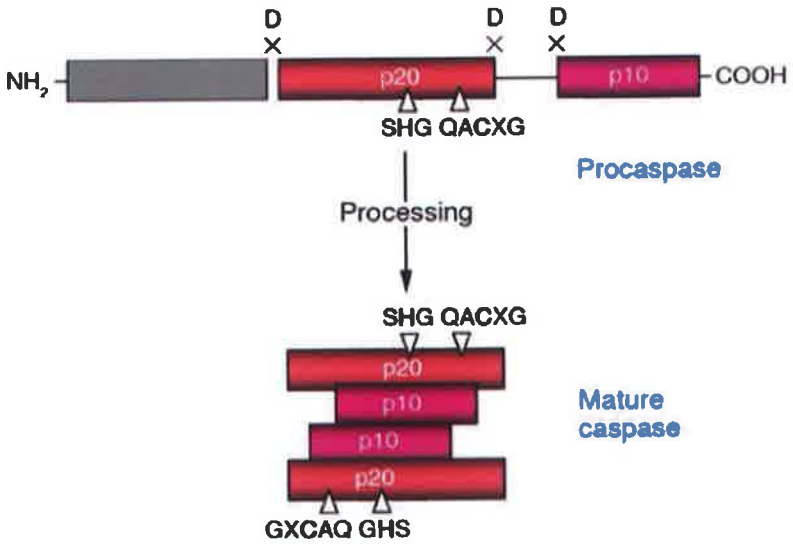

Figure 1-6 Caspase structure and caspase processing

A) Caspases contain three main domains: a prodomain of variable size, and large (p20) and small (p10) subunits that are sometimes separated by a small linker sequence. Activator and inflammatory caspases can contain caspase-recruitment domains (CARD) or death-effector domains (DED) to interact with apoptosis signalling molecules. Adapted from Degterev & Yuan 2008, *Nature Reviews Molecular Cell Biology* **B)** Following activation, the zymogens undergo proteolytic cleavage, the prodomain is removed and the p20 and p10 subunits are separated and rearranged. Adapted from Lavrik et al. 2005, *The Journal of Clinical Investigation.*

1.2.3 The intrinsic or mitochondrial apoptotic pathway

The apoptotic cascade can be triggered by various stimuli such as DNA- or organelle damage and proteasomal stress but also by growth factor withdrawal and other extracellular signals (Ganten et al. 2004; Gong et al. 2007). Two major pathways lead to apoptosis in mammalian cells: the intrinsic or mitochondrial apoptotic pathway and the extrinsic or death receptor pathway (Reimertz et al. 2000) (Figure 1-7). A third option involves the serine protease granzyme B, which is released by cytotoxic lymphocytes to kill virus-infected or tumour cells (Shi et al. 1992).

The intrinsic apoptotic pathway involves the mitochondria and is mainly induced by cytotoxic events such as DNA damage by drugs or radiation, leading to the activation of pro-apoptotic Bcl-2 family members as previously described (Song et al. 2003; Fulda & Debatin 2006). Pro-apoptotic Bcl-2 family member activation culminates in the oligomerisation of multidomain proteins Bak and Bax and pore formation in the outer mitochondrial membrane (Narita et al. 1998; Luetjens et al. 2001; Heiskanen et al. 1999). Mitochondrial outer membrane permeabilisation (MOMP) is accompanied by the loss of mitochondrial membrane potential and mitochondrial depolarisation (Düssmann et al. 2003). Various mitochondrial intermembrane space proteins are released, such as cytochrome *c*, second mitochondria-derived activator of caspases (Smac)/ direct inhibitor of apoptosis protein (IAP)-binding protein with low PI (DIABLO), apoptosis-inducing factor (AIF), the mitochondrial serine protease omi/ HtrA2 and endonuclease G (Candé et al. 2002; Saelens et al. 2004). Released cytochrome *c* binds to apoptotic protease-activating factor 1 (Apaf-1), thereby inducing the oligomerisation of Apaf-1 and the formation of the apoptosome (Zou et al. 1999). The apoptosome is a multiprotein complex consisting of several Apaf-1 molecules that form a heptameric wheel structure. In the presence of (d)ATP, initiator procaspase-9 is recruited to the complex by the interaction of the CARD domains of Apaf-1 and procaspase-9 (Li et al. 1997). Following apoptosome assembling, procaspase-9 dimerises and is processed into its active form. Active caspase-9 in turn triggers the activation of several downstream caspases, leading to a cascade of caspase-mediated cleavage reactions that culminate in the activation of executioner caspases caspase 3 and 7 (Li et al. 1997). The activation of executioner caspases results in the

cleavage of numerous cellular proteins and ultimately leads to the biochemical and morphological hallmarks of apoptosis (Nicholson & Thornberry 1997; Li et al. 1997; Pan et al. 1998). Caspase activity can be inhibited by proteins such as the X- chromosome linked inhibitor of apoptosis (XIAP), which can be deactivated by Smac/ DIABLO (Xia et al. 2007).

1.2.4 The extrinsic or death receptor pathway

The extrinsic apoptotic pathway can be induced by the activation of death receptors belonging to the tumour necrosis factor (TNF) receptor superfamily, which are expressed at the cell surface (Kischkel et al. 1995; Bertin et al. 1997; Ashkenazi & Dixit 1999; Pan et al. 1997). Death receptor ligands such as the FS7-associated cell surface antigen ligand (FasL/ CD95L) and the tumour necrosis factor-related apoptosis-inducing ligand (TRAIL) bind to a cysteine rich extracellular domain of their corresponding death receptors (Figure 1-7). The signal is then transduced via a transmembrane domain of the receptor that is embedded in the plasma membrane to an intra-cellular domain of the receptor that resides within the cytoplasm (Kischkel et al. 1995). In the TRAIL receptor pathway, binding of TRAIL to the death receptors 4 (DR4) and 5 (DR5) leads to their dimerisation, followed by death receptor aggregation into larger structures and the recruitment of adaptor proteins such as the Fas-associated protein with death domain (FADD) (Nitsch et al. 2000). FADD interacts with procaspase 8 and 10 via its death effector domain (DED) to form the death inducing signalling complex (DISC). Depending on the cell type, extrinsic apoptotic signalling can proceed via two pathways: in type I cells, active caspase-8 cleaves and activates executioner caspase-3, directly leading to nuclear fragmentation and ultimatively cell death (Scaffidi et al. 1998; Jost et al. 2009). In type II cells, caspase-8 instead cleaves the BH3-only protein Bid into truncated Bid (tBid), which in turn interacts with other Bcl-2 family member, leading to the activation of the mitochondrial apoptotic pathway (Wang et al. 1996; Li et al. 1998; Song et al. 2003).

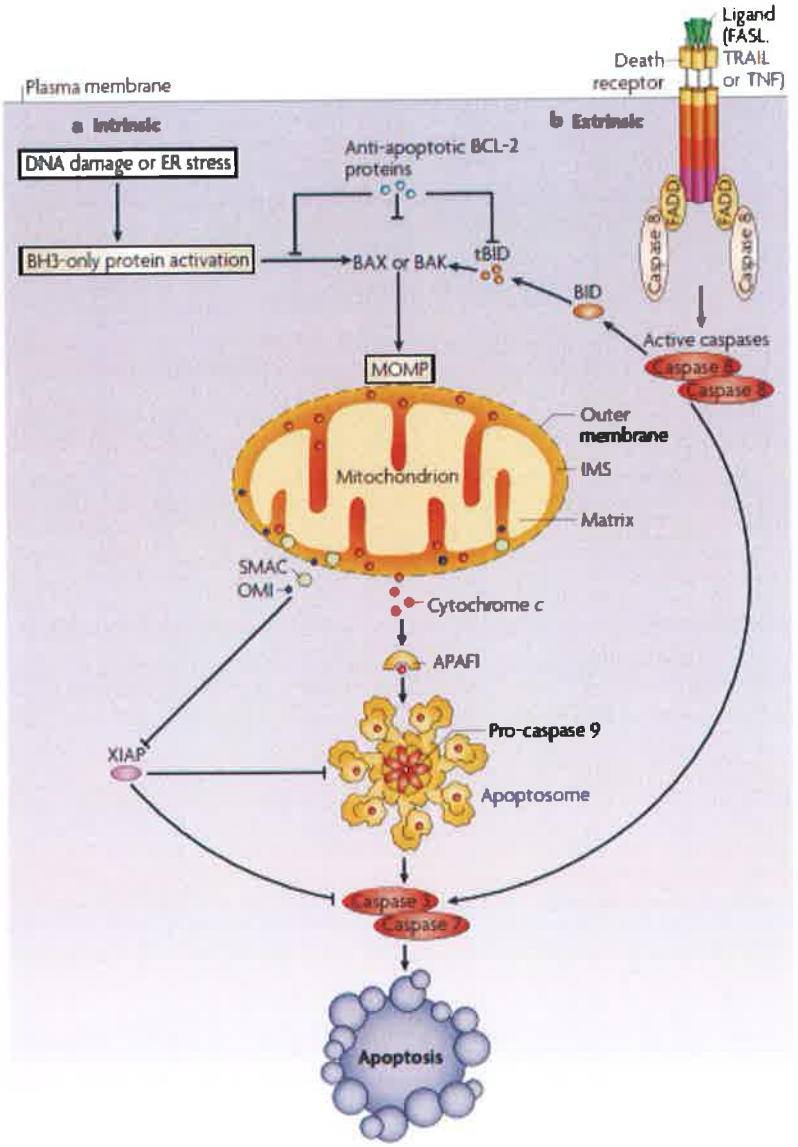

Figure 1-7 Intrinsic and extrinsic apoptotic pathway

A) DNA damage or ER stress activates the intrinsic apoptotic pathway, leading to activation of BH3-only proteins followed by Bak and Bax oligomerisation, resulting in MOMP. The released cytochrome *c* triggers the formation of the apoptosome and effector caspase activation, which execute cell death. **B)** The extrinsic apoptotic pathway is induced by ligand binding to the death receptors, which leads to DISC formation, caspase-8 activation and consequent effector caspase activation. In type II cells, caspase-8 mediates cleavage and activation of the BH3-only Bid, thereby activation the mitochondrial pathway. Adapted from Tait & Green 2010, *Nature Reviews*.

1.3 The aims of this study

Apoptosis plays a pivotal role in the maintanance of tissue homeostasis in multicellular organisms (Yuan & Horvitz 2004). Any disturbance leading to a misbalance between cell proliferation and cell death has disastrous consequences, causing either degenerative pathologies or increased growth and tumourigenesis (Meier et al. 2000). Precursors of pro- and anti-apoptotic proteins exist in a highly sensitive equilibrium within the cell (Weil et al. 1996; Stennicke & Salvesen 2000). The characteristic intrinsic dysregulation of pro-and anti-apoptotic proteins in many tumours, including glioblastomas, primes the cancerous cells to be less susceptible to apoptosis-inducing chemotherapeutics (Jia et al. 2010; Plati & Khosravi-Far 2008). In glioblastomas, a common pattern of apoptosis resistance is the upregulation of anti-apoptotic proteins and the downregulation or functional impairment of pro-apoptotic proteins, which is likely to interfer with treatment sensitivity (Cillessen et al. 2007). Activating alternative pathways of cell death could be one strategy to circumvent this problem (Castedo et al. 2004;). However, most drugs exert their antitumour activity mainly through apoptotic pathways (Roos et al. 2007).

In this study, the overall goal was to identify the molecular mechanisms that contribute to the resistance of glioblastoma multiforme to apoptosis-inducing treatment strategies. The first aim was investigate the expression of pro- and anti-apoptotic proteins critical to the execution of both the intrinsic and extrinsic pathways of apoptosis in a panel of glioma cell lines and GBM patient resected tumours. Our next goal was to determine if such protein expression profiles could be utilized to determine the sensitivity of the cell lines to various chemotherapeutics including the standard cytotoxic agent temozolomide, the novel therapeutic TRAIL and finally a combination of both. Importantly, we were also interested if the expression profiles of apoptotic proteins could be utilized to predict GBM patient progression free survival times. For both of these analyses, we aimed to compare and contrast two different statistical methods, single protein analysis and multivariate principle component analysis and a systems biology based mathematical model, APOPTO-CELL. The final aim of our study was to critically assess the role and regulation of the BH3-only protein Bim in the apoptotic death of glioma cells upon treatment with dual treatment strategy of TMZ and TRAIL.

2 Material and Methods

2.1 Material

Table 2-1 List of chemicals and general reagents

Chemical	Manufacturer
Ac-DEVD-AMC	BD Pharmingen, Biosciences, UK
Acrylamide/ bis-acrylamide (37.5:1) 40%	Sigma-Aldrich, Arklow, Ireland
Ampicillin sodium salt	Sigma-Aldrich, Arklow, Ireland
APS (Ammonium persulphate)	Sigma-Aldrich, Arklow, Ireland
Bromphenol blue	Sigma-Aldrich, Arklow, Ireland
BSA (Bovine Serum Albumine)	Thermo Fisher Scientific, Ireland
$CaCl_2$	Sigma-Aldrich, Arklow, Ireland
CHAPS	Biomol, Exeter, UK
Digitonin	Sigma-Aldrich, Arklow, Ireland
DMSO (dimethyl sulfoxide)	Sigma-Aldrich, Arklow, Ireland
EDTA disodium salt dihydrate	Sigma-Aldrich, Arklow, Ireland
EGTA	Sigma-Aldrich, Arklow, Ireland
Glycerol	Sigma-Aldrich, Arklow, Ireland
Glycerin	Sigma-Aldrich, Arklow, Ireland
HCl (37% hydrochloric acid)	Sigma-Aldrich, Arklow, Ireland
HEPES	Sigma-Aldrich, Arklow, Ireland
Isopropanol	Sigma-Aldrich, Arklow, Ireland
KCl	Sigma-Aldrich, Arklow, Ireland
Luria agar	Sigma-Aldrich, Arklow, Ireland
Luria broth base, Miller	Sigma-Aldrich, Arklow, Ireland
Methanol	Sigma-Aldrich, Arklow, Ireland
$MgCl_2$	Sigma-Aldrich, Arklow, Ireland
Milk powder	Marvel, Dunnes Stores, Dublin, Ireland
MTT (Thiazolyl Blue Tetrazolium	Sigma-Aldrich, Arklow, Ireland

Chemical	Manufacturer
Bromide)	
NaCl	Sigma-Aldrich, Arklow, Ireland
NaOH	Sigma-Aldrich, Arklow, Ireland
PBS tablets	Sigma-Aldrich, Arklow, Ireland
Phosphatase Inhibitor 2 (P5726)	Sigma-Aldrich, Arklow, Ireland
Phosphatase Inhibitor 2 (P0044)	Sigma-Aldrich, Arklow, Ireland
Protease Inhibitor cocktail (P8340)	Sigma-Aldrich, Arklow, Ireland
SDS (sodium dodecyl sulfate)	Sigma-Aldrich, Arklow, Ireland
Sucrose	Sigma-Aldrich, Arklow, Ireland
TEMED	Cell Signaling, Denvers, MA, USA
Tris base, ultra pure	Biomol, Exeter, UK
Triton-x-100	Sigma-Aldrich, Arklow, Ireland
Tween-20	Sigma-Aldrich, Arklow, Ireland
β-mercaptoethanol	Sigma-Aldrich, Arklow, Ireland

Table 2-2 List of cell culture reagents

Cell culture reagent	Manufacturer
Calcium phosphate transfection kit	Invitrogen, Biosciences, Ireland
DMEM medium cat no. 12-604	Lonza Ltd., Wokingham, UK
FBS (fetal bovine serum)	Sigma-Aldrich, Arklow, Ireland
L-glutamine, 200 mM solution	Sigma-Aldrich, Arklow, Ireland
Penicillin-Streptomycin solution	Sigma-Aldrich, Arklow, Ireland
RPMI-1640 medium, cat no. R0883	Sigma-Aldrich, Arklow, Ireland
Sodium pyruvate	Sigma-Aldrich, Arklow, Ireland
Trypsin/ EDTA solution	Sigma-Aldrich, Arklow, Ireland

Table 2-3 Kits and other consumables

Kit/ Consumable	Manufacturer
AmpliTaq Gold PCR Master Mix	Applied Biosystems®, Life Technologies, Dublin, Ireland
Annexin-V-FITC apoptosis detection kit	Biovision, Mountain View, CA, USA
BDFACS sheath fluid with surfactant	BD, Oxford, UK
Coomassie Plus (Bradford) Protein Assay Kit	Thermo Fisher Scientific, Dublin, Ireland
EndoFree Plasmid Maxi Kit	Qiagen, West Sussex, UK
EZ DNA-methylation Gold kit	Zymo Research Corporation, CA, USA
Immobilon Western chemiluminescent HRP substrate	Milipore, Carrigtwohill, Ireland
Micro BCA Protein Assay Kit, Pierce	Thermo Fisher Scientific, Dublin, Ireland
iBlot® transfer Kit	Invitrogen, Biosciences, Ireland
MycoAlert kit	Lonza Ltd., Wokingham, UK.
Nitrocellulose membrane, Protean BA 83, 2 μM	Schleicher & Schuell, Dassel, Germany
PageRuler Plus Prestained Protein ladder	Fermentas, Dublin, Ireland
Partec sheath fluid	Alpha Technologies, Co. Wicklow, Ireland
PI (propidium iodide) solution, 1 mg/ml	Sigma-Aldrich, Arklow, Ireland
PCR clean-up kit	Qiagen, West Sussex, UK
PCR gel extraction kit	Qiagen, West Sussex, UK
Quantitech SYBR Green I	Qiagen, West Sussex, UK
QIAamp DNA Mini Kit	Qiagen, West Sussex, UK
QuiaShredder Kit	Qiagen, West Sussex, UK
RNeasy mini kit	Qiagen, West Sussex, UK
Whatman paper, 1.5 mm thick	Schleicher & Schuell, Dassel, Germany

Table 2-4 Plastic ware

Product	Manufacturer
96-well plate, black, flat bottom, polystyrene	Greiner Bio-One, Cruinn Diagnostics Ltd., Dublin, Ireland
Culture flask T-175, T-75, T-25, vented	Sarstedt Ltd, Co. Wexford, Ireland
CryoTube vials, 1.8 ml	Biovision, Mountain View, CA, USA
Eppendorf tubes	Thermo Fisher Scientific, Dublin, Ireland
Flow cytometer plastic tubes, 3.5 ml, polystyrene	Sarstedt Ltd, Co. Wexford, Ireland
Petri dishes, 94 x 16 mm	Greiner Bio-One
Pipette tips, 0.1 – 10 µl, 2 – 200 µl, 100 – 1000 µl	Thermo Fisher Scientific, Dublin, Ireland
Plastic pipettes, sterile, 5 ml, 10 ml, 50 ml	Sarstedt Ltd, Co. Wexford, Ireland
Reaction tube, polypropylene, 15 ml, 50 ml	Sarstedt Ltd, Co. Wexford, Ireland
Tissue culture flasks, polyethylene, vented cap, 25 cm^2, 75 cm^2, 175 cm^2	Sarstedt Ltd, Co. Wexford, Ireland
Well plate, transparent, flat bottom; 6-, 24-, 96-wells	Sarstedt Ltd, Co. Wexford, Ireland
Nitrocellulose membrane, Protean BA 83, 2 µM	Schleicher & Schuell, Dassel, Germany
PageRuler Plus Prestained Protein ladder	Fermentas, Dublin, Ireland
Partec sheath fluid	Alpha Technologies, Co. Wicklow, Ireland
PI (propidium iodide) solution, 1 mg/ml	Sigma-Aldrich, Arklow, Ireland
PCR clean-up kit	Qiagen, West Sussex, UK
PCR gel extraction kit	Qiagen, West Sussex, UK
Quantitech SYBR Green I	Qiagen, West Sussex, UK

Table 2-5 Laboratory equipment

Instrument	Models	Manufacturer
-80°C freezer	Recvo	Thermo Fisher Scientific, Dublin, Ireland
Autoclave	Priorclave V150	Priorclave Ltd., Woolwich, UK
Bacterial incubator/shaker	Innova 44	New Brunswick Scientific, St. Albans, UK
BioRad electrophoresis system	Mini-PROTEAN 3 cell	Alpha Technologies, Co. Wicklow, Ireland
BioRad power supply	PowerPac HC or PowerPac basic	Alpha Technologies, Co. Wicklow, Ireland
Centrifuge	Sorvall RC-5B Plus	Unitech, Dublin, Ireland
Centrifuge with cooling function	Eppendorf 5810R	Unitech, Dublin, Ireland
Chemiluminescence imager	FujiFilm Las-3000, LAS-4000	Brennan and Company, Dublin, Ireland
Epifluorescence microscope	Nikon Eclipse TE300	MicronOptical
Flow cytometer	Cyflow ML 16	Partec, Münster, Germany
Freezer for sample storage	Powerpoint	Mason Technology, Dublin, Ireland
Fume hood	Chemflow CSC	Chemical System Control Ltd., Dublin, Ireland
GENios microplate reader	Infinite	Tecan, Crailsheim, Germany
iBlot® gel transfer device	iBlot	Invitrogen, Biosciences, Ireland
Ice machine	Porka KF185	Mason Technology
Light-Cycler	Light-Cycler 2.0	Roche
Light microscope	Nikon Eclipse TS100	MicronOptical
Liquid nitrogen tank	MVE Cryosystem 4000	Carl Stuart Ltd., Dublin, Ireland

Instrument	Models	Manufacturer
Mini-centrifuge	Jencons-PLS	Lennox
Nanodrop	2000	Thermo Fisher Scientific
Neubauer counting chamber	Hawksley & Son Ltd.	Lennox
pH meter	420 Orion digital	AGB Scientific Ltd., Dublin, Ireland
Pipette set (0.5 – 10 µl, 2 – 20 µl, 20 – 200 µl, 100 – 1000 µl)	Eppendorf Research adjustable	Unitech
PCR machine	MJ Research PTC-200 Peltier Thermal Cycler	Eppendorf
Precision scale	Ohaus Explorer Pro	Lennox
Scale	Ohaus Ranger	Lennox
Semi-dry transfer cell	Trans-Blot SD	Alpha Technologies
Table centrifuge with cooling function	Biofuge fresco	Heraeus, Newport Pagnell, UK
Thermomixer	Eppendorf comfort	Unitech
Tissue culture hood	MSC-Advantage	Thermo Fisher Scientific, Dublin, Ireland
Tissue culture incubator/ O_2-humidifier	Hera cell 150	Heraeus
Vortex mixer	Stuart SA8	Lennox
Water deionisation system	Barnstead Reverse Osmosiss	Mason Technology
Waterbath	1003	GFL, Burgwedel, Germany

2.2 Cell culture

2.2.1 Establishment of glioma cell lines

All human glioma cell lines were established and kindly provided by Dr. Donat Kögel, Experimental Neurosurgery, Center for Neurology and Neurosurgery, Goethe University Clinics Frankfurt, Germany.

Human tumour samples were obtained during craniotomies from the operating theatre of Neurosurgery, University Hospital Mainz, under sterile conditions from patients with histological documented brain tumours. Pathological and immunohistochemical analyses of the tumour specimens were performed in the Institute of Neuropathology in cryo sections and in formalin-fixed and paraffin-embedded tissues. Tumour specimens were classified according to the WHO system (Louis et al. 2007). Glioma cell lines MZ18, MZ51, MZ294 and MZ327 cell lines were derived from primary grade IV glioblastomas, MZ256 and MZ304 were derived from secondary or recurrent grade IV glioblastomas (Hetschko et al. 2007).

To isolate glioma cells, the tumour specimens were minced to a homogeneous compound with scalpels, suspended in 1 x physiological saline (PBS) and centrifuged at 400 x *g*. Pellets were resuspended in 10 ml Dulbecco's modified Eagle's medium (DMEM) containing 3.7 mg/ml NaHCO3, 10% fetal bovine serum, penicillin (100 units/ml), streptomycin (100 µg/ml) and L-glutamine (2 mmol/l), and cultivated at 37°C in a humidified incubator containing 5% CO_2.

Human glioma cell lines U87, U251, U343, U373 and A172 are commercially available cell lines (American Type Cell Culture (ATCC), Rockville, MD) derived from primary grade III/IV gliomas (Asai et al. 1994; Badie et al. 1994). The general term "glioma" is used to refer to both glioblastomas (WHO grade IV) and anaplastic gliomas (astrocytomas, oligoastocytomas, oligodendrogliomas) (WHO grade III) (Louis et al. 2007).

Table 2-6 Established glioma cell lines used in this study

Cell line	Tumour entity*	WHO grade	p53 status	MGMT status	Reference
MZ18	GBM	IV	unknown	unknown	(Hetschko et al. 2007)
MZ51	GBM	IV	unknown	unknown	(Hetschko et al. 2007)
MZ256	2° GBM	IV	unknown	unknown	(Hetschko et al. 2007)
MZ294	GBM	IV	unknown	unknown	(Hetschko et al. 2007)
MZ304	2° GBM	IV	unknown	unknown	(Hetschko et al. 2007)
MZ327	GBM	IV	unknown	unknown	(Hetschko et al. 2007)
U87	Glioma	III/IV	wildtype	negative/ positive	(Asai et al. 1994)
U251	Glioma	III/IV	mutant	negative	(Asai et al. 1994)
U343	Glioma	III/IV	wildtype	negative	(Asai et al. 1994)
U373	Glioma	III/IV	mutant	positive	(Badie et al. 1994)
A172	Glioma	III/IV	mutant	negative	(Badie et al. 1994)

GBM = glioblastoma multiforme (grade IV astrocytoma)

2nd GBM = secondary glioblastoma derived from lower-grade astrocytoma

Glioma = astrocytoma/ glioblastoma

*Classification according to WHO recommendations

2.2.2 Preparation of frozen samples and cell storage

For storage, cells were washed with 1 x PBS, trypsionized with 0.05% Trypsin/ EDTA, and spun for 3-5 min at 400 x *g*. Cells were washed again with 1 x PBS and resuspended in a 1:1 mixture of plain DMEM medium and a 80% FBS plus 20% glycerol freezing media stock. Samples were stored at -80°C in liquid N_2.

2.2.3 Defrosting cell lines and cell culture

Cells were shipped as frozen samples or stored in -80°C liquid nitrogen as replicates of the original samples. Cells were carefully defrosted by adding DMEM medium and spun at 400 x *g*, washed with 1 x PBS, resuspended in DMEM and cultivated as described above. Cells were passaged once weekly using trypsin/ EDTA. Cultures were discarded before they reached passage 20 and new frozen samples were cultivated as replacements. Cells were analysed every month for the presence of mycoplasm. For treatments cells were seeded at densities according to Table 2-7. Cell numbers were determined using a Neubauer haemocytometer.

Table 2-7 Seeding cell density

Dish		Area [mm^2]	Density (Seeding)	Density (Confluence)	Medium [ml]
Multi-well Plates	**6 wells**	962	0.3×10^6	1.2×10^6	2
	24 wells	200	0.5×10^5	2.0×10^5	0.5
	96 wells	50	1.25×10^2	0.5×10^5	0.15
Flasks	**T-25**	2500	0.7×10^6	2.8×10^6	5
	T-75	7500	2.1×10^6	8.4×10^6	10
	T-175	16000	4.9×10^6	19.6×10^6	25

2.2.4 Cancer cell line HeLa

The human cervix carcinoma cell line HeLa D98 was kindly provided by Markus Rehm, Physiology Department, Royal College of Surgeons in Ireland, Dublin, Ireland. This cell line was established in 1951 from a tumour sample of the patient Henrietta Lacks (Silberman 2010). The cells grow adherent with an epithelial morphology. HeLa cells have a modal number of 82 chromosomes and are 100% aneuploid. This cell line has very low p53 expression level due to the insertion of the human papilloma virus 18 (HPV 18) in the

genome. PHV 18 encodes for the E6 oncoprotein, which promotes the rapid degradation of p53 (Scheffner et al. 1990). HeLa cells have a doubling time of approximately 24 h. HeLa cells were cultivated in RPMI medium, containing 10% fetal bovine serum, penicillin (100 units/ml), streptomycin (100 µg/ml) and L-glutamine (2 mmol/l), at 37°C in a humidified incubator containing 5% CO_2. Cell line handling was carried out as described for glioma cell lines.

2.3 Patient samples

All human glioblastoma patient samples were kindly provided by Dr. Donat Kögel, Experimental Neurosurgery, Center for Neurology and Neurosurgery, Goethe University Clinics Frankfurt, Germany. Human tumour samples were obtained as described for glioma cell lines. The pellet resulting from tumour specimen homogenisation was directly mixed with SDS-lysis buffer (62.5 mmol/l Tris-Hcl (pH 6.8), 10% Glycerin, 2% SDS, 10 µM protease inhibitor cocktail) and samples were stored at -80°C (Table 2-8).

Table 2-8 Resected glioblastoma patient samples used in this study

# TS	Tumour entity	WHO grade	Age	Sex	PFS (in months)
1	GBM	IV	48	f	>17
2	GBM	IV	59	f	>16
3	GBM	IV	22	f	>15
4	GBM	IV	42	f	>12
6	GBM	IV	66	m	>11
7	GBM	IV	71	f	>16
8	2° GBM	IV	70	f	>10
9	GBM	IV	59	f	8
11	GBM	IV	59	m	7
13	GBM	IV	44	m	3
14	GBM	IV	55	f	5
16	GBM	IV	67	m	4
17	GBM	IV	64	f	<10 months
19	2° GBM	IV	66	m	<10 months
21	GBM	IV	55	f	<10 months
22	GBM	IV	53	f	<10 months
23	2° GBM	IV	55	f	<10 months

f = female, m = male

2nd GBM = secondary glioblastoma derived from lower-grade astrocytoma

PFS = progression-free survival

TS = tissue sample

samples 1 – 8 are classified as long-term PFS, samples 9 – 23 as short-term PFS

2.4 Bacterial work

The gram-negative bacterium *Escherichia coli* (*E. coli*) was used for the amplification of DNA plasmids, which were then transfected into mammalian cells. To avoid contaminations with other bacteria, all stock solutions and glassware were autoclaved for 20 min at 121°C. Work was carried out close to an open flame on laboratory benches sterilised with 70% ethanol.

2.4.1 Stock solution for bacterial work

LB (Luria Bertani) medium

1 litre of LB medium was made from of 15.5 g LB base mixed with deionised water and directly autoclaved. LB base consisted of tryptone, yeast extract and sodium chloride with final concentrations of 10 g/l. For the selective growth of transformed *E. coli*, 100 µg/ml ampicillin was added after the autoclavation.

LB Agar plates

40 g Luria agar was added to 1 litre LB medium before autoclaving it. LB agar was cooled down and antibiotic resistance was added, if required. After pouring the mixture into petri dishes, the agar plates were left to polymerise next to an open flame with a partially open lid.

0.1 M $CaCl_2$ buffer

2.2 g anhydrous calcium chloride and 30 ml glycerol were dissolved in 170 ml deionised water and autoclaved.

2.4.2 Generation of chemically competent cells

The strain Escherichia coli DH5α (in this work abbreviated as *E. coli*) was made competent using the calcium chloride method to take up plasmid DNA (Cohen et al. 1972; Hanhan 1983; Mandel & Higa 1992). Naïve, untransformed *E. coli* cell suspension was streaked on LB agar plates and incubated overnight at 37°C. A single *E. coli* colony was picked from the agar plate and grown overnight in 5 ml LB at 37°C, while shaking at 200 rpm. The overnight culture was added to 200 ml LB medium and grown at 37°C, 200 rpm, for approximately 2 h until an optical density OD_{600} was reached. The bacterial suspension was distributed into four 50 ml reaction tubes and centrifuged at 800 x g for 10 min at 4°C. The supernatant was poured off and the bacteria resuspended in 10 ml ice-cold 0.1 M $CaCl_2$ buffer and placed on ice for 30 min. The bacterial suspension was spun again and resuspended in 5 ml ice.cold 0.1 M $CaCl_2$ supplemented with 15% glycerol. Aliquots of 100 µl bacterial suspension were transferred into pre-cooled 1.5 ml micro tubes, shock-frozen in liquid nitrogen and stored at -80°C.

2.4.3 Transformation of competent *E. coli* cells

Frozen competent cells were thawed on ice. After adding 2 µl of the desired plasmid (Table 2-12), the cells were incubated on ice for 30 min. During this time the divalent Ca^{2+} cations coordinated a complex between the negatively charged DNA and the negatively charged lipopolysaccharides of the outer bacterial membrane (Panja et al 2008b). Plasmid uptake was induced by heatshocking the cells at 42°C in a water bath for 90 s, followed by recovery on ice for 2 min. The heat pulse led to pore formation in the bacterila membrane by reducing the lipid fluidity and faciliating the DNA uptake by lowering the membrane potential (Panja et al. 2008b). 800 µl LB medium was added to the cells. The cells were incubated for 1 h at 37°C and 600 rpm on a shaker to allow the expression of the antibiotic resistance gene, encoded on the plasmid. Different volumes of bacterial suspension (e.g. 25 µl and 100 µl) were plated out on LB plates containing the specific antibiotic for selection. LB plates were inverted and incubated overnight at 37°C. *E. coli* cells, which took up the

plasmid, were resistant against the antibiotic in the LB agar plate and could proliferate, while non-transformed cells died.

2.4.4 Plasmid extraction from transformed cells

After the transformation, a single colony from the LB plate was taken with a sterile filter tip to inoculate 5 ml LB medium with ampicilin. After letting the bacteria grow on a shaker (200 rpm) for 8 h at 37°C, the starter culture was added to 250 ml LB with ampicillin. The bacterial suspension was incubated overnight at 37°C and 200 rpm. On the following day the bacteria were collected and the plasmid DNA was isolated using EndoFree Plasmid Maxi kit (Table 2-3) according to manufacturer's instructions.

2.5 DNA analysis

2.5.1 RNA extraction

For total RNA extraction, cells were collected after addition of Trypsin/ EDTA and spun down for 5 min at 1000 x *g*. The RNeasy mini kit (Table 2-3) was used to extract the RNA according to manufacturer's instructions. RNA was stored at -80°C or directly purified using the QiaShredder kit according to manufacturer's instructions.

2.5.2 Quantitative Real Time PCR (qPCR)

Quantitative Real Time PCR (qPCR) was used to accurately measure the mRNA levels of genes using Sybr Green which binds to the minor groove of DNA causing it to fluoresce. Following each round of PCR the total fluorescence in the sample is measured which corresponds to the amount of DNA present after each cycle. The concentration of purified RNA extracts was measured using a nanodrop. First strand cDNA synthesis was performed as displayed in Table 2-9.

Table 2-9 Reverse transcription of RNA into cDNA

Incubation time	Temperature	Reagent	Volume
15 min	RT	RNA in water (1.5 µg)	17 µl
		DNAse I (Invitrogen)	1 µl
		10 x Buffer	2 µl
5 min, then on ice	65°C	+ EDTA (25 nM)	1 µl
2 min	25°C	+ random hexamers (200ng)	2 µl
		+ dNTPs (10 mM)	2 µl
		+ First Strand Buffer (5x) (Invitrogen)	8 µl
		+ DTT (0.1M)	4 µl
		+ RNase Out (Invitrogen)	2 µl
34 cycles: 10 min	25°C	+ Superscript II (Invitrogen)	2 µl
50 min	42°C		
15 min	70°C		

RT = Room temperature

Quantitative RT-PCR was performed using the Light-Cycler 2.0 and the QuantiTech SYBR green PCR kit.

Table 2-10 PCR Mix

Reagent	Volume
Sybr Green	10 µl
template cDNA (2µg)	2 µl
PrimerMix	1 µl
dH_2O	7 µl

Table 2-11 PCR program

	95°C	10 min
40 cycles	95°C	15 s
	60°C	30 s
	72°C	30 s
	72°C	10 min

The Primers were designed using the open source software Primer3 (sourceforge.net; http://frodo.wi.mit.edu/primer3/input.htm) (Table 2-12). Data analysis was performed using the Light-Cycler 4.0 software (Roche Applied Science).

Table 2-12 RT-PCR primers used in this study

Primers	Sequence
Bim forw	5'AGTGTGACCGAGAAGGTAGACAA'3
Bim rev	5'CATTGCACTGAGATAGTGGTT'3
PUMA forw	5'CCATCTCAGGAAAGGCTGTT'3
PUMA rev	5'ACGTTTGGCTCATTTGCTCT'3
Bid forw	5'GAGGAGCACAGTGCGGATTC'3
Bid rev	5'TGCGGAAGCTGTTGTCAGAA'3
β-actin forw	5'CACCCGTCTTCAGGGCTTCTTGGTTT'3'
β-actin rev	5'CATTTCACCATCTGGTTGGCTGGCTC'3

2.5.3 Genomic DNA extraction

Cells were first collected after addition of Trypsin/ EDTA and spun down for 5 min at 1000 x *g*. The *genomic* DNA was extracted using the QIAamp DNA Mini Kit following the instructions by the manufacturer. DNA was stored at -20°C to -80°C.

2.5.4 DNA gel electrophoresis

1 g agarose was dissolved in 100 ml Tris acetate EDTA buffer (TAE; 40 mM Tris-Hcl, 1 mM EDTA pH 8.0, 0.115% (v/v) glacial acetic acid in dH_2O) by heating in a microwave. The resulting gel was allowed to cool down to hand heat and 2 µl of ethidium bromide were added before casting the gel. After solidification the gel was immersed in TAE buffer. Meanwhile the DNA-samples were prepared by adding 6 x DNA loading buffer (15% (w/v) Ficoll, 0.001% (w/v) Bromphenol Blue in dH_20). The solidified gel was

immersed in TAE-Buffer and the samples were loaded before gel was connected to a voltage of 50 V. The DNA bands on the gel were then visualised with a LAS 3000 Image reader.

2.5.5 Methylation analysis

DNA methylation is an epigenetic event that affects cell function by altering gene expression (Quian & Brent 1997). Methylcytosines are generated by covalent addition of a methyl group to the 5-carbon of a cytosine in a CpG dinucleotide, catalyzed by DNA methyltransferase (DNMT). The methylation status of multiple CpG dinucleotides in the MGMT promoter fragment was analysed by direct Bisulfite genomic Sequencing PCR (BSP) (Frommer et al. 1992). A total of 500 ng of *genomic* DNA per cell line was bisulfite converted with the EZ DNA-methylation Gold kit using the alternative conversion reaction 2 as per manufacturer's instructions. During the reaction all cytosines which are not methylated are converted into tyrosines without affecting 5-methycytosine. PCR primers were designed using the open source program methyl primer express (www.appliedbiosystems.com/methylprimerexpress). BSP primers are designed to encompass the CpG without including them in the design of the primers.

Table 2-13 BSP primers used in this study

Primers	Sequence
BSP forw	5' ATGCGTAGATTGTTTTAGGTT'3
BSP rev	5' ACCACTCGAAACTACCACC'3

PCR was carried out using 20 ng of the bisulfite-treated DNA, 10 pmol of each primer, 25 µl of AmpliTaqGold PCR master mix and dH_2O along with a 1:5 dilution of DMSO.
PCR cycling conditions were as follows:

Table 2-14 Amplification of bisulfite converted *genomic* DNA

95°C	10 min
94°C	30 sec
58°C	45 sec
72°C	30 sec
72°C	10 min

Analysis via DNA electrophoresis verified the successfull PCR amplification. PCR products were either directly purified using the GeneJET™ PCR Purification Kit or after DNA gel electrophoresis, using the GeneJET™ Gel Extraction Kit. Samples were sent to MWG-Biotech for sequencing in both directions (http://www.mwg-biotech.com/). The BSP primers also served as sequencing primers. Resulting electropherograms were analyzed using the BIQ analyzer (Bock et al. 2005). and Chromas Lite (Technelysium Pty Ltd, Brisbane, Australia).

2.5.6 PCR Purification

PCR products were purified either directly after PCR amplification using the GeneJET™ PCR Purification Kit or after gel electrophoresis (1.5% agarose, 1xTAE buffer, 100 V) and excision of the band of interest on the gel, using the GeneJET™ Gel Extraction Kit. For gel extraction, gel slices were weighted and Binding Buffer was added 1:1 (volume: weight) to the gel slice. The gel mixture was incubated at 50-60°C for > 10 min with frequent mixing until the gel slice was completely dissolved. For PCR purification directly using the PCR product, 1:1 Binding Buffer (v/v) was added and mixed thoroughly. The following steps were conducted equally for both PCR purification and Gel extraction: Up to 800 µl of the solution per spin was transferred to a GeneJET™ purification column and centrifuged for 1 min at 13,000 rpm. Multiple spins were carried out if solution volume exceeded 800 µl. The flow-through was discarded, 100 µl Binding Buffer was added and the column was spun 1 min at 13,000 rpm. The flow-through was discarded, 700 µl Wash Buffer was added and the column was spun 1 min at 13,000 rpm. The flow-through was

discarded and the empty column was spun again for 1 min at 13,000 rpm to get rid of residual ethanol from the Wash Buffer. The column was placed into a fresh 1.5 ml Eppendorf tube. 40 µl Elution Buffer was added to the centre of the purification column membrane, the column was centrifuged for 1 min at 13,000 rpm and the DNA was stored at -20°C until further use.

2.5.7 Quantification of plasmid DNA, PCR products and RNA

DNA concentration was measured with a Nanodrop spectrophotometer Table 2-5) at an absorbance of 260 nm (A_{260}), the absorption maximum for nucleic acids. Plasmid DNA was measured as double-stranded DNA (DNA-50), PCR products after bisulfite conversion were measured as single-stranded DNA (ssDNA-30). RNA was measured at A_{230} (RNA-40). The Nanodrop was blanked with TE buffer or dH_2O and 1 µl well-mixed sample was added on the pedestal. The A_x value was multiplied by the constant factor for each sample (i.e. A_{260} with factor 50 for ds-DNA) by the Nanodrop software and displayed in µg/ml. Two readings were obtained typically for each sample and their mean derived. The absorbance at 280 nm (A_{280}) was measured simultaneously to examine the level of protein contamination. The A_{260}/ A_{280} ratio of pure DNA solution should be around 1.8.

2.6 Protein purification and analysis

2.6.1 Preparation of whole cell extracts

To examine protein levels and protein expression changes extracts from whole cells were examined. Cell cultures were trypsinised and collected with 1 x phosphate-buffered saline (PBS), spun at 400 *g* for 3 minutes and washed with PBS. Whole cell extracts were re-suspended in lysis buffer (62.5 mM Tris-HCl, pH 6.8, 10% (v/v) glycerin, 2% (w/v) SDS, 1 mM phenylmethylsulfonyl fluoride, 1 µg/ml pepstatin A, 1 µg/ml leupeptin, and 5 µg/ml aprotinin) and heated at 95 °C for 20 min and collected at 10,000 rpm for 30 seconds.

2.6.2 Cell fractionation after cytochrome *c* release

To monitor the release of cytochrome *c*, cells were fractioned after treatment into cytosolic extracts and pellets by selective plasma membrane permeabilisation. This involves using a permeabilisation buffer to compromise the plasma membrane, and release the cytosolic proteins into the extra-cellular fluid. The mitochondrial proteins and any other proteins residing in other organelles are not released as the permeabilisation buffer does not affect the membranes of other organelles in the cell. The cytosolic extract contains all cytosolic proteins, while the pellet fraction contains mitochondrial, nucleic and proteins from other cellular compartments that would not have been released when the plasma membrane was compromised. Each fraction can then be analysed to examine whether the protein of interest was located in the cell. This is useful to examine the release of mitochondrial proteins into the cytosol.

The cytosolic fraction was obtained first using permeablisation buffer (20 mM HEPES pH 7.4, 10 mM KCl, 1.5 mM $MgCl_2$, 1 mM EDTA, 250 nM sucrose, 100 µg/ml digitonin) (Ward et al, 2007). The permeabilisation buffer was left on cells for 5 min, during which time the plasma membrane ruptures, releasing cytosolic proteins. These extracts were then collected without damaging the cell layer and spun down for 5 minutes at 13000 *g*. Supernatants represent the cytosolic extracts and were stored at -80°C. Lysis buffer was then added to the remaining cells, disrupting any other organelle in these cells in order to release mitochondrial and nucleic proteins. The lysate was then collected, boiled for 25 minutes at 95 °C and stored at -80°C. Lysates containing the cell pellets or cytosolic cell extracts were then quantified for protein levels and analysed using Western blotting.

2.6.3 Quantification of total protein amount in a sample

The total protein concentration of each whole cell extract, cytosolic extract or pellet extract was measured using the Pierce Micro-BCA protein assay (Table 2-3). For calibration, a standard curve ranging from 0 – 12 µg was set up using a bovine serum albumin standard. 2 µl of each sample was added to 150 µl 0.9% NaCl and 150 µl of the

ABC mixture (ABC mixture consists of reagents A, B and C at ratios of 49:49:2). Samples and standards were performed in duplicate. As a control 2 µl of SDS lysis buffer was also measured. Samples and standards were incubated at RT for 45 min and the absorbance was measured at 560 nm. The average absorbances were calculated for each sample and standard. The slope of the BSA standard curve was used to calculate the protein concentration of each sample.

2.6.4 Protein separation using SDS-PAGE

Sodium dodecyl sulphate (SDS)-polyacrylamide gel electrophoresis was carried out as described by Sambrook and Maniatis (Sambrook et al. 1989). 10 – 15% resolving gels were casted, the stacking gel was prepared afterwards on top and 10- or 15-well-combs were inserted as space holders for sample loading. Percentage of the resolving gel was decided depending on the size of the protein of interest, the smaller the protein the higher the gel percentage used. Protein samples were prepared with SDS loading buffer (100 nM TRIS-Cl pH 6.8, 4% SDS, 0.2% bromophenol blue, 20% glycerol) and denatured at 95°C for 10 minutes. An equal amount of 20 µg protein was loaded onto each lane of the SDS-polyacrylamide gels. An electric field was applied across the gel, causing the negatively-charged proteins to migrate through the gel towards the positive electrode. Gels were run at a voltage of 80 V until the proteins had migrated through the stacking gel, and then at 120 V to drive the proteins through the resolving gel. Proteins migrate through the gel depending on their size – small proteins move more easily than larger proteins through the gel, so the smaller the protein the further it migrates through the gel. Along with the protein a molecular weight ladder was also run as a means of determining sample size (Fermentas Page Ruler Plus). The running buffer was composed of 25 mM Tris-Cl, pH 8.3, 250 mM glycine and 0.1% SDS. Once the proteins had migrated through the gel the current was stopped and gels were transferred to Nitrocellulose membranes.

Table 2-15 Composition of resolving gel

per 10 ml	10%	12%	15%
Acrylamide (40%)	2.50 ml	3.00 ml	3.75 ml
Tris 1.5 M pH 8.8	3.75 ml	3.75 ml	3.75 ml
H_2O	3.75 ml	3.25 ml	2.38 ml
APS (10%)	100 µl	100 µl	100 µl
SDS (10%)	100 µl	100 µl	100 µl
TEMED	5 µl	5 µl	5 µl

Table 2-16 Composition of stacking gel

per 10 ml	
Acrylamide (40%)	1.25 ml
Tris 1.5 M pH 6.8	1.25 ml
H_2O	7.45 ml
APS (10%)	100 µl
SDS (10%)	100 µl
TEMED	5 µl

2.6.5 Western Blotting

Once the proteins had migrated sufficiently through the gel, the proteins in the gel were transferred to nitrocellulose membranes. The membranes were subsequently probed with antibodies directed against specific proteins.

Protein transfer was performed either using the iBlot® gel transfer device and the iBlot kit or manually assembled and transferred using the semi-dry transfer cell. For manual protein transfer, gels were blotted to nitrocellulose membranes in transfer buffer (25 mM Tris, 192 mM glycine, 20% methanol (v/v), and 0.01% SDS). Membranes were placed on two pieces of Whatmann paper, pre-soaked in transfer buffer and the gel was placed on top of the membrane. Two more pieces of pre-soaked Whatmann paper were placed over the gel. Transfer cassettes were assembled and gels were transferred at 18 V for 60 min. The

electric charge drives negatively charged proteins from the gel onto the positively charged nitrocellulose membrane. The proteins will form a pattern on the nitrocellulose that is identical to the pattern they created in the gel.

2.6.6 Immunoblotting and protein detection

After western blotting, the nitrocellulose membranes were blocked with 5% nonfat dry milk in TBST (15 mM Tris-HCl, pH 7.5, 200 mM NaCl, and 0.1% Tween 20) for conventional antibodies or 3% BSA in TBST for phospho-antibodies at RT for 1 hour. The blocking step helps to prevent non-specific binding of antibodies to the membrane as the proteins in the blocking solution saturate the non-specific binding sites in the membrane. Membranes were incubated with the primary antibodies overnight at 4°C on a falcon tube rotator.

Primary antibodies are raised against a specific target in animals, most commonly rabbits, mice, rats and goats. The animal is immunized with the protein of interest and produces antibodies directed against this protein. These specific antibodies can then be extracted from the blood of the animal. A wide range of such antibodies are commercially available. When the membranes are incubated with a specific antibody, the antibody will bind to the target protein on the membrane. Secondary antibodies are directed against the primary antibody and have a probe or marker by which they can be detected, for example biotin labelling or horse radish peroxidase labelling. They recognise the primary antibody and attach to them specifically.

After incubation with the primary antibody, blots were washed with TBST 3 x 5 min and developed using the enhanced chemiluminescence detection reagent (Table 2-5). Chemiluminescence was detected at 12-bit dynamic range using a Fuji LAS 4000 CCD system (Fujifilm UK Ltd., Bedfordshire, UK). The chemiluminescence reagent recognises the peroxidase label on the secondary antibody and can thus be detected. Images were analysed and processed in Adobe® Photoshop®.

To verify an even amount of protein loading, the membranes were probed against β-actin or α-tubulin, two "housekeeping genes" that are expressed at high-levels constitutively in the sample.

Table 2-17 List of antibodies used in western blot analysis

Target	Source	Dilution	kDa	Manufacturer	Catalogue number
Akt (pan)	rabbit, M	1:1000	60	Cell Signaling, Denvers, MA, USA	#4691
p-Akt (Ser 473)	rabbit, M	1:1000	60	Cell Signaling, Denvers, MA, USA	# 4060
Apaf-1	rabbit, P	1:1000	130	Chemicon, Millipore, Molsheim, F	#16941
Bak	rabbit, P	1:100	30	Santa Cruz Biotech, Heidelberg, GER	sc-832
Bax	rabbit, P	1:100	23	Upstate, Dundee, UK	# 06-499
Bcl-2	mouse, M	1:50	26	Santa Cruz Biotech, Heidelberg, GER	sc-509
Bcl-w	rabbit, M	1:1000	18	Cell Signaling, Denvers, MA, USA	# 2724
Bcl-xL	mouse, M	1:250	30	Santa Cruz Biotech, Heidelberg, GER	sc-8392
Bid, tBid	rabbit, P	1:1000	15, 22	Cell Signaling, Denvers, MA, USA	#2002
Bim	rabbit, M	1:1000	12, 15, 23	Cell Signaling, Denvers, MA, USA	# 2933
Caspase-3	rabbit, P	1:1000	17, 19, 35	Cell Signaling, Denvers, MA, USA	# 9662
Cleaved caspase-3	rabbit, P	1:1000	17, 19	Cell Signaling, Denvers, MA, USA	# 9661

Target	Source	Dilution	kDa	Manufacturer	Catalogue number
Caspase-7	rabbit, P	1:1000	20, 35	Cell Signaling, Denvers, MA, USA	# 9492
Cleaved caspase-7	rabbit, P	1:1000	20	Cell Signaling, Denvers, MA, USA	# 9491
Caspase-8	mouse, M	1:500	54, 43/41, 18	Alexis, ENZO Life Sciences, UK	ALX-804-242
Caspase-9	rabbit, P	1:1000	17, 35, 37, 47	Cell Signaling, Denvers, MA, USA	# 9502
Cleaved caspase-9	rabbit, P	1:1000	17, 37	Cell Signaling, Denvers, MA, USA	# 9501
Cytochrome-*c*	mouse, M	1:1000	15	BD Biosciences, UK	556433
DR4	rabbit, P	1:1000	57	Abcam, Cambridge, UK	ab8415
DR5	rabbit, P	1:500	56	Abcam, Cambridge, UK	ab8416
ERK1/2 (pan) (p44/42 MAPK)	rabbit, M	1:1000	42, 44	Cell Signaling, Denvers, MA, USA	#4696
p-ERK1/2 (Thr 202/ Tyr 204)	rabbit, M	1:1000	42, 44	Cell Signaling, Denvers, MA, USA	#4370
FADD	mouse, M	1:1000	25	BD Biosciences, UK	610399
cFLIP	mouse, M	1:1000	55, 25	Alexis, ENZO Life Sciences, UK	ALX-804-428
FoxO3a (pan)	rabbit, M	1:1000	78, 82-96	Cell Signaling, Denvers, MA, USA	#2497
p-FoxO3a	rabbit, P	1:1000	78, 82-96	Cell Signaling, Denvers, MA, USA	#9464

Target	Source	Dilution	kDa	Manufacturer	Catalogue number
c-Jun (pan)	rabbit, M	1:1000	43, 48	Cell Signaling, Denvers, MA, USA	#9165
p-c-Jun	rabbit, M	1:1000	43, 48	Cell Signaling, Denvers, MA, USA	#3270
Mcl-1	mouse, M	1:1000	40	BD Biosciences, UK	559027
Noxa	mouse, M	1:1000	11	Abcam, Cambridge, UK	ab13654
PARP	rabbit, P	1:1000	24, 89, 116	Cell Signaling, Denvers, MA, USA	#9542
Cleaved PARP	rabbit, P	1:1000	89	Cell Signaling, Denvers, MA, USA	#9541
p53	rabbit, P	1:100	53	Santa Cruz Biotech, Heidelberg, GER	sc-6243
PUMA	rabbit, P	1:1000	23	ProSci Incorporated, CA, USA	#3041
Smac/ Diablo	mouse, M	1:1000	20	Cell Signaling, Denvers, MA, USA	#2954
XIAP	mouse, M	1:1000	55/54	BD Biosciences, UK	610763
β-Actin	mouse, M	1:5000	42	Sigma-Aldrich, Arklow, Ireland	A5441
α-Tubulin	mouse, M	1:5000	55	Sigma-Aldrich, Arklow, Ireland	T9026
Mouse-IgG	goat, P	1:5000		Millipore, Molsheim, F	AP124
Rabbit-IgG	goat, P	1:5000		Millipore, Molsheim, F	AP132P

M = monoclonal; P = polyclonal; p- = phospho; pan = total protein

2.6.7 Quantitative western blotting and densitometry analysis

For quantitative Western blotting, standard curves from HeLa cell extracts (5 – 20 µg) were run concurrently with the glioma cell line and patient lysates (20 µg) to ensure linearity of the signal detection range. The protein concentrations of the protein of interest within each glioma cell line and individual GBM patient sample were determined by comparison to signals from HeLa cell extracts, which served as controls. Digital densitometry was used to evaluate the protein levels from the images generated of the Western blots. The intensity of each band was calculated using the open source Image J software (http://rsbweb.nih.gov/ij) and Microsoft Exel. The background in each lane was substracted from the intensity of the protein bands. The intensity of the loading control (β-actin) is then deducted from the intensity of the band of interest to eliminate any differences in protein levels owing to uneven loading, so that each sample is normalized and can be compared. Protein levels are expressed as percentage of HeLa protein expression levels (set to 100 %).

2.7 Cell treatments and apoptosis induction

2.7.1 Transfection with calcium phosphate

In order to overexpress dominant-negative or constitutive-active versions of FoxO3a, foreign plasmid DNA was introduced into the cells via transfection. Calcium phosphate transfection (Table 2-3) is a chemical method to deliver the plasmid DNA into the host cell by forming transient pores in the cell membrane. Calcium phosphate faciliates the binding of DNA to the cell surface. DNA then enters the cell by endocytosis. Prior to carrying out experiments with transiently transfected cells, transfection optimization was carried out for each cell line. This optimization involved using calcium phosphate at different concentrations, combined with different concentrations of the plasmid in question. The condition that achieved the most efficient transfection result with the least cytotoxicity was then chosen for each cell type.

Cells were seeded 24 hours prior to transfection at a density according to Table 2-7 into 6-well and 24-well plates and incubated in a humidified CO_2 incubator at 37°C overnight. 3-4 hours before transfection, the media was exchanged and additional 3 ml media were added. For transfection of a 6-well-plate, each well containing 5 ml of media, 18 µl $CaCl_2$ (2 M) and 10 µg DNA were added to tube A and filled with sterile H_2O to a total volume of 150 µl per well. 150 µl of the phosphate buffer 2x HEPES Buffered Saline (HBS; 50 mM HEPES, 1.5 mM Na2HPO4, 280 mM NaCl, pH 7.1) were added to tube B. Solution A was then added dropwise to solution B with a pasteur pipette, while bubbling air through solution B with another pipette. A fine precipitate formed. This is important, because clumped DNA will not adhere to or enter the cell as efficiently. The mixture was incubated for 30 min RT. The precipitate was added dropwise to the media and cells were incubated overnight at 37°C in a humidified CO_2 incubator. The next day, the transfection mixture was removed from the cells and cell treatment was performed.

Table 2-18 Plasmids used in this thesis

Plasmid	Insert	Vector backbone	Bacterial resistance	Reference
HA-FoxO3a-TM (Addgene * plasmid #1788)	FoxO3a with triple mutated phosphorylation site	pECE	Amp^R	(Brunet et al. 1999)
HA-FoxO3a-DDB (Addgene * plasmid #8354)	FoxO3a lacking the DNA-binding site	pECE	Amp^R	(Brunet et al. 1999)
pECE (Addgene * plasmid #26453)	empty backbone vector	pECE	Amp^R	(Brunet et al. 1999)

* http://www.addgene.org; Michael Greenberg Lab plasmids

2.7.2 Treatment of cells with the standard therapy used clinically for the treatment of gliomas, temozolomide

Temozolomide (TMZ) is a DNA-alkylating agent that induces the intrinsic apoptotic pathway (Table 2-19) (Roos et al. 2007). A stock concentration of 0.5 M of TMZ in sterile DMSO was diluted into a working stock concentration of 75 mM. From the working stock concentrations, 2 µl of TMZ was added to 1 ml media to give a final concentration of 150 µM TMZ. Treatments were added to cells and DMSO was added as a control.

2.7.3 Induction of the intrinsic apoptotic pathway with staurosporine

Staurosporine (STS) is a kinase inhibitor that induces the intrinsic apoptotic pathway (Table 2-19) (Krohn et al. 1998). Staurosporine (Sigma) was diluted from the stock concentration of 10 mM in sterile DMSO to a working stock concentration of 10 µM. From the working stock concentrations, 100 µl of STS was added to 1 ml media to give a final concentration of 1 µM STS. Treatments were added to cells and DMSO was added as a control.

2.7.4 Activation of the extrinsic apoptotic pathway with TRAIL

Tumour necrosis factor-related apoptosis-inducing ligand (TRAIL) is a death receptor ligand that binds to human TRAIL receptor 1 (DR4) and TRAIL-R2 (DR5), leading to the induction of the extrinsic apoptotic pathway (Table 2-19) (Shah et al. 2005; Jaganathan et al. 2002). *Killer*TRAIL was diluted from the stock concentration of 0.5 M in sterile dH_20 to a working stock concentration of 20 µg/ml. From the working stock concentrations, 5 µl of TRAIL was added to 1 ml media to give a final concentration of 100 ng/ml TRAIL. Treatments were added to cells. In case of TRAIL treatment compared to TMZ treatment or treatment with TMZ and TRAIL combined, DMSO was added as a control.

2.7.5 Combination therapy with temozolomide and TRAIL

TMZ and TRAIL were prepared as described above from stock concentrations to working stock concentrations of TMZ in sterile DMSO and TRAIL in sterile dH_2O and added simultaneously to the cells at final concentration of TMZ (150 μM) and TRAIL (100 ng/ml) (TT). DMSO was added as a control.

2.7.6 Caspase- inhibition with zVAD

In order to analyse whether the cell death evident was caspase dependent, the pan caspase inhibitor Benzyloxycarbonyl-Val-Ala-Asp(*O*-methyl) fluoromethylketone (zVAD) (Table 2-19) was added as an additional control to experiments (Li et al. 1997). zVAD binds to the active site of cleaved caspases, thereby inhibiting them. zVAD was diluted from the stock concentration of 250 mM in sterile DMSO to a working stock concentration of 50 mM. From the working stock concentrations 1 μl zVAD was added to 1 ml media to give a final concentration of 50 μM zVAD. This was added to cells 1 hour prior to treatment.

2.7.7 Inhibition of PI3-K/ERK1/2 survival signalling

The ERK inhibitor PD98059 (Table 2-19) was used to analyse the role of survival signalling pathways in the regulation of Bim expression during TT treatment (Pang et al. 1995). PD98059 acts as a specific inhibitor to ERK1 and ERK2 enzymes at a concentration of 4 μM and 50 μM, respectively. For our experiments, a concentration of 15 μg/ml (~ 18 μM) was found to be most effective. A dilution from the stock concentration of 5 mg/ml in DMSO was prepared in dark and added 1 hour prior to the treatment to the cells.

2.7.8 c-Jun inactivation through JNK-inhibition

The ATP-competitive JNK inhibitor II (Table 2-19) was used to analyse the role of the transcription factor c-Jun in Bim regulation during treatment with TT (Ohba et al. 2009). Inhibition of c-Jun N-terminal protein kinase (JNK) inhibits c-Jun phosphorylation and c-Jun transcription. For our experiments, a final concentration of 5 µM was found to be effective. A dilution from the stock concentration of 50 mM in DMSO was prepared in dark and added 1 hour prior to the treatment to the cells.

Table 2-19 Summary of drugs and inhibitors

Reagent	stock conc	final conc	Manufacturer
JNK Inhibitor II	50 mM	5 µM	Calbiochem/ Merck Biosciences, Nottingham, UK
*Killer*TRAIL	0.5 M	100 ng/ml	Alexis, Alpha technologies
PD 98059 (ERK inhibitor)	5 mg/ml	15 µg/ml	Calbiochem/ Merck Biosciences, Nottingham, UK
Staurosporine	10 mM	1 µM, 3 µM	Alexis, Alpha technologies
Temozolomide	0.5 M	150 µM	Sigma-Aldrich, Arklow, Ireland
zVAD	250 mM	50 µM	Bachem, St. Helens, UK

2.8 Analysis of apoptosis

2.8.1 Cell viability (MTT) assay

Cell viability was assessed using the colorimetric MTT assay (Sylvester 2011). Glioma cells were seeded at 500 to 2,000 cells per well in 96-well, flat-bottomed plates, using wells per cell line and treatment, and cultured overnight at 37°C in a humidified CO_2-incubator. Cells were treated with drugs at the indicated timepoints and assessed for viability as follows: All media was removed and 150 µl of 3-(4,5-dimethylthiazol-2-yl)-2,5-diphenyltetrazoliumbromide (MTT) compound (yellow) in media (5 mg/ 10 ml media) was added to each well. Plates were incubated at 37°C in darkness for 4 hours, all liquid was

removed from the wells and 100 µl DMSO was added. MTT is reduced into formazan (purple) in metabolic active cells. Absorbance was measured by spectrophotometry at 540 nm with a plate reader (TECAN Reader), and cell viability was determined by calculating relative changes of absorbance compared to the DMSO control, which was set to 100% viability.

2.8.2 Microscopy and Hoechst staining of apoptotic cells

Condensed nuclei are a hallmark of apoptosis (Kerr et al. 1972). Cells were stained for 20 min with the dye Hoechst 33258 at a final concentration of 1µg/ml. Changes in nuclear morphology were detected by fluorescence microscopy using a filter for Hoechst 33258. Normal bright field images were taken to examine morphological changes such as cell shrinkage and membrane blebbing.

2.8.3 Flow cytometric analysis of apoptosis

Flow cytometry is a technique for counting cells or other subcellular organelle. It uses the principle of light scattering to generate data from various samples. The samples are passed through a laser path, and as they pass through they intercept the light source. This scatters the light and fluorochromes are excited to a higher energy state. This energy is released as a photon of light, which can be recorded. Flow cytometry was performed on a Partec Cyflow ML16 flow cytometer (Partec, Münster, Germany) equipped with a 488 nm argon ion laser. 10,000 gated events were acquired for each sample.

Cells were cultivated in 24-well culture dishes for flow cytometry analysis at densities outlined in Table 2-7. After certain time points cells were harvested at 400 *g* and washed in PBS. For cell death analysis, cells were incubated in 200 µl binding buffer (10 mM HEPES, 135 mM NaCl, 5 mM $CaCl_2$) containing Annexin-V FITC conjugate (5 µl/ml) (BioVision, Mountain View, CA, USA) and propidium iodide (PI) (2 µg/ml) at 37°C for 15 minutes. In apoptotic cells, the membrane phospholipid, phosphatidylserine, is translocated

from the inner surface of the plasma membrane to the outer surface where it is exposed. Annexin V is a Ca2+ dependent phospholipid-binding protein that has a high affinity for phosphatidylserine, and so the Annexin V binds to the phosphatidylserine that is exposed on apoptotic cells (Martin et al. 1995). Annexin V may be conjugated to a fluorochrome, such as FITC so that its levels can then be detected. Staining with FITC Annexin V is usually used in conjunction with propidium iodide (PI). Viable cells with intact membranes exclude PI, whereas the membranes of dead cells are permeable to PI. Staining with Annexin V and PI allows identification of early apoptotic cells - these cells would be PI negative, Annexin V positive. Necrotic cells would be PI positive, Annexin V positive, and healthy cells should be PI negative, Annexin V negative. Following incubation with Annexin V/PI cells were re-suspended in ice-cold binding buffer and analysed. According to gated regions, set up using controls (untreated cells, treated cells without staining, treated cells stained with Annexin V alone, treated cells stained with PI alone), levels of early apoptotic, apoptotic, necrotic or healthy cells could be identified Annexin V, an anticoagulant, is used to detect and measure apoptosis by binding to phosphatidylserine (PS) residues of apoptotic cells. PS are normally hidden within the plasma membrane and usually appear on the cell surface during apoptosis as one of the specific signals for recognition and removal of apoptotic cells by macrophages. As the apoptotic process progresses, cell membrane integrity is lost. The DNA specific viability dyes Propidium Iodide (PI) is used to distinguish between early apoptotic, late apoptotic, and dead cells. After apoptosis induction, cells were collected with trypsin-EDTA and incubated in 200 µl binding buffer (10 mM HEPES, 135 mM NaCl, and 5 mM $CaCl_2$) containing Annexin-V FITC conjugated (5 µl/ml) and PI (5µl/ml) for 10 min on ice. Additional 800 µl ice-cold binding buffer was added before measurement. Cells were subsequently analyzed on a flow cytometer. Annexin-V was excited with the 488 nm laser, and fluorescence emission was collected in the FL1 channel through a band-pass filter at 515 to 555 nm. PI was excited with the 488 nm laser and fluorescence was collected in the FL3 channel through a bandpass filter at 620 nm.

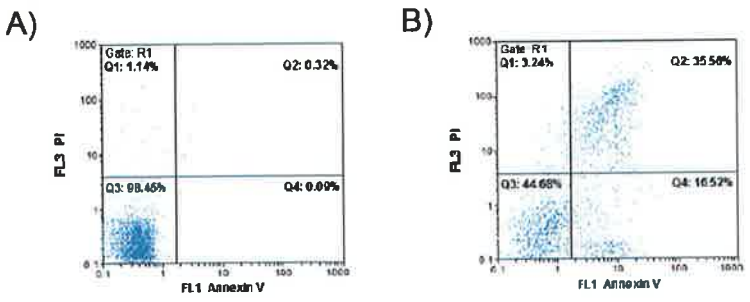

Figure 2-1 Flow cytometry gated regions

Annexin V and PI- positive cells were gated for in experiments examining apoptosis. The left upper quadrant represents PI- positive cells, while the right lower quadrant represents Annexin V- positive cells.

Data acquisition and analysis were performed using FlowMax software (Partec).

2.8.4 Determination of caspase-3-like protease activity

DEVDase activity was determined fluorometrically using N-benzyloxylcarbonyl-Asp-Glu-Val-Asp-7-amino-4-methyl-coumarin (DEVD-AMC) as the substrate (10 μM). Cleavage of DEVD-AMC to liberate free AMC was monitored in live cells by measuring fluorescence after treatment at 1- and 2-hour intervals. Protein content was determined using the Pierce Coomassie Plus protein assay reagent. Caspase activity was expressed as change in fluorescent units per hour and per microgram of protein.

2.9 Statistics

2.9.1 Statistical analysis

Data are given as mean ± S.E.M. For statistical comparison Student's t test for normal distributed data or Mann-Whitney U test for non-normal distributed data was used. P values

smaller than 0.05 were considered to be statistically significant. Data were analyzed and graphed using Microsoft Exel (Microsoft, Redmond, WA) and a trial version of GraphPad Prism 5 (GraphPad Software, Inc, La Jolla, USA).

2.9.2 Principal Component Analysis

In order to identify a pattern in the molecular expression profiles of glioma cell lines and glioblastoma patient samples, we utilised a comprehensive statistical method called Principal Component Analysis (PCA) (Han 2010). The PCA is a multivariate dimension reduction technique commonly used for pattern recognition analysis to discover molecular signatures in cancers (Brennan et al. 2009; Ringnér 2008; Han 2010). In this study, the influence of interrelated apoptotic proteins on the sensitivity to apoptosis-inducing treatments in glioma cell lines or the influence on progression-free survival time in GBM patients was analysed by identifying major components with the highest influence and revealing minor components with little influence on treatment sensitivity or survival time. A component represents a reduced number of original statistical samples, i.e. represents a fraction of the original variations in the protein expression levels of single proteins in the data set (glioma cell lines or GBM patient samples) The influence of each component is assessed by calculating the explained variance, thus indicating how well the component represents the original data set. The exclusion of minor components results in a representation of the original data set with reduced dimensions and reduced noise. Major components display those proteins that vary the most in their expression within the data set, thus revealing patterns in the data set. To avoid excluding too many components, the cumulative explained variance is assessed. The higher the cumulative explained variance of the remaining major components, the better the quality of the PCA in representing the original data set. Preferably, the PCA results in two or three major components that cumulate to 70 or more percent of explained variance, enabling an easy graphical representation of the original data set where each component is visualized as an axis.

$$component = c_1 * protein_1 + c_2 * protein_2 + ... + c_n * protein_n$$ **Equation 1**

As shown in equation 1, a component is calculated as a linear combination of the given proteins where the coefficients (c_n) show the impact of each protein to the component. A high absolute value of a coefficient shows that the according protein concentration has a high impact on the coordinates of the data point in the plot. Assigning properties of the samples, such as sensitivity to apoptosis inducing treatment, to the data points in the plot, might reveal a pattern of data clustering.

The PCAs were performed using a trial version of Minitab® 16.2.1 (Minitab, Inc, State College, Pennsylvania, USA).The specificity and sensitivity of a PCA was analysed using a two-tailed Fisher's exact test, p values at ≤ 0.05 were considered as significant.

2.10 Systems modelling

2.10.1 APOPTO CELL

In order to predict the likelihood of glioma cells (both glioma cell lines or GBM patient samples) to undergo apoptosis, we utilised a previously published model system called APOPTO CELL (Rehm et al. 2006; Huber et al. 2007; Hector et al. 2011) (http://systemsbiology.rcsi.ie/apopto-cell.html). APOPTO CELL is a computational model designed to simulate the late steps of the intrinsic apoptotic pathway, the apoptosome-dependent effector caspase activation of capsae-3 and -7 and the subsequent substrate cleavage. The model is based on a set of ordinary differential equations representing a reaction network of 53 reactions, 19 reaction partners and 75 reaction parameters and is implemented in MATLAB. APOPTO CELL was developed in HeLa cells and validated *in cellulo* and by adapting the model to cancer cell lines deficient in apoptosis signalling proteins (Rehm et al. 2006; O'Connor et al. 2008). The reaction network is initiated by cytochrome *c*-dependent apoptosome formation and mitochondrial Smac release while substrate cleavage by effector caspases is the model output (Huber et al, 2007). To generate substrate cleavage profiles for the glioblastoma cell lines and GBM patient samples, protein expression values for procaspases-9 and -3, XIAP, Smac, and Apaf-1, were calculated for

each individual patient sample and cell line in relation to concentrations as measured in HeLa cells (Rehm et al. 2006, supplementary material; Table 20). These absolute protein values served as input for APOPTO-CELL. The output displays substrate cleavage by caspase-3 and -7 after the release of cytochrome *c*. Varied substrate cleavage profiles were predicted at 60 min after the release of cytochrome *c*, ranging from <1% to 100%. Apoptosis susceptibility in GBM tumour resections and glioblastoma cell lines was defined as the ability to efficiently generate >80% substrate cleavage within this 60 min timeframe. A >80% substrate cleavage was chosen as it has previously been determined that this % enables apoptosis to proceed efficiently (Rehm et al. 2006). Drug sensitivity can be interpreted as the ability to perform substrate cleavage by caspase-3 or caspase-7 after the release of cytochrome *c*.

Table 2-20 HeLa protein concentrations for APOPTO CELL modelling

Protein	Initial concentration [μM]	References
Apaf-1	0.372	(Rehm et al. 2006; supplementary information 2)
Cytochrome *c*	10	(Waterhouse et al. 2001)
Procaspase-9	0.03	(Rehm et al. 2006; supplementary information 2)
Procaspase-3	0.12	(Rehm et al. 2006; supplementary information 2)
XIAP	0.063	(Rehm et al. 2006; supplementary information 2)
Smac	0.126	Estimated to be twice the XIAP conc. (Rehm et al. 2006; supplementary information 2)

3 Heterogeneous protein expression pattern within mitochondrial apoptotic pathway correlate with drug sensitivity in glioblastoma multiforme

3.1 Introduction

Glioblastoma multiforme (GBM) is characterized by histopathological and molecular heterogeneity (Bonavia et al. 2011). The broad category malignant glioma collectively refers to glioblastomas (WHO grade IV) and anaplastic gliomas (astrocytomas, oligoastocytomas, oligodendrogliomas) (WHO grade III) (Louis et al. 2007). Standard treatment includes surgical resection, followed by radiation and adjuvant chemotherapy, mainly with the cytotoxic drug temozolomide (TMZ) (Sarkaria et al. 2008). Although the prognosis remains poor and treatments are largely palliative, there are subsets of patients that show prolonged survival (Kraus et al. 2001; Krex et al. 2007; Das et al. 2011). However, the molecular mechanisms that determine short-term or long-term survival in GBM patients are largely unknown (Kraus et al. 2001).

The term progression-free survival (PFS) is often used to classify treatment success in GBM patients (Fallowfield & Fleissig 2011). It describes the length of time during and after treatment in which a patient is living with a disease that does not get worse. PFS can be used as predictor of overall survival (OS) (Halabi et al. 2009). PFS is often favoured as a measure in situations whereby a cure does not exist and it is intended to control the tumour (Halabi et al. 2009).

DNA damage caused by alkylating agents such as TMZ can be repaired by the DNA repair enzyme O^6-methylguanine-DNA methyltransferase (MGMT)) (Lindahl et al. 1982). Decreased activity of MGMT is associated with a favourable patient prognosis in some, but not all studies (Hegi et al. 2005; Costa et al. 2010).

Both radiotherapy and chemotherapy with most cytotoxic agents, including TMZ, mainly exert their antitumour effect by reactivating apoptosis, most commonly by the intrinsic or mitochondrial apoptotic pathway (Roos et al. 2007) (for details, see general introduction). The formation of the apoptosome, consisting of Apaf-1, procaspase-9 and cytochrome *c*, initiates the final step of apoptotic signalling, the activation of the caspase

cascade, leading to caspase-3- and -7 mediated cleavage of cellular proteins such as the poly (ADP-ribose) polymerase PARP and cell death (Li et al. 1997). Caspase activation can be inhibited by XIAP, which itself underlies the control of aberrant Smac in the cytosol after its release from the mitochondria (Rudy et al. 2008). The evasion of apoptosis is a typical hallmark of cancer and is often conferred by the up- or downregulation of pro- or anti-apoptotic proteins (Hanahan & Weinberg 2000). Therefore, the expression of these apoptotic proteins may be used as markers to predict therapy response and to establish a prognosis for cancer patients (Zlobec et al. 2006; Hector et al. 2011). For example, downregulation of pro-apoptotic Apaf-1 resulting from methylation silencing in acute leukemia has been implicated in chemoresistance and disease progression (Furukawa et al. 2005). Transcriptional downregulation of caspase-9 is a common event in colorectal cancer stage II patients (Shen et al. 2010). In non-Hodgkin's lymphoma, the inhibition of the apoptosis cascade downstream of Apaf-1 and caspase-9 is an important cause of therapy resistance (Cillessen et al. 2007). Overexpression of the caspase-inhibitor XIAP in renal cell carcinoma predicted a worse prognosis (Mizutani et al. 2007). Low caspase-3 levels have been associated with poor patients prognosis in Burkitt's lymphoma (Tirapelli et al. 2010; Nomura et al. 2008). In most glioblastoma low caspase-3 expression is common, however, systematic analyses examining how complex alterations between critical mediators of the intrinsic mitochondrial pathway may impact on the ability of glioblastomas to successfully evade death signalling pathways have rarely been performed.

3.1.1 Aims of this chapter

The aim of this study was to investigate whether the molecular expression profiles of key apoptotic proteins in the intrinsic mitochondrial pathway, namely Apaf-1, procaspase-9, procaspase-3, Smac and XIAP could be utilized to determine chemotherapeutic sensitivity in glioma cell lines and to predict outcome for patients with glioblastoma multiforme (GBM). We initially used a preclinical model of glioma cell lines and compared our findings within a more clinical setting, using a cohort of 17 GBM patient

resected tumour samples that originated from both long-term and short-term progression-free survivors (PFS).

Our first objective was to establish protein expression profiles of apoptotic proteins in the cell lines and patient samples. Our second objective was to correlate these profiles to treatment responses to temozolomide (TMZ) and progression-free survival times using two different statistical approaches: single protein expression analysis and a multivariate statistical method, the Principal Component Analysis (PCA) that combines all protein expression profiles while also highlighting differences in the expression levels of pro- and anti-apoptotic proteins. Our third aim was to utilise a systems medicine approach to predict both chemotherapeutic sensitivity of the cell lines and patient PFS times based on the simulated interaction of these critical players in the intrinsic mitochondrial pathways of apoptosis using the APOPTO CELL model.

3.2 Results

3.2.1 Heterogeneous response of glioma cell lines to standard chemotherapeutic therapy with temozolomide

Intrinsic or aquired resistance of cancer cells to standard therapies is the major cause of treatment failure (Cillessen et al. 2007). The current state-of-the-art chemotherapeutic for patients with glioblastomas is the DNA-alkylating drug temozolomide (TMZ) (Roos et al. 2007). To analyse chemotherapeutic sensitivity to TMZ in glioblastomas, we utilized a panel of 11 glioma cell lines, derived from patients suffering from grade III/IV tumours (Chapter 2; Table 2-6). TMZ was applied at a clinically relevant dose of 150 μM for 24, 48, 72, 96 and 120 hours (Agarwala & Kirkwood 2000). Cell viability was measured using the MTT cell viability assay at the indicated time points (Figure 3-1) (Sylvester 2011). We found that the current standard of care only shows effectiveness in five out of 11 glioma cell lines: Cell lines MZ18, MZ51, MZ256, MZ294, MZ304 and MZ327 were completely resistant to TMZ treatment and showed constant cell

survival rates above 50% (Figure 3-1 A). These cell lines were referred to as resistant or tolerant to the treatment (Cluster 1; Figure 3-1 A). The second group of cells, U87, U251, U343, U373 and A172 (Figure 3-1 B) showed significantly reduced cell viability below 50% after 72 hours to 120 hours TMZ treatment compared to control cells at 0 hours ($p \leq 0.05$ in Student's t test). These sensitive cell lines were grouped into cluster 2 (Figure 3-1 B). Thus, within the panel of glioma cell lines we identified two clearly distingushable TMZ responder groups.

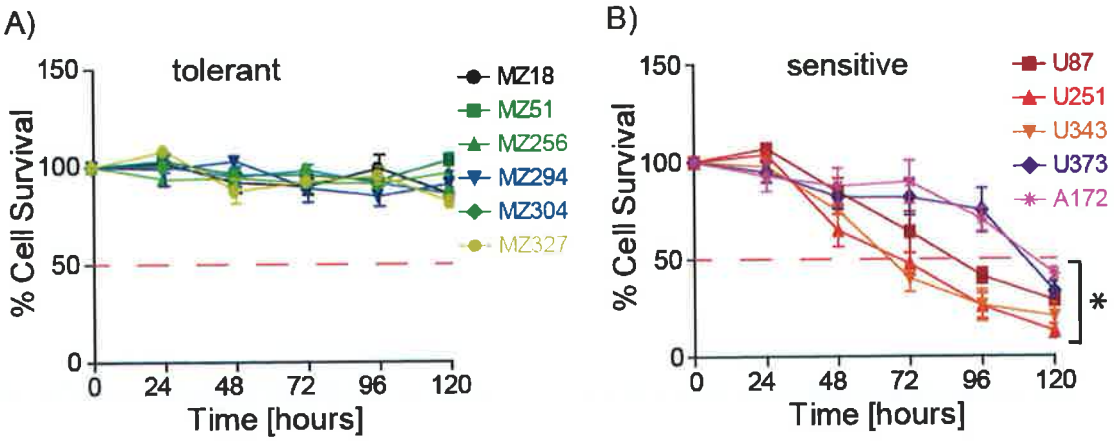

Figure 3-1 Heterogeneous drug response to TMZ in glioma cell lines

Assessment of cell survival during 120 hours TMZ treatment in 11 glioma cell lines. MTT assay following TMZ treatment (150 µM) for 24, 48, 72, 96 and 120 h. Red dashed lines indicate 50% cell survival. **A)** Cell lines MZ18, MZ51, MZ256, MZ294, MZ304 and MZ327 (tolerant/ cluster 1) did not show a decrease in cell number, **B)** Cell lines U87, U251, U343, U373 and A172 displayed < 50% cell survival rate after 72 h to 120 h treatment (sensitive/ cluster 2). Data points are means ± S.E.M of three independent experiments in sextuplicates (n=18); * indicates $p \leq 0.05$ between 0 and 120 h, Student's t test.

3.2.2 O^6-methylguanine DNA methyltransferase (MGMT) promoter methylation does not correlate with chemotherapeutic resistance to TMZ

We next analysed a possible molecular basis for the observed TMZ-drug resistance in our glioma cell lines by examining the activity of the DNA-repair enzyme O^6-methylguanine-DNA methyltransferase (MGMT) (Lindahl et al. 1982). MGMT can directly counteract the DNA-alkylating effect of TMZ (Brennand & Margison 1986; Bernd Kaina et al. 2007). The methylation status of the *MGMT* promoter may be associated with chemosensitivity to TMZ and patient outcome (Hegi et al. 2005; Hassel et al. 2010; Weller et al. 2010).

To assess whether MGMT expression and TMZ-resistance correlated in our cell lines, we analysed the methylation status of the *MGMT* promoter by direct Bisulfite Genomic Sequencing (Frommer et al. 1992; Park & Chapman 1994). The TMZ-sensitive cell line U251 and the TMZ-resistant cell line MZ294 were chosen as representatives. A 382 bp long DNA fragment of the *MGMT* promoter, from -202 bp to +180 bp relative to the transcription start site, was selected for methylation analysis (Figure 3-2). This region includes both a part of the promoter and the entire sequence of the first untranslated exon (Quian & Brent 1997). The selection represents a fraction of a previously described 508 bp fragment chosen to demonstrate the correlation between *MGMT* gene silencing and CpG methylation in this CpG island (Quian & Brent 1997). Shown in Figure 3-2 is the original *genomic* DNA sequence (labelled "g" for "*genomic*"; upper lane) compared to a computer generated sequence of a bisulfite conversion reaction of completely methylated DNA (labelled "B" for "Bisulfite"; lower lane). The positions of the Bisulfite genomic sequencing specific Primers (BSP) are indicated in red and orange. The methylation status of 47 CpG dinucleotides was analysed (green boxes) (Figures 3-2 and 3-3 B). The PCR amplification with Bisulfite genomic sequencing specific Primers (BSP) yielded products of the correct size ~400 bp (Figure 3-3 A). The samples were sequenced and approved for quality.

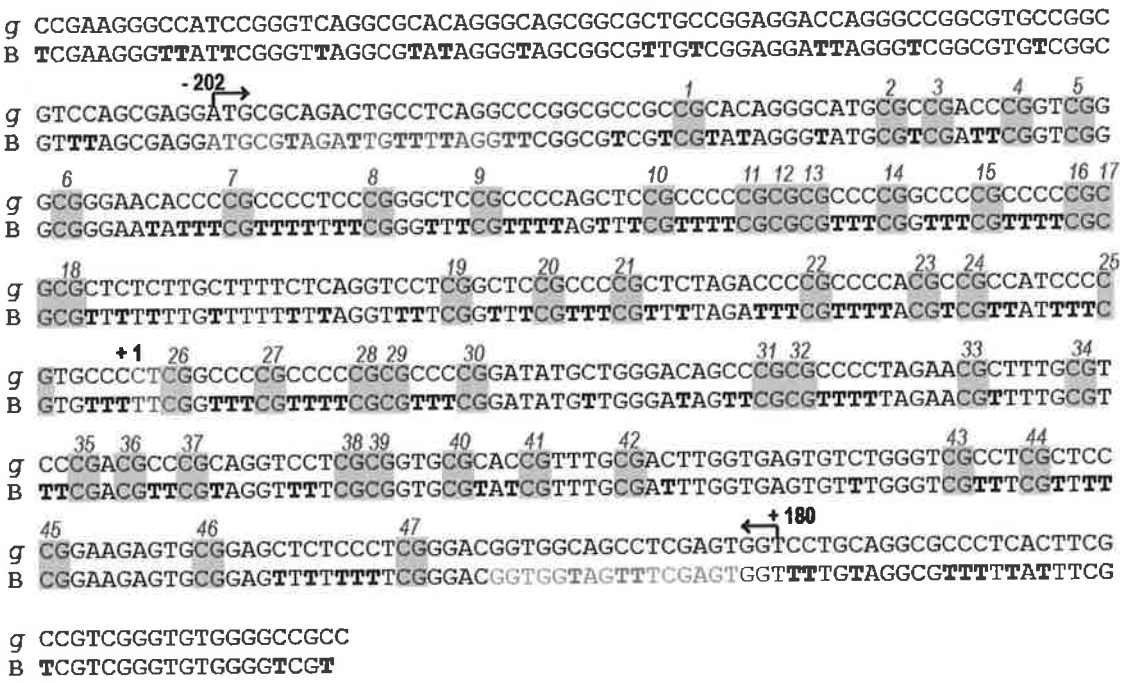

Figure 3-2 O^6-methylguanine DNA methyltransferase promoter fragment as chosen for methylation analysis

DNA sequence of a 382 bp fragment within the promoter region of *MGMT* -202 bp till +180 bp after start site of transcription (+1). 47 CpG dinucleotides were analysed for methylation. "g" genomic DNA; "B" Bisulfite converted methylated genomic DNA; bold = tyrosines resulting from cytosine conversion; green box = CpG dinucleotides; red = Bisulfite genomic Sequencing specific Primer (BSP) forward; orange = Bisulfite genomic Sequencing specific Primer (BSP) reverse.

The conversion ratio of all samples was ≥ 97%, which is considered a successful bisulfite reaction. TMZ-resistant cell line MZ294 and TMZ-sensitive cell line U251 displayed similar levels of *MGMT* promoter methylation, both below 50% (Table 3-1). The negative control represents an unmethylated *MGMT* promoter (0% methylation) that would result in full MGMT protein expression, which is correlated with TMZ resistance ("tolerant"). The positive control illustrates downregulation of MGMT expression through 100% *MGMT* promoter methylation, which is associated with TMZ-sensitivity ("sensitive").

Table 3-1 Analysis of MGMT promoter methylation

Cell line	% Methylation*		% Cell survival TMZ 120 h**		Correlation to TMZ sensitivity
MZ294	34.45	±16.16	91.21	±6.35	no
U251	49.45	±17.96	13.1	±3.51	yes
Neg Ctrl	0.0	±0	"tolerant"		-
Pos Ctrl	100	±0	"sensitive"		-

*mean of forward and reverse sequencing; ± SEM

** mean of three MTT assays in triplicate; ± SEM (see Figure 3-1)

Neg Ctrl = unmethylated converted DNA

Pos Ctrl = methylated converted DNA

The levels of *MGMT* Promoter methylation found in the cell line U251 could lead to a downregulation of MGMT protein levels, which correlates with TMZ-sensitivity in this cell line (Tang et al. 2011). However, levels of promoter methylation found in the MZ294 cell line were almost equally as high, therefore also indicating MGMT promoter silencing, an effect that did not correlate with the observed TMZ-resistance in MZ294 cells. Thus, these results show that the methylation status of the *MGMT* promoter is not a good predictor of TMZ treatment response in this panel of glioma cell lines and also highlighted that other resistance mechanisms might be at work.

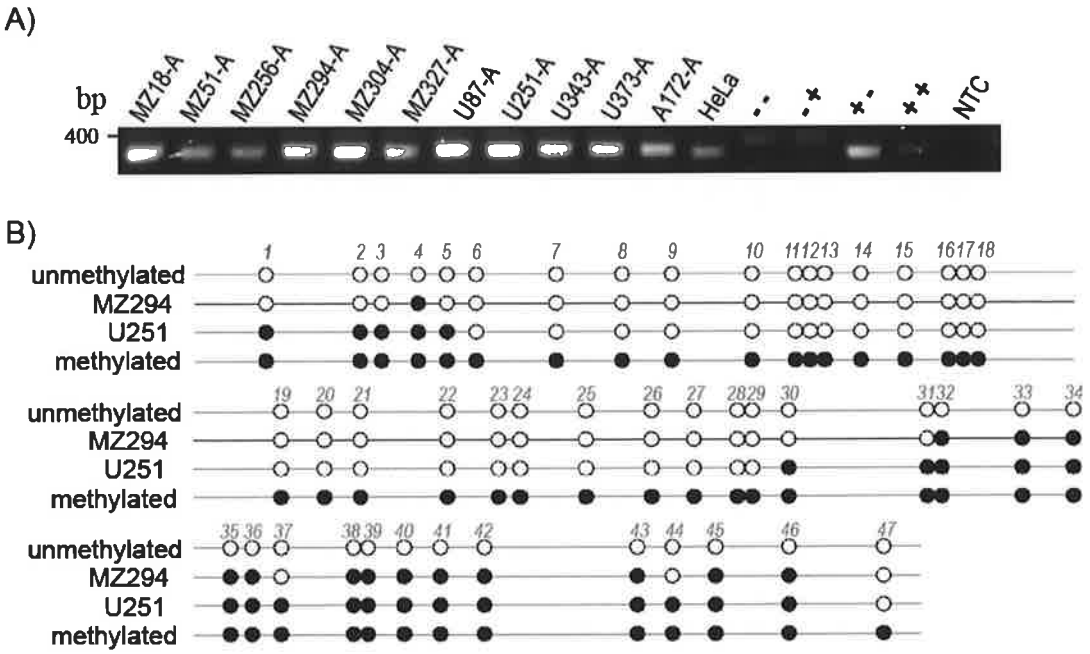

Figure 3-3 MGMT promoter methylation analysis in glioma cell lines

A) Representative DNA gel electrophoresis after Bisulfite conversion specific PCR. Amplification of biological triplicates. Controls "- -" unconverted unmethylated DNA; "-+" unconverted methylated DNA; "+-" converted unmethylated DNA; "++" converted methylated DNA; "NTC" no template control. **B)** Methylation analysis after sequencing. "Lollipop" scheme of CpG dinucleotide methylation. From top to bottom: negative control amplicon (unmethylated converted DNA), MZ294 amplicon, U251 amplicon and positive control amplicon (methylated converted DNA). White circles represent unmethylated CpG dinucleotides, black circles represent methylated CpG dinucleotides. MZ294 and U251 display similar methylation patterns.

3.2.3 Drug-sensitive glioma cell lines undergo caspase-dependent apoptosis after temozolomide treatment

The DNA damage caused by the DNA-alkylating agent TMZ can induce the intrinsic apoptotic pathway in glioma cells (Roos et al. 2007). Thus, we analysed whether the decrease in cell numbers in the TMZ-sensitive cluster 2 of cells was also associated with apoptosis within these cells. We performed Hoechst staining and monitored caspase-3 activity on Western Blots after TMZ (150 μM) treatment for 72 hours (Figure 3-4). The loss of viability in the cluster of TMZ-sensitive cell lines after treatment, represented here by the cell lines U251 and U343, was associated with the occurrence of condensed nuclei, shown as bright dots after staining with Hoechst 33258 (Figure 3-4 A & B). Other morphological changes characteristic of apoptosis, such as cell shrinkage, were visible in bright field images. Quantitative assessment of Hoechst- positive cells showed significantly elevated numbers of apoptotic cells in U251 and U343 cell lines (Figure 3-4 B). In contrast, only low levels of apoptotic cells were found in the TMZ-resistant cell lines MZ294 and MZ304 (Figure 3-4 A & B). Western Blot analysis identified increased levels of cleaved forms of caspase-3 (17 and 19 kDa) in sensitive cell lines U251 and U343, indicating caspase-3 activation (Figure 3-4 C). Subsequently, we found the fragmented form of PARP (f-PARP; 89 kDa), a direct caspase-3- substrate, after TMZ treatment, only in the drug-sensitive cell lines. Resistant cell lines MZ294 and MZ304 both did not show procaspase-3 activation or PARP fragmentation (Figure 3-4 C).

In conclusion, the observed decrease in cell numbers in sensitive cell lines following treatment with the alkylating agent TMZ (Figure 3-1) was associated with caspase-dependent apoptosis, whereas the TMZ-resistant cell lines did not show any signs of caspase activation and apoptosis.

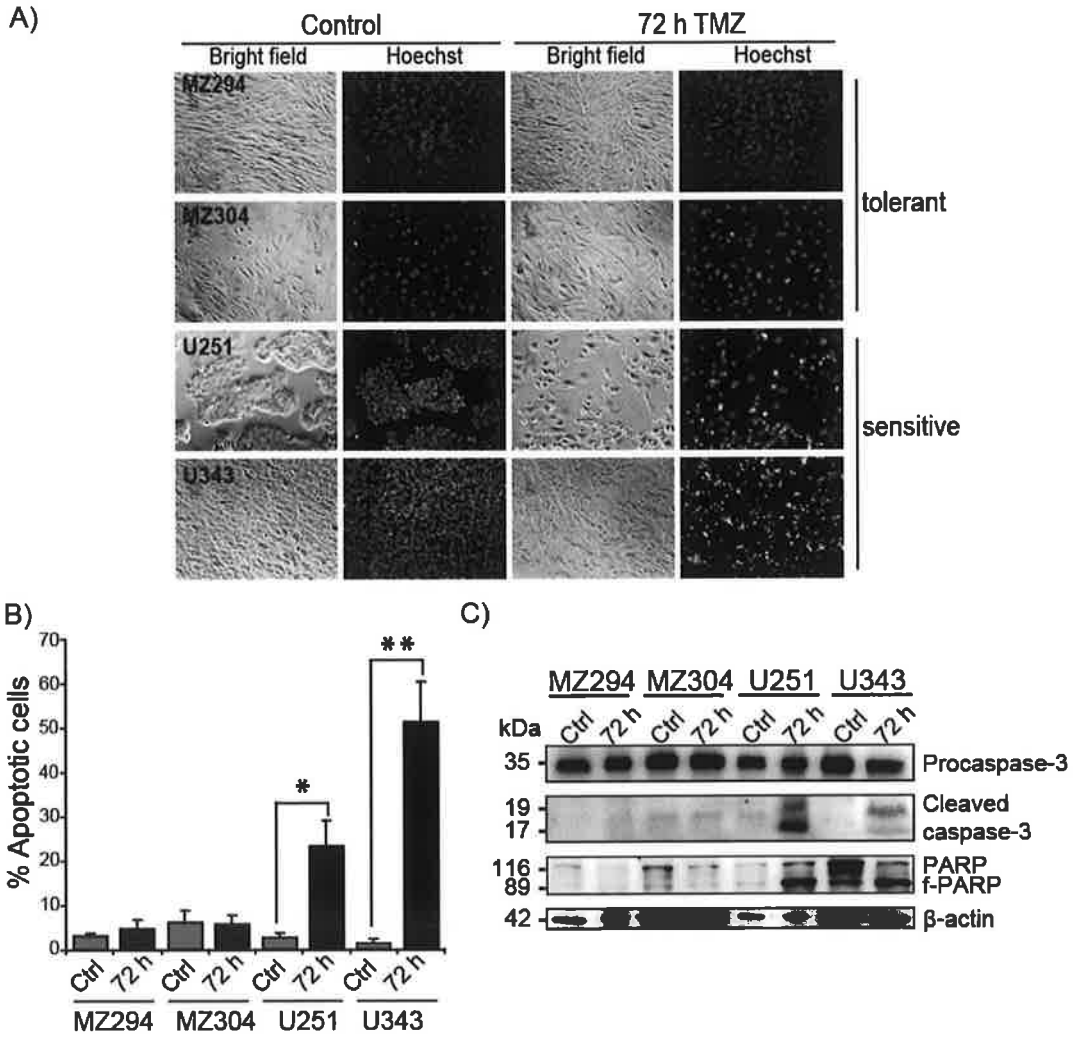

Figure 3-4 Apoptotic cell death in TMZ-sensitive cell lines

Representatives of both clusters, TMZ-resistant cell lines MZ294 and MZ304 and TMZ-sensitive cell lines U251 and U343, were treated with TMZ (150 μM) for 72 hours. **A)** Hoechst 33258-stained cells in bright field and UV-light microscopy. Condensation and fragmentation of the nuclear chromatin is clearly visible in U251 and U343 cells, but not in MZ294 and MZ304 cells. **B)** Count of Hoechst-positive cells. MZ294 and MZ304 displayed low amounts of apoptotic cells, while sensitive cell lines U251 and U343 showed significantly elevated levels of apoptotic cells. Data are means ± S.E.M from three independent experiments in triplicates; * indicates p value ≤ 0.07 and ** indicates p value ≤ 0.05, Student's t test. **C)** Western Blot showing procaspase-3 processing by cleavage into its active form and PARP fragmentation into f-PARP only in U251 and U343, but not in MZ294 and MZ304. β-actin was used as a loading control. Similar results were obtained in two different experiments.

3.2.4 TMZ-resistant cell lines show a delay in STS drug response

To further analyse the emerging pattern of chemotherapeutic sensitivity in our panel of cell lines, we utilised a second apoptotic stimulus, the broad-spectrum kinase inhibitor staurosporine (STS), which triggers apoptosis through a different mechanism, but also leads to the activation of the mitochondrial apoptotic pathway (Krohn et al. 1998). STS inhibits protein kinases through prevention of ATP-binding to the kinase and is not used in clinical settings due to its lack of specificity to tumour cells (Chae et al. 2000).

Cell viability was assessed via MTT assay after exposure to STS (1 μM) for 2, 6, 10, 16 and 24 hours (Figure 3-5). A significant decrease in cell numbers below 50% was found in cell lines U87, U251, U343, U373 and A172 after 10 hours of treatment (Figure 3-5 B; named sensitive or early responsive). Cell lines MZ18, MZ51, MZ256, MZ294 and MZ304 displayed only moderately reduced viability still above 50% after 10 hours treatment, although eventually undergoing cell death after 24 hours of drug exposure (Figure 3-5 A; termed tolerant or late responsive). MZ327, while here displayed in the same graph as the tolerant cluster of cells, demonstrated an intermediate response to STS treatment, with 48% survival after 10 hours of treatment (Figure 3-5 A).

Thus, the same groups of cells, previously identified to be TMZ-sensitive (U87, U251, U343, U373 and A172) or TMZ-resistant (MZ18, MZ51, MZ256, MZ294 and MZ304), were also forming STS-early response and STS-late response clusters, respectively, with the exception of the cell line MZ327 that showed a stronger response to STS treatment than expected after TMZ treatment. Therefore, because two apoptotic stimuli with different mechanism of apoptosis induction evoke the same pattern of treatment sensitivity in the panel of cell lines, it is plausible to assume that alterations in apoptosis signalling interfer with the execution of cell death in treatment-resistant glioma cell lines.

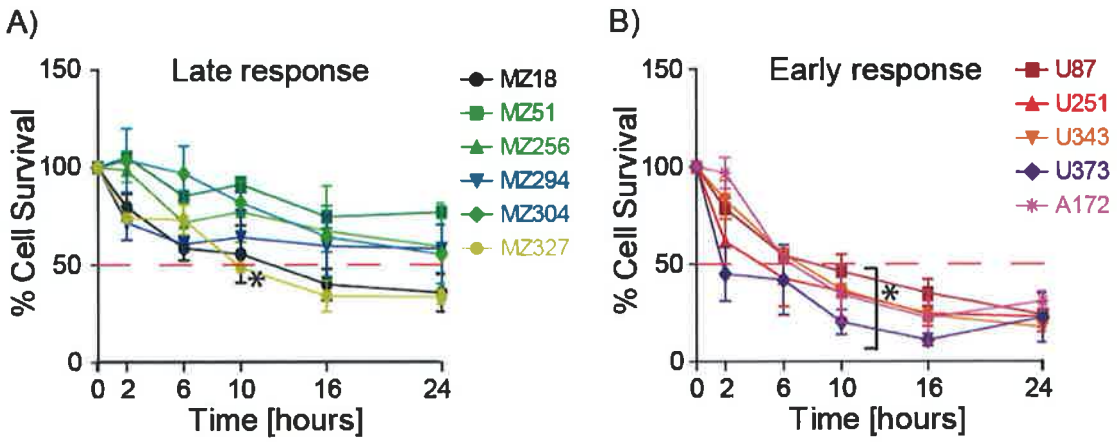

Figure 3-5 Glioma cell lines show similar responses to STS or TMZ treatment

Glioma cell viability during 24 h exposure to staurosporine (1 µM). MTT assay following STS for 2, 6, 10, 16 and 24 h. Red dashed lines mark 50% cell survival. **A)** At 10 h, TMZ-resistant cell lines MZ18, MZ51, MZ256, MZ294 and MZ304 (cluster 1; late response) displayed cell numbers above 50%. Levels of cell survival in MZ327 at 10 h were comparable to a sensitive cell line. **B)** TMZ-sensitive cell lines U87, U251, U343, U373 and A172 displayed less than 50% cell survival after 10 h STS treatment (cluster 2; early response). Data points are means ± SEM of three independent experiments in sextuplicates (n=18); * indicates $p \leq 0.05$, Student's t test.

3.2.5 TMZ-resistant cell lines are also less susceptible to STS-triggered activation of caspase-dependent apoptosis

In the previous paragraphs, we demonstrated that TMZ-sensitive cell lines underwent apoptosis after treatment, while TMZ-resistant cell lines showed no activation of caspase-dependent apoptotic signalling. To investigate whether apoptosis was also the preferred mode of cell death in glioma cell lines after STS treatment, we performed Hoechst staining of apoptotic cells and monitored procaspase-3 processing on Western Blots. Both STS-sensitive cell line U251 and STS-tolerant cell line MZ294 showed dramatic cell shrinkage after STS treatment for 10 hours (Figure 3-6 A, bright field image). However, the U251 cell line displayed significantly higher numbers of apoptotic cells than the MZ294 cell line following STS treatment at 3 μM for 10 hours (Figure 3-6 A and B), consistent with the previous observation that tolerant cell lines die later during STS treatment. In addition, caspase-3 activation and cleavage of its direct substrate PARP into f-PARP was only observed in the sensitive cell lines U251 and U343 (Figure 3-6 C), but not in the tolerant cell lines MZ294 and MZ304. Thus, STS treatment triggers caspase-dependent apoptosis in sensitive cell lines, while cell lines that were showing a late response in the reduction of cell numbers might undergo apoptosis later or even follow a different type of cell death.

The release of cytochrome *c* from mitochondria, a prerequisite for apoptosome-dependent effector caspase activation, was examined after 10 hours of drug exposure (STS 3 μM) (Figure 3-6 D) (Rehm et al. 2006). Cell cultures were separated into cytosolic and membrane fractions and analysed on Western Blots for cytochrome *c* protein content. Cytosolic extracts of both sensitive and tolerant cell lines U251 and MZ294 contained detectable levels of cytochrome *c* after treatment, although significantly lower in MZ294 (see general discussion).

Taken together, these results indicate an inhibition of the execution of apoptosis downstream of the mitochondria after the release of cytochrome *c* in treatment-tolerant glioma cell lines.

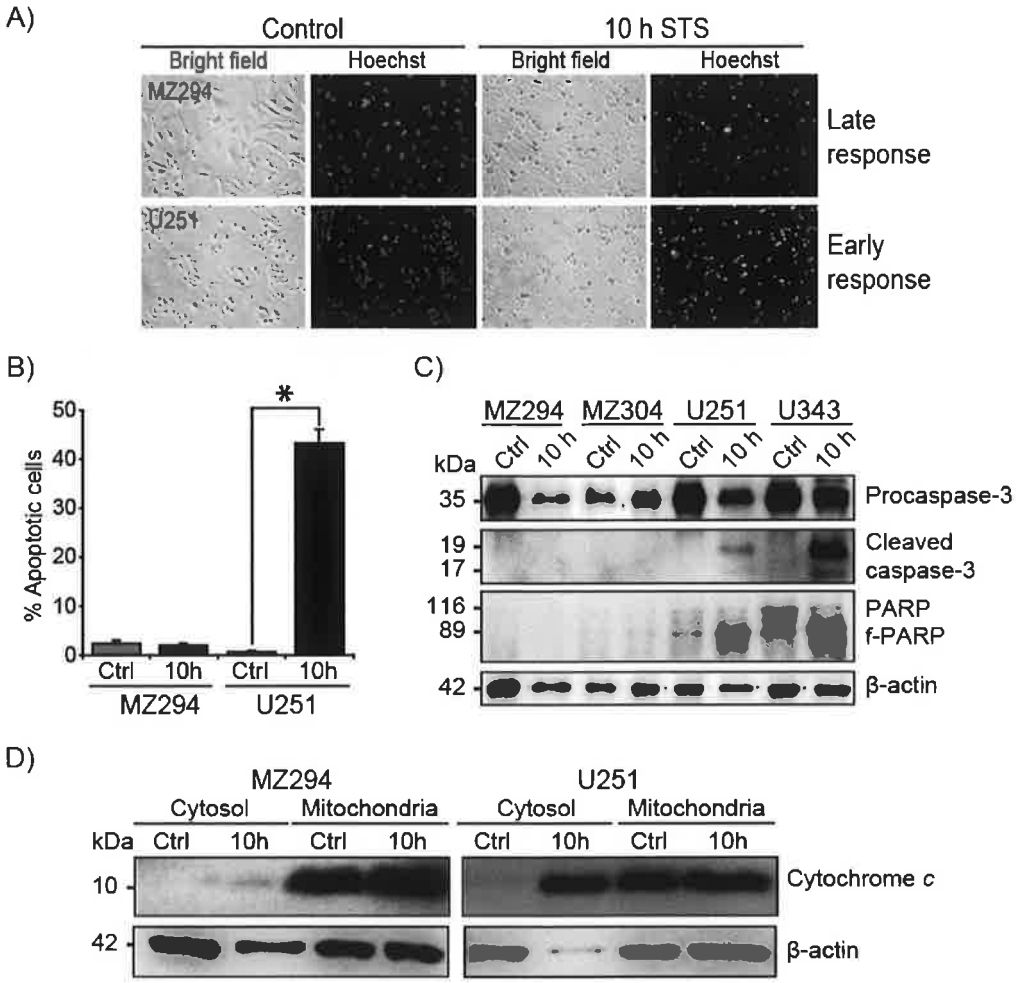

Figure 3-6 Characterization of cell death after STS treatment

A) and **B)** STS-resistant MZ294 and STS-sensitive U251 were treated with STS (3 μM) for 10 h. **A)** Bright field and UV-light microscopy images of Hoechst 33258-stained cells. Apoptotic nuclei were visible in U251 cells, but not in MZ294. **B)** Count of Hoechst-positive cells. U251 showed significantly elevated levels of apoptotic cells, MZ294 displayed low levels of apoptotic cells: means ± S.E.M from three independent experiments in triplicates; p values ≤ 0.05 were considered as significant; Student's t test. **C)** Western Blot after 10 h STS (1 μM). Caspase-3 activity was not found in drug-tolerant MZ294 and MZ304. Drug-sensitive U251 and U343 displayed processed procaspase-3 and PARP fragments (f-PARP). β-actin was used as a loading control. Experiments were repeated twice with similar results. **D)** Cytochrome *c* release assay and Western Blotting following STS treatment (3 μM) for 10 h. Cytochrome *c* protein was detected in STS-treated cytosolic fractions of U251 cells and to a lower extend in MZ294 cytosolic fractions. β-actin was used as a loading control. Experiments were repeated twice with similar results.

3.2.6 Glioma cell lines show differential expression of proteins involved in the intrinsic apoptotic pathway

Activators of the mitochondrial apoptotic pathway such as STS and TMZ culminate in the loss of mitochondrial outer membrane potential (MOMP) and cytochrome *c* release (Garrido et al. 2006). Consequent apoptosome formation and activation of effector caspases is a final step during apoptosis (Zou et al. 1999). Dysregulation of pro- and anti-apoptotic proteins is a common phenomenon in cancer and could be utilised to predict apoptosis resistance (Jia et al. 2010; Plati & Khosravi-Far 2008).

To analyse whether the apoptotic machinery downstream of the mitochondria is impaired in glioblastomas, we established expression profiles of the key pro- and anti-apoptotic proteins involved in apoptosome-dependent caspase activation: basal protein expression of Apaf-1, procaspase-9, XIAP, Smac and procaspase-3 in whole cell extracts of our panel of 11 glioma cell lines was visualized on Western Blots (Figure 3-7) and analysed by densitometry (Figure 3-8). Protein expression levels were normalised to the β-actin loading control and expressed relative to HeLa protein levels set at 100% (Figure 3-8). HeLa cells were chosen as a standard due to the availability of relative protein concentrations (Rehm et al. 2006, supplementary material).

All glioma cell lines (in grey and black) generally displayed low basal expression of pro-apoptotic Apaf-1 and procaspase-9 when compared to the HeLa cell line (Figure 3-8). The expression of the pro-apoptotic XIAP-inhibitor Smac was elevated in most glioma cell lines. We employed the Mann-Whitney test, a simple non-parametric test used to compare two independent groups of sampled data, to investigate drug-tolerant (dark grey) and drug–sensitive cell lines (black) (Mann & Whitney 1947). Significant differences between tolerant and sensitive cell lines were only found in the expression of pro-apoptotic procaspase-3, which was downregulated in tolerant cell lines ($p = 0.04$; Mann-Whitney test). Tendencies to higher XIAP expression levels in tolerant cell lines were not significant ($p = 0.12$; Mann-Whitney test). Expression levels of pro-apoptotic procaspase-9 ($p = 0.93$; Mann-Whitney test), Apaf-1 ($p = 0.93$; Mann-Whitney test) and Smac ($p = 0.24$; Mann-Whitney test) did not show significant differences between both clusters either.

In conclusion, sensitive and tolerant cell lines displayed highly heterogeneous protein expression levels within each cluster. With the exception of procaspase-3 expression, the examination of single protein levels in the panel of glioma cell lines did not reveal a strong pattern of molecular characteristics that could explain the previously observed cluster formation.

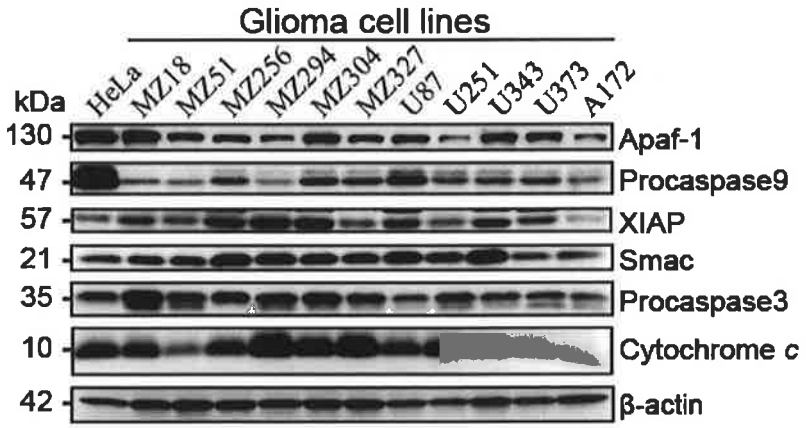

Figure 3-7 Differential protein expression of apoptotic proteins in glioma cell lines

Representative Western Blots showing basal Apaf-1, procaspase-9, XIAP, Smac, procaspase-3 and cytochrome *c* protein expression in glioma whole cell lysates. β-actin was used as a loading control. Data are representative of three independent experiments.

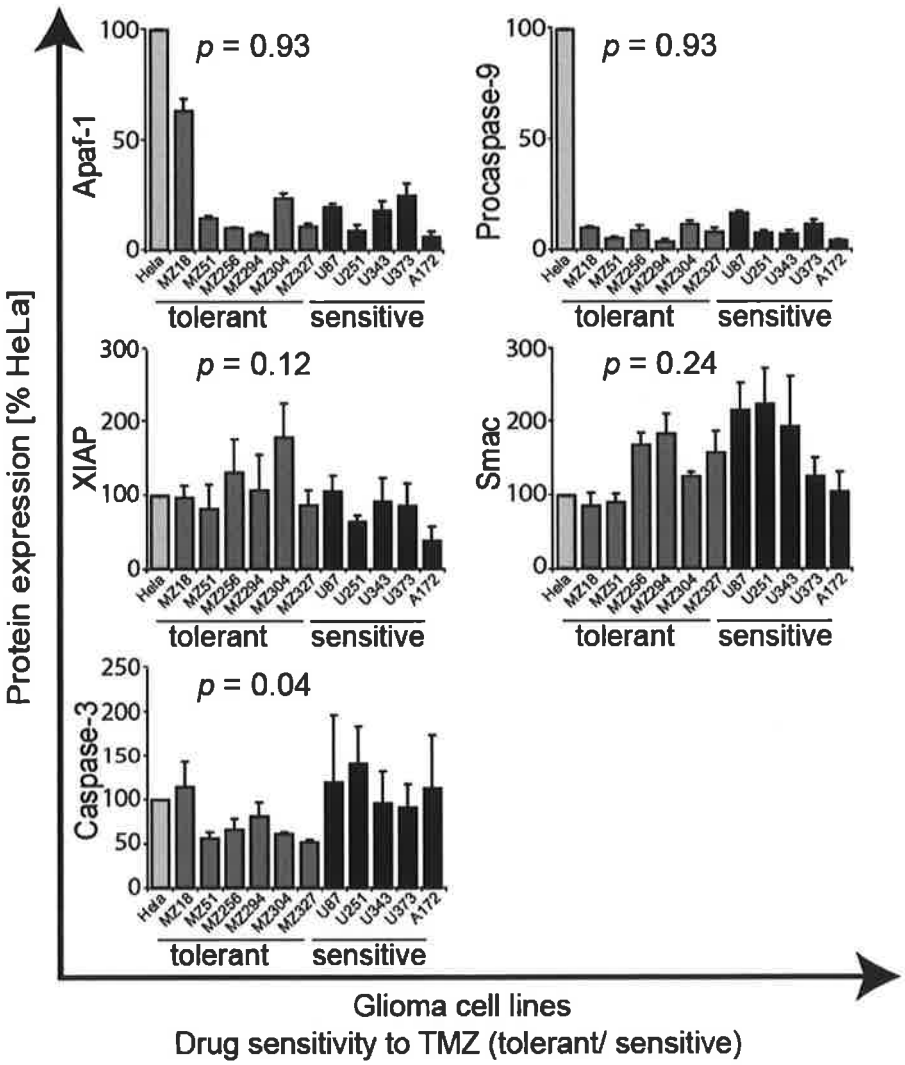

Figure 3-8 Densitometry analysis of apoptotic protein expression in glioma cell lines

Bar graphs displaying the densitometry analysis of the expression of Apaf-1, procaspase-9, XIAP, Smac and procaspase-3. TMZ sensitivity is indicated as dark grey (tolerant) and black (sensitive) bars, HeLa standard in light grey. Low levels of Apaf-1 and procaspase-9 were found in all glioma cell lines when compared with HeLa. TMZ-tolerant glioma cell lines showed lower expression of procaspase-3 when compared to sensitive glioma cell lines ($p = 0.04$; tendencies to elevated XIAP levels were not significant ($p = 0.12$) Data are means ± SEM of three Western Blots; values were normalised to β-actin and expressed relative to a HeLa standard set to 100%. p values ≤ 0.05 were considered as significant, Mann-Whitney test.

3.2.7 Glioma cell lines can be grouped into two distinct clusters that coincide with experimental drug response

In an approach to identify a common molecular signature in the protein expression profiles of drug-resistant and drug-sensitive glioma cell lines, we performed a pattern recognition analysis called principal component analysis (PCA). This highly sensitive multivariate statistical method is commonly used to discover molecular patterns in cancer (Dove et al. 1985; Brennan et al. 2009; Ringnér 2008; Han 2010) (see material and methods). The PCA is a dimension reduction technique which highlights those proteins that show the highest variance in their expression levels in the panel of glioma cell lines. Proteins with higher variance are given the priority, while proteins with the lowest variance are given less priority in the data display, thus enforcing a clearer pattern classification. The PCA can be used to capture meaningful biomarkers (Han 2010).

The protein expressions of procaspase-3, procaspase-9, XIAP, Smac and Apaf-1 in glioma cell lines relative to expression levels in HeLa cells (100%), as established in the previous chapter (Figures 3-7 and 3-8), were applied as a matrix in the PCA. The resulting first principal components, the principal component 1 (PC 1) and the principal component 2 (PC2) together explained 65% of the original variance in the data set. The analysis determined a strong influence of XIAP and medium influence of procaspase-9 and Apaf-1 expression levels on PC 1, PC2 was affected most by procaspase-3 and then by Smac expression levels (Table 3-2). Thus, apoptosis resistance in glioma cell lines might be determined by the expression of XIAP and procaspase-3.

Table 3-2 Coefficients in principal component analysis of glioma cell lines

Principal Component	Procaspase-3	Procaspase-9	XIAP	Smac	Apaf-1
PC1	-0.22	+0.52	+0.59	-0.24	+0.52
PC2	+0.67	+0.49	-0.10	+0.52	+0.14

The first principal component was graphed against the second principal component in a 2-dimensional plot (Figure 3-9). The results visualize the individual expression profiles of

single cell lines in relation to the expression profiles of all cell lines combined. Two groups of cell lines were distinguishable after principal component analysis: one group, consisting of MZ18, MZ51, MZ256, MZ294, MZ304 and MZ327, localized mainly in the upper quadrants of the coordination system (Figure 3-9). A second group of cell lines, U87, U251, U343, U373 and A172 settled in the lower quadrant of the grid (Figure 3-9). The colouring for drug sensitivity, red for sensitive, blue for tolerant and purple for intermediate, were applied manually after the PCA according to our previous results (Figures 3-1 and 3-5). We found that the clustering based on molecular expression profiles strongly coincided with the previously examined drug response to apoptotic stimuli (Figures 3-9, 3-1 and 3-5). The PCA analysis predicted STS drug response with 83.3% sensitivity and 100% specificity (two-tailed p value equalled 0.02 in Fisher's exact test) (Lalkhen & McCluskey 2008; Girardi et al. 2011). TMZ drug response was predicted with 100% sensitivity and 100% specificity, (two-tailed p value equalled 0.002 in Fisher's exact test).

Thus, resistant glioma cell lines display a distinct pattern of apoptotic protein expression that distinguishes them clearly from sensitive glioma cell lines. The PCA highlighted the most significant variants between tolerant and sensitive glioma cell lines, mainly the differences in procaspase-3 and XIAP expression. By applying this statistical method, we were able to clearly correlate the drug response to apoptotic stimuli to a possibly underlying cause, the dysregulation of components of apoptosome-dependent caspase-activation.

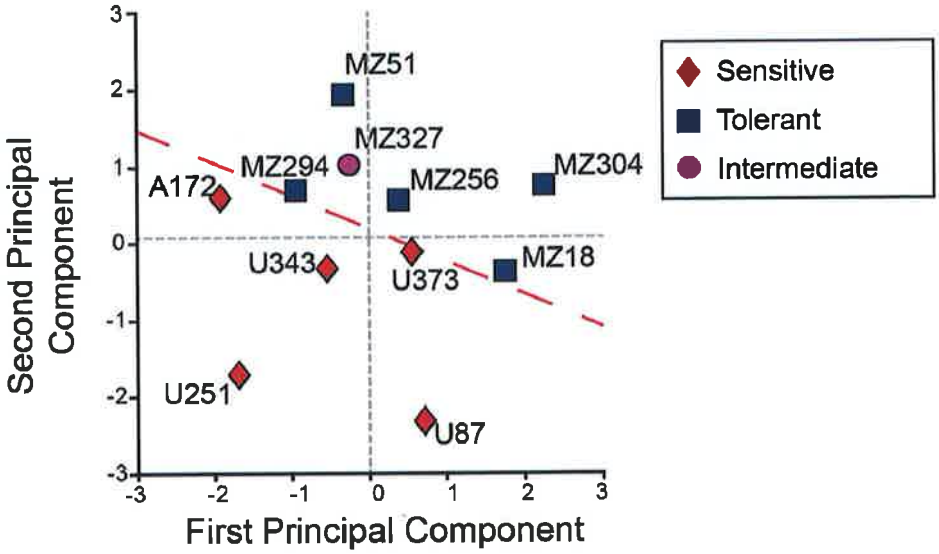

Figure 3-9 Principal component analysis (PCA) based on apoptotic protein expression profiles

Glioma cell lines were grouped in a two-dimensional coordinate system after PCA based on protein expression of procaspase-3, procaspase-9, XIAP, Smac and Apaf-1. The red dashed line indicates a possible separation between two groups: cluster 1 localized in the upper quadrants of the grid and consisted of the cell lines MZ18, MZ51, MZ256, MZ294, MZ304 and MZ327, cluster 2 settled in the lower quadrant of the grid and contained cell lines U87, U251, U343, U373 and A172. The colouring of tolerant cell lines in blue and sensitive cell lines in red was manually applied based on TMZ- and STS-drug response (Figure 3-1 and 3-5). MZ327 was labelled in purple to highlight its sensitivity to STS and its resistance to TMZ (intermediate). Data are based on mean values from three independent Western Blots normalised to β-actin loading control and expressed as percentage of HeLa expression (100%; Figure 3-8).

3.2.8 The APOPTO-CELL system predicts resistance and sensitivity to apoptosis induction in glioma cell lines

Next, we utilized a systems medicine approach, the APOPTO CELL model, to predict treatment sensitivity in glioma cell lines (Rehm et al. 2006; Huber et al. 2007). APOPTO CELL is a computational model of apoptosome-dependent effector caspase activation, developed with and based on HeLa cells (Rehm et al. 2006). APOPTO CELL has previously demonstrated its prognostic potential in a clinical application where it correctly predicted survival of colorectal cancer patients (Hector et al. 2011). Here, we used this system as a tool to test the likelihood of our panel of glioma cell lines to undergo apoptosis, thereby also proving the usability of this novel model in gliomas.

To calculate absolute protein quantities of procaspase-3, procaspase-9, XIAP, Smac and Apaf-1, we utilised the previously described protein expression profiles and expressed them relative to published protein concentrations for HeLa (Figure 3-8, Table 2-20) (Rehm et al. 2006, supplementary material). The determined protein concentrations of all five proteins (in µM) served as an input into the APOPTO-CELL program. Shown in Figure 3-10 is the output of APOPTO CELL, which predicts the probability of effector caspase activation within the cell lines. The modeled output displays simulated caspase-3 and caspase-7 substrate cleavage as a function over time following the release of cytochrome *c* (cyt *c*). Apoptosis execution was defined as 80% substrate cleavage (optimal substrate cleavage). HeLa cells achieved optimal substrate cleavage in 12 minutes after the release of cyt *c* (Figure 3-10 A). HeLa cells are thus considered highly susceptible to undergo apoptosis after receiving an apoptotic stimulus of the mitochondrial pathway (Markus Rehm et al. 2006).

Glioma cells were grouped based on their ability to undergo apoptosis: cell lines MZ18, MZ51, MZ256, MZ294 and MZ304 did not display optimal substrate cleavage (80%) within a 60 min time frame and should therefore be less likely to undergo apoptosis upon receiving an apoptotic stimulus. The MZ327 cell line should show a delay in substrate cleavage but nonetheless achieved optimal substrate cleavage within 60 minutes. Cell lines U87, U251, U343, U373 and A172 achieved optimal substrate cleavage (80%) within 20-36 minutes after the release of cytochrome *c* and are thus predicted to be sensitive to a drug

treatment strategy that aims to activate apoptosome-dependent cell death. By comparing our measured treatment sensitivities (Figures 3-1 and 3-5) with the APOPTO CELL outputs, we found that APOPTO CELL predicted STS drug response with 100% sensitivity and 100% specificity (two-tailed p value equalled 0.002 in Fisher's exact test). TMZ drug response was predicted with 100% sensitivity and 83.3% specificity (two-tailed p value equalled 0.02 in Fisher's exact test).

In conclusion, predictions made by APOPTO CELL show a strong association with the established drug sensitivity patterns (Figures 3-1 and 3-5) and resemble the correlation analyses made by single protein expression analysis and PCA (Figures 3-8 and 3-9).

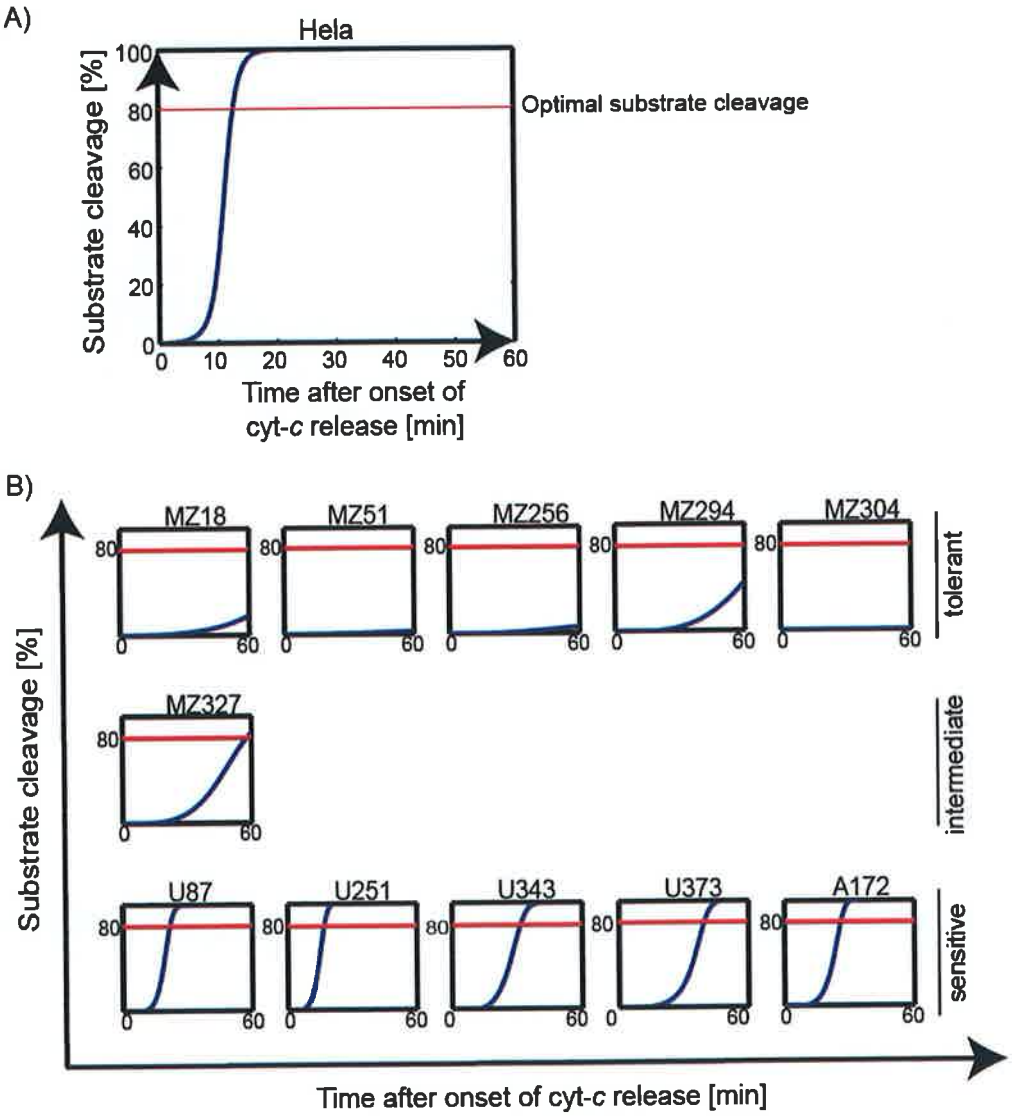

Figure 3-10 The APOPTO CELL model predicts drug sensitivity of glioma cell lines

Modelled output for caspase-3/-7 substrate cleavage as generated by APOPTO CELL. The likelihood of a cell line to undergo apoptosis is determined by its ability to reach optimal substrate cleavage (80%) within 60 min after the onset of cyt *c* release. **A)** Early substrate cleavage was predicted for HeLa. **B)** No substrate cleavage or a delayed substrate cleavage was predicted for glioma cell lines MZ18, MZ51, MZ256, MZ294 and MZ304 (tolerant). MZ327 reached 80% substrate cleavage almost exactly 60 min after the release of cyt *c* (intermediate). Early substrate cleavage was predicted for glioma cell lines U87, U251, U343, U373 and A172 (sensitive). Data input as absolute protein concentrations [μM] based on established protein expression profiles (Figure 3-8).

3.2.9 Analysis of protein expression in long-term and short-term progression-free survival (PFS) tissue samples from glioblastoma patients

Cancer cell lines are widely used as preclinical models to study cancer characteristics and to screen for potential therapeutic drugs, however, the cell lines sometimes display too little resemblance to the associated primary human tumours, depending on the subject of study (Lee et al. 2006; Romer & Curran 2005). Also, chemotherapeutic sensitivity to specific drugs is not always prognostic for the overall patients survival (van den Bent et al. 2011). Thus, we aimed to evaluate whether the identified pattern of apoptosis resistance in cultured glioma cells transferrable to the situation in a clinical setting with glioblastomas. We utilized a cohort of 17 GBM patient samples, consisting of 10 tissue specimens from short-term progression-free survivors (PFS < 10 months) and 7 samples representing long-term progression-free survivors (PFS ≥ 10 months) (Table 2-8). Progression-free survival time is defined as the length of time where a patient's cancer does not progress (Halabi et al. 2009).

Western Blot and densitometry analysis was performed on homogenized lysates of primary GBM tumour tissue samples (Table 2-8; Figures 3-11 and 3-12). Protein expression levels were normalised to the β-actin loading control and expressed relative to protein levels of a HeLa cell line set to 100%. We observed that protein expression profiles found in tumour tissue samples displayed a clear pattern that correlated well with patient follow-up data of progression-free survival in these patients (Table 2-8). Low protein expression of pro-apoptotic procaspase-9 was found in short-term PFS patient samples when compared to long-term PFS patient samples ($p = 0.0008$; Mann-Whitney Test). Anti-apoptotic XIAP levels were upregulated in short-term PFS and downregulated in long-term PFS ($p = 0.002$; Mann-Whitney Test). Pro-apoptotic Smac upregulation was found in long-term PFS ($p = 0.0008$; Mann-Whitney Test). The expression of pro-apoptotic procaspase-3 was also significantly higher in long-term PFS samples ($p = 0.004$; Mann-Whitney Test). Only the expression of Apaf-1 did not significantly differ between long-term and short-term PFS samples ($p = 0.66$; Mann-Whitney Test). Thus, GBM patient samples displayed a much more distinct molecular expression profile of apoptotic proteins than glioma cell lines (Figure 3-8). Significant differences between long-term and short-term progression-free

survivors were found in the expression of four out of five proteins. The downregulation of procaspase-3 in short-term PFS samples occurred in consistency with downregulation of procaspase-3 in resistant glioma cell lines (Figure 3-8). However, other similarities between glioma cell lines and patient samples could not be found.

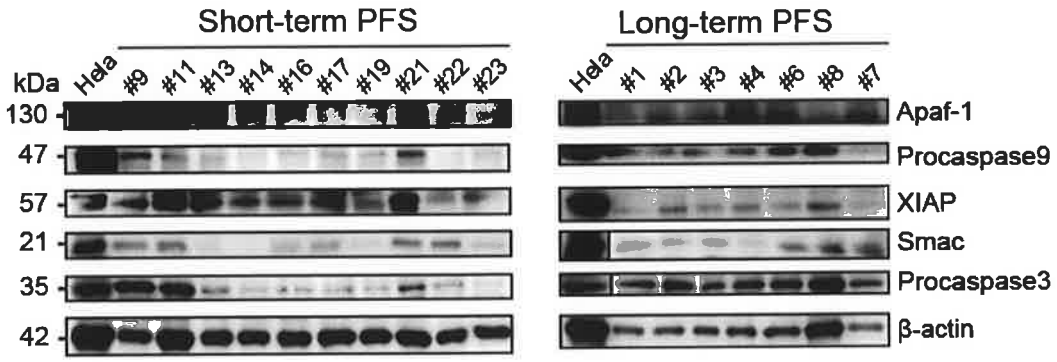

Figure 3-11 Glioblastoma patient samples differ in the basal protein expression of late pro- and anti-apoptotic proteins

Western Blots showing basal Apaf-1, procaspase-9, XIAP, Smac and procaspase-3 protein expression levels in GBM patient samples. PFS = progression-free survival; β-actin was used as loading control.

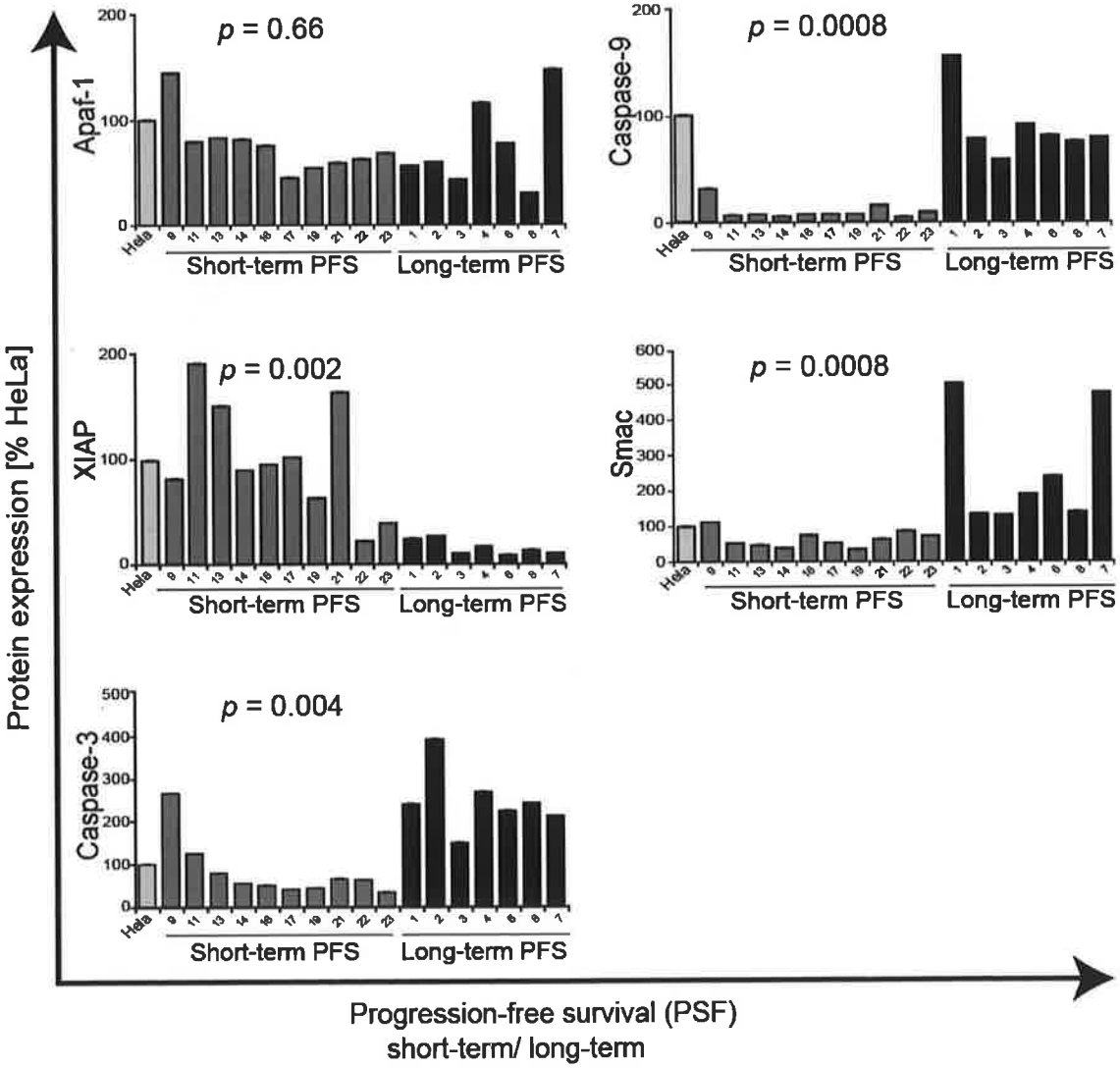

Figure 3-12 Densitometry analysis of apoptotic proteins in GBM patient samples

Protein expression of Apaf-1, procaspase-9, XIAP, Smac and procaspase-3 in GBM patient samples. Significant differences between short-term (grey bars) and long-term (black bars) PFS patient samples were found in the expression of procaspase-9, XIAP, Smac and procaspase-3. PFS = progression-free survival; $p \leq 0.05$ were considered significant; Mann-Whitney test.

3.2.10 GBM patient samples and glioma cell lines share a similar pattern of drug resistance

To further examine a correlation between apoptotic protein expression and tumour progression, we performed a PCA analysis on the protein expression profiles of GBM patient samples (Table 2-8). Expression levels of procaspase-3, procaspase-9, XIAP, Smac and Apaf-1 proteins in GBM patient samples (Figure 3-12) were used relative to expression levels in HeLa cells (100%) and entered as one data set in a PCA. The original variance in the matrix was explained with 71% by principal component 1 (PC 1) and principal component 2 (PC2). According to the analysis, procaspase-9 and Smac had the greatest influence on PC 1, while Apaf-1 and XIAP had a greater impact on PC 2 (Table 3-3). This could imply that procaspase-9 and Apaf-1 expression have a high influence on the progression-free survival time in patients.

Table 3-3 Coefficients in principal component analysis of GBM patient samples

Principal Component	Procaspase-3	Procaspase-9	XIAP	Smac	Apaf-1
PC1	0.477	0.55	-0.43	0.508	0.166
PC2	-0.086	-0.17	-0.343	-0.096	-0.915

GBM patient samples of short-term PFS were mainly found in the lower or left quadrants of the coordination system, long-term PFS GBM patient samples were located in the upper or right quadrants of the grid, divisible by an artificially drawn red dashed line (Figure 3-13). The PCA analysis predicted clustering of the cohort of patient samples into short-term and long-term progression-free survival with 100% sensitivity and 100% specificity (two-tailed p value equalled 0.00005 in Fisher's exact test). Thus, based on protein expression profiles of pro- and anti-apoptotic proteins, we were able to clearly distinguish between short-term and long-term progression-free survivors in glioblastomas. We can also conclude that despite the differences in their single protein expression, both treatment-

resistant glioma cell lines and short-term GBM patient samples show characteristics of an apoptosis-resistant phenotype.

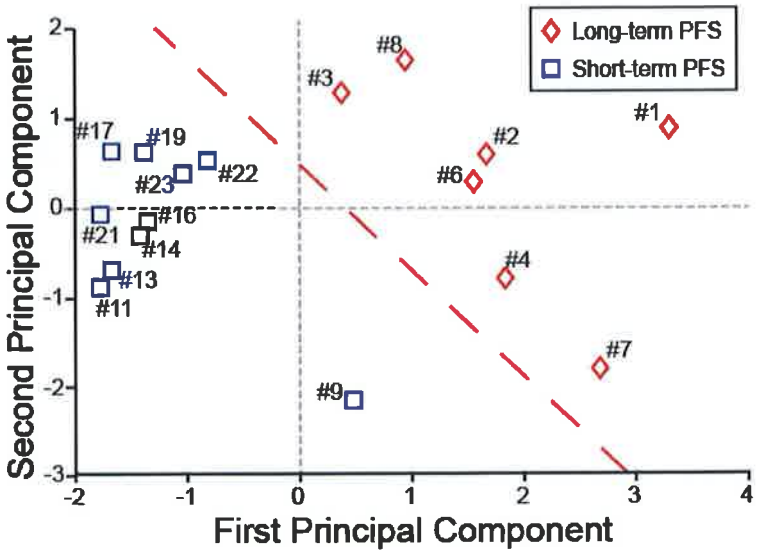

Figure 3-13 Predictions of patient survival coincided with patient follow-up data

Molecular expression profiles of GBM patient samples with different progression-free survival were combined in a principal component analysis (PCA). The red dashed line indicates a possible separation between short-term (blue rectangle) PFS patient samples on one side and long-term (red rectangle) PFS patient samples on the other side, respectively. Data was based on the protein expression of procaspase-3, procaspase-9, XIAP, Smac and Apaf-1 in 17 GBM patient samples relative to protein expression levels in a HeLa cell line (100%).

3.2.11 The APOPTO CELL model predicts long-term or short-term progression-free survival in GBM patient samples

In consistency with our previous strategy, we examined whether the APOPTO CELL model could also be utilised to predict progression-free survival time in GBM patient samples. Absolute protein amounts of procaspase-3, procaspase-9, XIAP, Smac and Apaf-1 (in μM) in GBM patient samples were calculated in relation to published protein concentrations for HeLa (Figure 3-11, Table 2-20) (Rehm et al. 2006, supplementary material). This served as an input into APOPTO CELL. The results are illustrated in Figure 3-14 as the probability of effector caspase-3 and -7 activation over time following the release of cytochrome *c* (cyt *c*). Optimal substrate cleavage is achieved at 80%. Patient samples that display the ability to undergo apoptosome-dependent caspase activation should be more likely to respond to a targeted therapy, thus leading to prolonged PFS. Long-term PFS tumour samples showed complete substrate cleavage (80%) within 60 minutes (Figure 3-14). Short-term PFS patient samples, with the exception of samples # 9 and # 22, did not show caspase-activation. APOPTO CELL predicted tumour progression based on treatment sensitivity with 77.77% sensitivity and 100% specificity (two-tailed *p* value equalled 0.0022624 in Fisher's exact test). Transferred to the patients, these results imply that the ability to undergo apoptosis is impaired in short-term progression-free survivors. Thus, the APOPTO CELL model can be utilised to predict progression-free survival time in GM patients.

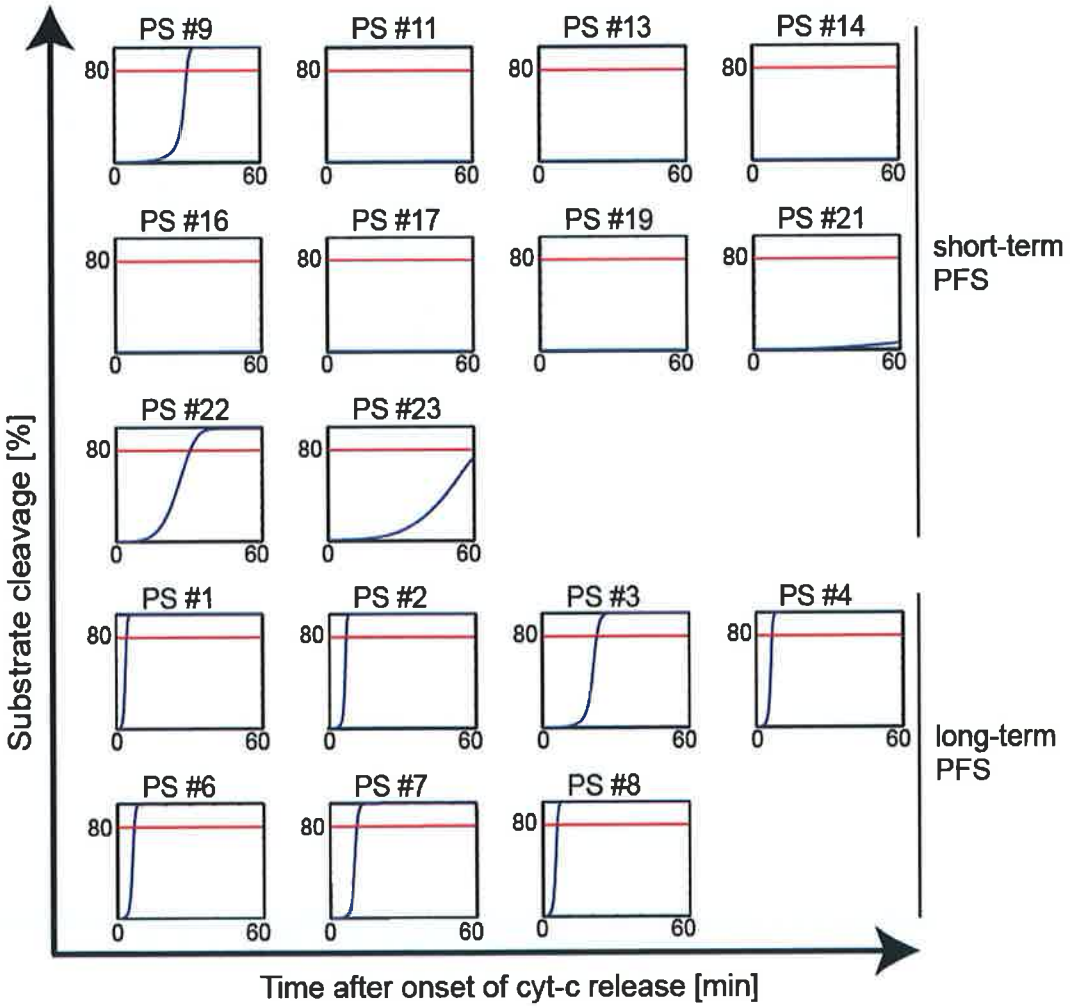

Figure 3-14 APOPTO-CELL predicts GBM patients progression

Modelled output signal for caspase-3/-7 substrate cleavage as generated by APOPTO CELL. Progression-free survival of patients is assumed to correlate with the ability of tumour cells to undergo apoptosis. Optimal substrate cleavage (80%) should occur within 60 min after the onset of cyt *c* release. Short-term PFS samples did not show sufficient substrate cleavage within 60 min, with the exception for samples #9 and #22. All long-term PFS samples showed early substrate cleavage within 60 min. Data input as absolute protein concentrations [μM] based on molecular expression profiles of procaspase-3, procaspase-9, XIAP, Smac and Apaf-1 in GBM patient samples.

3.3 Discussion

In this study, we demonstrated the usefulness of performing a comprehensive analysis of intrinsic apoptotic pathway components in glioblastoma to establish predictive marker for treatment response and patients survival. We first successfully correlated the imbalanced expression of pro-apoptotic procaspase-3, procaspase-9, Apaf-1 and Smac and anti-apoptotic XIAP to chemotherapeutic sensitivity towards the current standard chemotherapeutic agent, TMZ in a pre-clinical model using glioma cell lines (Figures 3-8, 3-9 and 3-10). A subpopulation within the panel of 11 glioma cell lines showed distinct features of an apoptosis resistant phenotype both on the molecular level and during treatment with two distinct apoptotic stimuli. We were able to predict the cellular response to treatment regimes that aim to reactivate the mitochondrial apoptotic pathway with high accuracy. We then transferred our findings into a clinical setting, using primary GBM patient samples with different progression-free survival follow-up data. The distinct expression of apoptotic proteins correlated well with the known patient outcome. Furthermore, we were able to demonstrate a common pattern of apoptotic protein expression in both cell lines and patient samples that could help to classify patients according to their susceptibility to a chosen drug regime, which could ultimatively lead to a more personalised therapy.

Inherent and acquired chemoresistance to DNA-alkylating agents is a severe limitation in the treatment of glioblastoma multiforme (GBM) (Sarkaria et al. 2008; Oliva et al. 2011). The underlying mechanisms that determine drug response in glioblastomas are not well understood. There is a high demand for novel predictive and prognostic biomarkers that allow identifying GBM patients that are most likely to respond to a specific therapy (Settle & Sulman 2011).

To analyse the effectiveness of current treatment regimes in gliomas, we initially tested 11 glioma cell lines derived from grade III/IV tumours for chemotherapeutic sensitivity to the standard chemotherapeutic TMZ (Table 2-6). TMZ was previously demonstrated to evoke a whole range of cellular responses in gliomas, including apoptosis, autophagy, senescence and growth inhibition (Zhang et al. 2010; Roos et al. 2007; York 2003; Mhaidat et al. 2007). In our investigations, only five out of 11 glioma cell lines

underwent apoptosis after three to five days treatment (U87, U251, U343, U373 and A172). The second group (MZ18, MZ51, MZ256, MZ304 and MZ327) displayed a cell viability steadily at about 90-100%. To better understand the observed treatment response, we analysed previously reported predictive factors that have been associated with chemoresistance to TMZ. These include epidermal growth factor (EGFR) overexpression, chromosomal 1p19q deletion, oncogene p53 overexpression, isocitrate dehydrogenase 1 (IDH1) status and most prominently expression of the DNA-repair enzyme O^6-methylguanine-DNA methyltransferase (MGMT) (Yan et al. 2009; Hegi et al. 2005; Hassel et al. 2010; Michael Weller et al. 2010). Downregulation of MGMT protein levels by *MGMT* promoter methylation is a common phenomenon in GBM and is often associated with increased treatment sensitivity to TMZ (M. E. Hegi et al. 2005). Controversially, other studies found no correlation between MGMT *gene* silencing and TMZ treatment response or overall patient survival (Rietschel et al. 2008; Costa et al. 2010; see general discussion). In the present study, we found equal levels of MGMT promoter methylation in a TMZ-tolerant (MZ294) and in a TMZ-sensitive (U251) cell line (34.35% ±16.16 and 49.45 ±17.96, respectively) (Figure 3-3, Table 3-1). The cell line U251 was previously reported to not express MGMT (van Nifterik et al. 2010). Thus, in our study, the observed methylation rate in both U251 and MZ294 cells is probably sufficient to effectively suppress MGMT protein expression. This would explain the observed TMZ sensitivity of the U251 cell line, but not the TMZ-resistance in the MZ294 cell lines. Therefore, we could not correlate the drug response of MZ294 cells to the MGMT status in this cell line. Taken together, our findings from methylation analysis suggest that other resistance mechanisms than the repair activity of MGMT might contribute to the observed TMZ-resistance in our subset of glioma cell lines.

We demonstrated that TMZ treatment triggered caspase-dependent apoptosis in the subset of sensitive glioma cells, but not in resistant cells (Figure 3-4). To characterise the ability of all cell lines to undergo apoptosis further, we tested a second apoptotic stimulus with a different mode of action, the broad spectrum kinase inhibitor staurosporine (STS). The microbal alcaloid was shown to induce the mitochondrial apoptotic pathway in a variety of cell types through the inhibition of protein kinases by preventing ATP-binding to

the kinases (Krohn et al. 1998; Chae et al. 2000; O'Reilly et al. 1993). In this study, we were able to demonstrate that despite differences in the way both drugs induce apoptosis, STS treatment evoked a similar pattern of drug sensitivity as demonstrated with TMZ: with the exception of MZ327, the TMZ-resistant cell lines (MZ18, MZ MZ18, MZ51, MZ256, MZ294 and MZ304) also underwent STS-induced apoptosis later than cell lines that were shown to be TMZ-sensitive (U87, U251, U343, U373 and A172). Thus, using two distinct apoptotic stimuli, we were able to discriminate between two drug responder groups, one group with high susceptibility to undergo apoptosis and a second group with low susceptibility to undergo apoptosis. Therefore, the involvement of apoptotic proteins in the underlying molecular mechanism of drug resistance appears to be likely.

The activation of the mitochondrial, caspase-dependent apoptotic pathway results in the release of cytochrome *c* (Li et al. 1997). This triggers the formation of the apoptosome, which consists of the adapter protein Apaf-1 and initiator caspase-9, leading to the cleavage and activation of effector caspase-3 and -7 (Liu et al. 1996; Li et al. 1997). We successfully demonstrated the release of cytochrome *c* in all glioma cell lines following apoptosis induction with STS (Figure 3-6). However, the low amounts of cytochrome *c* in the cytosol in drug-tolerant cell lines compared to drug-sensitive cell lines indicate that mechanisms upstream of the mitochondria might also impair the activation and execution of apoptosis.

In the study presented in this chapter, we established molecular expression profiles of the key apoptotic proteins downstream of mitochondrial apoptotic signalling, the anti-apoptotic caspase inhibitor XIAP and the pro-apoptotic proteins Apaf-1, procaspase-9, procaspase-3 and the XIAP inhibitor Smac. Expression profiles obtained from TMZ-resistant and TMZ-sensitive glioma cell lines were compared to a cohort of 17 patients with GBM grade IV (Table 2-8). The patient samples consisted of two subgroups, short-term (< 10 months) and long-term (≥ 10 months) progression-free survival (PFS), based on the provided patient data. Apoptotic proteins are often dysregulated in cancer, including the components of apoptosome-dependent caspase-activation, Apaf-1, procaspase-9, procaspase-3, Smac and XIAP (Hanahan & Weinberg 2000; Cillessen et al. 2007; Furukawa et al. 2005; Shen et al. 2010; Tirapelli et al. 2010; Nomura et al. 2008; Wagenknecht et al. 1999; Kim et al. 2004). Our single protein expression analysis revealed

a highly heterogeneous expression pattern of apoptotic proteins in glioma cell lines that only partially correlated with the expression pattern found in GBM patient samples. Glioma cell lines generally showed low levels of Apaf-1 and procaspase-9. Low Apaf-1 and procaspase-9 protein abundance could result in a lower frequency of apoptosome assembly. This could reduce the ability of glioma cells to undergo apoptosome-dependent caspase-activation, which could explain the generally low response of the panel of cell lines to cytotoxic agents. When comparing TMZ-resistant and TMZ-sensitive cell lines using the Mann-Whitney test, we found significant differences in the expression levels of procaspase-3, which points to a possible correlation between low levels of active caspase-3 and drug resistance in glioma cell lines. Expression profiles of GBM patient samples revealed highly significant differences between short-term and long-term PFS samples in four apoptotic proteins. Short-term PFS samples displayed reduced levels of procaspase-9 and procaspase-3 and increased levels of XIAP. Long-term PFS samples showed elevated levels of the XIAP-inhibitor Smac as well as procaspase-3. Thus, the only common characteristic of both cell lines and patient samples was the significantly reduced expression of procaspase-3 in resistant cell lines and in short-term PFS samples.

The use of the Mann-Whitney test is limited to single protein to treatment correlations and highly relies on the amount of samples in the analysis to get accurate results. We utilized a multivariate statistical method called principal component analysis (PCA) to combine multiple single protein expressions in a comprehensive analysis that more reflects the interrelationship of these proteins (Brennan et al. 2009; Ringnér 2008; Han 2010). The PCA enabled us to distinguish two groups within the panel of glioma cell lines based solely on the characteristic expression profiles of each cell line put into relation to all expression profiles. This method for pattern recognition does not directly correlate chemotherapeutic sensitivity to the expression of pro- and anti-apoptotic proteins. Thus, following the analysis, we compared the predicted separation into two distinct groups to the actual chemotherapeutic response in glioma cells, which matched with high precision. We found that the PCA predicted TMZ treatment response with high accuracy. The PCA highlighted the influence of XIAP and procaspase-3 expression on the sensitivity of glioma cell lines to apoptotic stimuli. Analysis of GBM patient samples together with the panel of

glioma cell lines also enabled us to discriminate two groups that strongly correlated with long-term and short-term survival. In this PCA, procaspase-9 and Apaf-1 expression was given the major impact on the predictions. In GBM patient samples, we also found high accuracy of the predictions made by the PCA. However, the evaluation of single protein concentrations alone in GBM also displayed a valid option to predict progression-free survival in GBM patients.

We also used a systems medical approach, the APOTO CELL model, to predict the likelihood of a cell to undergo apoptosome-dependent caspase activation (Markus Rehm et al. 2006; Huber et al. 2007). In our study, we were able to clearly discriminate between chemosensitive and resistant cell lines as well as between long-term and short-term progression-free survivors. APOPTO CELL also highlights the important role of XIAP, a presumption that is incorporated into the model system (Markus Rehm et al. 2006). APOPTO CELL was developed based on *in vitro* responses of a HeLa cell line to exposure to STS. In consistency, our results reveal that the highest accuracy of APOPTO CELL prediction was achieved for cell lines, while the predictions for patient samples showed a higher number of false positives (Figures 3-10 and 3-14). APOPTO CELL was also higher predictive of STS treatment outcome than of response to TMZ treatment. Thus, APOPTO CELL represents a reliable tool for the exploration of cellular response to a strong apoptotic stimulus and demonstrates its utility also as a diagnostic model to predict patients outcome.

In conclusion, this study identified distinct clusters of chemotherapeutic sensitivity with respect to the combined expression levels of components of the intrinsic apoptotic pathway downstream of the mitochondria. From the analysis, it was evident that gliomas mostly differ in their expression levels of XIAP and procaspase-3. Single protein expression analysis revealed major differences between glioma cell lines in the expression of procaspase-3. Our cohort of GBM patient samples could be separated based solely on the expression of procaspase-9, procaspase-3, XIAP and Smac. However, the induction of apoptosis is not only defined by the role of individual proteins but also by the relative abundance and the interaction of all proteins in a dynamic network (Hector et al. 2011). Thus, the advantage of using a comprehensive approach such as the PCA and APOPTO CELL in our study lies in a global view on key apoptotic proteins and their relation to each

other and how their interaction influences the drug response to common cytotoxic agents. Additionally, the use of the APOPTO CELL model is convenient because it represents a validated model system that enables us to investigate apoptosis sensitivity in a single specimen as opposed to the larger amount of samples that is required to perform a statistically accurate single protein or principal component analysis.

The development of computational models systems such as APOPTO CELL may one day lead to a more personalised and multi-targeted anti-cancer therapy.

Thus, a targeted therapy aiming at the apoptotic pathway after the mitochondria might provide a valid treatment option to overcome resistance in gliomas. Additionally, the protein expression of procaspase-9, procaspase-3, XIAP and Smac could be utilised as possible predictive markers in GBM patient samples.

4 Prediction of sensitivity to combination therapy in glioblastoma based on molecular expression profiling of pro- and anti-apoptotic proteins

4.1 Introduction

The intrinsic apoptotic pathway is tightly regulated by members of the Bcl-family of proteins (Anon 1998; Nemec & Khaled 2008; Strasser et al. 2005; Adams & S Cory 2007). Bcl-2, Bcl-x_L, Bcl-w and Mcl-1 are part of the anti-apoptotic Bcl-2 like group and interact with pro-apoptotic family members, consisting of the BH3-only proteins Bim, PUMA, Bid and Noxa, among others and the multidomain-proteins Bax and Bak (Ren et al. 2010). Members of the BH3-only family of proteins were shown to either activate Bax and Bak directly or indirectly by binding to the anti-apoptotic Bcl-2 like proteins, thereby releasing Bax and Bak. Bax then translocates to the mitochondria, where it homo-oligomerises with Bak, causing mitochondrial outer membrane permeabilisation (MOMP) (Adams & Cory 2007; Terrones et al. 2008). Dysregulation of pro-apoptotic Bcl-2 family members is a common phenomenon in cancer cells and effectively blocks mitochondrial apoptosis (Lowe et al. 2004; Schwarz et al. 2001; Johnson et al. 2003). Overexpression of the anti-apoptotic protein Bcl-2, for example, reduces the amount of released cytochrome *c*, which contributes to the observed apoptosis-resistant phenotype in gliomas (Schwarz et al. 2001). A promising novel therapy for treatment-resistant tumours, including malignant gliomas has emerged in the recent years in the form of the extracellular ligand tumour necrosis factor-related apoptosis-inducing ligand (TRAIL) (Shah et al. 2005; Jaganathan et al. 2002). TRAIL shows the advantage that it selectively kills tumour cells, with minimal toxicity to surrounding tissue. TRAIL induces apoptosis through binding to the death receptors DR4 and DR5 (also known as TRAIL-R1 and TRAIL-R2), leading to their dimerisation (Pan et al. 1997; von Haefen et al. 2004). The adaptor protein FADD (Fas-associated death domain) binds to the cell death receptors and in turn recruits procaspase-8, which completes the formation of the death inducing signalling complex (DISC) as an activation platform (Kischkel et al. 1995). The cellular FADD-like ICE inhibitory protein (cFLIP) negatively regulates caspase-8 function by competing with caspase-8 for binding FADD at the DISC

(Chang et al. 2002). In cell types that rely on the activation of the mitochondrial apoptotic pathways to execute death receptor signalling (type II cells), caspase-8 activation leads to the cleavage of the Bcl-2 family member Bid to truncated Bid (tBid) (Rudner et al. 2005). tBid then translocates to the mitochondria and induces the intrinsic apoptotic pathway via interactions with Bax and Bak (Sundararajan et al. 2001). Agonistic TRAIL receptor antibodies and human recombinant TRAIL are currently in clinical trials (Fox et al. 2010). TRAIL-induced apoptosis can occur independently of mutations in the transcription factor p53, a major cause of acquired apoptosis resistance in many types of cancer (Fox et al. 2010). Unfortunately, a large percentage of glioma cell lines show resistance to TRAIL-induced apoptosis (Rieger et al. 2007; Panner et al. 2010). The expression and activity of all pro-apoptotic members of the extrinsic apoptotic pathway is crucial for the execution of TRAIL (Kim et al. 2003; Irmler et al. 1997). Combination therapy of TRAIL with TMZ has been suggested as a new therapeutic option with increased potency for patients suffering from GBM (Hingten et al. 2008). Therefore, extending the protein expression analysis to components of both extrinsic and intrinsic apoptotic pathways potentially enlarges the amount of novel drug targets and possible biomarkers and may facilitate a more personalized therapy of patients with GBM.

4.1.1 Aims of this chapter

Mono-treatment with the current drug of choice TMZ has limited success in glioma cell cultures (Figure 3-1). In an effort to improve the performance of glioma therapy, we aimed to investigate the effectiveness of a novel therapeutic, the TNF-related apoptosis inducing ligand (TRAIL), and to analyse the advantage of combination therapy with TMZ and TRAIL in gliomas (Hingten et al. 2008; Uzzaman et al. 2007).

In chapter 3, we identified molecular expression patterns of apoptotic proteins that strongly correlated with chemotherapeutic sensitivity to TMZ in glioma cell lines and with progression-free survival in glioblastoma patient samples. The analysis was limited to components of apoptosome-dependent caspase-activation, a final step during mitochondrial apoptosis after the loss of mitochondrial outer membrane potential (MOMP) and the release

of cytochrome *c* (Markus Rehm et al. 2002). In this study, our aim was to extend the previous analysis by analysing apoptotic proteins involved in the intrinsic apoptotic pathway upstream of the mitochondria, namely the Bcl-2 family of proteins, and by measuring components of the extrinsic apoptotic pathway. Our final goal was to correlate treatment sensitivity to mono-therapy with TMZ or TRAIL or combination therapy with TMZ and TRAIL to the basal expression of these apoptotic proteins.

4.2 Results

4.2.1 Combination therapy with TMZ and TRAIL enhances cell death in glioma cells

The current standard of care, administration of the cytotoxic drug temozolomide (TMZ), was only effective in five of eleven glioma cell lines (Figure 3-1). In order to improve treatment outcome, we utilised TRAIL to activate death receptor signalling, thereby engaging a second apoptotic pathway. The same panel of 11 glioma cell lines as used in chapter 3 (Table 2-6) was treated with TRAIL alone (100 ng/ml) or a combination of TRAIL and TMZ (150 µM) for 24, 48 and 96 hours and analysed using the MTT cell viability assay. Cell lines were displayed in two separate graphs according to the previously examined TMZ-sensitivity to faciliate comparison of cell survival rates after mono TMZ treatment to those obtained after mono TRAIL or dual TMZ- and TRAIL treatment for 24, 48 and 96 hours (Figures 3-1 and 4-1). Glioma cell line A172 showed the highest sensitivity to TRAIL treatment alone with cell survival rates dropping significantly below 50% already after 48 hours (Figure 4-1 A). MZ256 cell numbers decreased below 75%, but still above 50% after 96 hours of treatment (Figure 4-1 B). Cell lines MZ18, MZ51, MZ294, MZ304 and MZ327 (Figure 4-1 A) and U87, U251, U343 and U373 (Figure 4-1 B) did not show a decrease in cell number after TRAIL treatment.

Drug response was generally increased in glioma cell lines after combinatorial treatment with TMZ and TRAIL (Figure 4-1 C-D). The strongest effect was found in U251 cells and A172 cells after 48 hours, with significantly decreased cell viability after 48 hours

(Figure 4-1 D). Cell numbers in cell lines U87 and U343 dropped below 50% after 96 hours treatment (Figure 4-1 D). MZ327, MZ18 and U373 cells displayed cell survival below 75% at 96 h, but still above 50% (Figure 4-1 C-D). Cell lines MZ51, MZ256, MZ294 and MZ304 remained tolerant to the combinatorial treatment (Figure 4-1 C).

The cell survival in the cell line U251 after combined TMZ- and TRAIL-treatment was further reduced when compared to cell survival following single TMZ or TRAIL treatment alone, thus indicating a synergistic effect of both drugs in U251 (see Figure 5-1). Decreased cell survival rates, but to a lesser extend than in U251, were also found in U373 and MZ18. Levels of cell death in A172 did not succeed cell death rates after TRAIL administration alone, indicating that A172 is mainly sensitive to TRAIL treatment and to a lesser extend to TMZ after 96 and 120 hours (Figure 3-1). U87 and U343 cell lines both displayed low differences between TMZ sensitivity and TMZ and TRAIL combined sensitivity.

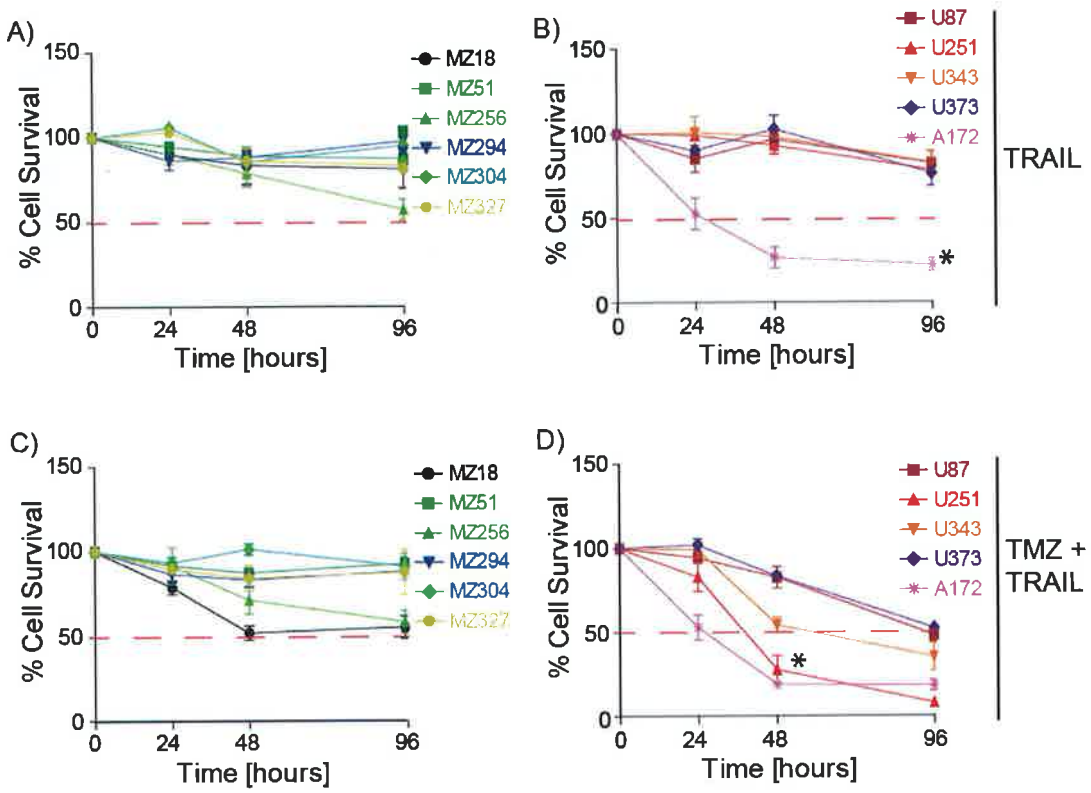

Figure 4-1 Drug response to TRAIL alone and TMZ plus TRAIL in combination

Assessment of cell survival during four days of TRAIL treatment (100 ng/ml) and combination treatment with TMZ (150 µM) and TRAIL (100 ng/ml) in 11 glioma cell lines. MTT assay following treatment for 24 h, 48 h and 96 h. Red dashed lines indicate 50% cell survival. **A) and B)** TRAIL treatment. Cell lines MZ18, MZ51, MZ294, MZ304 and MZ327 and U87, U251, U343 and U373 did not show a decrease in cell number. MZ256 cell survival was below 75% after 96 h, A172 survival below 50% after 48 h. **C) and B)** TT treatment.. MZ51, MZ256, MZ294 and MZ304 cells were tolerant to the treatment, MZ327, MZ18 and U373 displayed survival below 75% at 96 h and U87, U251, U343 and A172 below 50% at 96 h. Synergistic effect of both drugs was observed in U251 cells after 48 h treatment and to a lesser extend in MZ18 and U373 cells after 96 hours. **A and B)** Data points are means ± SEM of three independent experiments in sextuplicates; * indicates $p \leq 0.005$, Student's t test.

The drug sensitivity of our panel of glioma cell lines is summarized in Table 4-1. Treatment response was classified as tolerant (-) when the survival was above 75% after 96 hours, low response (+) below 75%, but above 50% survival after 96 hours, medium response (++) below 50% survival after 96 hours and high response (+++) below 50% after 48 hours treatment.

Table 4-1 Sensitivity to TMZ, TRAIL or combination of TMZ and TRAIL

Cell line	TMZ (150 μM) (Figure 3-1)	TRAIL (100 ng/ml)	TMZ (150 μM) + TRAIL (100 ng/ml)
MZ18	-	-	+
MZ51	-	-	-
MZ256	-	+	+
MZ294	-	-	-
MZ304	-	-	-
MZ327	-	-	-
U87	++	-	++
U251	++	-	+++
U343	++	-	++
U373	+	-	++
A172	+	+++	+++

-	Tolerant
+	Cell survival below 75% after 96 hours treatment; low response
++	Cell survival below 50% after 96 hours treatment; medium response
+++	Cell survival below 50% after 48 hours treatment; high response

4.2.2 Bcl-2 protein family expression in glioma cell lines

In chapter 3, we analysed the expression of apoptotic proteins that function downstream of the mitochondria in the intrinsic apoptotic pathway. Expression of the Bcl-2 family of proteins, key regulators of apoptosis that mainly act upstream of the mitochondria, is also regularly distorted in cancer cells (Lowe et al. 2004). TMZ and TRAIL can both activate the mitochondrial pathway depending on the expression and activity of Bcl-2 family members (Schwarz et al. 2001; Johnson et al. 2003; Vogler et al. 2008; Gillissen et al. 2010; Hingten et al. 2008). The overexpression of anti-apoptotic proteins can effectively block the cellular response to TRAIL, thus rendering the cancer cells resistant to TRAIL treatment (Huang & Sinicrope 2008; Gillissen et al. 2010; Johnson et al. 2003). To explain cellular responsiveness in glioma cell lines to single therapy with TMZ or TRAIL or combination therapy with TMZ and TRAIL (Figure 4-1), we established protein expression profiles of Bcl-2 family members. Expression levels of pro-apoptotic BH3-only proteins Bim, PUMA, Noxa and Bid, anti-apoptotic Bcl-2 like family members Bcl-2, Bcl-x_L, Mcl-1 and Bcl-w and pro-apoptotic multidomain proteins Bak and Bax were analysed in whole cell extracts using western blotting and densitometry analysis (Figures 4-2 and 4-3). Protein expression levels were normalised to the β-actin loading control and expressed relative to HeLa protein levels set at 100%. Glioma cell lines were labelled according to sensitivity to dual TMZ and TRAIL treatment (TT) for 96 hours (Table 4-1) (Figure 4-3).

All glioma cell lines showed elevated expression of the anti-apoptotic proteins Bcl-2 and Bcl-x_L and decreased protein levels of Bcl-w and Mcl-1 when compared to HeLa (Figures 4-2 and 4-3 B). The multidomain proteins Bak and Bax were generally overexpressed in glioma cell lines when compared to HeLa (Figure 4-3 C). Expression of the BH3-only protein Bim is highly heterogeneous: High Bim expression levels were found in U251 and U343 cell lines, intermediate expression in MZ256 and MZ304 and a general downregulation of Bim was eminent in the rest of the cell lines (Figure 4-3 A). Expression of PUMA, Noxa and Bid was also highly heterogeneous.

When analysing varied drug responder groups, glioma cell lines show significant differences in the expression of Bcl-2 family members: In single TMZ-treatments, the

Mann-Whitney test revealed significant differences between TMZ-sensitivity (U87, U251, U343, U373 and A172) and TMZ-resistant (MZ18, MZ51, MZ294, MZ304 and MZ327) cell lines only in the protein levels of Bcl-x_L ($p = 0.04$; TMZ) (Figure 4-3 B).

Mann-Whitney tests were also performed to compare protein expression in TRAIL-responsive cell lines (A172 and MZ256) and TRAIL-resistant cell lines (MZ18, MZ51, MZ256, MZ294, MZ304, MZ327, U87, U251, U343 and U373), but no significant difference was found (Figure 4-3).

In dual TMZ and TRAIL treatment, a statistical significance between TT-tolerant cell lines (MZ51, MZ294, MZ304 and MZ327) and TT-sensitive cell lines (MZ18, MZ256, U87, U251, U343, U373 and A172) was found in the expression levels of Noxa ($p = 0.05$; TT) and Bcl-w ($p = 0.02$; TT) (Figure 4-3 A and B). However, Bcl-w expression was generally low in glioma cell lines, indicating that the observed differences in Bcl-w levels might not have a major impact on apoptosis.

Thus, the single protein analysis highlights a possible correlation between low Bcl-x_L protein expression and TMZ-sensitivity and between high Noxa protein expression and combinatorial TMZ and TRAIL-sensitivity. However, a significant protein expression signature within the Bcl-2 family of proteins that would clearly predict chemosensitivity to all therapies could not be identified.

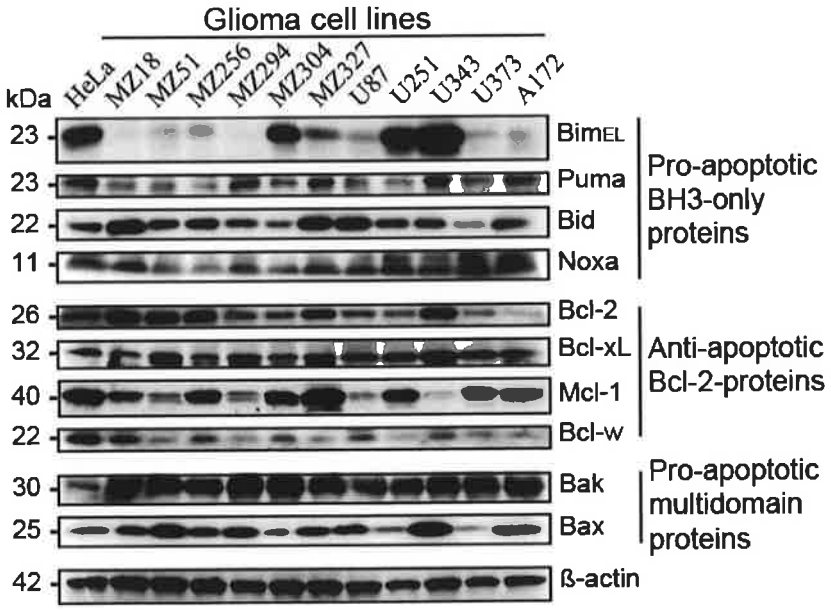

Figure 4-2 Bcl-2 protein family expression in glioma cell lines

Molecular expression analysis of pro- and anti-apoptotic members of the Bcl-2 family of proteins in glioma cell lines. Representative western blots showing expression levels of pro-apoptotic BH3-only proteins Bim, PUMA, Bid and Noxa, anti-apoptotic Bcl-2, Bcl-x_L, Mcl-1 and Bcl-w and pro-apoptotic multidomain proteins Bak and Bax. Data are representative of two to three independent experiments. β-actin was used as a loading control.

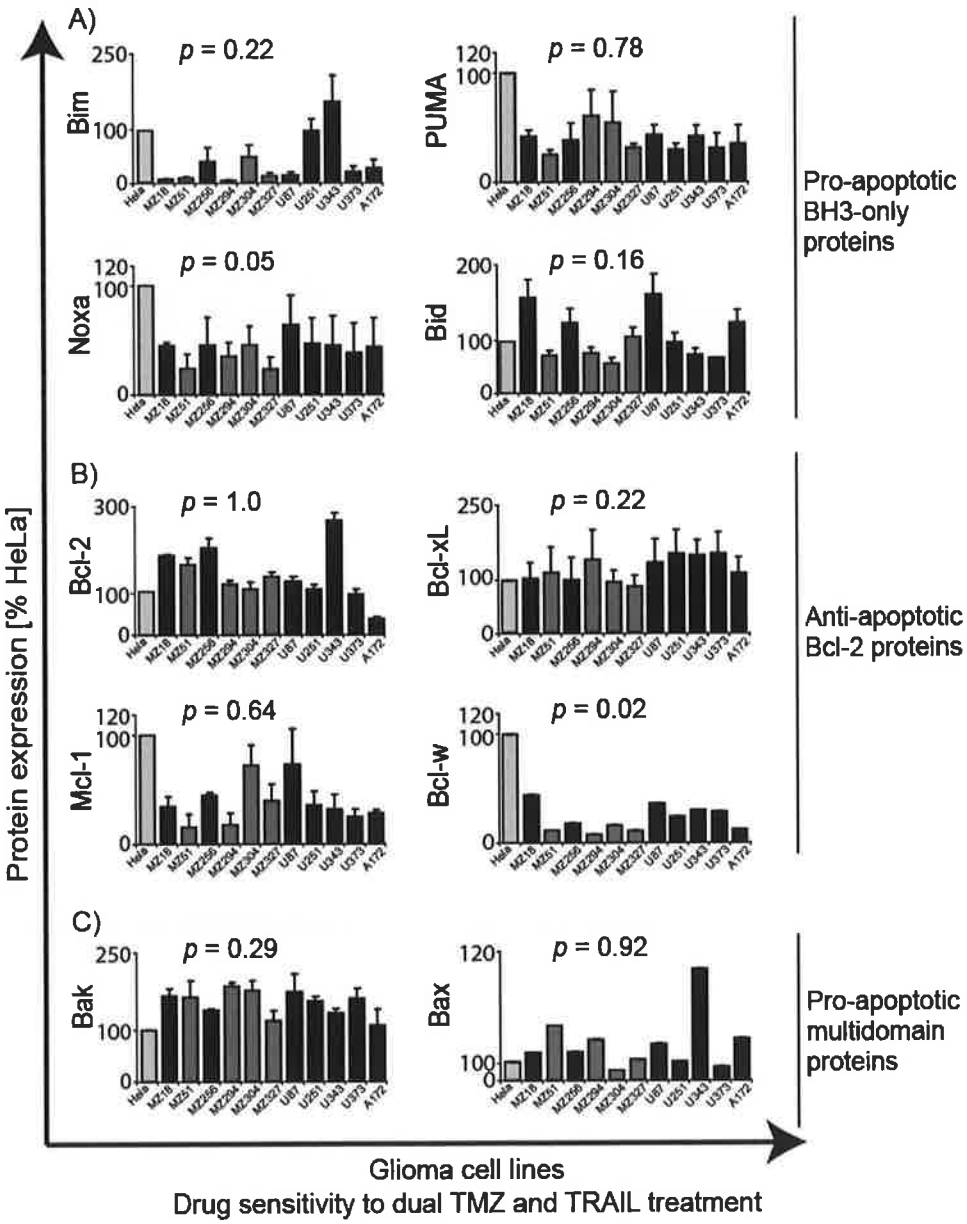

Figure 4-3 Expression profiles of the Bcl-2 family of proteins

Densitometry analysis of molecular expression patterns of the Bcl-2 family of proteins. Bars are labelled according to responsiveness to dual TMZ and TRAIL therapy, dark grey (tolerant), black (sensitive), Hela standard (light grey). **A)** Pro- apoptotic BH3-only's. Differential expression patterns for Bim were found in glioma cell lines, with MZ256, MZ304, U251 and U343 displaying high Bim levels, and the other cell lines showing downregulation of Bim. Significant downregulation of Noxa in TT-resistant cells in comparison to TT-sensitive cells. **B)** Anti-apoptotic

Bcl-2's. Low levels of Bcl-w and Mcl-1 were found in comparison to HeLa. Bcl-w expression was significantly different between sensitive and resistant cells, but also showed high differential expression within each group. **C)** Pro-apoptotic multidomain-proteins. Differential expression of Bax and overexpression of Bak is without statistical significance. Data are means ± SEM of two - three western blots; Values were normalised to β-actin and expressed relative to HeLa standard set to 100%. p values ≤ 0.05 were considered significant; Mann-Whitney test.

4.2.3 Distorted expression of the Bcl-2 family of proteins in GBM patient samples

As explained in chapter 3, cancer cell lines as a preclinical model sometimes do not display the same molecular features as the associated primary human tumour (Lee et al. 2006; Romer & Curran 2005). It is therefore advisable to verify the described expression pattern of Bcl-2 family members in glioma cell lines in glioblastoma patient samples (Figure 4-3). We performed western blot and densitometry analysis on homogenized lysates of tumour tissue samples in the cohort of 17 GBM specimens (Chapter 2, Table 2-8; Figures 4-4 and 4-5). The GBM patient cohort consisted of 10 short-term progression-free survival samples (PFS > 10 months) and 7 long-term progression-free survival samples (PFS ≤ 10 months). Protein expression levels were normalised to the β-actin loading control and expressed relative to protein levels of a HeLa cell line set to 100%.

In all GBM patient samples, we found elevated expression levels of anti-apoptotic Bcl-2 like proteins Bcl-2 and Bcl-x_L when compared to HeLa, in consistency with the findings in glioma cell lines (Figures 4-3 and 4-5 B). The BH3-only protein Bim was generally downregulated in GBM patient samples (Figure 4-5 A).

When comparing short-term and long term progression-free survivors, we found that Bcl-2 and Bcl-w were significantly upregulated in short-term survival patients (p = 0.003 and p = 0.0008, respectively; Mann-Whitney test) (Figure 4-5 B). However, as in glioma cell lines, Bcl-w was also highly heterogeneously expressed between individual samples. No significant difference in Bim expression was found between short-term and long term PFS samples (p = 0.81; Mann-Whitney test) (Figure 4-5 A). Protein expression of the multidomain protein Bak was elevated in the majority of long-term PFS samples,

except for sample #3 and #7 ($p = 0.009$; Mann-Whitney test) (Figure 4-5 C). Thus, glioma cell lines share common characteristics with GBM patients in the general overexpression of anti-apoptotic proteins Bcl-2 and Bcl- x_L. Additional, both treatment-resistant glioma cell lines and short-term progression-free survivors show higher expression of Bcl-2 (Bcl-x_L in glioma cell lines) and Bcl-w.

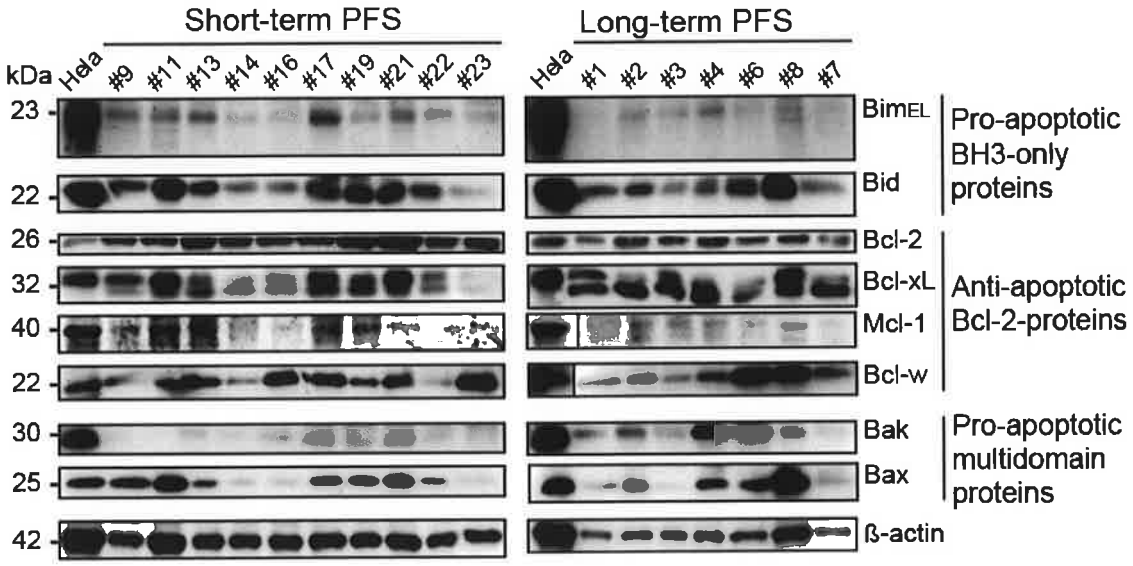

Figure 4-4 Expression of Bcl-2 family members in GBM patient samples

Western blots showing protein expression of Bcl-2 family members Bim, Bid, Bcl-2, Bcl-x_L, Mcl-1, Bcl-w, Bak and Bax in glioblastoma patient samples with short-term or long-term PFS. The BH3-only protein Bim was generally low expressed in GBM patient samples. PFS = progression-free survival; β-actin was used as loading control.

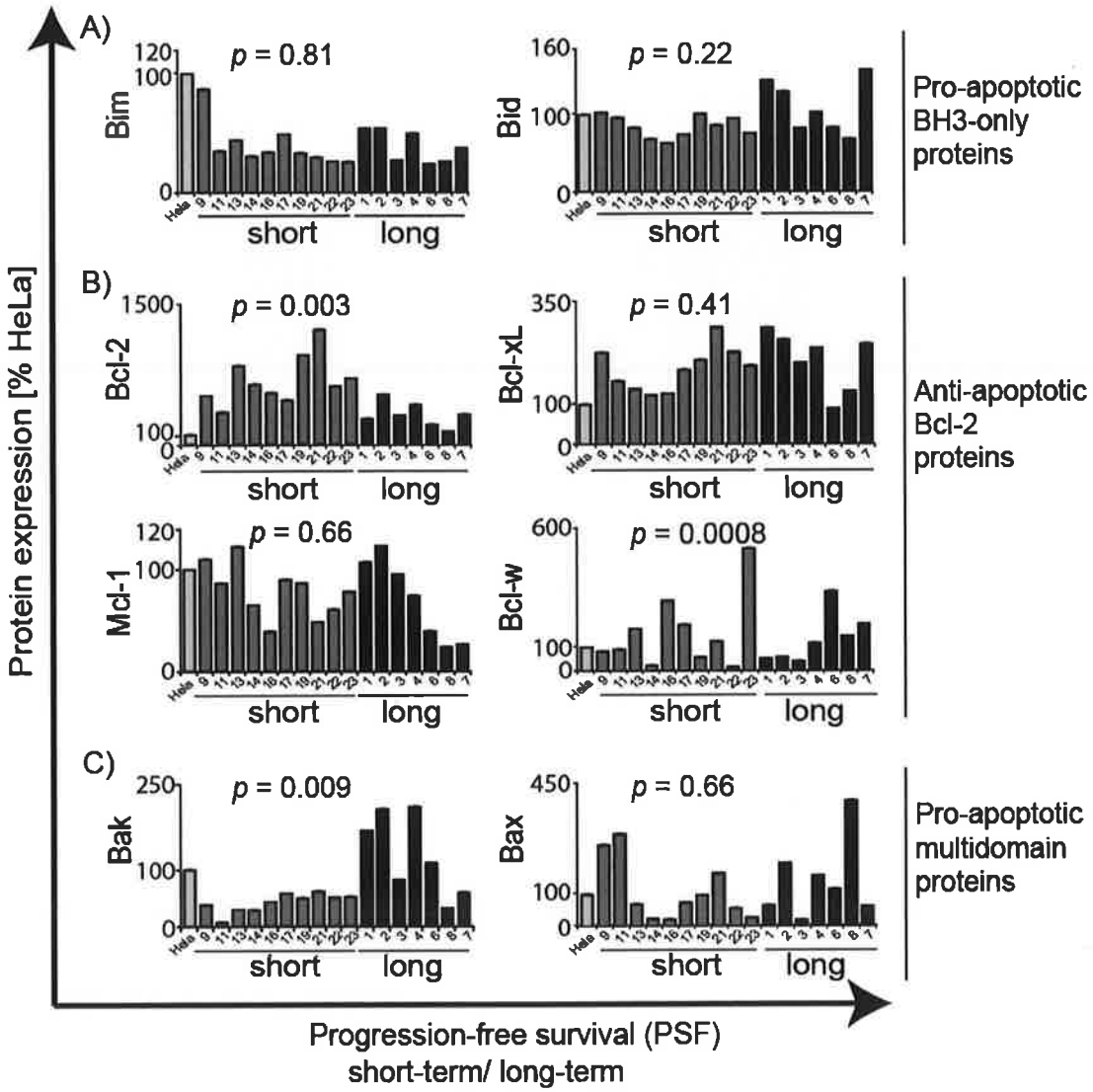

Figure 4-5 Densitometry analysis of Bcl-2 family members in GBM patient samples

Protein expression of Bcl-2 family members Bim, Bid, Bcl-2, Bcl-x_L, Mcl-1, Bcl-w, Bak and Bax in glioblastoma patient samples with long-term and short-term progression-free survival (PFS). Bars are labelled dark grey for short-term PFS and black for long-term PFS; Hela standard in light grey. **A)** Pro-apoptotic BH3-only proteins. Bim protein was generally low expressed in glioblastoma patient samples when compared to HeLa. **B)** Anti-apoptotic Bcl-2's. Bcl-2 and Bcl-x_L were overexpressed in comparison to HeLa. Bcl-2 protein levels were higher in short-term PFS than in long-term PFS. **C)** Pro-apoptotic multidomain proteins. Significant higher expression levels of Bak in long-term PFS than in short term PFS. Data represent one western blot per protein, protein levels

were normalised to ß-actin and expressed as percentage of HeLa (set at 100%). $p \leq 0.05$ were considered significant; Mann-Whitney test.

4.2.4 Chemosensitivity in glioma cell lines can only partially be correlated with distorted Bcl-2 family member expression

Next, we utilized the Principal Component Analysis (PCA) as previously described in chapter 3 to investigate if a pattern in the expression of Bcl-2 family members in glioma cell lines could explain the drug responses to TMZ, TRAIL or dual TMZ and TRAIL treatment (Figures 4-1 and 4-3). Expression levels of Bim, PUMA, Noxa, Bid, Bcl-2, Bcl-x_L, Mcl-1, Bcl-w, Bak and Bax in glioma cell lines (Figure 4-3) were used relative to expression levels in HeLa cells (100%) in the PCA. Figure 4-6 displays a two-dimensional coordination system, in which the glioma cell lines are clustered based on their individual protein expression profiles of Bcl-2 family members in relationship to protein expression profiles as found in all glioma cell lines. Principal Component 1 (PC 1) and Principal Component 2 (PC 2) together explained 45.6% of the variance in the data set (Table 4-2). Bim, Bax and Bcl-x_L expression variation had the highest influence on PC 1. Bcl-2 and Noxa had the highest impact on PC 2. Therefore, the expression of Bim and Bcl-2 could have a strong influence on treatment response in glioma cell lines.

Table 4-2 Coefficients in PCA based on Bcl-2 family expression in glioma cell lines

PC	Bim	PUMA	Noxa	Bid	Bcl-2	Bcl-xL	Mcl-1	Bcl-w	Bak	Bax
1	0.498	-0.156	0.294	-0.212	0.285	0.445	-0.262	0.133	-0.142	0.459
2	0.168	0.275	-0.455	0.243	0.561	-0.240	0.298	0.257	0.064	0.314

Areas of assumed drug sensitivities (set to 100% specificity) were drawn around those cell lines that showed experimental sensitivity to TRAIL, TMZ or TMZ and TRAIL (taken from Figure 4-1; Table 4-1). The area of TRAIL sensitivity (blue box) contained TRAIL-sensitive cell lines A172 and MZ256. TRAIL-resistant cell line MZ294 also localized in this area as a false positive of the PCA. The area of TMZ sensitivity was drawn around cell

lines U87, U251, U343, U373 and A172 and falsely included TMZ-resistant cell lines MZ51, MZ256 and MZ294. Combined TMZ and TRAIL sensitivity is assumed around MZ18, MZ256, U87, U251, U343, U373 and A172, the resistant cell lines MZ51 and MZ294 also falsely located in this area.

The PCA predicted positive response to TRAIL treatment in glioma cell lines with 66.66% sensitivity (two-tailed p value equalled 0.05 in Fisher's exact test). TMZ effect was predicted with 62.5% sensitivity (two-tailed p value equalled 0.18 in Fisher's exact test). The sensitivity to combined TMZ and TRAIL was 77.77% (two-tailed p value equalled 0.11 in Fisher's exact test).

In conclusion, the comprehensive analysis of the Bcl-2 family members did not enable us to clearly distinguish between cell lines that are sensitive or resistant to either TMZ or TRAIL or dual TMZ and TRAIL treatment.

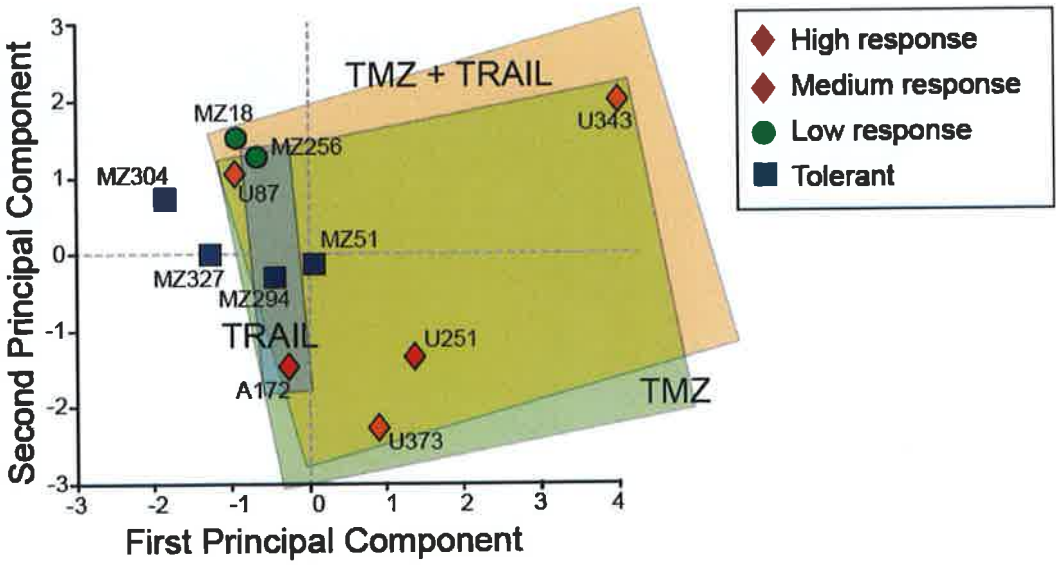

Figure 4-6 Clustering of glioma cell lines based on drug response in a Bcl-2 family expression-dependent PCA

PCA plot based on protein expression profiles of Bcl-2 family members in glioma cell lines. Clustering of glioma cells did not correlate well with the actual drug response to single TMZ or TRAIL treatment or to combination therapy with TMZ and TRAIL. Areas of assumed TRAIL sensitivity (blue box), TMZ sensitivity (green box) and TMZ plus TRAIL sensitivity (orange box), are indicated. Individual cell lines are labelled according to combined TMZ and TRAIL treatment sensitivity as explained in the legend and in Table 4-1.

4.2.5 Tumour progression in glioblastomas can only partially be correlated with distorted Bcl-2 family member expression

Next, we performed a Principal Component Analysis on the protein expression profiles of Bcl-2 family members in the cohort of GBM patient samples. Expression levels of Bim, Bid, Bcl-2, Bcl-x_L, Mcl-1, Bcl-w, Bak and Bax in GBM patient samples (Figure 4-4) were used relative to expression levels in HeLa cells (100%). The original variance in the matrix was explained by 52.8% with Principal Component 1 (PC 1) and Principal Component 2 (PC2). PC 1 was plotted against PC 2 in a 2-dimensional grid (Figure 4-7). Bcl-x_L, Bak and Bid had the highest influence for the first PC, Bax, Bcl-2 and Bcl-w for the second PC (Table 4-3). Therefore, the progression-free survival time in GBM patient samples might be influenced by the expression of Bcl-x_L and Bax (Figure 4-7).

Table 4-3 Coefficients in PCA of GBM patient samples

PC	Bim	Bid	Bcl-2	Bcl-xL	Mcl-1	Bcl-w	Bak	Bax
1	0.417	0.443	-0-016	0.471	0.378	0.257	0.444	-0.013
2	0.209	0.261	-0.499	-0.044	-0.191	-0.434	0.005	0.642

GBM patient samples of short-term PFS were found in the lower quadrants of the coordination system, long-term PFS GBM patient samples were mainly located in the upper quadrants of the grid. Two short-term PFS samples and one long-term sample were falsely placed on the wrong side, respectively.

The PCA analysis predicted clustering of the GBM patient samples into short-term and long-term progression-free survival with 85.71% sensitivity and 80% specificity (two-tailed *p* value equalled 0.02 in Fisher's exact test).

Thus, similar to findings made in glioma cell lines, GBM patient samples are only inefficiently clustered according to their progression-free survival time when utilising protein expression profiles of the Bcl-2 family of proteins. In conclusion, analysis of the Bcl-2 family alone might be insufficient to recognise a clear molecular pattern in glioblastomas.

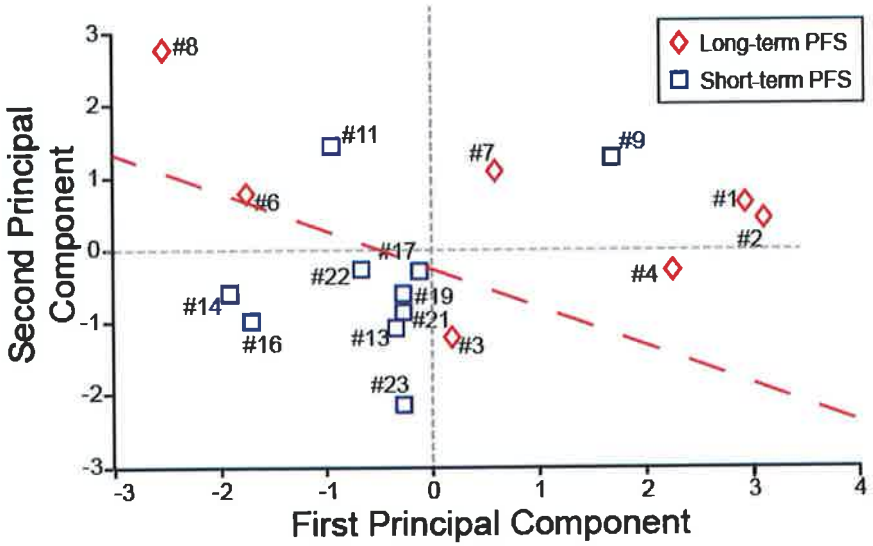

Figure 4-7 Clustering of GBM patient samples based on drug response in a Bcl-2 family expression-dependent PCA

Coordination system illustrating clusters according to tumour progression in GBM patient samples. Dashed red line indicates a possible separation between short-term (blue rectangle) PFS patient samples and long-term (red rectangle) PFS patient. Three values were positioned on the wrong side in the coordination system. Data was based on the protein expression of Bim, Bid, Bcl-2, Bcl-x_L, Mcl-1, Bcl-w, Bak and Bax in 17 GBM patient samples relative to protein expression levels in a HeLa cell line (100%).

4.2.6 Glioma cell lines show differential protein expression of compounds of the intrinsic apoptotic pathway

As reported in chapter 3, treatment response to TMZ-monotherapy can be predicted with high accuracy by analysing the components of apoptosome-dependent caspase-activation in the intrinsic apoptototic pathway in a PCA (Figure 3-1, 3-8 and 3-9). However, our PC analysis based on the Bcl-2 family of proteins (Figure 4-3) could not exactly predict chemotherapeutic sensitivity to single TRAIL or combination of TMZ and TRAIL treatment in glioma cell lines (Figure 4-4). The ligand TRAIL activates the extrinsic apoptotic pathway by binding to death receptors at the cell surface (Pan et al. 1997). We therefore analysed five additional proteins that are involved in the initial steps of cell death receptor signalling: the TRAIL-receptors DR4 and DR5, the anti-apoptotic caspase-8 homologue $cFLIP_L$, caspase-8 and the adaptor molecule FADD (Figure 4-8 and Figure 4-9). Values were normalised to β-actin and expressed relative to HeLa standard set to 100%. The death receptors DR4 and DR5 and caspase-8 were generally low expressed in glioma cell lines when compared to HeLa cells (Figure 4-9). The Mann-Whitney test for significance was performed between TRAIL-, TMZ- or TT-responder groups. Following mono-therapy with the direct inducer of death receptor signalling TRAIL, we found no significant difference between the two TRAIL-responder groups, TRAIL-resistant (MZ18, MZ51, MZ294, MZ304, MZ327, U87, U251, U343 and U373) and TRAIL-sensitive cell lines (MZ256 and A172) (Figures 4-1 and 4-9). We also correlated the response to single TMZ treatment to expression of death receptor signalling components and found no significant difference between TMZ-resistant (MZ18, MZ51, MZ256, MZ294, MZ304 and MZ327) and TMZ-sensitive cell lines (U87, U251, U343, U373 and A172) (Figures 3-1 and 4-1; Table 4-1). When comparing dual TMZ and TRAIL treatment, however, we found significant differences in the expression levels of procaspase-8 (p = 0.02; TT; Mann-Whitney test) between TT-resistant (MZ51, MZ294, MZ304 and MZ327) and TT-sensitive cell lines (MZ18, MZ256, U87, U251, U343, U373 and A172) (Figures 4-1 and 4-9, indicated as TT-sensitive (black bars) and TT-resistant (dark grey bars) in the graph). Thus, the response to combination therapy with TMZ and TRAIL might be determined by the expression on procaspase-8.

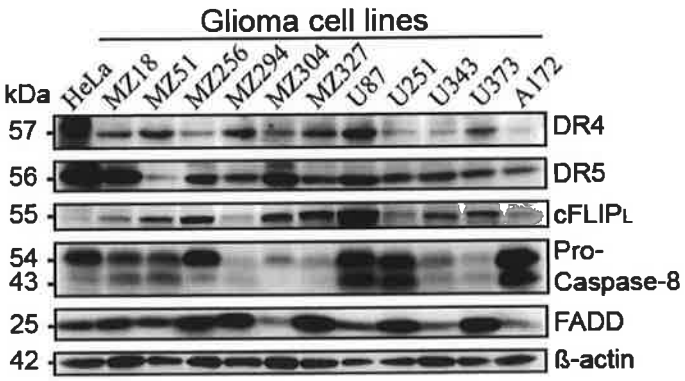

Figure 4-8 Protein expression of apoptotic proteins involved in the extrinsic pathway

Representative western blots showing expression of components involved in death receptor signalling in glioma cell lines: DR4, DR4, $cFLIP_L$, caspase-8 and FADD were analysed in whole cell lysates. β-actin was used as a loading control. Data are representative of three independent experiments.

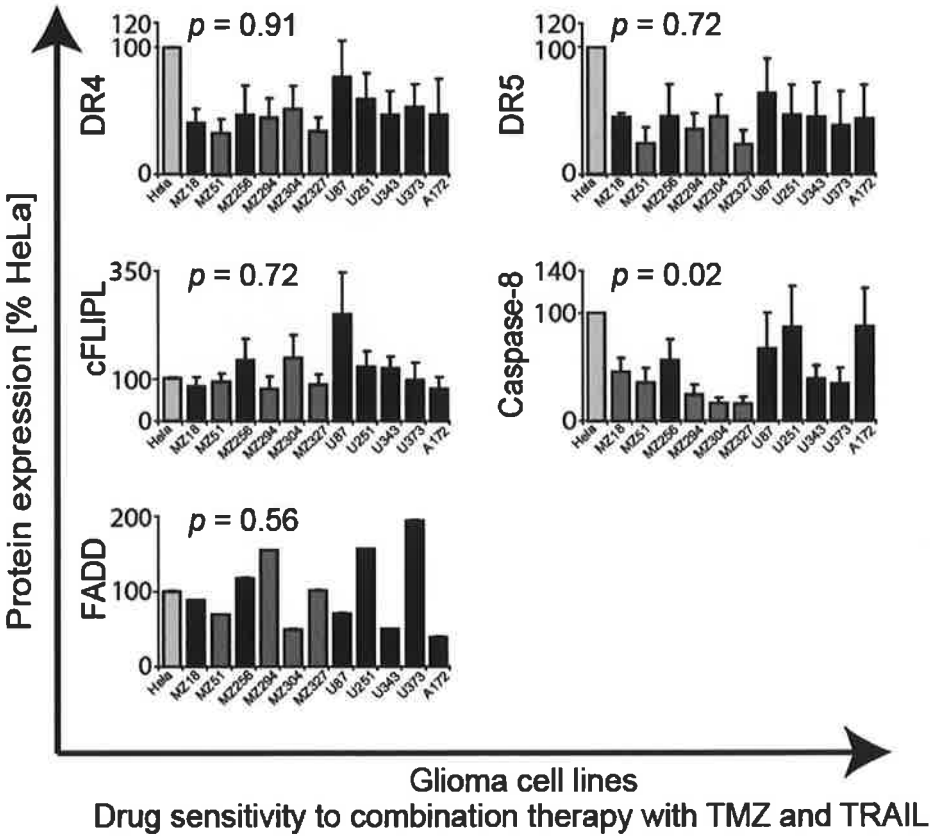

Figure 4-9 Expression of components of cell death receptor signalling in glioma cell lines

Densitometry analysis of western blots monitoring the expression of components of death receptor signalling, DR4, DR4, $cFLIP_L$, caspase-8 and FADD. Bars are labelled for TT sensitivity in dark grey (tolerant), black (sensitive), Hela standard (light grey). DR4, DR5 and caspase-8 were generally low expressed in glioma cell lines when compared to HeLa cells. Caspase-8 expression was significantly lower in tolerant cell lines compared to sensitive cell lines. Data are representative of one western blot or means ± S.E.M of three western blots; Values were normalised to β-actin and expressed relative to HeLa standard set to 100%. p values ≤ 0.05 were considered significant; Mann-Whitney test.

4.2.7 Comprehensive cluster analysis of 21 components involved in both intrinsic and extrinsic apoptotic pathways

In chapter 3, we demonstrated that the drug response of our panel of glioma cell lines to cytotoxic agents could be predicted with high accuracy by the analysis of proteins involved in late steps of apoptotic signalling after MOMP. Chemotherapeutic sensitivity to TRAIL or a combination therapy with TMZ and TRAIL, however, cannot be sufficiently explained by the analysis of Bcl-2 family members, which act upstream of the mitochondria (Figures 4-6 and 4-7). In our final Principal Component Analysis, we combined the protein expression profiles of 21 pro-and anti-apoptotic proteins in glioma cell lines: proteins involved in apoptosome-dependent caspase activation (Figure 3-7), the Bcl-2 family of proteins (Figure 4-2) and components of death receptor signalling (Figure 4-8). Protein expression levels were used relative to expression levels in HeLa cells (100%). The calculated Principal Component 1 (PC 1) and Principal Component 2 (PC 2) together explained 48.7% of the variance in the data set (Table 4-4). DR4, DR5, cFLIP, caspase-3 and caspase-9 had the highest influence on PC 1. XIAP, Mcl-1, Noxa, and Bcl-x_L had the highest impact on PC 2.

Thus, the sensitivity of glioma cell lines to a combination therapy with TMZ and TRAIL most likely depends on the expression levels of TRAIL-receptors, the anti-apoptotic protein XIAP and Bcl2-like proteins.

Table 4-4 **Coefficients in PCA of 21 components of the intrinsic and extrinsic apoptotic pathways**

Protein	PC 1	PC 2
Caspase-3	0.299	-0.233
Caspase-9	0.286	0.262
XIAP	0.037	0.406
Smac	0.247	-0.116
Apaf-1	0.068	0.193
Bim	0.114	-0.183
PUMA	0.074	0.219
Noxa	0.196	-0.335
Bid	0.177	0.116
Bcl-2	-0.014	0.089
Bcl-x_L	0.203	-0.334
Mcl-1	0.232	0.335
Bcl-w	0.275	0.057
Bak	0.137	0.171
Bax	-0.026	-0.139
DR4	0.383	0.007
DR5	0.372	0.078
$cFLIP_L$	0.313	0.196
Caspase-8	0.201	-0.245
FADD	0.043	-0.193
Cytochrome *c*	0.242	-0.172

Figure 4-10 illustrates the clustering of glioma cell lines according to a common molecular pattern in a two-dimensional coordination system after PCA on expression profiles of 21 pro- and anti-apoptotic proteins. Based on our previous analysis of drug sensitivity (Table 4-1) we were able to define areas with high probability of response to TMZ, TRAIL or TMZ and TRAIL (100% sensitivity and 100% specificity; two-tailed p values equalled 0.002 for TMZ treatment, 0.02 for TRAIL treatment and 0.003 for dual TMZ and TRAIL treatment in Fisher's exact test). No "false positives", i.e. resistant cell lines in close proximity to cell lines with a specific drug sensitivity were identified. Our results show that there is a clear correlation between the established molecular expression profiles and sensitivity to TMZ or TRAIL mono-therapy and to combination therapy with TMZ and TRAIL.

Thus, by analysing the expression of components of both the extrinsic and intrinsic apoptotic pathway, we were able to predict cellular response to mono- and dual therapy with high accuracy.

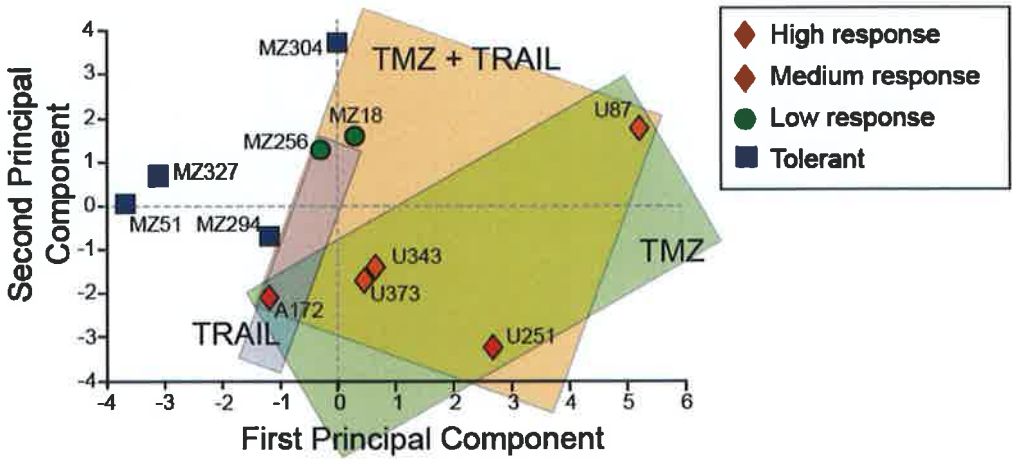

Figure 4-10 PCA analysis of extrinsic and intrinsic apoptotic pathway components in glioma cell lines

PCA blot based on the expression of 21 pro-and anti-apoptotic proteins in glioma cell lines. The distribution of the cell lines correlated strongly with the individual drug response to TMZ, TRAIL or dual TMZ and TRAIL treatment. Areas of assumed TRAIL sensitivity (blue box), TMZ sensitivity (green box) and TMZ plus TRAIL sensitivity (orange box), are indicated. Individual cell lines are labelled according to combined TMZ and TRAIL treatment sensitivity as explained in the legend and in Table 4-1.

4.3 Discussion

In this chapter, we analysed the potential of utilising the protein expression profiles of Bcl-2 family members alone or in combination with proteins involved in upstream signalling of the death receptor pathway and downstream signalling following the release of cytochrome *c* and apoptosome-dependent caspase-activation, to predict treatment sensitivity to mono therapy with TMZ or TRAIL or to dual therapy with TMZ and TRAIL in glioblastomas (Figures 4-1, 4-3, 4-6, 4-9 and 4-10). Protein expression profiles of the Bcl-2 family of proteins in glioma cell lines beard similarities to profiles found in GBM patient samples, thus indicating a common pattern of apoptotic dysregulation in glioblastomas (Figures 4-3 and 4-5).

Cell death in cancer cells is determined by a complex interplay of pro- and anti-apoptotic proteins (Dai & Grant 2007; Gillissen et al. 2003; Adams & Cory 1998). One of the most promising novel approaches of cancer therapy that has emerged in recent years is the targeting of death receptor signalling (Kischkel et al. 1995; Elias et al. 2009; Papenfuss et al. 2008). We initially investigated chemotherapeutic sensitivity to mono-therapy with TRAIL (100 ng/ml) (Figure 4-1 A and B). Resistance of many types of cancer, including glioma cell lines, to mono-therapy with TRAIL has been previously reported and can be caused by the overexpression of anti-apoptotic Bcl-2-like proteins (Fakler et al. 2009; Vogler et al. 2008; Gillissen et al. 2010; Rieger et al. 2007; Panner et al. 2010). Pronounced resistance against TRAIL was also found in our study: from the 11 cell lines investigated in this study, only one cell line, A172, was highly responsive to single TRAIL-treatment, and a second cell line, MZ256, showed low response. In our experiments, the response of U87 and U251 to TRAIL alone at the chosen time point was considerably low. However, another study from Hetschko et al. showed that treatment with a higher TRAIL dose (250 ng/ml instead of 100 ng/ml as in our experiments) can trigger high cell death rates in U87 and U251 cells, while the cell lines U373 and MZ18 still showed resistance (Hetschko et al. 2007). Therefore, U87 and U251 are sensitive to TRAIL depending on the drug dose.

A combination therapy with TMZ and TRAIL, however, was highly effective at a low dose of TRAIL in U251 cells and also increased cell death in other glioma cell lines, in accordance with previously published results (Uzzaman et al. 2007) (Figure 4-1; Tables 2-6

and 4-1): The administration of TMZ (150 μM) and TRAIL (100 ng/ml) in combination affected seven cell lines (MZ18, MZ256, U87, U251, U343, U373 and A172) and thus more cell lines than after mono-therapies with each drug alone (Figures 3-1 and 4-1). Comparison of cell survival rates after mono-therapies with those from combination therapy yet revealed that dual TMZ and TRAIL-treatment effectively potentiated chemotherapeutic sensitivity in just in three cell lines: MZ18, U251 and U373 displayed a stronger response to combination therapy than to mono-therapy with each drug alone. The cell line U251 exibited the highest response to combination therapy (Figure 4-1 D). The synergistic effect of TMZ and TRAIL on the U251 cell line will be further investigated in chapter 5 (Figure 5-2). The effectiveness of a combination of death receptor signalling-inducing agents and the standard therapy TMZ on cell viability has been previously demonstrated (Uzzaman et al. 2007; Hingten et al. 2008; Roth et al. 2011). Administration of the death receptor ligand APO010 accompanied by TMZ was shown to trigger caspase-dependent cell death in glioma cells (Roth et al. 2011). The cell death ligand TRAIL and TMZ were described to act in synergy to increase apoptosis in glioma cell lines and neuronal stem cells (NSC) (Uzzaman et al. 2007; Hingten et al. 2008). Thus, combination therapy with TMZ and TRAIL is a highly promising treatment strategy and should be considered in the therapy of for treatment-resistant glioblastomas.

Our previous results showed that TMZ-sensitivity in glioma cell lines can be predicted with high accuracy using single protein expression analysis, comprehensive multivariate analysis (PCA) and the computational model system APOPTO CELL (Figures 3-8, 3-9 and 3-10) based on a systemic approach that combines expression profiles of component of apoptosome-dependent caspase-activation (chapter 3). This approach was limited to the intrinsic apoptotic pathway downstream of the mitochondria and was not predictive of TRAIL or TMZ and TRAIL sensitivity (Figure 3-6). The Bcl-2 family of proteins is mainly involved in the regulation of apoptosis upstream of the mitochondria (Nemec & Khaled 2008; Adams & Cory 1998; Wong & Puthalakath 2008). Bcl-2 Family members were shown to undergo up- or downregulation in TMZ- or TRAIL-induced apoptosis. Overexpression of Bcl-2 and Bcl-x_L is associated with apoptosis inhibition and increased tumour resistance to most chemotherapy agents (Amundson et al. 2000; Meike

Vogler et al. 2009; Johnson et al. 2003; Olopade et al. 1997; Jiang et al. 2003). Downregulation of BH3-only proteins also contributes to a resistant phenotype, as BH3-only proteins mediate the cytotoxic responses elicited by most chemotherapeutic agents (Adams & Cory 2007). Our single protein analysis revealed high levels of the anti-apoptotic proteins Bcl-2 and Bcl-x_L and low levels of the pro-apoptotic BH3-only protein Bim in most glioma cell lines (Figure 4-3; Table 2-8). BH3-only proteins PUMA and Noxa were also downregulated, while pro-apoptotic Bak protein levels were increased in all glioma cell lines. Inhibition of Bak by Mcl-1 can contribute to TRAIL resistance, however, in our analysis we found low Mcl-1 protein levels in glioma cell lines (Gillissen et al. 2010). Inbetween glioma cell lines with different sensitivities to combination therapy with TMZ and TRAIL, we only found differences in the expression of the BH3-only protein Noxa, which was significantly higher in cell lines that were sensitive to combination treatment. Bcl-w expression levels showed a statisical difference in the analysis, but dispayed a highly heterogeneous expression pattern within each group (Figure 4-3). In conclusion, analysis of single protein expression did not reveal a clear pattern that enabled us to distinguish treatment-sensitive cell lines from treatment-resistant cell lines in mono- and dual drug therapy.

Consistant with glioma cell lines, GBM patient samples displayed high levels of anti-apoptotic Bcl-2 and Bcl-xL and low levels of pro-apoptotic Bim (Figures 4-3 and 4-5). Between GBM patient samples, we found significantly elevated levels of Bcl-2 in short-term PFS samples compared to long-term PFS, in consistency to previous results (Jiang et al. 2003). Levels of the pro-apoptotic multidomain protein Bak were significantly decreased in short-term PFS samples compared to long-term PFS. Delft et al. demonstrated that inhibition of Bcl-2 by the BH3-mimetic ABT-373 induces apoptosis via Bak and Bax (Delft et al. 2006). Targeting Bcl-2 activity leads to the release of multidomain proteins such as Bak and could, thus, provide a possible treatment strategy in the group of short-term survival patients in addition to combination therapy with TMZ and TRAIL. In conclusion, single protein analysis of Bcl-2 family members in glioma cell lines and GBM patient samples revealed general characteristics of treatment-resistant tumours. The differences between treatment-sensitive and treatment-resistant cell lines and short-term

and long-term progression-free survivors GBM however lacked a strong pattern that would enable us to clearly predict drug response or progression-free survival. We incorporated the protein expression profiles of Bcl-2 family members in a Principal Component analysis (PCA) as previously described (Figures 3-9 and 3-13). The PCA analysis correlated chemotherapeutic sensitivity and progression-free survival time, respectively with the expression of Bcl-2 family members with only medium accuracy (Figures 4-6 and 4-7). "False positive" were included in the predictions for cell line sensitivity to all treatments as well as for progression-free survival of GBM patients, leading to a decreased specificity and sensitivity of the analysis. Thus, the analysis of molecular expression profiles of Bcl-2 family members alone showed limited implications as a diagnostic tool.

In addition, we analyzed the cell death receptor pathway only in glioma cell lines and found downregulation of the TRAIL receptors DR4 and DR5 in all cell lines (Figure 4-9). A significant difference between TT-sensitive and TT-resistant cell lines was evident in the expression levels of procaspase-8 (Figure 4-9). Both downregulation of DR4 and DR5 and downregulation of procaspase-b8 could severely affect dual drug action: Downregulation of caspase-8 by promoter methylation was shown to interfer with TRAIL sensitivity and has also been linked to glioma development and GBM relapse (Capper et al. 2009). Another study implies that an upregulation of DR5 by pharmacological inhibitors sensitises glioma cells to TRAIL-induced apoptosis, an interesting treatment option for glioblastomas (Hetschko et al. 2008).

In our final analysis, we combined all 21 molecular expression profiles in glioma cell lines, consisting of apoptotic proteins after the mitochondria (Figures 3-8, 4-3 and 4-9), the Bcl-2 family of proteins and components of cell death signalling, in one Principal Component Analysis (Figure 4-10). When comparing the results from molecular expression profiling with cell viability rates after TMZ, TRAIL or combination TMZ and TRAIl treatment, we found that cell death suscebtibility was correctly assigned for all cell lines with high accuracy (100%). Thus, based on the expression of components of both extrinsic and intrinsic apoptotic pathways, we were able to successfully generate treatment-specific preditions of cellular responsiveness. This molecular analysis can be further exploited to

identify novel targets and might in the future proof itself useful in the prediction of therapy outcome and in the development of new treatment strategy in glioblastoma patients.

Additional remark: The differential expression of Bim in glioma cell lines, although not significant between drug responder groups, might be connected to the origin of the tumour: Bim protein expression was exceptionally high in the cell lines U251 and U343, two cell lines of grade III/ IV origin, and moderately increased in cell lines MZ256 and MZ304 when compared to the rest of the glioma cell lines, though still lower than in HeLa. MZ256 and MZ304 are are derived from secondary GBM (see Table 2-6). We also found generally low levels of Bim in GBM patients (Figure 4-5). In colorectal cancer, repression of Bim was associated with tumour progression towards a metastatic phenotype (Greenhough et al. 2010). We therefore assume that the downregulation of Bim is a frequent event in the progression and *de novo* emergence of malignant gliomas, which could contribute to a general impairment of apoptotic signalling. Thus, tumours with high intrinsic expression levels of Bim might be more suceptible to treatment regimes that aim at the reactivation of the apoptotic pathway, a question that we persued in the following chapter 5.

5 The role of Bim during TMZ-and TRAIL-induced cell death in malignant gliomas

5.1 Introduction

The pro-apoptotic BH3-only protein Bim of the Bcl-2 family of proteins is involved in the regulation of the mitochondroal apoptotic pathway (Nordigården et al. 2009; Essafi et al. 2005). Upregulation of Bim triggers the release of cytochrome *c* from the mitochondria, thereby inducing apoptosome-formation and ultimately cell death. Active, unsequestered Bim can either directly interact with the multidomain proteins Bax and Bak, thereby inducing their oligomerisation and translocation to the mitochondria, or indirectly by binding to anti-apoptotic Bcl-2 like proteins, thus causing the release of Bak and Bax (Du et al. 2011). Bim, as well as other BH3-only proteins, Bid and PUMA, can interact with all anti-apoptotic members of the Bcl-2 family of proteins (Labi et al. 2006).

Alternative splicing of Bim *m*RNA gives rise to three major isoforms, Bim_S, Bim_L and Bim_{EL}, among others (Bouillet et al. 2001). The largest isoform, Bim_{EL} contains two ubiquitination sites, three extracellular signal-regulated kinase (ERK) phosphorylation sites, one JNK phosphorylation site and one transmembrane site.

Bim_{EL} can be regulated both at transcriptional and post-translational levels by two major cell survival pathways, the mitogen activated protein kinase (MAPK)/ ERK1/2 – and the phospoatidylinositol 3-kinase (P13K)/ Akt pathways (Roy et al. 2010). The protein kinase Raf, part of tyrosine receptor (RTK) signalling, can activate both pathways, which, cell type specific, leads to opposing cellular responses (Zimmermann & Moelling 1999). Both Akt and ERK pathways also interact with each other to regulate growth in tumour cells (Maines 2007). At transcriptional level, at least three different transcription factors have been described to control Bim expression via binding to specific binding sites on the *Bim* promoter (Biswas et al. 2007). The forkhead box O3 (FoxO3a /FKHR) transcription factor activates Bim expression via two conserved FoxO binding sites in the *Bim* promoter and can be suppressed by ERK1/2 or Akt-mediated phosphorylation (Wang et al. 2011). The transcription factor c-Jun carries two major JNK phosphorylation sites and is activated by JNK phosporylation (Biswas et al. 2007). And finally, cell-cycle controlled Cdk4/ E2F/

Myb signalling was shown to activate *bim* expression following growth factor withdrawal (Biswas et al. 2007).

Post-translationally, Bim_{EL} is negatively regulated by phosphorylation by ERK and Akt, which target the protein for ubiquitination and proteasomal degradation (Biswas & Greene 2002). Another class of MAP kinases, the c-Jun N-terminal kinase JNK, positively regulates Bim_{EL} activity by phosphorylation, which leads to the release of Bim from binding to the anti-apoptotic protein Bcl-2 (Strasser et al. 2006; Putcha et al. 2003; Hu et al. 2008).

Bim repression has been demonstrated in colorectal cancer and in glioblastoma and might be an important step during tumourigenesis (Austin & Cook 2005; Greenhough et al. 2010). A Bim-targeted therapy has the advantage of tumour selectivity and may lead to a more effective treatment strategy against resistant glioblastomas (Akiyama et al. 2009).

5.1.1 Aims of this chapter

In this chapter, we aim to elucidate the role and the regulation of the BH3-only protein Bim during the apoptotic cell death of glioma cells induced by the combination therapy of TMZ and TRAIL. Our previous results showed that cell death was enhanced in the U251 cell line after combination therapy with TMZ and TRAIL (Figure 4-1). U251 cells also displayed high basal levels of the pro-apoptotic BH3-only protein Bim, while other cell lines including MZ294 and glioblastoma patient samples showed significant downregulation of Bim (Figure 4-3). We therefore hypothesize that Bim plays a pivotal role in TMZ- and TRAIL-mediated cell death in glioblastomas (Han et al. 2006). Thus, our first objective was to examine in detail the role of Bim in the treatment-sensitive U251 cell line. In addition, we aim to investigate chemoresistance in a cell line that shows high resistance to all applied treatments, MZ294, based on the assumption that Bim protein levels are actively downregulated in resistant glioma cells.

5.2 Results

5.2.1 TMZ and TRAIL act in synergy and enhance apoptosis in the drug-sensitive cell line U251

The majority of glioma cell lines, 9 of 11, showed resistance to mono-therapy with TRAIL alone, mono therapy with TMZ was only effective in 5 of 11 glioma cell lines (Figures 3-1 and 4-1). The administration of TMZ and TRAIL in combination (TT treatment) caused decreased cell viability in 7 of 11 cell lines, 3 of those showed increased cell death rates when compared to cell viability after TMZ or TRAIL treatment alone (Figure 4-1). The cell line U251 displayed the highest decrease in cell viability following treatment with combination therapy with TMZ and TRAIL (Figure 4-1). In contrast the MZ294 cell line did not respond to any of the treatments when applied alone or in combination (Figure 4-1). Initially, we aimed to analyze whether the observed loss of cell viability was caused by enhanced apoptosis when applying both drugs in combination. MZ294 and U251 cells were treated with TMZ (150 µM) or TRAIL (100 ng/ml) or TMZ (150 µM) and TRAIL (100 ng/ml) combined for 48 hours and subsequently analyzed with Annexin V/ Propodium Iodide (PI) staining by flow cytometry (Figure 5-1 A). The sensitive cell line U251 showed high levels of Annexin V-stained and PI-positive cells after TMZ and TRAIL treatment when compared to TMZ- or TRAIL-treated cells alone already after 48 h treatment. MZ294 cells did not undergo apoptosis after treatments. Additionally, Hoechst-staining against apoptotic nuclei after 48 hour TMZ and TRAIL treatment revealed significantly increased levels of apoptotic nuclei in U251 cells, but not in MZ294 (Figure 5-1 B).

Thus, the levels of cell death after combined treatment with TMZ and TRAIL for 48 hours was greater than the sum of cell death rates after mono-therapy, indicating a synergistic effect of both drugs in glioma cell line U251 (adapted from Webb's theory, Webb 1966).

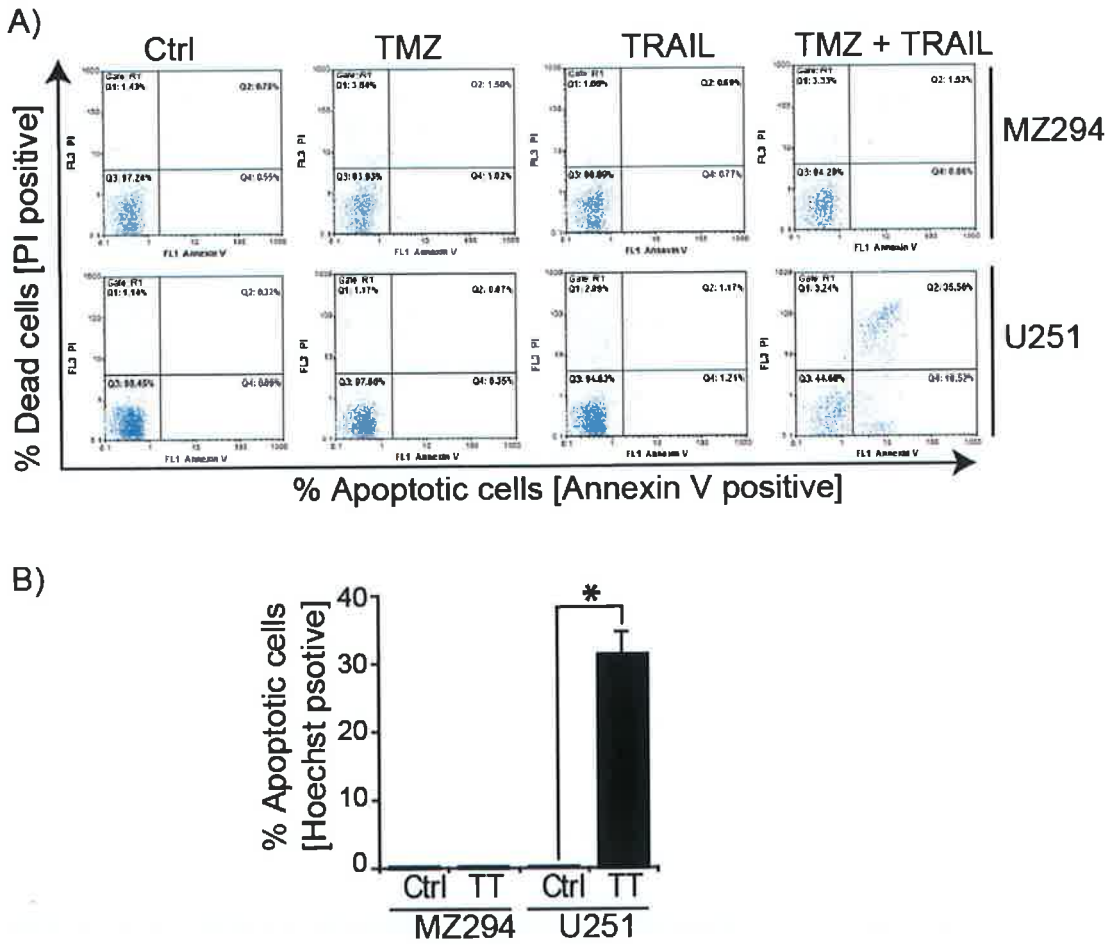

Figure 5-1 TMZ and TRAIL act in synergy to enhance apoptosis in the glioma cell line U251

Treatments of glioma cell lines U251 and MZ294 for 48 h with TMZ (150 μM), TRAIL (100 ng/ml) or dual TMZ (150 μM) and TRAIL (100 ng/ml) (TT). **A)** Flow cytometry analysis of Annexin V- and PI-stained cells. Elevated levels of early apoptotic cells (Annexin V positive) and dead cells (PI positive) were found after TT treatment in U251 when compared to TMZ or TRAIL treatments alone, indicating a synergistic effect of both drugs in combination that enhanced cell death in the U251 cell line. MZ294 cells did not undergo apoptosis. Experiments were performed in triplicates and repeated at least once with similar results. **B)** Hoechst-staining following TT treatment. Significantly increased numbers of apoptotic cells were observed in U251, low levels of apoptotic cells in MZ294. Data represent means ± S.E.M of three independent experiments in triplicates; * indicates $p \leq 0.01$, Student's t test.

5.2.2 Caspase-dependent apoptosis after dual TMZ and TRAIL treatment in the U251 cell line

In chapter 3, we showed that the TMZ-sensitive cell line U251 underwent caspase-dependent apoptosis after 72 hours TMZ treatment, while the MZ294 cell line did not show any characteristics of apoptotic cell death (Figure 3-4). We next aimed to confirm that the enhanced apoptotic cell death after 48 h of TMZ and TRAIL combination treatment in U251 cells was also caspase-dependent. U251 cells were treated with TMZ (150 µM) or TRAIL (100 ng/ml) or a combination with TMZ and TRAIL (150 µM/ 100 ng/ml) for 48 hours (Figure 5-2). The processing of proaspase-3 (35 kDa) into its active forms (17, 19 kDa) was visualized on a Western Blot (Figure 5-2 A). Active caspase-3 was evident in U251 cell lysates after TT treatment. In addition, precursor forms (above 19 kDa) of active caspase-3 were found after treatment with TRAIL alone in U251. TMZ-treated U251 cells did not show procaspase-3 cleavage at this early timepoint, in consistency with the occurrence of apoptotic cell death after 72 hours mono TMZ treatment compared to 48 hours after combination treatment in this cell line (Figure 5-2). We also utilised a caspase-3 activity assay that monitors DEVD-substrate cleavage and we found significantly elevated levels of active caspase-3 after dual TMZ and TRAIL treatment in U251 cells (Figure 5-2 B). Fragmentation of the natural caspase-3 substrate PARP was analyzed on a Western Blot (Figure 5-2 C).Visible f-PARP (89 kDa) occurred after treatment in U251, but not in MZ294. The application of the general caspase- inhibitor benzyloxycarbonyl-Val-Ala-Asp(*O*-methyl) fluoromethylketone (zVAD) (50 µM) for 1 hour before TMZ and TRAIL treatment prevented the fragmentation of PARP during TMZ and TRAIL treatment in U251 cells (Li et al. 1997).

Therefore, the activation of executioner caspase-3, PARP fragmentation and the prevention of substrate cleavage by caspase-3 inhibition indicated that the enhanced TMZ- and TRAIL-induced apoptotic cell death in U251 was indeed caspase-dependent.

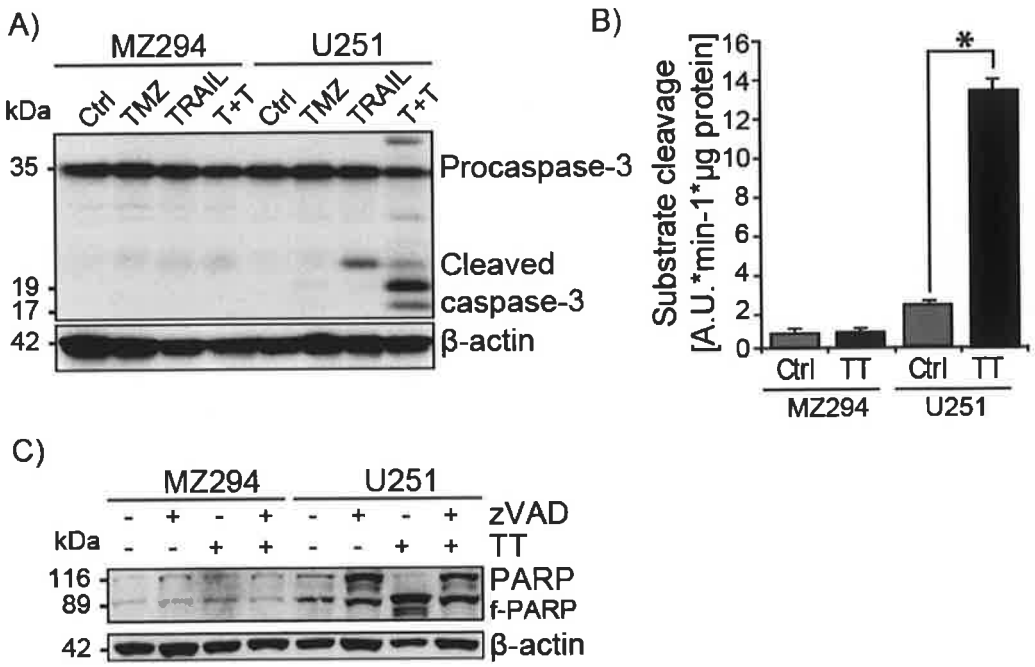

Figure 5-2 Caspase-dependent apoptosis after TMZ and TRAIL in combination

Treatments of U251 and MZ294 for 48 h with TMZ (150 µM), TRAIL (100 ng/ml) or TMZ plus TRAIL (TT). **A)** Western Blots showing caspase-3 activation by cleavage. Caspase-3 activation was observed in U251 after TT treatment and to a minimal amount after TRAIL alone. Experiments were repeated twice with similar results. **B)** Caspase-3 activity assay measuring DEVD-substrate cleavage. Caspase-3 activity was 14-fold elevated in U251 after TT treatment for 48 h. Data are means ± S.E.M of three independent experiments in triplicates; * indicates $p \leq 0.01$, Student's t test. **C)** Western blots monitoring PARP fragmentation, a caspase-3 substrate, in U251 after TT and caspase-inhibition by zVAD (50 µM]. PARP fragmentation was observed after TT treatment in U251, which was prevented by addition of zVAD.

5.2.3 Upregulation of Bim protein levels following TMZ and dual TMZ and TRAIL treatment in U251 cells

In Chapter 4, we showed that the glioma cell lines U25 and U343 displayed highly elevated levels of the BH3-only protein Bim when compared to HeLa (Figure 4-3). The cell lines MZ256 and MZ304 displayed higher Bim expression levels than other glioma cell lines, but still below Bim levels as found in HeLa cells (Figure 4-3). The rest of the glioma cell lines, including MZ294, showed significantly low levels of Bim. Additionally, Bim expression levels were also decreased in GBM patient samples, indicating that a downregulation of Bim activity might be important in the development of malignant glioblastomas (Figure 4-5) (Austin & Cook 2005; Greenhough et al. 2010). Out of those four glioma cell lines with elevated Bim expression, only U251 was sensitive to the synergistic effect of TMZ and TRAIL in combination (Figures 4-1 and 5-1). To analyse whether Bim expression was involved in the apoptotic cell death following mono therapy with TMZ in the drug-sensitive cell line U251, we first analysed Bim_{EL} protein expression levels during a time course experiment with TMZ (150 μM) for 24, 48, 72 and 96 hours and compared this to levels found in the TMZ-resistant cell line MZ294 (Figure 5-3). Western Blot and densitometry analysis revealed a further increase in Bim protein levels in U251 cells during TMZ treatment. Bim_{EL} protein levels in MZ294 were only slighly increased and might not be sufficient for the execution of apoptosis. Thus, the upregulation of Bim protein expression during TMZ administration in U251 cells points to a role of Bim in TMZ-induced mitochondrial apoptosis.

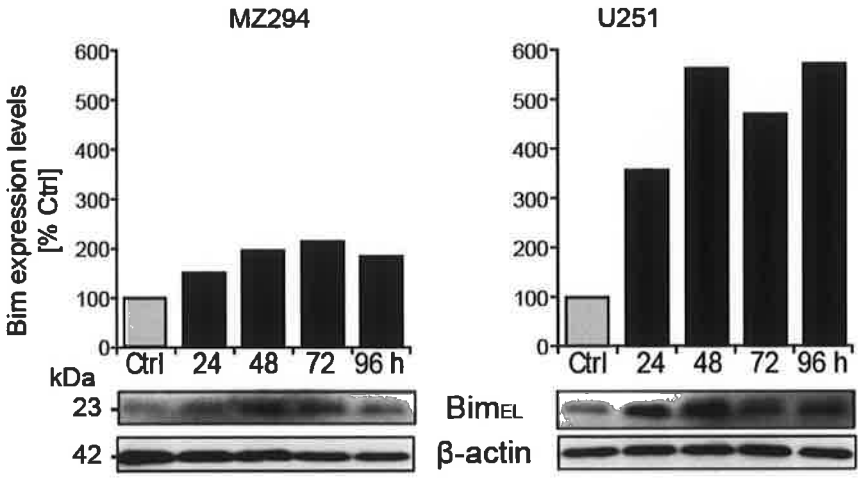

Figure 5-3 Upregulation of Bim protein levels following TMZ treatment in the U251 cell lines

Western Blot and densitometry analysis of single representative blots. U251 and MZ294 were treated with TMZ (150 μM) for 0- 96 hours. Protein levels of Bim were elevated in U251, indicating novel protein synthesis induced by TMZ treatment. Insignificant Bim upregulation was observed in MZ294. β-actin was used as a loading control. Experiments were repeated once with similar results.

Subsequently, we analyzed Bim protein expression in a time course experiment with combined TMZ (150 μM) and TRAIL (100 ng/ml) for 6, 12, 24 and 48 hours (Figure 5-4 A). Western Blot and densitometry analysis revealed that Bim protein levels were elevated beginning at 12 hours and peaked at 24 hours in U251 cells, while MZ294 cells displayed unchanged Bim protein expression. Bim protein levels dropped after 48 hours of treatment in U251 cells, which coincided with the time point of cell death in this cell line.

To examine if any other Bcl-2 family members and components of the extrinsic apoptotic pathway played a role in the apoptotic death elicited by the TT treatment strategy, a similar time course experiment was performed in both U251 and MZ294 cell lines Figure 5-4 B). Western Blot analysis showed upregulation of the BH3-only protein PUMA after 24 hours treatment in U251 cells. Mcl-1 levels slightly decreased, while Bcl-2 levels remained constant. Neither the activation of procaspase-8 by cleavage nor processing of the BH3-only protein Bid into its active form tBid was evident in our analysis. In addition, protein levels of the TRAIL-receptor DR4 were steady during the treatment. Somewhat in contrast, MZ294 cells displayed an upregulation in the levels of Bcl-2, while Mcl-1 levels decreased during treatment. The expression of the BH3-only proteins, PUMA and DR4 expression did not change. Finally, procaspase-8 and Bid were not processed into their active forms.

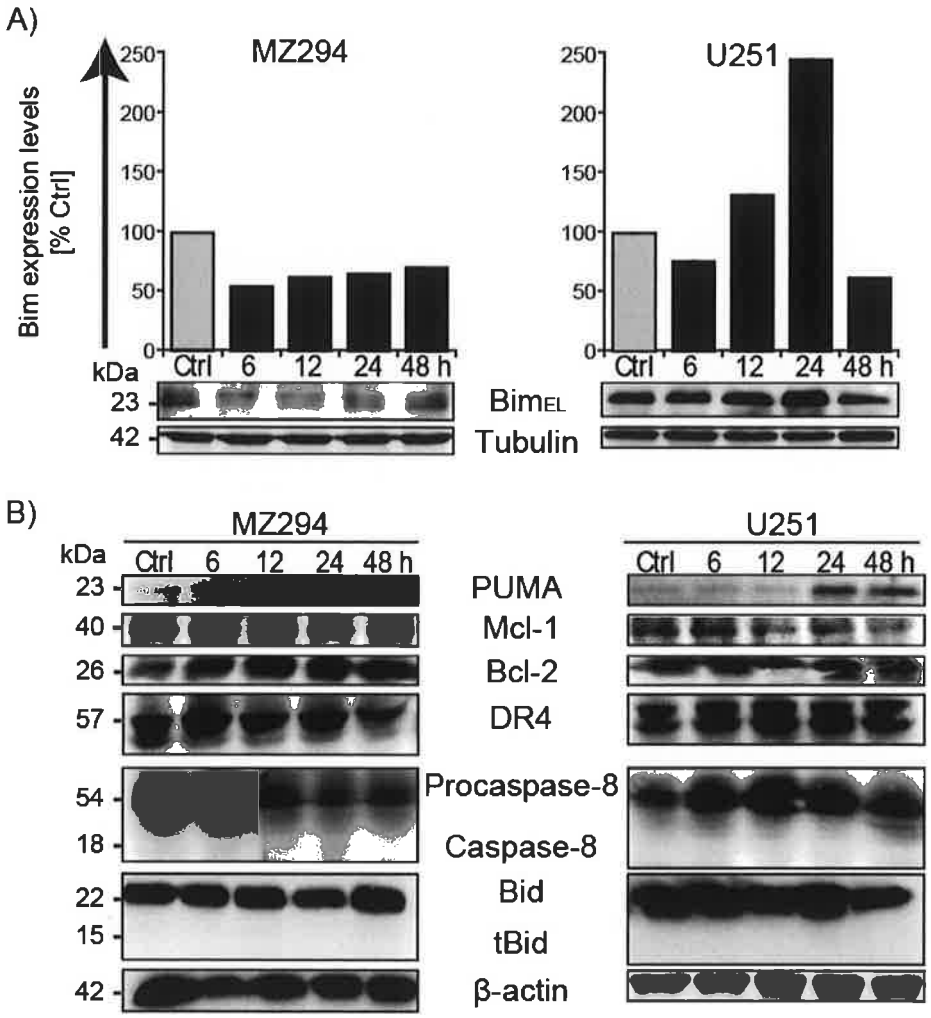

Figure 5-4 Upregulation of pro-apoptotic Bcl-2 family members BIM and PUMA in U251 cells after dual TMZ and TRAIL treatment

Cell lines U251 and MZ294 were treated with TMZ (150 μM) and TRAIL (100 ng/ml) for 6, 12, 24 and 48 h. **A)** Western Blot and densitometry analysis of single representative blots; TT treatment. Elevated Bim and PUMA protein levels were found in U251 cells after 12 h and 24 h of treatment, respectively. No Bim or PUMA upregulation was found in MZ294 cells. Tubulin was used as a loading control. Results are representative of three independent experiments **B)** Western Blot analysis of Bcl-2 family members and death receptor signalling associated proteins. Puma levels were upregulated in U251 cells. Bid cleavage into its active form was not observed, nor was caspase-8 activation in U251 cells. β-actin was used as a loading control. Experiments were repeated twice with similar results.

To analyze if the upregulation of Bim and PUMA protein levels was a direct result of the induction of *gene* expression of the corresponding genes, we measured relative *m*RNA levels in the TMZ and TRAIL-treated U251 cells using quantitative PCR (qRT-PCR; Figure 5-5). *Bim* gene expression was significantly elevated up to ninefolds after 48 hours treatment. *PUMA* gene expression was already significantly elevated up to tenfolds after 24 hours of treatment. Relative *Bid* mRNA levels did not significantly increase. Such elevated mRNA levels indicated that the observed increase in Bim and PUMA protein levels had a transcriptional component, which correlated with an increase of apoptosis. Thus, we hypothesise that both of these BH3-only proteins could potentially play a role in the apoptotic death of U251 cells following TMZ and TRAIL treatment. However, as discussed previously, Bim showed exceptionally high basal protein levels in the sensitive cell line U251, while most glioma cell lines and GBM patient samples expressed low basal levels of Bim (Figures 4-3 and 4-5). Intrinsic PUMA expression in the sensitive U251 cells though did not greatly differ from expression in other cell lines, such as the resistant cell line MZ294 (Figure 4-3). Therefore, we initially focused on the regulation of Bim protein expression in both U251 and MZ294 cells.

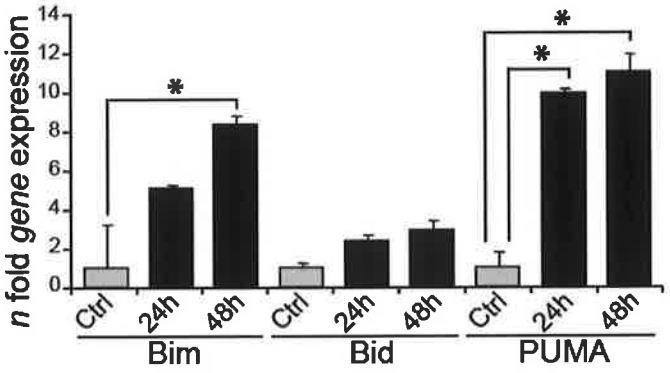

Figure 5-5 Induction of Bim and PUMA *gene* expression after dual TMZ and TRAIL treatment

Cell lines U251 and MZ294 were treated with TMZ (150 μM) and TRAIL (100 ng/ml) for 24 and 48 h. RT-PCR analysis showing Bim, Bid and PUMA *m*RNA levels in U251 cells. Bim and PUMA gene expression is significantly increased after 24 h and 48 h treatment, indicating direct upregulation following the treatment regime. β-actin was used as a control. Date are means ± S.E.M of three independent experiments in triplicates; * mark $p \leq 0.05$, Student's t test.

5.2.4 Transcription factors c-Jun and Foxo3a are both activated following combined TMZ and TRAIL treatment

Bim *gene* expression has been shown to be regulated by the transcription factors c-Jun and FoxO3a (Biswas 2007; Xia et al. 2007; Guan et al. 2011). c-Jun can be activated through phosphorylation by the c-Jun activating kinase (JNK), while FoxO3a needs to be dephosphorylated in order to be transported into the nucleus. In an effort to identify if these transcription factors were active in either the drug-sensitive cell line U251 or the drug-resistant cell line MZ294, the cell lines were treated with TMZ (150 μM) and TRAIL (100 ng/ml) in a time course experiments of 48 hours and analysed by Western Blotting and densitometry (Figure 5-6). U251 cells displayed higher amounts of phosphorylated c-Jun proteins in the initial 24 hours following treatment, which further increased at 36 and 48 hours (Figure 5-6 A). Phospho-c-Jun levels in MZ294 did not change significantly during treatment (Figure 5-6 A). A decrease in phospho-FoxO3a levels, which marks the activation of FoxO3a by de-phosphorylation, was visible at 12 and 24 hours following treatment in U251 cells (Figure 5-6 B). In contrast, in the MZ294 cell line, FoxO3a was initially deactivated, as highlighted by an increase in its phosphorylation levels at 6 hours, before levels of phospho-FoxO3a returned to similar levels expressed in untreated control cells.

Thus, the transcription factors c-Jun and FoxO3a both displayed -increased activity in U251 cells only, which correlated with the upregulation of Bim expression following TMZ and TRAIL treatment in this cell line.

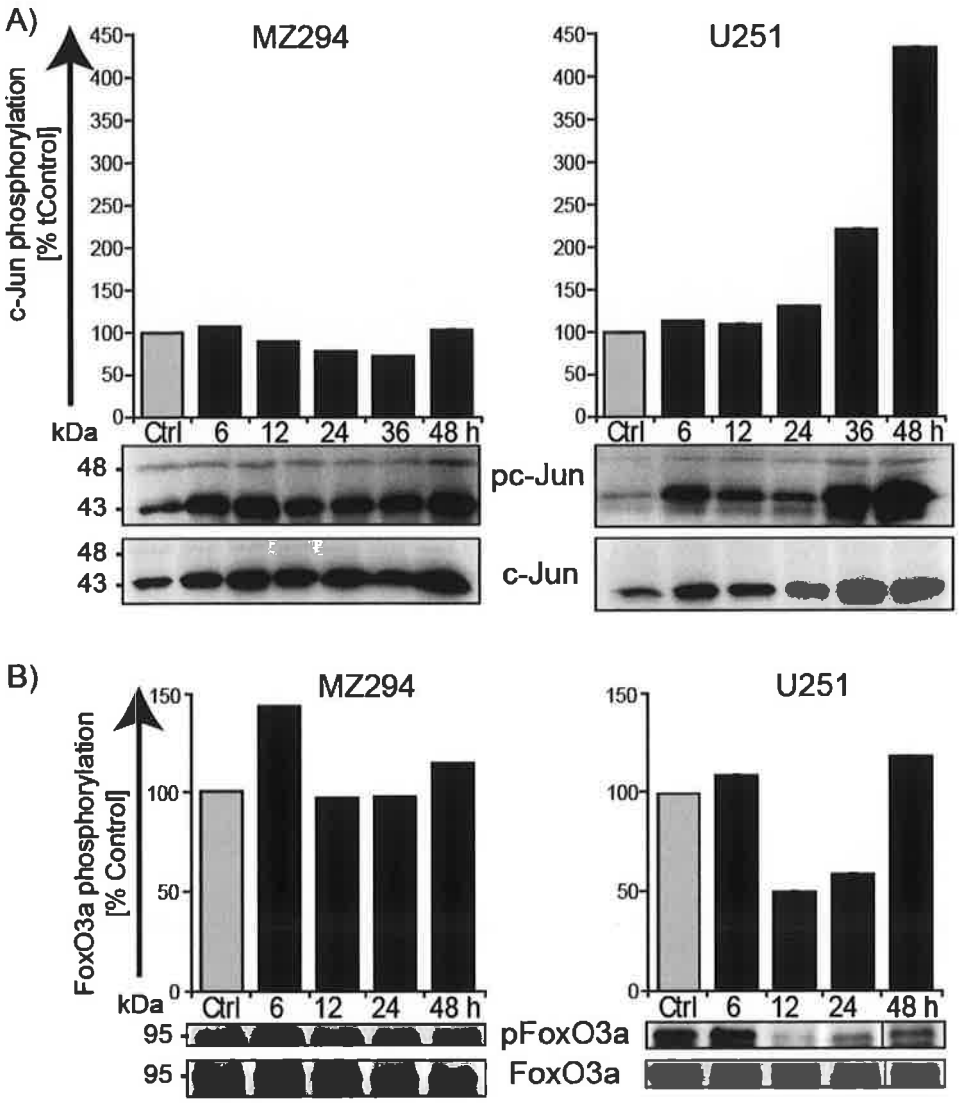

Figure 5-6 Activation of transcription factors c-Jun and Foxo3a after combination of TMZ and TRAIL

A) Western Blot and densitometry analysis of single representative blots monitoring c-Jun activation by phosphorylation in comparison to total c-Jun levels. Levels of active c-Jun were elevated after TT treatment in U251 cells. Amounts of phosphorylated c-Jun did not significantly change in MZ294 cells. Total c-Jun levels were used as a control. Experiments were repeated twice with similar results. **B)** Western Blot and densitometry analysis of single representative blots showing FoxO3a activation by de-phosphorylation. FoxO3a was activated in U251 cells and de-activated in MZ294 cells. Total FoxO3a levels were used as a control. Experiments were performed three times with similar results.

5.2.5 Bim expression in U251 cells is regulated independently of JNK/ c-Jun activity

Phosphorylation of the transcription factor c-Jun by the c-Jun N-terminal kinase (JNK) results in its activation. In order to determine if c-Jun played a pivotal role in the transcriptional regulation of Bim, we applied the JNK-inhibitor SP600125 to prevent c-Jun activity during treatment with TMZ and TRAIL (Ohba et al. 2009). U251 cells were pre-incubated with JNK-Inhibitor SP600125 (5 μM) for 1 hour, followed by combination TMZ (150 μM) and TRAIL (100 ng/ml) treatment for 24 or 48 hours (Figure 5-7). Successful inhibition of c-Jun phosphorylation was visualized on Western Blots following 24 hours treatment (Figure 5-7 A). Levels of phosphorylated c-Jun after JNK inhibition were decreased when compared to total c-Jun protein levels, indicating the deactivation of c-Jun. Expression levels of Bim in SP600125-pre-treated cells did not differ from those found in treated cells without JNK-inhibition (Figure 5-7 A). In addition, quantitative assessment of apoptotic cells after staining with Hoechst 33258 revealed no significant differences in the amounts of apoptotic cells following dual TMZ and TRAIL treatment (48 hours) when compared to levels of cell death achieved by pre-incubation with SP600125 followed by dual TMZ and TRAIL treatment (Figure 5-7 B). Finally, flow cytometry analysis of Annexin V/ PI stained cells after 48 hours TMZ and TRAIL treatment found similar amounts of apoptotic cells (Annexin V^+) with or without JNK inhibition with SP600125 (Figure 5-7 C).

Therefore, the observed concomitant activation of the c-Jun transcription factor and upregulation of Bim protein levels during the apoptotic death of U251 cells following combined TMZ and TRAIL treatment most likely occurred independently of each other. We reasoned that *Bim* gene expression in U251 cells during combined TMZ and TRAIL treatment was controlled by another transcription factor.

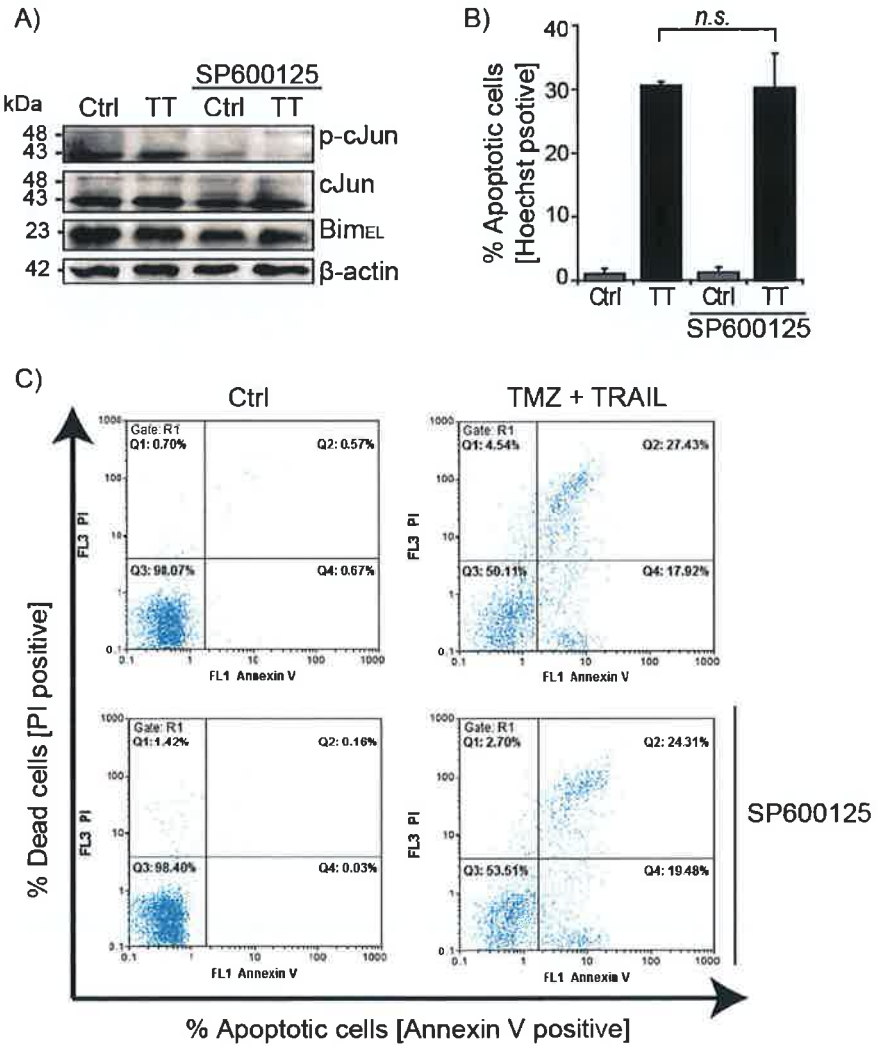

Figure 5-7 Bim expression is regulated independently of JNK/ c-Jun activity during TMZ and TRAIL treatment in U251 cells

U251 cells were pre-treated for 1 h with JNK inhibitor SP600125 (5 μM), followed by addition of TMZ (150 μM) and TRAIL (100 ng/ml) for 24 h and 48 h. **A)** Western Blots of U251 cells treated for 24 h with TT. Inhibition of JNK prevented c-Jun activation, but did not change Bim expression levels. β-actin was used as a control. Experiments were performed twice with similar results. **B)** Count of Hoechst-positive cells after 48 h treatment. No significant differences were found between the amount of apoptotic cells after dual TMZ and TRAIL treatment alone and with pre-incubation with SP600125. Data are means ± S.E.M of two independent experiments; n.s. = not significant. **C)** Flow cytometry analysis of treated cells (48 h). Annexin V $^{+}$ cells represent apoptotic cells, PI^{+} stained cells show already dead cells. JNK inhibition did not interfere with apoptosis induction following TT treatment in U251. Experiments have been performed twice with similar results.

5.2.6 The transcription factor FoxO3a regulates Bim expression during TMZ- and TRAIL- induced apoptosis

Next, we analyzed the impact of FoxO3a activity on Bim expression during treatment in U251 cells. The cells were transfected with two FoxO3a constructs, the dominant-negative FoxO3a-DDB plasmid, which lacks the DNA-binding domain, and the constitutive-active FoxO3a-TM plasmid, which has sustained activity due to three ("triple") mutated phosphorylation sites (Brunet et al. 1999). 24 hours after transfection, U251 cells were treated with TMZ (150 µM) and TRAIL (100 ng/ml) combined for 24 or 48 hours (Figure 5-8). Western Blot analysis revealed that Bim protein levels in U251 cells were elevated following the overexpression of constitutive active FoxO3a-TM and subsequent dual treatment with TMZ and TRAIL for 24 hours when compared to the cells transfected with an empty control vector (vehicle), amd then treated with TMZ and TRAIL (Figure 5-8 A). In contrast, the overexpression of dominant-negative FoxO3a-DDB led to lower Bim protein levels in U251 cells when compared to the vehicle control after TMZ and TRAIL for 24 h (Figure 5-8 B). Next, following transfection 48 hours TMZ and TRAIL treatment, U251 cells were stained with Annexin V/ PI analysed by flow cytometry analysis (Figure 5-8 C). A decrease in the numbers of apoptotic cells (Annexin V^+) when compared to the vehicle control was evident after the overexpression of the dominant-negative construct FoxO3a-DDB when compared to the TT treated cells which overexpressed the vehicle control. The overexpression of constitutive active FoxO3a-TM caused slightly increased amounts of apoptotic cells (Annexin V^+).

Therefore, we conclude that the transcription factor FoxO3a is involved in the upregulation of Bim protein levels during TMZ and TRAIL-induced cell death in U251 cells.

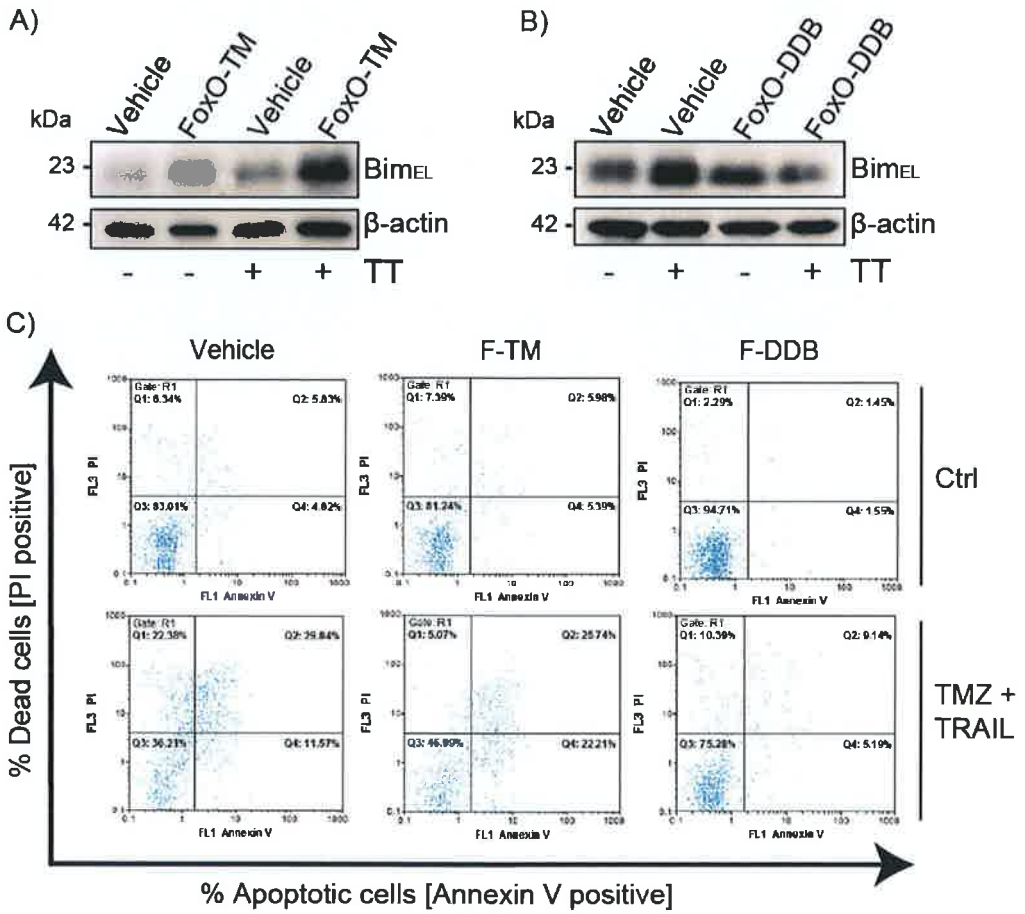

Figure 5-8 FoxO3a activity regulates Bim expression in U251

Transfection with constitutive- active Foxo3a-TM and dominant-negative FoxO3a-DDB plasmids, followed by TMZ (150 μM) and TRAIL (100 ng/ml) treatments for 24 h and 48 h in the U251 cell line. Empty vector pECE served as vehicle control. **A)** Western Blot monitoring Bim expression after FoxO3a-TM transfection and 24 h TT treatment. Overexpression of FoxO3a-TM led to increased Bim expression levels after treatment β-actin was used as a control **B)** Western Blot showing Bim protein levels after FoxO3a-DDB transfection and 24 h TT treatment. Decreased Bim levels were found in FoxO3a-DDB overexpressing and TT-treated cells. β-actin was used as a control. **C)** Flow Cytometry analysis of Annexin B and PI stained cells after 48 h TT treatment. Apoptotic cell death was significantly reduced following overexpression of FoxO3a-DDB and TT treatment. FoxO3a-TM overexpression increases the amount of apoptotic cells after TT treatment.

5.2.7 Activation of Akt survival signalling does not prevent cell death

It is known that FoxO3a activity can be negatively controlled by protein kinase B (Akt), which is part of the PTEN/ PI3K/ Akt signalling pathway, and by the extracellular signal-regulated kinase ERK, a component of MAPK/ERK signalling (Brunet et al. 1999; Wang et al. 2011). Abberantly active survival pathways are a common phenomenon in cancer cells and were shown to interact with apoptotic pathways (Marani et al. 2004; Iglesias-Serret et al. 2007; Reginato et al. 2003; Beere 2005; Elgendy et al. 2011; Lowe et al. 2004; Herr & Debatin 2001; Maddika et al. 2007). We first analyzed the activity of Akt by monitoring its phosphorylation status on a Western Blot and subsequent densitometry analysis (Figure 5-9). Sensitive U251 cells and resistant MZ294 cells were treated with TMZ (150 µM) and TRAIL (100 ng/ml) for 6, 12, 24 and 48 hours. Elevated amounts of phosphorylated Akt compared to total amounts of Akt protein were found in U251 cells after 6 hours during the treatment and these levels further increased at later timepoints. In contrast, MZ294 cells showed minimal activation of Akt by phosphorylation, over the timecourse experiment, which further decreased.

From these results we hypothesized that Akt survival signalling was not a critical component of the intrinsic survival mechanism of the MZ294 cell line to TMZ and TRAIL treatment. Furthermore, the observed activation of Akt in the drug-sensitive cell line U251 points to a minor role of Akt signalling in the survival strategy of U251 cells.

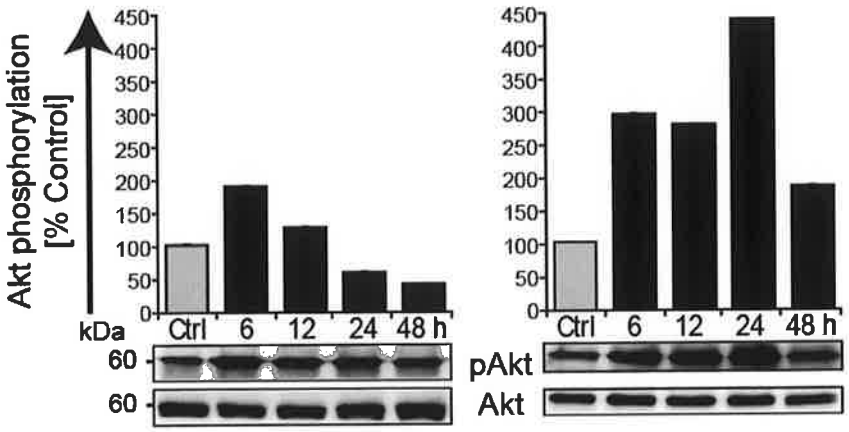

Figure 5-9 Activation of Akt survival signalling by the combination therapy of TMZ and TRAIL does not prevent cell death in U251 cells

Western Blot and densitometry analysis of single representative blots. TMZ (150 μM) and TRAIL (100 ng/ml) (TT) treatment for 0 - 48 h. Activation of Akt by phosphorylation was found in both MZ294 and U251 cells after 6 h. Akt phosporylation was intensified in U251cells at 24 h, but downregulated in MZ294 cells. Total amounts of Akt served as control. Experiments were repeated twice with similar results.

5.2.8 Inhibition of ERK1/2 activity enables Bim upregulation and leads to growth inhibition in a formerly drug-resistant cell line

Next, we examined ERK1/2 activitation by phosphorylation after dual TMZ and TRAIL treatment. U251 and MZ294 cells were treated with TMZ (150 µM) and TRAIL (100 ng/ml) for 6, 12, 24 and 48 hours and analyzed by Western Blotting and densitometry analysis (Figure 5-10 A). High levels of phosphorylated, active ERK1/2 were detected in MZ294 cells at 6 hours after treatment and these levels remained elevated for 24 hours. In contrast, U251 cells did not display any evidence of ERK1/2 activation (Figure 5-10 A).
Next, MZ294 cells were pre-treated with the ERK1/2 specific inhibitor PD98059 (15 µg/ml) for 1 hour, followed by 24 hours dual TMZ and TRAIL treatment and subsequent Western Blot analysis (Figure 5-10 B). Bim protein levels were significantly elevated following ERK inhibition in both untreated control and TT treated cells. The activation of FoxO3a by dephosporylation was also indicated by the decrease of phosphorylated FoxO3a in comparison to total FoxO3a. Finally, treatment with the ERK inhibitor PD98059 and subsequent TMZ and TRAIL administration revealed that cell numbers in the MZ294 cell line were significantly decreased after eight days of treatment (Figure 5-10 C). This effect though was most likely caused by growth inhibition and not by cell death in MZ294 cells, as observations through a microscope did not reveal an increase in dead cell numbers (data not shown).

In conclusion, MZ294 cell lines showed increased activity of the ERK1/2 survival signalling pathway after treatment with TMZ and TRAIL, which could be blocked by ERK1/2 inhibition, leading to a reduced proliferation rate in these cells. This indicates that the MAPK/ ERK1/2 pathway is involved in the resistant mechanisms of MZ294 cells. Furthermore, we showed that the activity of Bim correlated with the activation of the transcription factor FoxO3a, which could be induced by the inhibition of ERK1/2. Thus, we hypothesise that Bim levels are kept in check by survival signalling in MZ294 cells, resulting in its ability to resist treatment with TMZ and TRAIL.

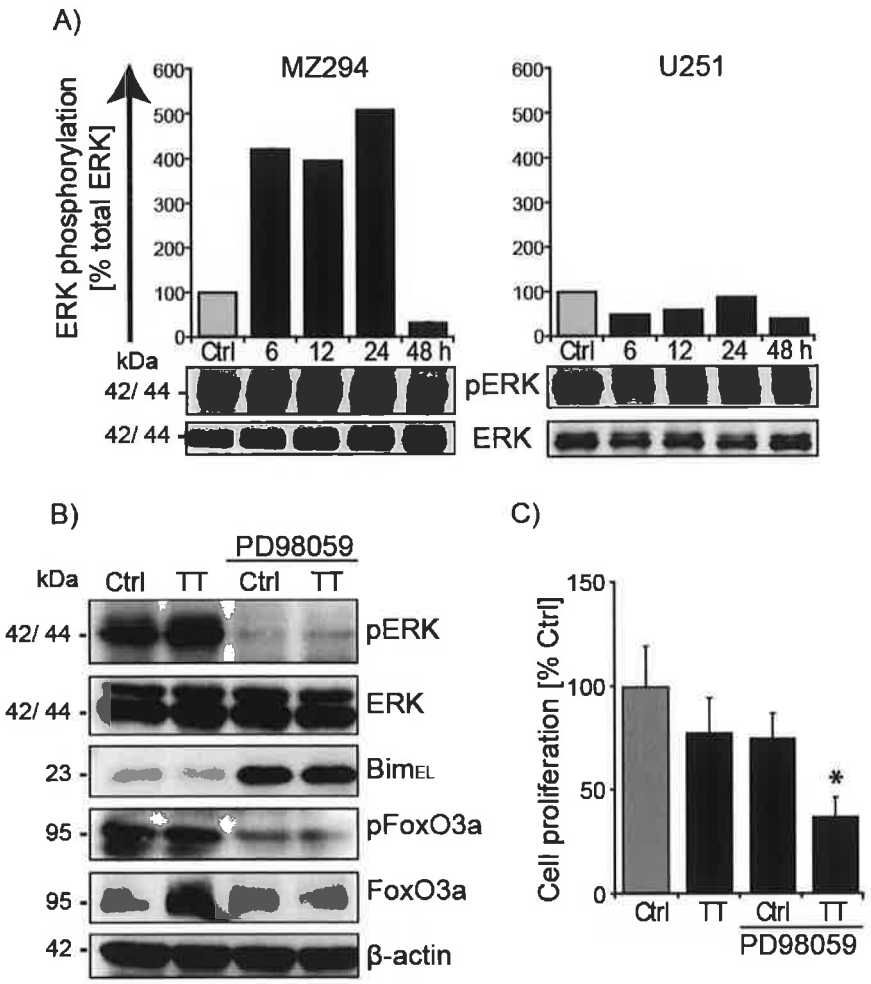

Figure 5-10 Inhibition of ERK1/2 activity enables Bim upregulation and leads to growth inhibition in a formerly drug-resistant cell line

A) Western Blot and densitometry analysis of single representative blots. Monitoring of ERK phosphorylation following dual TMZ (150 μM) and TRAIL (100 ng/ml) treatment during a 48 h time course in MZ294 and U251 cells. High levels of phosphorylated, active ERK were found in MZ294 cells already 6 h after TT treatment, U251 cells did not show activation of ERK signalling. Blots are representatives of three independent experiments with similar results. **B)** Western Blot analysis of MZ294 cells after 1 h pre-treatment with the ERK inhibitor PD98059 (15 μg/ml) and subsequent TT for 24 h. Bim protein levels were elevated after ERK inhibition in both control and TT-treated cells. In addition, FoxO3a was dephosphorylation. **C)** MTT analysis after 1 h pre-treatment with PD98059 and concomitant incubation with TT for 8 days. Cell growth was significantly reduced in the MZ294 cell line. Results are presented as mean ± S.E.M of three independent experiments; * indicates $p \leq 0.005$, Student's t test.

5.3 Discussion

In this study, we examined the role of Bim during TMZ-and TRAIL-induced cell death in malignant gliomas. Initially, we found that the U251 cell line succumbed to an earlier apoptotic death upon combined treatment with the DNA-alkylating agent TMZ and the death receptor ligand TRAIL than compared to treatment with either drug alone, indicating a synergistic effect of these drugs in combination in U251 cells (Figures 3-1, 4-1 and 5-1). Synergy is defined to occur when the effect of two drugs exceeds the effect of each drug treatment given individually (Webb 1966). Synergistic effects have been previously demonstrated for TRAIL in connection with DNA-damaging therapies, for example 5-fluorouracil (5-FU) or with kinase inhibitors such as sorafenib (von Haefen et al. 2004; Katz et al. 2009).

We also demonstrated that combined TMZ and TRAIL treatment led to caspase-dependent apoptosis in U251 cells, as evidenced by the activation of procaspase-3 and subsequent cleavage of the caspase substrate PARP, which was prevented by the application of the caspase inhibitor zVAD (Bender et al. 2010) (Figure 5-3). Therefore, we conclude that TMZ and TRAIL act in synergy to evoke caspase-dependent apoptosis in the glioma cell line U251. As it was demonstrated in chapter 4, U251 cells displayed high basal levels of the pro-apoptotic BH3-only protein Bim (Figure 4-3). In contrast, most glioma cell lines and glioblastoma patient samples showed extreme downregulation of Bim expression, as previously illustrated in chapter 4 (Figures 4-3 and 4-5). Bim repression has been demonstrated in colorectal cancer and in glioblastoma and might be an important step during tumourigenesis (Austin & Cook 2005; Greenhough et al. 2010). The pro-apoptotic function of Bim is regulated both at transcriptional and post-transcriptional level (Marchand et al. 2012; Iglesias-Serret et al. 2007). In our study, we observed transcriptionally induced upregulation of pro-apoptotic BH3-only proteins Bim and PUMA following combined TMZ and TRAIL treatment in the U251 cell line, which correlated with the onset and execution of apoptosis (Figures 5-4 and 5-5).

In contrast, the MZ294 cell line was resistant to either mono-therapy with TMZ or TRAIL alone or combined TMZ and TRAIL treatment, which was also evident by the lack of caspase-3 activity and apoptotic cells following either treatment regimes (Figures 3-1, 4-

1, 5-1 and 5-2). In consistency, the pro-apoptotic BH3-only protein Bim was only insufficiently upregulated in MZ294 cells (Figure 5-4).

TRAIL-induced apoptosis can occur via both mitochondrial-dependent and mitochondrial-independent apoptotic pathways (Suliman et al. 2001). A dependency of TRAIL-signalling via the mitochondria (Type II cells) was previously reported for glioma cells (Boya & Kroemer 2008; Hetschko et al. 2007). In chapter 4, we demonstrated that essential elements of death receptor signalling are expressed in most glioma cell lines (Figure 4-9), including the adaptor protein FADD, which is required for cell death receptor DR4 and DR5-mediated cell death. FADD, DR4 and DR5 are equally expressed in U251 and MZ294 cells, indicating the presence of a functional TRAIL signalling pathway in both cell lines (Figure 4-8) (Petak et al. 2003; Puduvalli et al. 2005). Petak et al. also reported that TRAIL-induced activation of Bax was inhibited by Bcl-x_L and Bcl-2 (Petak et al. 2003). Bcl-x_L is overexpressed in both U251 and MZ294 cells and the expression of Bcl-x_L is generally high in gliomas, which could arguably be one of the reasons why TRAIL treatment alone showed so little effect in most glioma cell lines (Figures 4-1 and 4-3). The BH3-only protein Bid is usually described as the main mediator of TRAIL-induced, mitochondrial dependent apoptosis and functions as a link between the extrinsic and the intrinsic apoptotic pathway in type II cells (Rudner et al. 2005). In our study, we examined procaspase-8 and Bid activation during TMZ- and TRAIL-induced cell death, but we could not find any evidence that TRAIL signalled via caspase-8/ t-Bid occured in the treatment-sensitive U251 cells. This contradicted previous findings that demonstrated combined TRAIL and TMZ treatment of glioma cell lines activated procaspase-8 via the extrinsic pathway of apoptosis (Uzzaman et al. 2007). Despite repeated efforts we did not see similar results in our experiments and hypothesise that the differences observed are due to differing concentrations of TRAIL and incubation periods being used between the two groups. Caspase-8 -independent mechanisms of TRAIL-induced cell death have been demonstrated previously in rhabdomyosarcoma cells (Petak et al. 2003). In their work, Petak et al. show that TRAIL signalling occured through sphingosine-mediated Bax activation, resulting in cytochrome *c* release from the mitochondria, thereby circumventing caspase-8-mediated activation of Bid. Other studies found evidence for an involvement of caspase-10 in a

TRAIL-induced, caspase-8-independent cell death (Kischkel et al. 2001). Another mechanism, proposed by Holler et al., assumes that death receptor signalling may induce receptor interacting protein (RIP) kinase activity, leading to necrosis, which is also independent of caspase-8 activity, although this most likely does not apply to our experiments, as we see caspase-3-dependent apoptosis following TMZ and TRAIL treatment (Figure 5-2) (Holler et al. 2000). Thus, caspase-8 -independent TRAIL signalling via the mitochondria may occur during TMZ and TRAIL-induced cell death in the U251 cell line.

However, despite the possibility that TRAIL signalling, independent of caspase-8, leads to Bid cleavage into its active form tBid, we observed that Bid was not cleaved during dual TMZ and TRAIL treatment (Figure 5-4) (Terrones et al. 2008). Yet Bid cleavage might not be essential for TRAIL-induced apoptosis, as it has been shown during caspase-independent excitotoxic apoptosis in hippocampal neurons that full length Bid was sufficient to induce apoptosis (König et al. 2007). König et al. demonstrated that translocation of full length Bid from the cytosol to the mitochondria was required to trigger the release of pro-apoptotic factors. This could culminate in caspase-dependent cell death, which we found in our cell lines, as demonstrated by the activity of caspase-3 (Figure 5-2). However, another possibility which is supported by Han et. al is an alternative cross-talk mechanism between the TRAIL receptor death signalling pathway and the mitochondria that involves Mcl-1 and Bim (Han et al. 2006). In their study it was demonstrated that TRAIL-activated caspase-3 can lead to the degradation of Mcl-1, thereby releasing Bim, which in turn mediates a Bax-dependent apoptotic cascade. In our experiments we found slightly decreased levels of Mcl-1, which would strengthen this assumption (Figure 5-4). In conclusion, a possible role of full length Bid in dual TMZ and TRAIL-mediated apoptosis cannot be excluded. However, taking into account that U251 cells displayed high basal levels of Bim, it seems plausible that Bim activation plays a pivotal role during apoptosis in this cell line and that the role of Bim exceeds the contribution of Bid to TMZ- and TRAIL-induced cell death. We therefore hypothesise that Bim acts at the intersection of the extrinsic and intrinsic apoptotic pathways in U251 cells (Han et al. 2006).

To investigate the regulation of Bim further, we examined the activity of c-Jun and FoxO3a, two transcription factors that have been shown to control Bim expression (Biswas et al. 2007; Sunters et al. 2006; Guan et al. 2011a; Khatri et al. 2010). We demonstrated that both c-Jun and FoxO3a activation took place concomitantly with Bim upregulation during TMZ- and TRAIL-treatment. The kinase c-Jun can be activated through phosphorylation via the c-Jun N-terminal kinase (JNK) (Marchand et al. 2012). JNK is a mitogen-activated protein kinase (MAPK) that can also post-transcriptionally control Bim function by direct phosphorylation, thereby positively regulating Bim activity (Putcha et al. 2003). TMZ has been previously demonstrated to activate JNK in glioma cells (Ohba et al. 2009). In addition, it was speculated that the JNK pathway may play a role in sensitizing glioma cells to TMZ treatment, which was demonstrated in U87 cells (Ohba et al. 2009). In U251 cells, however, we found that inhibition of JNK/ c-Jun with the JNK-specific inhibitor SP600125 did not decrease TMZ-and TRAIL-induced apoptosis. Furthermore, we found that *Bim* gene regulation was also not effected as a result of JNK inhibition, thereby suggesting that Bim expression was controlled by transcriptional regulators other than c-Jun. Therefore, we examined the role of FoxO3a in the upregulation of Bim protein levels. By overexpression of a dominant-negative FoxO3a construct (Brunet et al. 1999; Brunet et al. 2001), we were able to demonstrate that inhibition of FoxO3a led to decreased Bim levels and to a reduction in TMZ- and TRAIL-induced apoptosis. In contrast, the overexpression of a constitutive active version of FoxO3a (Brunet et al. 1999; Brunet et al. 2001) further increased Bim protein levels. Apoptosis was not significantly increased. Thus, FoxO3a regulates Bim expression during TMZ- and TRAIL-induced apoptosis in U251 glioma cells. Furthermore, it was evident that FoxO3a-induced Bim expression correlated with the increased apoptotic cell death of this cell line.

FoxO3a activity can be negatively controlled by two major survival pathways, the PTEN/ PI3K/ Akt and the Raf/ MAPK/ ERK1/2 signalling pathways (Wang et al. 2011). We found elevated levels of active Akt in the TMZ- and TRAIL-sensitive cell line U251 during treatment, whereas resistant MZ294 cells did not show significant activation of Akt (Figure 5-9). Akt or protein kinase B is usually regarded as a survival factor that promotes cell survival (Brunet et al. 1999; Golding et al. 2009). The occurrence of highly elevated

levels of phosphorylated Akt in U251 cells, which actually undergo apoptosis could therefore suggest that Akt activity is insufficient to inhibit apoptosis in U251 cells. However, it has also been shown that the uncontrolled activation of Akt can have the very opposite effect and promote apoptosis, based on cell type and stimulus (van Gorp et al. 2006; Choi et al. 2010). Further testing will be needed to elucidate the role of Akt during TMZ- and TRAIL-induced apoptosis in U251 cells.

Analysis of ERK1/2 activity revealed significantly increased levels of phosphorylated ERK in MZ294 cells during TMZ- and TRAIL treatment (Figure 5-10 A). In U251 cells, ERK1/2 was not activated and even further downregulated following treatment. It has been previously demonstrated that ERK1/2 can directly regulate FoxO3a through phosphorylation, thereby promoting FoxO3a-degradation via its E3-ligase MDM2 (Yang et al. 2008). We found that the inhibition of ERK1/2 activity led to the activation of FoxO3a and a strong upregulation of the BH3-only protein Bim (Figure 5-10 B). Blockage of ERK1/2 -promoted cell survival led to a reduced proliferation rate in the formerly treatment-resistant cell line MZ294 (Figure 5-10 C). Therefore, Bim expression was negatively regulated by ERK1/2 / FoxO3a survival signalling in the cell line MZ294 and potentially in other treatment resistant tumours. Additionally, ERK1/2 activity plays also a role in the repression of Bim (Greenhough et al. 2010). Post-transcriptional modification of Bim via direct protein phosphorylation by ERK1/2 and consequent degradation of Bim was associated with tumour progression to a metastatic phenotype.

In conclusion, our study highlights the role of the Raf/ MAPK/ ERK1/2 signalling pathway, involving FoxO3a activity, in the control of Bim expression and protein stability. The development of chemotherapeutics aiming specifically at Bim as an executioner of cell death could greatly enhance therapy for patients suffering from GBM. Novel inhibitors and enhancers targeting the ERK1/2/ FoxO3a/ Bim axis should, therefore, be included into a multitargeted therapy for treatment-resistant gliomas.

6 General Discussion

6.1 Apoptosis resistance and aberrant cell survival signalling in glioblastoma multiforme

Glioblastoma multiforme is the most aggressive form of primary brain tumour, with fatal consequences for the patient (Louis et al. 2007; Bonavia et al. 2011). The high mortality rate due to a fast tumour progression and an invasive phenotype combined with the complete lack of a cure make these tumours one of the biggest challenge in cancer research (Stupp et al. 2005; Johnson & O'Neill 2011; Friedman 2007). Despite recent therapeutic advances, current available treatment options only marginally improve patient outcome (Hetschko et al. 2008). Molecular profiling of various types of cancer, including glioblastoma is a promising opportunity for the development of new therapies and prognostic markers (Settle & Sulman 2011; Jung et al. 2011).

In this thesis, we analysed the role of apoptosis resistance in glioblastoma by correlating expression profiles of apoptotic proteins to chemotherapeutic sensitivity and progression-free survival in glioma cell lines and GBM patient samples, respectively (Figure 3-7, 3-11, 4-2 and 4-4). Many studies implicate that the expression and activity of various components of the apoptotic signalling cascade influences the decision of cell death or survival (Irmler et al. 1997; Hanahan & Weinberg 2000; Cillessen et al. 2007; Furukawa et al. 2005; Shen et al. 2010; Tirapelli et al. 2010; Nomura et al. 2008; Kim et al. 2004; Amundson et al. 2000; Vogler et al. 2009; Johnson et al. 2003; Olopade et al. 1997; Jiang et al. 2003; Greenhough et al. 2010; Sträter et al. 2010; Herr & Debatin 2001). For example, loss of death receptor DR4 and DR5 expression, high expression of FLIP and the loss of caspase-8 expression all contribute to the inhibition of the extrinsic apoptotic pathway (Kim et al. 2003; Irmler et al. 1997). Anti-apoptotic Bcl-2 family members such as Bcl-2 and Bcl-x_L are regularly overexpressed, while their pro-apoptotic counterparts, BH3-only proteins, are downregulated in many types of tumours, which effectively blocks the activation and the execution of the mitochondrial apoptotic pathway (Schwarz et al. 2001; Johnson et al. 2003). Bcl-2 family members are also crucial for the mediation of death receptor signalling in type II cells (Fecker et al. 2006; Wong & Puthalakath 2008; Hetschko

et al. 2007; Raisova et al. 2001). In type II cells, activation of the extrinsic apoptotic pathway culminates in the engagement of the mitochondrial apoptotic pathway (Rudner et al. 2005). Dysregulation of proteins involved in apoptosome formation and the caspase cascade are also common, including executioner caspase-3, which is regularly low expressed in gliomas (Tirapelli et al. 2010; Nomura et al. 2008). Overexpression of the caspase-inhibitor XIAP affects both extrinsic and intrinsic apoptotic pathways (Wagenknecht et al. 1999). The dysregulation of apoptosis has been shown to contribute to cancer formation, development and resistance (Plati & Khosravi-Far 2008).

In our study, the analysed glioma cell lines and GBM patient samples also displayed extensive alterations in the expression of various apoptotic signalling components (Figures 3-7, 3-11, 4-2, 4-4 and 4-9). In all glioma cell lines and all GBM patient samples, we found up- or downregulation of members of both extrinsic and intrinsic apoptotic pathways, when compared to the cervix carcinoma cell line HeLa.

In most glioma cell lines, the pro-apoptotic proteins procaspase-8 and 9, Apaf-1, Bim, PUMA, Noxa, DR4 and DR5 were generally low expressed, while the anti-apoptotic proteins Bcl-2, Bcl-x_L and to some extent XIAP were commonly high expressed in comparison to HeLa (Figures 3-7, 4-2 and 4-9). Glioma cell lines also generally responded later to STS treatment when compared to the more sensitive HeLa cell line (data not shown). Thus, all glioma cell lines showed typical characteristics of highly malignant tumour cells that exceeded the attributes of other, less malignant cancer types.

In addition, apoptosis-resistant cell lines showed even higher levels of certain anti-apoptotic proteins, namely XIAP and Bcl-x_L and much lower levels of pro-apoptotic procaspase-3, Smac, Bim and Noxa than apoptosis-sensitive cell lines (Figures 3-7, 4-2 and 4-9). Especially the overexpression of XIAP and Bcl-x_L, which affects both apoptotic pathways, probably has a severe impact on the ability of tumour cells to undergo apoptosis, in accordance with published findings (Shoji et al. 2011; Fakler et al. 2009). Several studies indicate that overexpression of Bcl-x_L or Bcl-2 efficiently blocks cytochrome *c* release, thereby preventing mitochondrial apoptosis (Kojima 1998; Garrido et al. 2006; Schwarz et al. 2001). In consistency, we demonstrated that though both apoptosis-resistant and apoptosis-sensitive cell lines were capable of releasing cytochrome *c* after apoptosis

induction with a strong stimulus, the amount of released cytochrome *c* in the resistant cell line, which also showed higher Bcl-x_L levels, was much lower than in the sensitive cell line (Figure 3-6 D). Therefore, the characteristic differences between treatment-resistant and treatment-sensitive cell lines indicate that treatment failure is caused by a shift in the balance of pro- and antiapoptotic proteins towards apoptosis resistance.

Most GBM patient samples also displayed a general overexpression of Bcl-2 and Bcl-x_L and low levels of Bim (Figures 3-12 and 4-5). However, short- and long-term PFS patient samples show highly significant differences in their protein expression and little common features. Short-term survival PFS overexpressed XIAP and Bcl-2 and downregulated Bak, while long-term PFS patient samples showed higher expression of procaspase-3, procaspase-9, Smac and Bak. Thus, our correlation analyses confirmed the interrelationship between this characteristic upregulation of anti-apoptotic proteins and downregulation of pro-apoptotic proteins and a short progression-free survival time (Figures 3-13 and 4-7).

Taken together, gliomas showed strong suppression of apoptosis which confers a survival advantage to the cells (Hanahan & Weinberg 2000; Lowe et al. 2004). Several studies indicate that such an intrinsic or acquired apoptosis resistance is a major complication during chemo- and radiotherapy of many cancer patients (Guan et al. 2011; Zhang & Fang 2005; Bargou et al. 1995; Vogler et al. 2007; Baylin 2011). Thus, our findings demonstrate that one underlying cause of treatment failure in glioma cell lines and of a shortened progression-free survival time in GBM patients is the obvious apoptosis resistance in these cells and tumour specimens, mainly conferred by overexpression of XIAP and anti-apoptotic Bcl-2-like proteins.

Defects in the apoptotic machinery in cancer cells are often accompanied by aberrantly active survival pathways (Lowe et al. 2004; Herr & Debatin 2001; Maddika et al. 2007). Survival signalling is distinct from apoptotic signalling, but interactions between survival and apoptotic pathways are common (Marani et al. 2004; Iglesias-Serret et al. 2007; Reginato et al. 2003; Beere 2005; Elgendy et al. 2011). Aquired dysregulation of cellular pathways can arise from alterations of the genome during targeted therapies (Sawyers

2009). Tumour progression is driven by the accumulation of additional mutations (Loeb & Loeb 2000). In chronic myelogeneous leukemia, which harbour the BCE-ABL mutation, the use of drugs against single oncoproteins, for example the drug imatinib against, or against gastrointestinal stromal tumour, promotes the seletion for secondary mutations within the same gene (Al-Ali et al. 2004; Bertucci et al. 2006). This renders the previous treatment ineffective and the tumour resistant to common therapy regimes. Mutations driven by the selective pressure of targeted therapies can also lead to drug antagonism through increased signalling involving alternative survival pathways (Sawyers 2009).

The Ras survival signalling pathway is the subject of extensive studies since the 1980s and was shown to have a strong impact on oncogenesis and tumour biology (DeFeo et al. 1981; Parada et al. 1982; Ellis et al. 1982; Mccubrey et al. 2007). Ras can be activated by receptor tyrosine kinases (RTK) such as EGFR and PDGFR. Alterations in EGFR expression are highly frequent mutations in glioblastomas (Louis et al. 2007). Elevated EGFR activity can result from gene mutations such as the vIII EGFR variant that renders the receptor insensitive to normal control mechanisms (Burger et al. 2001; Cemeus et al. 2008). However, *EGFR* gene amplifications and rearrangements are the most common form of EGFR mutation in glioblastoma (Ekstrand et al. 1991; Burger et al. 2001). Constitutive activation of Ras/ RAF/ ERK1/2 signalling can also result from elevated B-Raf kinase activity (Sheridan et al. 2008). The V600E mutation in B-Raf results in an increase in resistance to apoptosis induction by chemotherapeutic drugs and promotes ERK-dependent phosphorylation of Bim (Sheridan et al. 2008). However, BRAF V600E mutations are not very common, while *BRAF* copy number gain is a frequent event in glioblastomas (Deimling et al. 2010). Activation of Ras culminates in the induction of multiple downstream factors, including MAP kinases, which are direct downstream effectors of Ras, leading to activation of the Ras/ RAF/ ERK1/2 pathway, or the induction of the peripheral P13K/ Akt pathway (Meier et al. 2007; Meier et al. 2005).

The present study demonstrates the involvement of the Ras/ RAF/ ERK1/2 pathway in chemoresistance of glioma cell lines to a combination therapy with TMZ and TRAIL (Figure 5-10). The apoptosis resistant glioma cell line MZ294 displayed upregulation of ERK1/2, but no upregulation of Akt after treatment (Figures 5-9 and 5-10). This increased

activity of survival signalling is a common response to chemotherapy with cytotoxic agents (Mandic et al. 2001; Fingas et al. 2011). We showed that the direct inhibition of ERK1/2 activity with the inhibitor PD98059 (Pang et al. 1995) followed by dual drug treatment with TMZ and TRAIL lead to growth inhibition in the MZ294 cell line (Figure 5-10 C). Thus, apoptosis resistance in glioma cell lines is partially conferred by aberrant Ras/ RAF/ ERK1/2 signalling.

We also demonstrated that the Ras/ RAF/ ERK1/2 pathway is involved in the regulation of the pro-apoptotic protein Bim in gliomas (Figure 5-10 B). Following ERK1/2 inhibition, MZ294 cells displayed upregulation of Bim concomitantly with activation of the Bim transcription factor FoxO3a. It is known that FoxO3a activity is under the direct control of ERK1/2 (Yang et al. 2008). In the sensitive glioma cell line U251, we demonstrated that the transcription factor FoxO3a, but not JNK/ c-Jun, is involved in the upregulation of Bim following treatment (Figures 5-6, 5-7 and 5-8). Also, Bim protein stability can also be negatively regulated by ERK activity, leading to the ubiquitination and degradation of Bim via the proteasome (Luciano et al. 2003). Thus, irregular Ras/ RAF/ ERK1/2 signalling could transcriptionally inhibit Bim expression via FoxO3a, and possibly also post-transcriptionally via ERK1/2 mediated phosphorylation. This intrinsic inhibition of Bim expression in resistant cell lines could directly interfer with their ability to undergo cell death.

Taken together, the extensive dysregulation of apoptotic proteins and the increased activity of survival signalling in gliomas, as displayed here in this study, reflects on the multiresistant phenotype of glioblastomas, in consistency with previous findings (Vaupel 2004; Pàez-Ribes et al. 2009). Therefore, it might be necessary to develop novel treatment combinations that aim at multiple targets in both apoptotic and survival signalling pathways in order to overcome treatment resistance in glioblastomas.

6.2 Identification of novel biomarkers to predict patients outcome

The complexity and heterogeneity of glioblastomas has made it difficult to make prognostic determinations based purely on clinicopathological characteristics (Bonavia et al. 2011). New insights into the molecular mechanisms behind drug resistance can facilitate the identification of diagnostic markers and the development of novel apoptosis-inducing chemotherapeutics (Souglakos et al. 2009). Several molecular markers for glioblastomas provide predictive and prognostic information, including O^6-methylguanine-DNA methyltransferase (MGMT) promoter methylation status, which is associated with treatment response to TMZ in patients (Hegi et al. 2005; Kitange et al. 2009; Sarkaria et al. 2008; Shah et al. 2011). The MGMT *gene* encodes for a DNA-repair enzyme that counteracts the DNA-alkylating effects of the standard GBM therapy TMZ, thereby possibly contributing to GBM resistance (Brennand & Margison 1986; van Nifterik et al. 2010). Downregulation of MGMT protein expression was shown to result from epigenetic methylation of the MGMT promoter (Watts et al. 1997). Epigenetic alterations do not change the DNA sequence, but modify the genome by DNA methylation and histone deacetylation, which results in *gene* silencing (Killian et al. 2001; Boumber & Issa 2011). During DNA methylation, methyl groups are added to cytosines to create 5-methylcytosines. A correlation between epigenetic MGMT *gene* silencing and prolonged patient survival was first demonstrated by Hegi et al. (Hegi et al. 2008). In their study, Hegi et al. argue that high levels of MGMT activity may be an important determinant of TMZ treatment failure and could be utilized as a prognostic marker to classify patients. However, the clinical application of this marker is controversially discussed (Costa et al. 2010; Tang et al. 2011; Preusser et al. 2008). Multiple studies provided evidence for a correlation between MGMT promoter methylation and patient survival (Kitange et al. 2009; Sarkaria et al. 2008; Shah et al. 2011; Hegi et al. 2008; van Nifterik et al. 2010). On the contrary, other investigators were unable to associate patient outcome with MGMT promoter methylation (Tang et al. 2011; Costa et al. 2010; Preusser et al. 2008). In their studies, Tang et al. and Costa et al. reported the frequency of MGMT methylation among Chinese and Portuguese GBM patients, respectively. They found no statistically significant association between MGMT promoter methylation and the outcome of GBM patients treated with

temozolomide. In melanoma, MGMT expression was associated with tolerance to TMZ treatment, but not with patients outcome (Hassel et al. 2010). The clinical significance of MGMT status as a biomarker thus warrants further evaluation in a larger scale.

About 80% of primary glioblastoma display a phenotype of global hypermethylation (Alonso et al. 2003; Gonzalez-Gomez et al. 2003; van den Bent et al. 2011). This mechanism is a primary step during tumourigenesis, leading to the silencing of several tumour suppressor genes (Gonzalez-Gomez et al. 2003). Van den Bent et al. also argue that general hypermethylation serves as a better predictive marker for patients survival than MGMT promoter methylation, which requires further investigations (van den Bent et al. 2011).

In our study, we analyzed the promoter methylation status of MGMT in glioma cell lines. A TMZ-sensitive and a TMZ-resistant cell line displayed similar levels of promoter methylation, indicating that MGMT activity is impaired in both cell lines to an equal amount (Figure 3-3 and Table 3-1). Consequently, it is possible that other resistance mechanisms than the MGMT repair activity might be at work in the glioma cell lines that we used in this study. It has been implied that such a MGMT-independent TMZ-resistance can be associated with hyperactivity of the PI3K-signalling pathway (Gaspar et al. 2010). Another possibility for TMZ resistance as we demonstrate here in this thesis is the previously discussed apoptosis resistance. Aberrant methylation can influence the expression of a wide range of apoptotic proteins such as caspase-3, Apaf-1, caspase-8, Bcl-2 and Bax, among others (Hervouet et al. 2010; Martinez et al. 2007; Furukawa et al. 2005; Yakovlev et al. 2010). Thus, MGMT promoter methylation as we observed in glioma cell lines might indicate that other genes are also silenced by methylation, such as apoptotic proteins, which contributes to the treatment resistance in glioblastomas. However, global hypermethylation in resistant or sensitive gliomas was not investigated in this study. Still, based on our MGMT promoter methylation analysis, we conclude that MGMT promoter methylation is not a highly predictive marker for TMZ sensitivity in the panel of glioma cell lines that we used in this study, a complication that was also encountered by Blough et al. and Gaspar et al. in their studies (Blough et al. 2010; Gaspar et al. 2010).

In order to predict treatment outcome and progression-free survival with higher accuracy, we here demonstrated the advantage of performing a comprehensive analysis of apoptotic protein expression. In chapter 3, we showed that the susceptibility of gliomas to single, cytotoxic agents can be determined by the assessment of components of the mitochondrial apoptotic pathway. As discussed in chapter 4, cellular response to single drugs that engage the extrinsic apoptotic pathway and to combination therapy with drugs that stimulate both apoptotic pathways were best predicted by assessment of components of both apoptotic cascades. The individual apoptotic protein analyses correlated well with treatment sensitivity and progression-free survival in gliomas. This was confirmed by using a more sensitive, multivariate statistical approach (PCA) that combined the molecular expression profiles of the interactive protein network in comprehensive correlation analyses (Figures 3-9, 3-13, 4-6, 4-7 and 4-10). The PCA highlighted a common pattern of protein expression, thereby indicating that the observed correlation to treatment response was not coincidental. The computational model APOPTO CELL, which simulates the interaction of proteins involved in mitochondrial apoptosis, also correctly predicted cellular response and patients outcome, in consistency with the PCA (Figures 3-10 and 3-14). Systems biology has recently emerged as a promising approach to assess the complexity of treatment resistance, using both experimental data and computational modelling (Kitano 2002; Peri et al. 2003). The analysis of cellular networks, including apoptotic and survival signalling, enables us to understand how cancer cells function. The usability of the APOPTO CELL model as a predictive tool was previously demonstrated in colorectal cancer (Hector et al. 2011). Thus, the expression analysis of apoptotic proteins provided valuable information about the status of apoptosis resistance in gliomas. The described correlation methods and the computational model APOPTO CELL were highly predictive of cellular treatment response and progression-free survival and could be utilised as a personalised approach to identify patients that will most likely respond to a chosen treatment regime.

6.3 Outlook: Therapeutic intervention and personalised medicine

Differential protein expression can be found within individuals, but also within the tumour (Rice et al. 2010; Bonavia et al. 2011). The establishment of the molecular signature of individual tumour specimens could eventually lead to a more personalised therapy (Hector et al. 2011; Weller et al. 2010).

The analysis of apoptotic and survival signalling pathways in this study revealed several possible targets that could be utilised to improve and extend current treatment regimes. The most prominent signature of gliomas that we found was the differential expression of pro-apoptotic caspase-3 and anti-apoptotic XIAP and Bcl-x_L, among other protein alterations which we discussed in the chapters. XIAP overexpression in cancer cells may select for tumour cell survival following various apoptotic stimuli. This protein is the most potent member of the caspase-inhibitory (IAP) family, partly due to its ability to directly inhibit the enzymatic activity of caspases (Schimmer et al. 2006). Members of the inhibitor of apoptosis (IAP) family play key roles in the suppression of apoptosis (Deveraux et al. 1998; Wagenknecht et al. 1999). Downregulation or inhibition of XIAP can influence the expression and the activity of various proteins both involved in extrinsic and intrinsic apoptotic signalling, most prominently by releasing caspases (Wagenknecht et al. 1999; Siegelin et al. 2009). A promising novel strategy involves the use of IAP inhibitors in combination with other drugs (Siegelin et al. 2009; Fakler et al. 2009; Meike Vogler et al. 2008; Kim et al. 2004). Small molecule XIAP inhibitors in combination with TRAIL were shown to effectively abolish XIAP activity, leading to the circumvention of the mitochondrial pathway in Bcl-2-overexpressing type II cells (Fakler et al. 2009). Another strategy involves the use of proteasome inhibitors such as bortezomib, which prevent the degradation of ubiquitylated proteins by the proteasome, a large multi-subunit complex with intrinsic proteolysis activity (Teicher et al. 1999). One effect of bortezomib treatment is the downregulation of XIAP (Kahana et al. 2011). Bortezomib also stabilises pro-apoptotic Bcl-2 proteins and is already in use in therapy for mantle cell lymphoma and relapsed multiple myeloma (Twombly 2003; Witzig 2005). Finally, the administration of roscovitine, a Cdc2/ Cdk2 inhibitor, was also demonstrated to indirectly downregulate XIAP, contributing to the amplification of caspase cascades and thereby promotes TRAIL-

mediated apoptosis (Kim et al. 2004). The use of Smac mimetics, the natural XIAP inhibitor, also offers an interesting therapeutic opportunity (Hossbach et al. 2009; Berger et al. 2011).

To conclude, in this study, we identified a characteristic pattern of extensive dysregulation of pro- and anti-apoptotic proteins in glioma cell lines and GBM patient samples. We successfully correlated chemotherapeuic sensitivity and progression-free survival time with the individual expression profiles of these pro- and anti-apoptotic proteins, using two statistical approaches and one computational model system. The comprehensive analysis of pro- and anti-apoptotic proteins as presented here could be utilised to predict apoptosis resistance with high accuracy (Jia et al. 2010; Plati & Khosravi-Far 2008). Finally, we showed that the survival signalling pathway Ras/RAF/ERK1/2 is involved in the promotion of cell growth, partly mediated by the downregulation of Bim expression via FoxO3a, a direct target of Erk1/2 phosphorylation. Thus, the long term aim of this work is to support a more personal approach to anti-cancer therapies, where the individual characteristics of each patient is taking into account to assist finding the most fitting type of treatment.

References

Adams, J. M. and Cory, S. (2007). The Bcl-2 apoptotic switch in cancer development and therapy. *Oncogene*, **26**(9), 1324-1337.

Adams, J. M. and Cory, S. (1998). The Bcl-2 Protein Family : Arbiters of Cell Survival. *Science* **281**, 1322-1326.

Agarwala, S. S. and Kirkwood, J. M. (2000). Temozolomide, a Novel Alkylating Agent with Activity in the Central Nervous System , May Improve the Treatment of Advanced Metastatic Melanoma. *The Oncologist* **5**, 144-151.

Akiyama, T., Dass, C. R., Choong, P. F. M. (2009). Bim-targeted cancer therapy : A link between drug action and underlying molecular changes. *Molecular Cancer Therapeutics* **8** (December), 1-8.

Al-Ali, H. K., Heinrich, M.C., Lange, T., Krahl, R., Mueller, M., Müller, C., Niederwieser, D., Druker, B. J.,Deininger, M. W. N. (2004). High incidence of BCR-ABL kinase domain mutations and absence of mutations of the PDGFR and KIT activation loops in CML patients with secondary resistance to imatinib. *The Hematology Journal* **5**(1), 55-60.

Alonso, M. E., Bello, M. J., Gonzalez-Gomez, P., Arjona, D., Lomas, J., de Campos, J. M., Isla, A., Sarasa, J. L., Rey, J. A. (2003). Aberrant promoter methylation of multiple genes in oligodendrogliomas and ependymomas. *Cancer Genetics and Cytogenetics* **144**(2), 134-42.

Amundson, S.A., Myers, T.G., Scudiero, D., Lines, C.C., Kitada, S., Reed, J.C., & Fornace, A.J. (2000). An Informatics Approach Identifying Markers of Chemosensitivity in Human Cancer Cell Lines. *Cancer Research* **60**(21), 6101-6110.

Asai, A., Miyagi, Y., Sugiyama, A., Gamanuma, M., Hong, S. H., Takamoto, S., Nomura, K., Matsutani, M., Takakura, K., Kuchino, Y. (1994). Negative effects of wild-type p53 and s-Myc on cellular growth and tumorigenicity of glioma cells. Implication of the tumor suppressor genes for gene therapy. *Journal of Neurooncology*, **19**(3), 259-268.

Ashkenazi, A. and Dixit, V.M. (1999). Apoptosis control by death and decoy receptors. *Current Opinion in Cell Biology*, **11**(2), 255-60.

Austin, M. and Cook, S. J. (2005). Increased expression of Mcl-1 is required for protection against serum starvation in phosphatase and tensin homologue on chromosome 10 null mouse embryonic fibroblasts, but repression of Bim is favored in human glioblastomas. *The Journal of biological Chemistry* **280**(39), 33280-33288.

Badie, B., Hunt, K., Economou, J. S., Black, K. L. (1994). Stereotactic delivery of a recombinant adenovirus into a C6 glioma cell line in a rat brain tumor model. *Neurosurgery* **35**(5), 910-916.

Bargou, R. C., Daniel, P. T., Mapara, M. Y., Bommert, K., Wagener, C., Kallinich, B., Royer, H. D., Dörken, B. (1995). Expression of the bcl-2 gene family in normal and malignant breast tissue: low bax-alpha expression in tumor cells correlates with resistance towards apoptosis. *International journal of cancer* **60**(6), 854-859.

Baylin, S. B. (2011). Resistance , epigenetics and the cancer ecosystem. *Nature Medicine* **17**(3), 288-289.

Beere, H. M. (2005). Death versus survival : functional interaction between the apoptotic and stress-inducible heat shock protein pathways. *The Journal of Clinical Investigation* **115**(10), 2633-2639.

Bender, A., Opel, D., Naumann, I., Kappler, R., Friedman, L., von Schweinitz, D., Debatin, K. M., Fulda, S. (2010). PI3K inhibitors prime neuroblastoma cells for chemotherapy by shifting the balance towards pro-apoptotic Bcl-2 proteins and enhanced mitochondrial apoptosis. *Oncogene*, **103**, 1-10.

Berger, R., Jennewein, C., Marschall, V., Karl, S., Cristofanon, S., Wagner, L., Vellanki, S. H., Vellanki, S. H., Hehlgans, S., Rödel, F., Debatin, K. M., Ludolph, A. C., Fulda, S. (2011). NF-κB is required for Smac mimetic-mediated sensitization of glioblastoma cells for γ-irradiation-induced apoptosis. *Molecular Cancer Therapeutics* **10**(10), 1867-18.

Bertin, J., Armstrong, R. C., Ottilie, S., Martin, D. A., Wang, Y., Banks, S., Wang, G. H., Senkevich, T. G., Alnemri, E. S., Moss, B., Lenardo, M. J., Tomaselli, K. J., Cohen, J. I. (1997). Death effector domain-containing herpesvirus and poxvirus proteins inhibit both Fas- and TNFR1-induced apoptosis. *Biochemistry* **94**(4), 1172-1176.

Bertucci, F., Goncalves, A., Monges, G., Madroszyk, A., Guiramand, J., Moutardier, V., Noguchi, T., Dubreuil, P., Sobol, H. (2006). Acquired resistance to imatinib and secondary KIT exon 13 mutation in gastrointestinal stromal tumour. *Oncology Reports*, **16**(1), 97-101.

Biswas, S. C. and Greene, L. A. (2002). Nerve Growth Factor (NGF) Down-regulates the Bcl-2 Homology 3 (BH3) Domain-only Protein Bim and Suppresses Its Proapoptotic Activity by Phosphorylation. *Biochemistry* **277**(51), 49511-49516.

Biswas, S. C., Shi, Y., Sproul, A., Greene, L. A. (2007). Pro-apoptotic Bim Induction in Response to Nerve Growth Factor Deprivation Requires Simultaneous Activation of Three Different Death Signaling Pathways. *Journal of Biological Chemistry* **282**(40), 29368 - 29374.

Blough, M. D., Westgate, M. R., Beauchamp, D., Kelly, J. J., Stechishin, O., Ramirez, A. L., Weiss, S., Cairncross, J. G. (2010). Sensitivity to temozolomide in brain tumor initiating cells. *Neurooncology* **12**(7), 756-760.

Blough, M. D., Zlatescu, M. C., Cairncross, J. G. (2007). O 6 -Methylguanine-DNA Methyltransferase Regulation by p53 in Astrocytic Cells. *Cancer Research* **67**(2), 580-584.

Bock, C., Reither, S., Mikeska, T., Paulsen, M., Walter, J., Lengauer, T. (2005). BiQ Analyzer: visualization and quality control for DNA methylation data from bisulfite sequencing. Bioinformatics, **21**(21), 4067-4068.

Bodey, B., Bodey, V., Siegel, S. E., Nasir, A., Coppola, D., Hakam, A., Kaiser, H. E. (2004). Immunocytochemical detection of members of the caspase cascade of apoptosis in high-grade astrocytomas. *In Vivo (Athens, Greece)* **18**(5), 593-602.

Bonavia, R., Inda, M. D. M., Cavenee, W. K., Furnari, F. B. (2011). Heterogeneity Maintenance in Glioblastoma: A Social Network. *Cancer research* **71**(12), 4055-4060.

Bouillet, Philippe, Zhang, L. C., Huang, D. C. S., Webb, G. C., Bottema, C. D. K., Shore, P., Eyre, H. J., Sutherland, G. R., Adams, J. M. (2001). Gene structure , alternative splicing , and chromosomal localization of pro-apoptotic Bcl-2 relative Bim. *Mammalian Genome* **168**, 163-168.

Boumber, B. Y. and Issa, J. P. (2011). Epigenetics in Cancer : What's the Future? *Oncology* **25**(3), 1-13.

Boya, P. and Kroemer, G. (2008). Lysosomal membrane permeabilization in cell death. *Oncogene* **27**, 6434-6451.

Brennan, C., Momota, H., Hambardzumyan, D., Ozawa, T., Tandon, A., Pedraza, A., Holland, E. (2009). Glioblastoma subclasses can be defined by activity among signal transduction pathways and associated genomic alterations. *Public Library of Science one*, **4**(11), e7752-7762.

Brennand, J. and Margison, G. P. (1986). Reduction of the toxicity and mutagenicity of alkylating agents in mammalian cells harboring the Escherichia coli alkyltransferase gene. *Biochemistry* **83**(17), 6292-6296.

Brunet, A., Bonni, A., Zigmond, M. J., Lin, M. Z., Juo, P., Hu, L. S., Anderson, M. J., Arden, K. C., Blenis, J., Greenberg, M. E. (1999). Akt promotes cell survival by phosphorylating and inhibiting a Forkhead transcription factor. *Cell* **96**(6), 857-868.

Brunet, A., Park, J., Tran, H., Hu, L. S., Hemmings, B. A., Greenberg, M. E. (2001). Protein kinase SGK mediates survival signals by phosphorylating the forkhead transcription factor FKHRL1 (FOXO3a). *Molecular and Cellular Biology* **21**(3), 952-965.

Burger, P C, Pearl, D. K., Aldape, K., Yates, A. J., Scheithauer, B. W., Passe, S. M., Jenkins, R. B., James, C. D. (2001). Small cell architecture--a histological equivalent of

EGFR amplification in glioblastoma multiforme? *Journal of Neuropathology and Experimental Neurology* **60**(11), 1099-1104.

Byrne, G. I. and Ojcius, D. M. (2004). Chlamydia and apoptosis: life and death decisions of an intracellular pathogen. *Microbiology* **2**(10), 802-808.

Candé, C., Cohen, I., Daugas, E., Ravagnan, L., Larochette, N., Zamzami, N., & Kroemer, G. (2002). Apoptosis-inducing factor (AIF): a novel caspase-independent death effector released from mitochondria. *Biochimie* **84**(2-3), 215-222.

Cao, V. T., Jung, T.-Y., Jung, S., Jin, S.-G., Moon, K.-S., Kim, I.-Y., Kang, S.-S., Park, C. S., Lee, K. H., Chae, H. J. (2009). The correlation and prognostic significance of MGMT promoter methylation and MGMT protein in glioblastomas. *Neurosurgery* **65**(5), 866-875.

Capper, D., Gaiser, T., Hartmann, C., Habel, A., Mueller, W., Herold-Mende, C., von Deimling, A., Siegelin, M. D. (2009). Stem-cell-like glioma cells are resistant to TRAIL/Apo2L and exhibit down-regulation of caspase-8 by promoter methylation. *Acta Neuropathologica* **117**(4), 445-456.

Castedo, M., Perfettini, J.-L., Roumier, T., Valent, A., Raslova, H., Yakushijin, K., Horne, D., Feunteun, J., Lenoir, G., Medema, R., Vainchenker, W., Kroemer, G. (2004). Mitotic catastrophe constitutes a special case of apoptosis whose suppression entails aneuploidy. *Oncogene* **23**(25), 4362-4370.

Cemeus, C., Zhao, T. T., Barrett, G. M., Lorimer, I. A., Dimitroulakos, J. (2008). Lovastatin enhances gefitinib activity in glioblastoma cells irrespective of EGFRvIII and PTEN status. *Journal of Neurooncology* **90**, 9-17.

Chae, H. J., Kang, J. S., Byun, J. O., Han, K. S., Oh, S. M., Kim, H. M., Chae, S. W., Kim, H. R. (2000). Molecular mechanism of staurosporine-induced apoptosis in osteoblasts. *Pharmacological Research* **42**(4), 373-381.

Chai, J., Wu, Q., Shiozaki, E., Srinivasula, S. M., Alnemri, E. S., Shi, Y. (2001). Crystal Structure of a Procaspase-7 Zymogen : Mechanisms of Activation and Substrate Binding. *Cell* **107**, 399-407.

Chang, D. W., Xing, Z., Pan, Y., Algeciras-Schimnich, A., Barnhart, B. C., Yaish-ohad, S., Peter, M. E., Yang, X. (2002). c-FLIP L is a dual function regulator for caspase-8 activation and CD95-mediated apoptosis. *EMBO Journal* **21**(14), 3704-3714.

Chen, S., Dai, Y., Harada, H., Dent, P., Grant, S. (2007). Mcl-1 down-regulation potentiates ABT-737 lethality by cooperatively inducing Bak activation and Bax translocation. *Cancer Research*, **67**(2), 782-791.

Chipuk, J. E., Moldoveanu, T., Llambi, F., Parsons, M. J., Green, D. R. (2010). The BCL-2 Family Reunion. *Molecular Cell* **37**(3), 299-310.

Choi, H. R., Shin, J. W., Lee, H. K., Kim, J. Y., Huh, C. H., Youn, S. W., Park, K. C. (2010). Potential redox-sensitive Akt activation by dopamine activates Bad and promotes cell death in melanocytes. *Oxidative Medicine and Cellular Longevity* **3**(3), 219-224.

Cillessen, S. A. G. M., Hess, C. J., Hooijberg, E., Castricum, K. C. M., Kortman, P., Denkers, F., Vos, W., van de Wiel, M. A., Schuurhuis, G. J., Ossenkoppele, G. J., Meijer, C. J. L. M., Oudejans, J. J. (2007). Inhibition of the intrinsic apoptosis pathway downstream of caspase-9 activation causes chemotherapy resistance in diffuse large B-cell lymphoma. *Clinical Cancer Research* **13**(23), 7012-7021.

Clark, A. S., Deans, B., Stevens, M. F., Tisdale, M. J., Wheelhouse, R. T., Denny, B. J., Hartley, J. A. (1995). Antitumor imidazotetrazines. 32. Synthesis of novel imidazotetrazinones and related bicyclic heterocycles to probe the mode of action of the antitumor drug temozolomide. *Journal of Medicinal Chemistry* **38**(9), 1493-1504.

Cohen, S. N., Chang, A. C., Hsu, L. (1972). Nonchromosomal antibiotic resistance in bacteria: genetic transformation of Escherichia coli by R-factor DNA. *Proceedings of the National Academy of Sciences of the United States of America* **69**(8), 2110-2114.

Costa, B. M., Caeiro, C., Guimaraes, I., Damasceno, M., Reis, R. (2010). Prognostic value of MGMT promoter methylation in glioblastoma patients treated with temozolomide-based chemoradiation: A Portuguese multicentre study. *Oncology Reports* **23**(6), 1655-1662.

Cosulich, S. C., Worrall, V., Hedge, P. J., Green, S., Clarke, P. R. (1997). Regulation of apoptosis by BH3 domains in a cell-free system. *Current Biology* **7**(12), 913-920.

Dai, Y. and Grant, S. (2007). Targeting multiple arms of the apoptotic regulatory machinery. *Cancer Research* **67**(7), 2908-2011.

Das, P., Puri, T., Jha, P., Pathak, P., Joshi, N., Suri, V., Sharma, M. C., Sharma, B. S., Mahapatra, A. K., Suri, A., Sarkar, C. (2011). A clinicopathological and molecular analysis of glioblastoma multiforme with long-term survival. *Journal of Clinical Neuroscience* **18**(1), 66-70.

DeFeo, D., Gonda, M. A., Young, H. A., Chang, E. H., Lowy, D. R., Scolnick, E. M., Ellis, R. W. (1981). Analysis of two divergent rat genomic clones homologous to the transforming gene of Harvey murine sarcoma virus. *Biochemistry* **78**(6), 3328-3332.

Degterev, A. and Yuan, J. (2008). Expansion and evolution of cell death programmes. *Molecular Cell Biology* **9**(5), 378-390.

Degterev, A., Boyce, M., Yuan, J. (2003). A decade of caspases. *Oncogene* **22**(53), 8543-8567.

Deimling, A. V., Korshunov, A., Hartmann, C. (2010). The Next Generation of Glioma Biomarkers : MGMT Methylation , BRAF Fusions and IDH1 Mutations. *Brain Pathology* **21**(22), 74-87.

Delft, M. F. V., Wei, A. H., Mason, K. D., Vandenberg, C. J., Chen, L., Czabotar, P. E., Willis, S. N., Scott, C. L., Day, C. L., Cory, S., Adams, J. M., Roberts, A. W., Huang, D. C S. (2006). The BH3 mimetic ABT-737 targets selective Bcl-2 proteins and efficiently induces apoptosis via Bak / Bax if Mcl-1 is neutralized. *Cancer Cell* **10**(November), 389-399.

Demaria, S., Pikarsky, E., Karin, M., Coussens, L. M., Chen, Y.-C., El-Omar, E. M., Trinchieri, G., Dubinett, S. M., Mao, J. T., Szabo, E., Krieg, A., Weiner, G. J., Fox, B. A., Coukos, G., Wang, E., Abraham, R. T., Carbone, M., Lotze, M. T. (2010). *Journal of Immunotherapy* **33**(4), 335-351.

Deveraux, Q. L., Roy, N., Stennicke, H. R., Van Arsdale, T., Zhou, Q., Srinivasula, S. M., Alnemri, E. S., Salvesen, G. S., Reed, J. C. (1998). IAPs block apoptotic events induced by caspase-8 and cytochrome c by direct inhibition of distinct caspases. *The EMBO journal* **17**(8), 2215-2223.

Dewson, G., Kratina, T., Sim, H. W., Puthalakath, H., Adams, J. M., Colman, P. M., Kluck, R. M. (2008). To Trigger Apoptosis, Bak Exposes Its BH3 Domain and Homodimerizes via BH3: Groove Interactions. *Molecular Cell* **30**(3), 369-380.

Dove, S., Coats, E., Scharfenberg, P., Franke, R. (1985). 7-substituted-4-hydroxyquinoline-3-carboxylic acids as inhibitors of dehydrogenase enzymes and of the respiration of Ehrlich ascites tumor cells: multivariate analysis and quantitative structure-activity relationship for polar substituents. *Journal of Medicinal Chemistry* **28**(4), 447-451.

Du, Han, Wolf, J., Schafer, B., Moldoveanu, T., Chipuk, J. E., Kuwana, T. (2011). BH3 domains other than Bim and Bid can directly activate Bax/Bak. *The Journal of Biological Chemistry*, **286**(1), 491-501.

Düssmann, H., Rehm, M., Kögel, D., Prehn, J. H. M. (2003). Outer mitochondrial membrane permeabilization during apoptosis triggers caspase-independent mitochondrial and caspase-dependent plasma membrane potential depolarization: a single-cell analysis. *Journal of Cell Science* **116**(Pt 3), 525-536.

Ekstrand, A. J., James, C. D., Cavenee, W. K., Seliger, B., Pettersson, R. F., Collins, V. P. (1991). Genes for epidermal growth factor receptor, transforming growth factor alpha, and epidermal growth factor and their expression in human gliomas in vivo. *Cancer Research* **51**(8), 2164-2172.

Elgendy, M., Sheridan, C., Brumatti, G., Martin, S. J. (2011). Oncogenic Ras-Induced Expression of Noxa and Beclin-1 Promotes Autophagic Cell Death and Limits Clonogenic Survival. *Molecular Cell* **42**(1), 23-35.

Elias, A., Siegelin, M. D., Steinmüller, A., von Deimling, A., Lass, U., Korn, B., Mueller, W. (2009). Epigenetic silencing of death receptor 4 mediates tumor necrosis factor-related apoptosis-inducing ligand resistance in gliomas. *Clinical Cancer Research* **15**(17), 5457-5465.

Ellis, L., Clauser, E., Morgan, D. O., Edery, M., Roth, R. A., Rutter, W. J. (1986). Replacement of insulin receptor tyrosine residues 1162 and 1163 compromises insulin-stimulated kinase activity and uptake of 2-deoxyglucose. *Cell* **45**, 721-32

Ellis, R. W., DeFeo, D., Furth, M. E., Scolnick, E. M. (1982). Mouse cells contain two distinct ras gene mRNA species that can be translated into a p21 onc protein. *Molecular and cellular biology* **2**(11), 1339-1345.

Essafi, A., Mattos, S. F. de, Hassen, Y. A. M., Soeiro, I., Mufti, G. J., Thomas, N. S. B., Medema, R. H., Lam, E. W. F. (2005). Direct transcriptional regulation of Bim by FoxO3a mediates STI571-induced apoptosis in Bcr-Abl-expressing cells. *Oncogene* **24**, 2317-2329.

Ewings, K. E., Hadfield-, K., Wiggins, C. M., A, J., Balmanno, K., Degenhardt, K., White, E., Cook, S. J. (2007). ERK1/2-dependent phosphorylation of Bim. *EMBO Journal* **26**(12), 2856-2867.

Fakler, M., Loeder, S., Vogler, M., Schneider, K., Jeremias, I., Debatin, K. M., Fulda, S. (2009). Small molecule XIAP inhibitors cooperate with TRAIL to induce apoptosis in childhood acute leukemia cells and overcome Bcl-2-mediated resistance. *Blood* **113**(8), 1710-1722.

Fallowfield, L. J. and Fleissig, A. (2011). The value of progression-free survival to patients with advanced-stage cancer. *Nature Clinical Oncology* **9**(1), 41-47.

Fecker, L. F., Geilen, C. C., Tchernev, G., Trefzer, U., Assaf, C., Kurbanov, B. M., Schwarz, C., Schwarz, C., Daniel, P. T., Eberle, J. (2006). Loss of proapoptotic Bcl-2-related multidomain proteins in primary melanomas is associated with poor prognosis. The Journal of investigative dermatology, **126**(6), 1366-1371.

Fingas, C. D., Bronk, S. F., Werneburg, N. W., Mott, J. L., Guicciardi, M. E., Cazanave, S. C., Mertens, J. C., Sirica, A. E., Gores, G. J. (2011). Myofibroblast-derived PDGF-BB promotes Hedgehog survival signaling in cholangiocarcinoma cells. *Expert Opinion on Biological Therapy* **54**(6), 2076-2088.

Fox, N. L., Humphreys, R., Luster, T. A., Klein, J. (2010). Tumor necrosis factor-related apoptosis-inducing ligand (TRAIL) receptor-1 and receptor-2 agonists for cancer therapy. *Genome* **10**(1) 1-18.

Friedman, H. S. (2007). State-of-the-art Therapy for Glioblastoma Multiforme. *US Oncological Disease*, 16-17.

Friedman, H. S., Kerby, T. (2000). Temozolomide and Treatment of Malignant Glioma 1. *Clinical Cancer Research* **6**(7), 2585-2597.

Frommer, M., McDonald, L. E., Millar, D. S., Collis, C. M., Watt, F., Grigg, G. W., Molloy, P. L., Paul, C L. (1992). A genomic sequencing protocol that yields a positive display of 5-methylcytosine residues in individual DNA strands. *Genetics* **89**(5), 1827-1831.

Fulda, S. and Debatin, K. M. (2006). Extrinsic versus intrinsic apoptosis pathways in anticancer chemotherapy. *Oncogene* **25**(34), 4798-811.

Furnari, F.B., Fenton, T., Bachoo, R. M., Mukasa, A., Stommel, J. M., Stegh, A., Hahn, W. C., Ligon, K. L., Louis, D. N., Brennan, C., Chin, L., Depinho, R. A., Cavenee, W. K. (2007). Malignant astrocytic glioma : genetics , biology , and paths to treatment. *Genes & Development* **21**, 2683-2710

Furukawa, Yutaka, Sutheesophon, K., Wada, T., Nishimura, M., Saito, Y., Ishii, H., & Furukawa, Y. (2005). Methylation silencing of the Apaf-1 gene in acute leukemia. *Molecular Cancer Research* **3**(6), 325-34.

Galluzzi, Lorenzo, Kepp, O., & Kroemer, G. (2009). RIP kinases initiate programmed necrosis. *Journal of Molecular Cell Biology* **1**(1), 8-10.

Ganten, T. M., Haas, T. L., Sykora, J., Stahl, H., Sprick, M. R., Fas, S. C., Krueger, a, Weigand, M. A., Grosse-Wilde, A., Stremmel, W., Krammer, P. H., Walczak, H. (2004). Enhanced caspase-8 recruitment to and activation at the DISC is critical for sensitisation of human hepatocellular carcinoma cells to TRAIL-induced apoptosis by chemotherapeutic drugs. *Cell Death and Differentiation* **11**, S86-96.

Garcia-Calvo, M., Peterson, E. P., Rasper, D. M., Vaillancourt, J. P., Zamboni, R., Nicholson, D. W., Thornberry, N. A. (1999). Purification and catalytic properties of human caspase family members. *Cell Death and Differentiation* **6**, 362-369.

Garrido, C., Galluzzi, L., Brunet, M., Puig, P. E., Didelot, C., Kroemer, G. (2006). Mechanisms of cytochrome c release from mitochondria. *Cell Death and Differentiation* **13**, 1423-1433.

Gaspar, N., Marshall, L., Perryman, L., Bax, D. a, Little, S. E., Viana-Pereira, M., Sharp, S. Y., Vassal, G., Pearson, A. D. J., Reis, R. M., Hargrave, D., Workman, P., Jones, Chris. (2010). MGMT-independent temozolomide resistance in pediatric glioblastoma cells associated with a PI3-kinase-mediated HOX/stem cell gene signature. *Cancer Research* **70**(22), 9243-9252.

Ghavami, S., Hashemi, M., Ande, S. R., Yeganeh, B., Xiao, W., Eshraghi, M., Bus, C. J., Kadkhoda, K., Wiechec, E., Halayko, A. J. (2009). Apoptosis and cancer: mutations within caspase genes. *Journal of Medical Genetics* **46**, 497-510.

Giam, M, Huang, D. C. S., Bouillet, P. (2008). BH3-only proteins and their roles in programmed cell death. *Oncogene* **27** Suppl 1, S128-136.

Gilley, J., Coffer, P. J., Ham, J. (2003). FOXO transcription factors directly activate bim gene expression and promote apoptosis in sympathetic neurons. *The Journal of Cell Biology*, **162**(4), 613-22.

Gillissen, B., Essmann, F., Graupner, V., Stärck, L., Radetzki, S., Dörken, B., Schulze-Osthoff, K., Daniel, P. T. (2003). Induction of cell death by the BH3-only Bcl-2 homolog Nbk/Bik is mediated by an entirely Bax-dependent mitochondrial pathway. *The EMBO Journal* **22**(14), 3580-3590.

Gillissen, B., Wendt, J., Richter, A., Richter, A., Müer, A., Overkamp, T., Gebhardt, N., Preissner, R., Belka, C., Dörken, B., Daniel, P. T. (2010). Endogenous Bak inhibitors Mcl-1 and Bcl-xL: differential impact on TRAIL resistance in Bax-deficient carcinoma. *The Journal of Cell Biology* **188**(6), 851-862.

Girardi, V., Carbognin, G., Camera, L., Bonetti, F., Manfrin, E., Pollini, G., Pozzi Mucelli, R. (2011). Inflammatory breast carcinoma and locally advanced breast carcinoma: characterisation with MR imaging. *La Radiologia medica* **116**(1), 71-83.

Glick, D., Barth, S., Macleod, K. F. (2010). Autophagy: cellular and molecular mechanisms. *The Journal of Pathology* **221**, 3-12.

Golding, S. E., Rosenberg, E., Valerie, N., Hussaini, I., Frigerio, M., Cockcroft, X. F., Chong, W. Y., Hummersone, M., Rigoreau, L., Menear, K. A., O'Connor, M. J., Povirk, L. F., van Meter, T., Valerie, K. (2009). Improved ATM kinase inhibitor KU-60019 radiosensitizes glioma cells, compromises insulin, AKT and ERK prosurvival signaling, and inhibits migration and invasion. *Molecular Cancer Therapeutics* **8**(10), 2894-2902.

Gong, Y., Somwar, R., Politi, K., Balak, M., Chmielecki, J., Jiang, X., Pao, W. (2007). Induction of BIM is essential for apoptosis triggered by EGFR kinase inhibitors in mutant EGFR-dependent lung adenocarcinomas. *PLoS medicine* **4**(10), e294.

Gonzalez-Gomez, P., Bello, M. J., Arjona, D., Lomas, J., Alonso, M. E., De Campos, J. M., Vaquero, J., Isla, A., Gutierrez, M., Rey, J. A. (2003). Promoter hypermethylation of multiple genes in astrocytic gliomas. *International Journal of Oncology* **22**(3), 601-608.

Greenhough, A., Wallam, C. A., Hicks, D. J., Moorghen, M., Williams, A. C., Paraskeva, C. (2010). The proapoptotic BH3-only protein Bim is downregulated in a subset of colorectal cancers and is repressed by antiapoptotic COX-2 / PGE 2 signalling in colorectal adenoma cells. *Oncogene* **29**(23), 3398-3410.

Guan, H., Song, L., Cai, J., Huang, Y., Wu, J., Yuan, J., Li, J., Li, M. (2011). Sphingosine Kinase 1 Regulates the Akt/FOXO3a/Bim Pathway and Contributes to Apoptosis Resistance in Glioma Cells. *Public Library of Science one*, **6**(5), e19946.

Guckenberger, M., Mayer, M., Buttmann, M., Vince, G. H., Sweeney, R. A., Flentje, M. (2011). Prolonged survival when temozolomide is added to accelerated radiotherapy for glioblastoma multiforme. *Strahlentherapie und Onkologie* **187**(9), 548-554.

Halabi, S., Vogelzang, N. J., Ou, S.-S., Owzar, K., Archer, L., Small, E. J. (2009). Progression-free survival as a predictor of overall survival in men with castrate-resistant prostate cancer. *Journal of Clinical Oncology* **27**(17), 2766-2771.

Han, H. (2010). Nonnegative principal component analysis for mass spectral serum profiles and biomarker discovery. *BMC Bioinformatics* **11** (Suppl 1), S1.

Han, J., Goldstein, L. A., Gastman, B. R., Rabinowich, H. (2006). Interrelated Roles for Mcl-1 and BIM in Regulation of TRAIL-mediated Mitochondrial Apoptosis. *Journal of Biological Chemistry* **281**(15), 10153-10163.

Hanahan, D. (1983). Studies on transformation of Escherichia coli with plasmids. *Journal of Molecular Biology* **166**(4), 557-580.

Hanahan, D. andWeinberg, R. A. (2000). The hallmarks of cancer. *Cell* **100**(1), 57-70.

Hassel, J. C., Sucker, a, Edler, L., Kurzen, H., Moll, I., Stresemann, C., Spieth, K., Mauch, C., Rass, K., Dummer, R., Schadendorf, D. (2010). MGMT gene promoter methylation correlates with tolerance of temozolomide treatment in melanoma but not with clinical outcome. *British Journal of Cancer* **103**(6), 820-826.

Hector, S. and Prehn, J. H. M. (2009). Apoptosis signaling proteins as prognostic biomarkers in colorectal cancer: A review. *BBA - Reviews on Cancer* **1795**(2), 117-129.

Hector, S., Rehm, M., Schmid, J., Kehoe, J., McCawley, N., Dicker, P., Murray, F., et al. (2011). Clinical application of a systems model of apoptosis execution for the prediction of colorectal cancer therapy responses and personalisation of therapy. *Gut* Epublished ahead

of print; http://gut.bmj.com/content/early/2011/11/14/gutjnl-2011-300433.abstract (accessed 27 February 2012)

Hegi, M. E., Diserens, A.-C., Gorlia, T., Hamou, M.-F., de Tribolet, N., Weller, M., Kros, J. M., Hainfellner, J. A., Mason, W., Mariani, L., Bromberg, J. E. C., Hau, P., Mirimanoff, R. O., Cairncross, J. G., Janzer, R. C., Stupp, R. (2005). MGMT gene silencing and benefit from temozolomide in glioblastoma. *The New England Journal of Medicine* **352**(10), 997-1003.

Hegi, M. E., Liu, L., Herman, J. G., Stupp, R., Wick, W., Weller, M., Mehta, M. P., Gilbert, M. R. (2008). Correlation of O 6 -Methylguanine Methyltransferase (MGMT) Promoter Methylation With Clinical Outcomes in Glioblastoma and Clinical Strategies to Modulate MGMT Activity. *Journal of Clinical Oncology* **26**(25), 4189-4199.

Heiskanen, K. M., Bhat, M. B., Wang, H.W., Ma, J., Nieminen, A.L. (1999). Mitochondrial Depolarization Accompanies Cytochrome c Release During Apoptosis in PC6 Cells. *Biochemistry* **274**(9), 5654 -5658.

Hellwig, C. T. and Rehm, M. (2012). TRAIL Signaling and Synergy Mechanisms Used in TRAIL-Based Combination Therapies. *Molecular Cancer Therapeutics* **11**(1), 3-13.

Herr, I. and Debatin. K. M. (2001). Cellular stress response and apoptosis in cancer therapy. *Blood* **98**(9), 2603-2614.

Hervouet, E., Vallette, F. M., Cartron, P. F. (2010). Impact of the DNA methyltransferases expression on the methylation status of apoptosis-associated genes in glioblastoma multiforme. *Cell Death & Disease* **1**, e8.

Hess, J., Angel, P., Schorpp-Kistner, M. (2004). AP-1 subunits: quarrel and harmony among siblings. *Journal of Cell Science* **117**(Pt 25), 5965-5973.

Hetschko, H., Voss, V., Seifert, V., Prehn, J. H. M., Kögel, D. (2008). Upregulation of DR5 by proteasome inhibitors potently sensitizes glioma cells to TRAIL-induced apoptosis. *FEBS Journal* **275**, 1925-1936.

Hetschko, H., Voss, V., Horn, S., Seifert, V., Prehn, J. H. M., Kögel, D. (2007). Pharmacological inhibition of Bcl-2 family members reactivates TRAIL-induced apoptosis in malignant glioma. *Journal of Neurooncology* **86**(3), 265-272.

Hingten, S., Ren, X., Terwilliger, E. (2008). Targeting multiple pathways in gliomas with stem cell and viral delivered S-TRAIL and Temozolomide. *Molecular Cancer Therapy* 7(11), 3575-3585.

Holler, N., Zaru, R., Micheau, O., Thome, M., Attinger, A., Valitutti, S., Bodmer, J. L., Schneider, P., Seed, B., Tschopp, J. (2000). Fas triggers an alternative, caspase-8-

independent cell death pathway using the kinase RIP as effector molecule. *Nature Immunology* **1**(6), 489-95.

Homma, T., Fukushima, T., Vaccarella, S., Yonekawa, Y., Di Patre, P. L., Franceschi, S., Ohgaki, H. (2006). Correlation among pathology, genotype, and patient outcomes in glioblastoma. *Journal of Neuropathology and Experimental Neurology* **65**(9), 846-854.

Hossbach, J., Michalsky, E., Henklein, P., Jaeger, M., Daniel, P. T., Preissner, R. (2009). Inhibiting the inhibitors: retro-inverso Smac peptides. *Peptides* **30**(12), 2374-2379.

Hu, A., Barrett, T., Flavell, R. A., Davis, R. J., Hübner, A. (2008). Multisite phosphorylation regulates Bim stability and apoptotic activity. *Molecular Cell* **30**(4), 415-425.

Huang, S. and Sinicrope, F. A. (2008). BH3 Mimetic ABT-737 Potentiates TRAIL-Mediated Apoptotic Signaling by Unsequestering Bim and Bak in Human Pancreatic Cancer Cells. *Cancer Research* **68**(8), 2944-2951.

Huber, H. J., Rehm, M., Plchut, M., Düssmann, H., Prehn, J. H. M. (2007). APOPTO-CELL — a simulation tool and interactive database for analyzing cellular susceptibility to apoptosis. *Bioinformatics* **23**(5), 648-650.

Iglesias-Serret, D., de Frias, M., Santidrián, A. F., Coll-Mulet, L., Cosialls, A. M., Barragán, M., Domingo, A., Gil, J., Pons, G. (2007). Regulation of the proapoptotic BH3-only protein BIM by glucocorticoids, survival signals and proteasome in chronic lymphocytic leukemia cells. *Leukemia* **21**(2), 281-7.

Irmler, M., Thome, M., Hahne, M., Schneider, P., Hofmann, K., Steiner, V., Bodmer, J. L., Schröter, M., Burns, K., Mattmann, C., Rimoldi, D., French, L. E., Tschopp, J. (1997). Inhibition of death receptor signals by cellular FLIP. *Nature* **388**(6638), 190-195.

Jaganathan, J., Petit, J. H., Lazio, B. E., Singh, S. K., Chin, L. S. (2002). Tumor necrosis factor-related apoptosis-inducing ligand-mediated apoptosis in established and primary glioma cell lines. *Neurosurgical Focus* **13**(3), ecp1.

Jesenberger, V. and Jentsch, S. (2002). Deadly encounter: ubiquitin meets apoptosis. *Molecular Cell Biology* **3**(2), 112-21.

Jette, C. A., Flanagan, A. M., Ryan, J., Pyati, U. J., Carbonneau, S., Stewart, R. A., Langenau, D. M., Look, A. T., Letai, A. (2008). BIM and other BCL-2 family proteins exhibit cross- species conservation of function between zebrafish and mammals. *Cell Death and Differentiation* **15**, 1063-1072.

Jia, L., Srinivasula, S. M., Liu, F. T, Newland, A. C., Fernandes-Alnemri, T., Alnemri, E. S., Kelsey, S. M.(2010). Apaf-1 protein deficiency confers resistance to cytochrome c – dependent apoptosis in human leukemic cells. *Blood* **98**(2), 414-421.

Jiang, Z., Zheng, X., Rich, K. M. (2003). Down-regulation of Bcl-2 and Bcl-xL expression with bispecific antisense treatment in glioblastoma cell lines induce cell death. *Journal of Neurochemistry* **84**, 273-281.

Johnson, D. R. and O'Neill, B. P. (2011). Glioblastoma survival in the United States before and during the temozolomide era. *Journal of Neurooncology*, Epub http://www.springerlink.com/content/r46781t171221218/ , 11-16 (accessed 27 February 2012)

Johnson, T. R., Stone, K., Nikrad, M., Yeh, T., Zong, W. X., B, C., Nesterov, A., Kraft, A. S. (2003). The proteasome inhibitor PS-341 overcomes TRAIL resistance in Bax and caspase 9-negative or Bcl-xL overexpressing cells. *Oncogene* **22**, 4953-4963.

Jost, P. J., Grabow, S., Gray, D., Mckenzie, M. D., Nachbur, U., Huang, D. C. S., Bouillet, P., Thomas, H. E., Borner, C., Silke, J., Strasser, A., Kaufmann, T. (2009). XIAP discriminates between type I and type II. *Nature* **460**, 1035-1039.

Jung, Y., Joo, K. M., Seong, D. H., Choi, Y. L., Kong, D.-S., Kim, Y., Kim, M. H., Jin, J., Suh, Y. L., Seol, H. J., Shin, C. S., Lee, J. I., Kim, J. H., Song S. Y., Nam D.H. (2011). Identification of prognostic biomarkers for glioblastomas using protein expression profiling. *International Journal of Oncology* **40**(4), 1122-1132.

Kahana, S., Finniss, S., Cazacu, S., Xiang, C., Lee, H.-kyung, Brodie, S., Goldstein, R. S., Roitman, V., Slavin, S., Mikkelsen, T., Brodie, C. (2011). Proteasome inhibitors sensitize glioma cells and glioma stem cells to TRAIL-induced apoptosis by PKCε-dependent downregulation of AKT and XIAP expressions. *Cellular Signalling* **23**(8), 1348-1357.

Kaina, Bernd, Christmann, M., Naumann, S., Roos, W. P. (2007). MGMT: key node in the battle against genotoxicity, carcinogenicity and apoptosis induced by alkylating agents. *DNA repair* **6**(8), 1079-1099.

Katz, S. I., Zhou, L., Chao, G., Smith, C. D., Ferrara, T., Wang, W., Dicker, D. T., El-deiry, W. S. (2009). Sorafenib inhibits ERK1/2 and MCL-1L phosphorylation levels resulting in caspase-independent cell death in malignant pleural mesothelioma. *Cancer Biological Therapy* **8**(24), 2406-2416.

Kerr, J. F., Wyllie, A. H., Currie, A. R. (1972). Apoptosis: a basic biological phenomenon with wide-ranging implications in tissue kinetics. *British Journal of Cancer* **26**(4), 239-257.

Kesari, S. (2011). Understanding glioblastoma tumor biology: the potential to improve current diagnosis and treatments. *Seminars in Oncology* **38**(6) Suppl 4, S2-S10.

Khatri, S., Yepiskoposyan, H., Gallo, C. A., Tandon, P., Plas, D. R. (2010). FOXO3a Regulates Glycolysis via Transcriptional Control of Tumor Suppressor TSC1. *Journal of Biological Chemistry* **285**(21), 15960 -15965.

Killian, J. K., Cell, M., Reik, W., Dean, W. (2001). Epigenetic Reprogramming in Mammalian Development. *Science* **293**(August), 1089-1093.

Kim, E. H., Kim, S. U., Shin, D. Y., Choi, K. S. (2004). Roscovitine sensitizes glioma cells to TRAIL-mediated apoptosis by downregulation of survivin and XIAP. *Oncogene* **23**(2), 446-456.

Kim, H. S., Lee, J. W., Soung, Y. H., Park, W. S., Kim, S. Y., Lee, J. H., Park, J. Y., et al. (2003). Inactivating mutations of caspase-8 gene in colorectal carcinomas. *Gastroenterology* **125**(3), 708-715.

Kischkel, F. C., Hellbardt, S., Behrmann, I., Germer, M., Pawlita, M., Krammer, P. H., Peter, M. E. (1995). Cytotoxicity-dependent APO-1 (Fas/CD95)-associated proteins form a death-inducing signaling complex (DISC) with the receptor. *The EMBO journal* **14**(22), 5579-5588.

Kischkel, F. C., Lawrence, D. A., Tinel, A., LeBlanc, H., Virmani, A., Schow, P., Gazdar, A., Blenis, J., Arnott, D., Ashkenazi, A. (2001). Death receptor recruitment of endogenous caspase-10 and apoptosis initiation in the absence of caspase-8. The *Journal of Biological Chemistry* **276**(49), 46639-46646.

Kitange, G. J., Carlson, B. L., Schroeder, M. A., Grogan, P. T., D, J., Decker, P. A., Wu, W., James, C. D., Sarkaria, J. N (2009). Induction of MGMT expression is associated with temozolomide resistance in glioblastoma xenografts. *Neuro-Oncology* **11**, 281-291.

Kitano, H. (2002). Computational systems biology. *Nature* **420**, 206-210.

Kojima, H. (1998). Abrogation of Mitochondrial Cytochrome c Release and Caspase-3 Activation in Acquired Multidrug Resistance. *Journal of Biological Chemistry* **273**(27), 16647-16650.

Kokkinakis, D. M., Moschel, R. C., Vuong, T. H., Reddy, M. V., Schold, S. C., Pegg, A. E. (1996). Mechanism of depletion of O6-methylguanine-DNA methyltransferase activity in rat tissues by O6-Benzyl-2'-deoxyguanosine. Role of metabolism. *In Vivo (Athens, Greece)* **10**(3), 297-306.

Kondo, N., Takahashi, A., Ono, K., Ohnishi, T. (2010). DNA Damage Induced by Alkylating Agents and Repair Pathways, 2010. *Journal of Nucleic Acids* 2010 published online http://www.ncbi.nlm.nih.gov/pmc/articles/PMC2989456/?tool=pubmed

Kraus, J. A., Wenghoefer, M., Glesmann, N., Mohr, S., Beck, M., Schmidt, M. C., Schröder, R., et al. (2001). TP53 Gene Mutations, Nuclear p53 Accumulation, Expression of Waf/p21, Bcl-2, and CD95 (APO-1/Fas) Proteins are not Prognostic Factors in De Novo Glioblastoma Multiforme. *Journal of Neuro-Oncology* **52**(3), 263-272.

Krex, D., Klink, B., Hartmann, C., Deimling, A. V., Pietsch, T., Simon, M., Sabel, M., Steinbach, J. P., Heese, O., Reifenberger, G. (2007). Long-term survival with glioblastoma multiforme. *Brain* **130**, 2596-2606.

Krohn, A. J., Preis, E., Prehn, J. H. M. (1998). Staurosporine-Induced Apoptosis of Cultured Rat Hippocampal Neurons Involves Caspase-1-Like Proteases as Upstream Initiators and Increased Production of Superoxide as a Main Downstream Effector. *The Journal of Neuroscience* **18**(20), 8186-8197.

Kuwana, T., & Newmeyer, D. D. (2003). Bcl-2-family proteins and the role of mitochondria in apoptosis. *Current Opinion in Cell Biology* **15**, 691-699.

Kyprianou, N., English, H. F., Isaacs, J. T. (1990). Programmed cell death during regression of PC-82 human prostate cancer following androgen ablation. *Cancer Research* **50**(12), 3748-3753.

König, H. G., Rehm, M., Gudorf, D., Krajewski, S., Gross, A., Ward, M. W., Prehn, J. H. M. (2007). Full Length Bid is sufficient to induce apoptosis of cultured rat hippocampal neurons. *BMC Cell Biology* **8**, 1-8.

Labi, V, Erlacher, M., Kiessling, S., Villunger, A. (2006). BH3-only proteins in cell death initiation, malignant disease and anticancer therapy. *Cell Death and Differentiation* 13, 1325-1338.

Lalkhen, A. G., McCluskey, A. (2008). Clinical tests: sensitivity and specificity. *Continuing Education in Anaesthesia, Critical Care & Pain* **8**(6), 221-223.

Lavrik, I. N., Golks, A., Krammer, P. H. (2005). Caspases : pharmacological manipulation of cell death. *Journal of Clinical Investigation* **115**(10), 2665-2672.

Lee, J., Kotliarova, S., Kotliarov, Y., Li, A., Su, Q., Donin, N. M., Pastorino, S., Purow, B. W., Christopher, N., Zhang, W., Park, J. K., Fine, H. A. (2006). Tumor stem cells derived from glioblastomas cultured in bFGF and EGF more closely mirror the phenotype and genotype of primary tumors than do serum-cultured cell lines. *Cancer Cell* **9**(5), 391-403.

Lenhard, R. E. (1996) Cancer statistics: a measure of progress. *CA: a cancer journal for clinicians* **46**(1), 3-4.

Letai, Anthony. (2005). Pharmacological manipulation of Bcl-2 family members to control cell death. *The Journal of Clinical Investigations* **115**(10), 2648-2655.

Li, H., Zhu, H., Xu, C. J., Yuan, J. (1998). Cleavage of BID by caspase 8 mediates the mitochondrial damage in the Fas pathway of apoptosis. *Cell* **94**(4), 491-501.

Li, Nijhawan, D., Budihardjo, I., Srinivasula, S. M., Ahmad, M., Alnemri, E. S., Wang, X. (1997). Cytochrome c and dATP-Dependent Formation of Apaf-1 / Caspase-9 Complex Initiates an Apoptotic Protease Cascade. *Cell* **91**, 479-489.

Lindahl, T., Demple, B., Robins, P. (1982). Suicide inactivation of the E. coli O6-methylguanine-DNA methyltransferase. *The EMBO journal* **1**(11), 1359-1363.

Liu, X., Kim, C. N., Yang, J., Jemmerson, R., Wang, X. (1996). Induction of Apoptotic Program in Cell-Free Extracts : Requirement for dATP and Cytochrome c. *Cell* **86**, 147-157.

Llambi, F., & Green, D. R. (2011). Apoptosis and oncogenesis: give and take in the BCL-2 family. *Current Opinion in Genetics & Development* **21**(1), 12-20.

Loeb, K. R. and Loeb, L. A. (2000). Significance of multiple mutations in cancer. *Carcinogenesis* **21**(3), 379-85.

Lopez, H., Zhang, L., George, N. M., Liu, X., Pang, X., Evans, J. J. D., Targy, N. M., Luo, Xu. (2010). Perturbation of the Bcl-2 Network and an Induced Noxa / Bcl-xL Interaction Trigger Mitochondrial Dysfunction Following DNA Damage. Journal of Biological Chemistry **14**(20), 15016-15026.

Louis, D. N. (2006). Molecular Pathology of Malignant Gliomas. *Annual Review of Pathology* **1**, 97-117.

Louis, D. N., Ohgaki, H., Wiestler, O. D., Cavenee, W. K., Burger, P. C., Jouvet, A., Scheithauer, B. W., Kleihues, P. (2007). The 2007 WHO Classifcation of Tumours of the Central Nervous System. *Acta Neuropathologica* **114**, 97-109.

Lowe, S. W., Cepero, E., Evan, G. (2004). Intrinsic tumour suppression. *Nature* **432**(7015), 307-315.

Luciano, F., Jacquel, A., Colosetti, P., Herrant, M., Cagnol, S., Pages, G., Auberger, P. (2003). Phosphorylation of Bim-EL by Erk1 / 2 on serine 69 promotes its degradation via the proteasome pathway and regulates its proapoptotic function. *Oncogene* **22**, 6785-6793.

Luetjens, M. C., Kögel, D., Reimertz, C., Ußmann, H. D., Renz, A., Schulze-Osthoff, K., Nieminen, A. L., Poppe, M., Prehn, J. H. M. (2001). Multiple Kinetics of Mitochondrial Cytochrome c Release in Drug-Induced Apoptosis. *Molecular Pharmacology* **60**(5), 1008-1019.

Maddika, S., Rao, S., Panigrahi, S., Paranjothy, T., Weglarczyk, K., Zuse, A., Eshraghi, M., Manda, K. D., Wiechec, E., Los, M. (2007). Cell survival , cell death and cell cycle pathways are interconnected : Implications for cancer therapy. *Drug Resistance Update* **10**, 13-29.

Maines, M. D. (2007). Biliverdin reductase: PKC interaction at the cross-talk of MAPK and PI3K signaling pathways. *Antioxidants & Redox Signaling* **9**(12), 2187-2195.

Maiuri, M. C., Zalckvar, E., Kimchi, A., Kroemer, G. (2007). Self-eating and self-killing: crosstalk between autophagy and apoptosis. *Molecular Cell Biology* **8**(9), 741-752.

Mandel, M. and Higa, A. (1992). Calcium-dependent bacteriophage DNA infection. 1970. *Biotechnology* **24**, 198-201.

Mandic, A., Viktorsson, K., Heiden, T., Hansson, J., Shoshan, M. C. (2001). The MEK1 inhibitor PD98059 sensitizes C8161 melanoma cells to cisplatin-induced apoptosis. *Melanoma Research* **11**(1), 11-19.

Mann, H. B., and Whitney, D. R. (1947). On a test of whether one of two random variables is stochastically larger than the other. *The Annals of Mathematical Statistics.*

Marani, M., Hancock, D., Lopes, R., Tenev, T., Downward, J., Lemoine, N. R. (2004). Role of Bim in the survival pathway induced by Raf in epithelial cells. *Oncogene* **23**, 2431-2441.

Marchand, B., Tremblay, I., Cagnol, S., Boucher, M. J. (2012). Inhibition of glycogen synthase kinase-3 activity triggers an apoptotic response in pancreatic cancer cells through JNK-dependent mechanisms. *Carcinogenesis*, 0(0), 1-9.

Martin, S J, Reutelingsperger, C. P., McGahon, A. J., Rader, J. A., van Schie, R. C., LaFace, D. M., Green, D. R. (1995). Early redistribution of plasma membrane phosphatidylserine is a general feature of apoptosis regardless of the initiating stimulus: inhibition by overexpression of Bcl-2 and Abl. *The Journal of Experimental Medicine* **182**(5), 1545-1556.

Martinez, R., Setien, F., Voelter, C., Casado, S., Quesada, M. P., Schackert, G., Esteller, M. (2007). CpG island promoter hypermethylation of the pro-apoptotic gene caspase-8 is a common hallmark of relapsed glioblastoma multiforme.
Carcinogenesis **28**(6), 1264-1268.

Mccubrey, J. A., Steelman, L. S., Chappell, W. H., Abrams, S. L., Wong, E. W. T., Chang, F., Lehmann, B., et al. (2007). Roles of the Raf / MEK / ERK pathway in cell growth , malignant transformation and drug resistance. *Biochimica et Biophysica Acta* **1773**, 1263 - 1284.

Mckenzie, M. D., Jamieson, E., Jansen, E. S., Scott, C. L., Huang, D. C. S., Bouillet, P., Allison, J., et al. (2010). Glucose Induces Pancreatic Islet Cell Apoptosis That Requires the BH3-Only Proteins Bim and Puma and Multi-BH Domain Protein Bax. *Diabetes* **59**, 644-652.

Meier, F, Busch, S., Lasithiotakis, K., Kulms, D., Garbe, C., Maczey, E., Herlyn, M., Schittek, B. (2007). Combined targeting of MAPK and AKT signalling pathways is a promising strategy for melanoma treatment. *The British Journal of Dermatology* **156**(6), 1204-1213.

Meier, Friedegund, Schittek, B., Busch, S., Garbe, C., Smalley, K., Satyamoorthy, K., Li, G., Herlyn, M. (2005). The RAS/RAF/MEK/ERK and PI3K/AKT signaling pathways present molecular targets for the effective treatment of advanced melanoma. *Frontiers in Bioscience* **10**, 2986-3001.

Meier, P., Finch, A., Evan, G. (2000). Apoptosis in development. *Nature* **407**(6805), 796-801.

Mhaidat, N. M., Zhang, X. D., Allen, J., Avery-Kiejda, K. A., Scott, R. J., Hersey, P. (2007). Temozolomide induces senescence but not apoptosis in human melanoma cells. *British Journal of Cancer* **97**, 1225 – 1233.

Miller, C. R., Dunham, C. P., Scheithauer, B. W., Perry, A. (2006). Significance of necrosis in grading of oligodendroglial neoplasms: a clinicopathologic and genetic study of newly diagnosed high-grade gliomas. *Journal of Clinical Oncology* **24**(34), 5419-5426.

Mirimanoff, R.-O., Gorlia, T., Mason, W., Van den Bent, M. J., Kortmann, R.-D., Fisher, B., Reni, M., Brandes, Alba, A., Curschmann, J., Villa, S. Cairncross, G., Allgeier, A., Lacombe, D. Stupp, R. (2006). Radiotherapy and temozolomide for newly diagnosed glioblastoma: recursive partitioning analysis of the EORTC 26981/22981-NCIC CE3 phase III randomized trial. Journal of clinical oncology **24**(16), 2563-2569.

Mizutani, Y., Nakanishi, H., Li, Y. N., Matsubara, H., Yamamoto, K., Sato, N., Shiraishi, T., Nakamura, T., Mikami, K., Okihara, K., Takaha, N., Ukimura, O., Kawauchi, A., Nonomura, N., Bonavida, B., Miki, T. (2007). Overexpression of XIAP expression in renal cell carcinoma predicts a worse prognosis. *International Journal of Oncology* **30**(4), 919-925.

Munoz-Pinedo, C., Guido-Carrion, A., Goldstein, J. C., Fitzgerald, P., Newmeyer, D. D., Green, D. R. (2006). Different mitochondrial intermembrane space proteins are released during apoptosis in a manner that is coordinately initiated but can vary in duration. *PNAS* **103**(31) 11573-11578.

Murakami, Y., Miller, J. W., Vavvas, D. G. (2011). RIP kinase-mediated necrosis as an alternative mechanisms of photoreceptor death. *Oncotarget* **2**(6), 497-509.

Mérino, D., Giam, M., Hughes, P. D., Siggs, O. M., Heger, K., Reilly, L. A. O., Adams, J. M., et al. (2009). The role of BH3-only protein Bim extends beyond inhibiting Bcl-2–like prosurvival proteins. *Journal of Cell Biology* **186**(3), 355-362.

Narita, M., Shimizu, S., Ito, T., Chittenden, T., Lutz, R. J., Matsuda, H., Tsujimoto, Y. (1998). Bax interacts with the permeability transition pore to induce permeability transition and cytochrome c release in isolated mitochondria. *Proc. Natl Acad. Sci. USA* **95**(25), 14681-14686.

Nemec, K. N. and Khaled, A. R. (2008). Therapeutic Modulation of Apoptosis : Targeting the BCL-2 Family at the Interface of the Mitochondrial Membrane. *Yonsei Medical Journal* **49**(5), 689 - 697.

Nicholson, D. W. and Thornberry, N. A. (1997). Caspases: killer proteases. *Trends in Biochemical Sciences* **22**(8), 299-306.

Nicholson, D. W., Ali, A., Thornberry, N. A., Vaillancourt, J. P., Ding, C. K., Gallant, M., Gareau, Y., Griffin, P. R., Labelle, M., Lazebnik, Y. A. (1995). Identification and inhibition of the ICE/CED-3 protease necessary for mammalian apoptosis. *Nature* **376**(6535), 37-43.

Nitsch, R., Bechmann, I., Deisz, R. A., Haas, D., Lehmann, T. N., Wendling, U., Zipp, F. (2000). Human brain-cell death induced by tumour-necrosis-factor-related apoptosis-inducing ligand (TRAIL). *The Lancet* **356**, 827-828.

Nomura, Y., Yoshida, S., Karube, K., Takeshita, M., Hirose, S., Nakamura, S., Yoshino, T., Kikuchi, M., Ohshima, K. (2008). Estimation of the relationship between caspase-3 expression and clinical outcome of Burkitt's and Burkitt-like lymphoma. *Cancer Science* **99**(8), 1564-1546.

Nordigården, A., Kraft, M., Eliasson, P., Labi, V., Lam, E. W., Villunger, A., Jo, J. I. (2009). BH3-only protein Bim more critical than Puma in tyrosine kinase inhibitor – induced apoptosis of human leukemic cells and transduced hematopoietic progenitors carrying oncogenic FLT3. *Blood* **113**(10), 2302-2311.

Ohba, S., Hirose, Y., Kawase, T., Sano, H. (2009). Inhibition of c-Jun N-terminal kinase enhances temozolomide-induced cytotoxicity in human glioma cells. Journal of *Neurooncology* **95**(3), 307-16.

Oliva, C. R., Moellering, D. R., Gillespie, G. Y., Griguer, C. E. (2011). Acquisition of Chemoresistance in Gliomas Is Associated with Increased Mitochondrial Coupling and Decreased ROS Production. *PloS one*, **6**(9), e24665.

Olopade, O. I., Adeyanju, M. O., Safa, A. R., Hagos, F., Mick, R., Thompson, C. B., Recant, W. M. (1997). Overexpression of BCL-x protein in primary breast cancer is associated with high tumor grade and nodal metastases. *The Cancer Journal from Scientific American* **3**(4), 230-237.

O'Connor, L., Strasser, A., Reilly, L. A. O., Hausmann, G., Adams, J. M., Cory, S., & Huang, D. C. S. (1998). Bim : a novel member of the Bcl-2 family that promotes apoptosis. *EMBO Journal* **17**(2), 384-395.

O'Connor, C.L., Anguissola, S., Huber, H. J., Dussmann, H., Prehn, J. H. M., Rehm, M. (2008). Intracellular signaling dynamics during apoptosis execution in the presence or absence of X-linked-inhibitor-of-apoptosis-protein. *Biochimica et biophysica acta* **1783**, 1903-1913.

O'Reilly, S. M., Newlands, E. S., Glaser, M. G., Brampton, M., Rice-Edwards, J. M., Illingworth, R. D., Richards, P. G., Kennard C., Colquhoun I. R., Lewis P. (1993). Temozolomide: a new oral cytotoxic chemotherapeutic agent with promising activity against primary brain tumours. *European Journal of Cancer* **29A**(7), 940-2.

Pan, G., O'Rourke, K., Dixit, V. M. (1998). Caspase-9, Bcl-XL, and Apaf-1 form a ternary complex. *The Journal of Biological Chemistry* **273**(10), 5841-5845.

Pan, G., O'Rourke, K., Chinnaiyan, A. M., Gentz, R., Ebner, R., Ni, J., Dixit, V. M. (1997). The receptor for the cytotoxic ligand TRAIL. *Science* **276**(5309), 111-113.

Pang, L., Sawada, T., Decker, S. J., Saltiel, A. R. (1995). Inhibition of MAP kinase kinase blocks the differentiation of PC-12 cells induced by nerve growth factor. *The Journal of Biological Chemistry* **270**(23), 13585-13588.

Panja, S., Aich, P., Jana, B., Basu, T. (2008a). How does plasmid DNA penetrate cell membranes in artificial transformation process of Escherichia coli? *Molecular Membrane Biology* **25**(5), 411-422.

Panja, S., Aich, P., Jana, B., Basu, T. (2008b). Plasmid DNA binds to the core oligosaccharide domain of LPS molecules of E. coli cell surface in the CaCl2-mediated transformation process. *Biomacromolecules* **9**(9), 2501-2509.

Panner, A., Crane, C. A., Weng, C., Feletti, A., Fang, S., Parsa, A. T., Pieper, R. O. (2010). Ubiquitin-specific protease 8 links the PTEN-Akt-AIP4 pathway to the control of FLIPS stability and TRAIL sensitivity in glioblastoma multiforme. Cancer research, **70**(12), 5046-53.

Papenfuss, K., Cordier, S. M., Walczak, H. (2008). Death receptors as targets for anti-cancer therapy. *Journal of Cellular and Molecular Medicine* **12**(6B), 2566-85.

Parada, L. F., Tabin, C. J., Shih, C., Weinberg, R. A. (1982). Human EJ bladder carcinoma oncogene is homologue of Harvey sarcoma virus ras gene. *Nature* **297**(5866), 474-478.

Park, J. G. and Chapman, V. M. (1994). CpG island promoter region methylation patterns of the inactive-X-chromosome hypoxanthine phosphoribosyltransferase (Hprt) gene. *Molecular and Cellular Biology* **14**(12), 7975-7983.

Patel, M., McCully, C., Godwin, K., Balis, F. M. (2003). Plasma and cerebrospinal fluid pharmacokinetics of intravenous temozolomide in non-human primates. Journal of Neurooncology **61**(3), 203-207.

Peri, S., Navarro, J. D., Amanchy, R., Kristiansen, T. Z., Jonnalagadda, C. K., Surendranath, V., Niranjan, V., Muthusamy, B., Gandhi, T. K. B., Gronborg, M., Ibarrola, N., Deshpande, N., Shanker, K.,Shivashankar, H. N., Rashmi, B. P., Ramya, M. A., Zhao, Z., Chandrika, K. N., Padma, N., Harsha, H. C., Yatish, A. J., Kavitha, M. P., Menezes, M., Choudhury, D. R., Suresh, S., Ghosh, N., Saravana, R., Chandran, S., Krishna, S., Joy, M., Anand, S. K., Madavan, V., Joseph, A., Wong, G. W., Schiemann, W. P., Constantinescu, S. N., Huang, L., Khosravi-Far, R., Steen, H., Tewari, M., Ghaffari, S., Blobe, G. C., Dang, C. V., Garcia, J. G. N., Pevsner, J., Jensen, O. N., Roepstorff, P., Deshpande, K. S., Chinnaiyan, A. M., Hamosh, A., Chakravarti, A., Pandey, A. (2003). Development of human protein reference database as an initial platform for approaching systems biology in humans. *Genome Research* **13**(10), 2363-2371.

Perry, A., Aldape, K. D., George, D. H., Burger, P. C. (2004). Small cell astrocytoma: an aggressive variant that is clinicopathologically and genetically distinct from anaplastic oligodendroglioma. *Cancer* **101**(10), 2318-26.

Petak, I., Vernes, R., Szucs, K. S., Anozie, M., Izeradjene, K., Douglas, L., Tillman, D. M., Phillips, D. C., Houghton, J. A. (2003). A caspase-8-independent component in TRAIL/Apo-2L-induced cell death in human rhabdomyosarcoma cells. *Cell death and Differentiation* **10**(6), 729-739.

Plati, J., Khosravi-Far, R. (2008). Dysregulation of Apoptotic Signalling in Cancer: Molecular Mechanisms and Therapeutic Opportunities. *J Cell Biochem.* **104**(4), 1124-1149.

Preusser, M., Charles Janzer, R., Felsberg, J., Reifenberger, G., Hamou, M.-F., Diserens, A.-C., Stupp, R., Gorlia, T., Marosi, C. (2008). Anti-O6-methylguanine-methyltransferase (MGMT) immunohistochemistry in glioblastoma multiforme: observer variability and lack of association with patient survival impede its use as clinical biomarker. *Brain Pathology* **18**(4), 520-532.

Puduvalli, V. K., Sampath, D., Bruner, J. M., Nangia, J., Xu, R., Kyritsis, A. P. (2005). TRAIL-induced apoptosis in gliomas is enhanced by Akt-inhibition and is independent of JNK activation. *Apoptosis* **10**(1), 233-243.

Putcha, G. V., Le, S., Frank, S., Besirli, C. G., Clark, K., Chu, B., Alix, S., et al. (2003). JNK-Mediated BIM Phosphorylation Potentiates BAX-Dependent Apoptosis. *Neuron* **38**, 899-914.

Puthalakath, H. and Strasser, A. (2002). Keeping killers on a tight leash : transcriptional and post- translational control of the pro-apoptotic activity of BH3- only proteins. *Cell Death and Differentiation* **9**, 505-512.

Puthalakath, Hamsa, Huang, D. C. S., Reilly, L. A. O., King, S. M., Strasser, A. (1999). The Proapoptotic Activity of the Bcl-2 Family Member Bim Is Regulated by Interaction with the Dynein Motor Complex. *Molecular Cell* **3**, 287-296.

Pàez-Ribes, M., Allen, E., Hudock, J., Takeda, T., Okuyama, H., Viñals, F., Inoue, M., Bergers, G., Hanahan, D., Casanovas, O. (2009). Antiangiogenic therapy elicits malignant progression of tumors to increased local invasion and distant metastasis. *Cancer Cell* **15**(3), 220-231.

Qi, X. J., Wildey, G. M., Howe, P. H. (2006). Evidence that Ser87 of BimEL is phosphorylated by Akt and regulates BimEL apoptotic function. *The Journal of Biological Chemistry* **281**(2), 813-823.

Quian, X. C., Brent, T. P. (1997). Methylation Hot Spots in the 5' Flanking Region Denote Silencing of the 06-Methylguanine-DNA Methyltransferase Gene. *Cancer Research* **57**, 3672-3677.

Raisova, M., Hossini, A. M., Eberle, J., Riebeling, C., Wieder, T., Sturm, I., Daniel, P. T., Orfanos, C. E., Geilen, C. C. (2001). The Bax/Bcl-2 ratio determines the susceptibility of human melanoma cells to CD95/Fas-mediated apoptosis. The Journal of Investigative Dermatology **117**(2), 333-340.

Ray, S. K., Patel, S. J., Welsh, C. T., Wilford, G. G., Hogan, E. L., Banik, N. L., Carolina, S. (2002). Molecular Evidence of Apoptotic Death in Malignant Brain Tumors Including Glioblastoma Multiforme: Upregulation of Calpain and Caspase-3. *Journal of Neuroscience Research* **69**, 197-206.

Reed, John C. (2008). Bcl-2 family proteins and hematologic malignancies : history and future prospects. *Blood* **111**(7), 3322-3330.

Reginato, M. J., Mills, K. R., Paulus, J. K., Lynch, D. K., Sgroi, D. C., Debnath, J., Muthuswamy, S. K., et al. (2003). Integrins and EGFR coordinately regulate the pro-apoptotic protein Bim to prevent anoikis. *Nature Cell Biology* **5**(8), 733-741.

Rehm, Markus, Huber, H. J., Dussmann, H. (2006). Systems analysis of effector caspase activation and its control by X-linked inhibitor of apoptosis protein. *EMBO Journal* **25**(18), 4338-4349.

Rehm, Markus, Duessmann, H., Ja, R. U., Tavare, J. M., Koegel, D., Prehn, J. H. M. (2002). Single-cell Fluorescence Resonance Energy Transfer Analysis Demonstrates That Caspase Activation during Apoptosis Is a Rapid Process. *The Journal of Biological Chemistry* **277**(27), 24506 -24514.

Reimertz, C., Kögel, D., Rami, A., Chittenden, T., Prehn, J. H. M. (2000). Gene expression during ER stress – induced apoptosis in neurons: induction of the BH3-only protein Bbc3 / PUMA and activation of the mitochondrial apoptosis pathway. *The Journal of Cell Biology* **162**(4), 587-597.

Ren, D., Takeuchi, O., Jeffers, J. R., Zambetti, G. P., Hsieh, J. J., & Cheng, E. H. (2011). BID, BIM, and PUMA Are Essential for Activation of the BAX- and BAK-Dependent Cell Death Program. *In Vitro* **1390**(2010), 10-14,

Rice, S. D., Heinzman, J. M., Brower, S. L., Ervin, P. R., Song, N., Shen, K., Wang, D. (2010). Analysis of chemotherapeutic response heterogeneity and drug clustering based on mechanism of action using an in vitro assay. *Anticancer Research* 30(7), 2805-2811.

Rieger, J., Frank, B., Weller, M., Wick, W. (2007). Mechanisms of resistance of human glioma cells to Apo2 ligand/TNF-related apoptosis-inducing ligand. *Cellular Physiology and Biochemistry* **20**(1-4), 23-34.

Rietschel, P., Wolchok, J. D., Krown, S., Gerst, S., Jungbluth, A. a, Busam, K., Smith, K., Orlow, I., Panageas, K., Chapman, P. B. (2008). Phase II study of extended-dose temozolomide in patients with melanoma. *Journal of Clinical Oncology* **26**(14), 2299-304.

Ringnér, M. (2008). What is principal component analysis? *Nature biotechnology* **26**(3), 303-304.

Tsujimoto. Y. (1998). Role of Bcl-2 family proteins in apoptosis: apoptosomes or mitochondria? Genes Cells **3**(11), 697-707.

Romer, J. and Curran, T. (2005). Targeting medulloblastoma: small-molecule inhibitors of the Sonic Hedgehog pathway as potential cancer therapeutics. *Cancer Research* **65**(12), 4975-4978.

Roos, W. P., Batista, L. F. Z., Naumann, S. C., Wick, W., Weller, M., Menck, C. F. M., Kaina, B. (2007). Apoptosis in malignant glioma cells triggered by the temozolomide-induced DNA lesion O 6 -methylguanine. *Oncogene* **26**, 186-197.

Roth, P., Hasenbach, K., Aulwurm, S., Wolpert, F., Tabatabai, G., Wick, W., & Weller, M. (2011). APO010, a synthetic hexameric CD95 ligand, induces human glioma cell death in vitro and in vivo. *Neuro-Oncology* **13**(2), 155 - 164.

Roy, S. K., Srivastava, R. K., Shankar, S. (2010). Inhibition of PI3K/AKT and MAPK/ERK pathways causes activation of FOXO transcription factor, leading to cell cycle arrest and apoptosis in pancreatic cancer. *Journal of Molecular Signaling* **5**(10), 1-13.

Rudner, J., Jendrossek, V., Lauber, K., Daniel, P. T., Wesselborg, S., Belka, C. (2005). Type I and type II reactions in TRAIL-induced apoptosis -- results from dose-response studies. *Oncogene* **24**(1), 130-140.

Rudy, A., López-Antón, N., Barth, N., Pettit, G. R., Dirsch, V. M., Schulze-Osthoff, K., Rehm, M., Prehn, J. H. M., Vogler, M., Fulda, S., Vollmar, A. M. (2008). Role of Smac in cephalostatin-induced cell death. *Cell Death and Differentiation* **15**(12), 1930-1940.

Saelens, X., Festjens, N., Vande Walle, L., van Gurp, M., van Loo, G., Vandenabeele, P. (2004). Toxic proteins released from mitochondria in cell death. *Oncogene* **23**(16), 2861-2874.

Sambrook, J., Fritsch, E., Maniatis, T. (1989). Molecular Cloning: A Laboratory Manual, 2nd Edition. *Cold Spring Harbor Press NY*, 18.47-18.59.

San José-Eneriz, E., Agirre, X., Jiménez-Velasco, A., Cordeu, L., Martín, V., Arqueros, V., Gárate, L., Fresquet, V., Cervantes, F., Martinéz-Climent, J., Heiniger, A., Torres, A., Prósper, F., Roman-Gomez, J. (2009). Epigenetic down-regulation of BIM expression is associated with reduced optimal responses to imatinib treatment in chronic myeloid leukaemia. *European Journal of Cancer* **45**, 1877-1889.

Sarkaria, J. N., Kitange, G. J., James, C. D., Plummer, R., Calvert, H., Weller, M., & Wick, W. (2008). Mechanisms of Chemoresistance to Alkylating Agents in Malignant Glioma. *Clinical Cancer Research* **14**(10), 2900-2908.

Savill, J. (1997). Recognition and phagocytosis of cells undergoing apoptosis. *British Medical Bulletin* **53**(3), 491-508.

Savill, James, Fadok, V., Henson, P., Haslett, C. (1993). Phagocyte recognition of cells undergoing apoptosis. *Immunology today* **14**(3), 131-136.

Sawyers, C. L. (2009). Shifting paradigms: the seeds of oncogene addiction. *Nature Medicine* **15**(10), 1158-1161.

Scaffidi, C., Fulda, S., Srinivasan, A., Friesen, C., Li, F., Tomaselli, K. J., Debatin, K. M., et al. (1998). Two CD95 (APO-1/Fas) signaling pathways. *The EMBO journal* **17**(6), 1675-1687.

Scheffner, M., Werness, B. A., Huibregtse, J. M., Levine, A. J., Howley, P. M. (1990). The E6 oncoprotein encoded by human papillomavirus types 16 and 18 promotes the degradation of p53. *Cell* **63**(6), 1129-1136.

Schimmer, A. D., Dalili, S., Batey, R. A., Riedl, S. J. (2006). Targeting XIAP for the treatment of malignancy. Cell Death and Differentiation **13**(2), 179-188.

Schwarz, C. S., Evert, B. O., Seyfried, J., Schaupp, M., Kunz, W. S., Vielhaber, S., Klockgether, T., Wu, U. (2001). Overexpression of bcl-2 Results in Reduction of Cytochrome c Content and Inhibition of Complex I Activity. *Biochemical and Biophysical Research Communications* **280**(4), 1021-1027.

Settle, S. H., Sulman, E. P. (2011). Tumor profiling: development of prognostic and predictive factors to guide brain tumor treatment. *Current Oncology Reports*, **13**(1), 26-36.

Shah, K., Tung, C.-H., Breakefield, X. O., Weissleder, R. (2005). In vivo imaging of S-TRAIL-mediated tumor regression and apoptosis. *Molecular Therapy* **11**(6), 926-931.

Shah, N., Lin, B., Sibenaller, Z., Ryken, T., Lee, H., Yoon, J.-geun, Rostad, S., et al. (2011). Comprehensive Analysis of MGMT Promoter Methylation : Correlation with MGMT Expression and Clinical Response in GBM. Analyzer, 6(1).

Shen, X.-G., Wang, C., Li, Y., Wang, L., Zhou, B., Xu, B., Jiang, X., Zhou, Z. G., Sun, X. F. (2010). Downregulation of caspase-9 is a frequent event in patients with stage II colorectal cancer and correlates with poor clinical outcome. *Colorectal Disease* **12**(12), 1213-1218.

Sheridan, C., Brumatti, G., Martin, S. J. (2008). Oncogenic B-RafV600E inhibits apoptosis and promotes ERK-dependent inactivation of Bad and Bim. *The Journal of Biological Chemistry* **283**(32), 22128-22135.

Shi, L., Kraut, R. P., Aebersold, R., Greenberg, A. H. (1992). A natural killer cell granule protein that induces DNA fragmentation and apoptosis. *The Journal of Experimental Medicine* **175**(2), 553-566.

Shinjyo, T., Kuribara, R., Inukai, T., Hosoi, H., Kinoshita, T., Miyajima, A., Houghton, P. J., et al. (2001). Downregulation of Bim, a Proapoptotic Relative of Bcl-2 , Is a Pivotal Step in Cytokine-Initiated Survival Signaling in Murine Hematopoietic Progenitors. *Molecular Cell Biology* **21**(3), 854-864.

Shoji, K., Tsubaki, M., Yamazoe, Y., Satou, T., Itoh, T., Kidera, Y. (2011). Mangiferin Induces Apoptosis by Suppressing Bcl-xL and XIAP Expressions and Nuclear Entry of NF-κB in HL-60 Cells. *Archives of Pharmacal Research* (Seoul), **34**(3), 469-475.

Siegelin, M D, Gaiser, T., Siegelin, Y. (2009). The XIAP inhibitor Embelin enhances TRAIL-mediated apoptosis in malignant glioma cells by down-regulation of the short isoform of FLIP. *Neurochemistry International* **55**(6), 423-430.

Song, J., Petruk, K. C., Meir, E. G. V. (2003). TRAIL Triggers Apoptosis in Human Malignant Glioma Cells Through Extrinsic and Intrinsic Pathways. *Brain Pathology* **13**, 539-553.

Souglakos, J., Philips, J., Wang, R., Marwah, S., Silver, M., Tzardi, M., Silver, J., Ogino, S., Hooshmand, S,, Kwak, E., Freed, E., Meyerhardt, J. A., Saridaki, Z., Georgoulias, V., Finkelstein, D., Fuchs, C. S., Kulke, M. H., Shivdasani, R. A. (2009). Prognostic and predictive value of common mutations for treatment response and survival in patients with metastatic colorectal cancer. *British Journal of Cancer* **101**(3), 465-472.

Stennicke, H. R., Salvesen, G. S. (2000). Caspases - controlling intracellular signals by protease zymogen activation. *Biochimica et biophysica acta* **1477**(1-2), 299-306.

Stennicke, H. R., Deveraux, Q. L., Humke, E. W., Reed, J. C., Dixit, V. M., Salvesen, G. S. (1999). Caspase-9 can be activated without proteolytic processing. *The Journal of Biological* Chemistry **274**(13), 8359-62.

Stevens, M. F., Hickman, J. A., Langdon, S. P., Chubb, D., Vickers, L., Stone, R., Baig, G., Goddard, C., Gibson, N. W., Slack, J. A.. (1987). Antitumor activity and pharmacokinetics in mice of 8-carbamoyl-3-methyl-imidazo[5,1-d]-1,2,3,5-tetrazin-4(3H)-one (CCRG 81045; M & B 39831), a novel drug with potential as an alternative to dacarbazine. *Cancer Research* **47**(22), 5846-5852.

Strasser, A, Harris, A. W., Vaux, D. L., Webb, E., Bath, M. L., Adams, J. M., Cory, S. (1990). Abnormalities of the immune system induced by dysregulated bcl-2 expression in transgenic mice. *Current topics in microbiology and immunology*, **166**, 175-181.

Strasser, Andreas, Puthalakath, H., Bouillet, P., Huang, D. C. S., Connor, L. O., Reilly, L. A. O., Cullen, L., Cory, S., Adams, J. M. (2006). The Role of Bim, a Proapoptotic BH3-Only Member of the Bcl-2 Family , in Cell-Death Control. *Annals of the New York Academy of Science* **917**, 541-548.

Strasser, Andreas (2005). The Role Of BH3-Only Proteins In The Immune System. *Immunology* **5**(March), 189-200.

Sträter, J., Herter, I., Merkel, G., Hinz, U., Weitz, J., Möller, P. (2010). Expression and prognostic significance of APAF-1, caspase-8 and caspase-9 in stage II/III colon

carcinoma: caspase-8 and caspase-9 is associated with poor prognosis. *International journal of cancer/ Journal International du Cancer* **127**(4), 873-880.

Stupp, R., Mason, W. P., van den Bent, M. J., Weller, M., Fisher, B., Taphoorn, M. J. B., Belanger, K., Brandes, A. A., Marosi, C., Bogdahn, U., Curschmann, J., Janzer, R. C., Ludwin, S. K., Gorlia, T., Allgeier, A., Lacombe, D., Cairncross, J. G., Eisenhauer, E., Mirimanoff, R. O. (2005). Radiotherapy plus concomitant and adjuvant temozolomide for glioblastoma. *The New England Journal of Medicine*, **352**(10), 987-996.

Suliman, A., Lam, A., Datta, R., Srivastava, R. K. (2001). Intracellular mechanisms of TRAIL: apoptosis through mitochondrial-dependent and -independent pathways. *Oncogene* **20**(17), 2122-2133.

Sundararajan, R., Cuconati, a, Nelson, D., White, E. (2001). Tumor necrosis factor-alpha induces Bax-Bak interaction and apoptosis, which is inhibited by adenovirus E1B 19K. The Journal of Biological Chemistry, **276**(48), 45120-45127.

Sunters, A., Ferna, S., Mattos, D., Stahl, M., Brosens, J. J., Zoumpoulidou, G., Saunders, C. A., Coffer, P. J., Medema, H., Coombes, R. C., Lam, E. W. (2003). FoxO3a Transcriptional Regulation of Bim Controls Apoptosis in Paclitaxel-treated Breast Cancer Cell Lines. *Biochemistry* **278**(50), 49795-49805.

Sunters, A., Madureira, P. A., Pomeranz, K. M., Aubert, M., Brosens, J. J., Cook, S. J., Burgering, B. M. T., et al. (2006). Paclitaxel-Induced Nuclear Translocation of FOXO3a in Breast Cancer Cells Is Mediated by c-Jun NH 2 -Terminal Kinase and Akt. *Cancer Research* **66**(1), 212-220.

Sylvester, P. W. (2011). Optimization of the tetrazolium dye (MTT) colorimetric assay for cellular growth and viability. *Methods in Molecular Biology* **716**, 157-68.

Tait, S. W. G. and Green, D. R. (2010). Mitochondria and cell death: outer membrane permeabilization and beyond. *Molecular Cell Biology* **11**(9), 621-32.

Tang, K., Jin, Q., Yan, W., Zhang, W. (2011). Clinical correlation of MGMT protein expression and promoter methylation in Chinese glioblastoma patients. *Medical Oncology*, Epub online. http://www.springerlink.com/content/t60346172674g689/
(Accessed 27 February 11)

Teicher, B. A., Ara, G., Herbst, R., Palombella, V. J., Adams, J. (1999). The proteasome inhibitor PS-341 in cancer therapy. *Clinical Cancer Research* **5**(9), 2638-45.

Terrones, O., Etxebarria, A., Landajuela, A., Landeta, O., Antonsson, B., Basan, G. (2008). BIM and tBID Are Not Mechanistically Equivalent When Assisting BAX to Permeabilize Bilayer Membranes. *Journal of Biological Chemistry* **283**(12), 7790 -7803.

Tirapelli, L. F., Bolini, P. H. N. A., Tirapelli, D. P. D. C., Peria, F. M., Becker, A. N. P., Saggioro, F. P., Carlotti Jr, C. G. (2010). Caspase-3 and Bcl-2 expression in glioblastoma: an immunohistochemical study. *Arquivos de neuro-psiquiatria* **68**(4), 603-607.

Twombly, R. (2003). First proteasome inhibitor approved for multiple myeloma. *Journal of the National Cancer Institute* **95**(12), 845.

Uzzaman, M., Keller, G., Germano, I. M. (2007). Enhanced proapoptotic effects of tumor necrosis factor-related apoptosis-inducing ligand on temozolomide-resistant glioma cells. *Journal of Neurosurgery* **106**(4), 646-651.

Vaupel, P. (2004). Tumor microenvironmental physiology and its implications for radiation oncology. *Seminars in Radiation Oncology* **14**(3), 198-206.

Vogler, M, Dürr, K., Jovanovic, M., Debatin, K. M., Fulda, S. (2007). Regulation of TRAIL-induced apoptosis by XIAP in pancreatic carcinoma cells. *Oncogene* **26**(2), 248-257.

Vogler, Meike, Butterworth, M., Majid, A., Walewska, R. J., Sun, X.-M., Dyer, M. J. S., & Cohen, G. M. (2009). Concurrent up-regulation of BCL-XL and BCL2A1 induces approximately 1000-fold resistance to ABT-737 in chronic lymphocytic leukemia. *Blood* **113**(18), 4403-4413.

Vogler, Meike, Walczak, H., Stadel, D., Haas, T. L., Genze, F., Jovanovic, M., Gschwend, J. E., et al. (2008). Targeting XIAP bypasses Bcl-2-mediated resistance to TRAIL and cooperates with TRAIL to suppress pancreatic cancer growth in vitro and in vivo. *Cancer research* **68**(19), 7956-7965.

Wagenknecht, B., Glaser, T., Naumann, U., Ku, S., Isenmann, S., Ba, M., Korneluk, R., et al. (1999). Expression and biological activity of X-linked inhibitor of apoptosis (XIAP) in human malignant glioma. *Cell Death and Differentiation* **95**, 370-376.

Wang, K., Yin, X. M., Chao, D. T., Milliman, C. L., Korsmeyer, S. J. (1996). BID: a novel BH3 domain-only death agonist. *Genes & Development* **10**(22), 2859-69.

Wang, X, Chen, W. R., Xing, D. (2011). A pathway from JNK through decreased ERK and Akt activities for FOXO3a nuclear translocation in response to UV irradiation. *Journal of Cellular Physiology* (May 2011), 1-45.

Waterhouse, N. J., Goldstein, J. C., von Ahsen, O., Schuler, M., Newmeyer, D. D., Green, D. R. (2001). Cytochrome c maintains mitochondrial transmembrane potential and ATP generation after outer mitochondrial membrane permeabilization during the apoptotic process. *The Journal of Cell Biology*, **153**(2), 319-328.

Watts, G. S., Pieper, R. O., Costello, J. F., Peng, Y. M, Dalton, W. S., Futscher, B. W. (1997). Methylation of Discrete Regions of the O 6 -Methylguanine DNA Methyltransferase (MGMT) CpG Island Is Associated with Heterochromatinization of the MGMT Transcription Start Site and Silencing of the Gene. *Microbiology* **17**(9), 5612-5619.

Webb, J. L. (1966). Enzyme and Metabolic Inhibitors. Library (Vol. **III**).

Weil, M., Jacobson, M. D., Coles, H. S., Davies, T. J., Gardner, R. L., Raff, K. D., Raff, M. C. (1996). Constitutive expression of the machinery for programmed cell death. *The Journal of Cell Biology*, **133**(5), 1053-1059.

Weller, M., Wick, W., Hegi, M. E., Stupp, R., Tabatabai, G. (2010). Should biomarkers be used to design personalized medicine for the treatment of glioblastoma? *Future Oncology* (London, England) **6**(9), 1407-1414.

Willis, S. N., and Adams, J. M. (2010). Life in the balance : how BH3-only proteins induce apoptosis. *Molecular Cell* **17**(6), 617-625.

Witzig, T. E. (2005). Current treatment approaches for mantle-cell lymphoma. *Journal of Clinical Oncology* **23**(26), 6409-6414.

Wong, W. W. L. and Puthalakath, H. (2008). Bcl-2 Family Proteins: The Sentinels of the Mitochondrial Apoptosis Pathway. *Life* 60(6), 390-397.

Woods, N. T., Yamaguchi, H., Lee, F. Y., Bhalla, K. N., Wang, H. G. (2007). Anoikis, initiated by Mcl-1 degradation and Bim induction, Is deregulated during oncogenesis. *Cancer Research* **67**(22), 10744-10752.

Xia, S., Li, Y., Rosen, E. M., Laterra, J. (2007). Ribotoxic Stress Sensitizes Glioblastoma Cells to Death Receptor – Induced Apoptosis : Requirements for c-Jun NH 2 -Terminal Kinase and Bim. *Molecular Cancer Research* **5**(August), 783-792.

Yakovlev, A., Khafizova, M., Abdullaev, Z., Loukinov, D., Kondratyev, A. (2010). Epigenetic regulation of caspase-3 gene expression in rat brain development. *Gene* **450**(1-2), 103-108.

Yan, H., Parsons, D. W., Jin, G., McLendon, R., Rasheed, B. A., Yuan, W., Kos, I., Batinic-Haberle, I., Jones, S., Riggins, G. J., Friedman, H., Friedman, A., Reardon, D., Herndon, J., Kinzler, K. W., Velculescu, V. E., Vogelstein, B., Bigner, D. D. (2009). IDH1 and IDH2 mutations in gliomas. *The New England Journal of Medicine*, **360**(8), 765-773.

Yanamandra, N., Kondraganti, S., Srinivasula, S. M., Gujrati, M., Olivero, W. C., Dinh, D. H., Rao, J. S. (2004). Activation of caspase-9 with irradiation inhibits invasion and angiogenesis in SNB19 human glioma cells. *Oncogene* **23**(13), 2339-2346.

Yang, J.Y., Zong, C. S., Xia, W., Yamaguchi, H., Ding, Q., Xie, X., Lang, J. Y., Lai, C. C., Chang, C. J., Huang, W. C., Huang, H., Kuo, H. P., Lee, D. F., Li, L. Y., Lien, H. C., Cheng, X., Chang, K. J., Hslao, C. D., Tsai, F. J., Tsai, C. H., Sahin, A. A., Muller, W. J., Mills, G. B., Yu, D., Hortobadyi, G. N., Hung, M. C. (2008). ERK promotes tumorigenesis by inhibiting FOXO3a via MDM2-mediated degradation. *Nature Cell Biology* **10**(2), 138-148.

Yang, W., Dolloff, N. G., El-Deiry, W. S. (2008). ERK and MDM2 prey on FOXO3a. *Nature Cell Biology* **10**(2), 125-126.

York, N. (2003). Inhibition of DNA repair for sensitizing resistant glioma cells to temozolomide. *The Journal of Neurosurgery* **99**, 1047-1052.

Youle, R. J. and Strasser, A. (2008). The BCL-2 protein family: opposing activities that mediate cell death. *Molecular Cell Biology* **9**(1), 47-59.

Yuan, J. and Yankner, B. A. (2000). Apoptosis in the nervous system. *Nature* **407**(6805), 802-809.

Yuan, Junying and Horvitz, H. R. (2004). A First Insight into the Molecular Mechanisms of Apoptosis. *Cell* **S116**(1993), 53-56.

Zhang, Lidong and Fang, B. (2005). Mechanisms of resistance to TRAIL-induced apoptosis in cancer. *Cancer Gene Therapy* **12**(3), 228-237.

Zhang, W. B., Wang, Z., Shu, F., Jin, Y.H., Liu, H.Y, Wang, Q. J, Yang, Y. (2010). Activation of AMP-activated protein kinase by temozolomide contributes to apoptosis in glioblastoma cells via p53 activation and mTORC1 inhibition. *The Journal of Biological Chemistry* **285**(52), 40461-40471.

Zimmermann, S., Moelling, K. (1999). Phosphorylation and regulation of Raf by Akt (protein kinase B). *Science* **286**(5445), 1741-1744.

Zlobec, I., Vuong, T., Compton, C. C. (2006). The predictive value of apoptosis protease-activating factor 1 in rectal tumors treated with preoperative, high-dose-rate brachytherapy. *Cancer* **106**(2), 284-286.

Zou, H., Li, Y., Liu, X., Wang, X. (1999). An APAF-1.cytochrome c multimeric complex is a functional apoptosome that activates procaspase-9. *The Journal of Biological Chemistry* **274**(17), 11549-11556.

van Gorp, A. G. M., Pomeranz, K. M., Birkenkamp, K. U., Hui, R. C.Y., Lam, E. W. F., Coffer, P. J. (2006). Chronic protein kinase B (PKB/c-akt) activation leads to apoptosis induced by oxidative stress-mediated Foxo3a transcriptional up-regulation. *Cancer Research* **66**(22), 10760-10769.

van Nifterik, K. a, van den Berg, J., van der Meide, W. F., Ameziane, N., Wedekind, L. E., Steenbergen, R. D. M., Leenstra, S., Lafleur, M. V. M., Slotman, B. J., Stalpers, L. J. A., Sminia, P. (2010). Absence of the MGMT protein as well as methylation of the MGMT promoter predict the sensitivity for temozolomide. *British Journal of Cancer* **103**(1), 29-35.

van den Bent, M. J., Gravendeel, L. a M., Gorlia, T., Kros, J. M., Lapre, L., Wesseling, P., Teepen, J., et al. (2011). A hypermethylated phenotype in anaplastic oligodendroglial brain tumors is a better predictor of survival than MGMT methylation in anaplastic oligodendroglioma: a report from EORTC study 26951. *Clinical Cancer Research* **17**(22), 7147-7155.

von Haefen, C., Gillissen, B., Hemmati, P. G., Wendt, J., Güner, D., Mrozek, A., Belka, C., Dörken, B., Daniel, P. T. (2004). Multidomain Bcl-2 homolog Bax but not Bak mediates synergistic induction of apoptosis by TRAIL and 5-FU through the mitochondrial apoptosis pathway. *Oncogene* **23**(50), 8320-8332.